# Physiological characterisation of transcranial magnetic stimulation (TMS) using functional magnetic resonance imaging (fMRI)

Sven Bestmann

Thesis submitted for the degree of PhD in Neurological Studies

Institute of Neurology

University College London

University of London

February 2004

# Abstract

Despite its widespread use, a striking lack of knowledge exists regarding the mechanism of action of transcranial magnetic stimulation (TMS). This thesis describes the physiological characterisation of repetitive TMS (rTMS) to the motor system by means of functional magnetic resonance imaging (fMRI).

A detailed analysis of imaging artefacts arising from the simultaneous application of TMS-fMRI was conducted and subsequently, strategies were presented for unperturbed TMS-fMRI.

Physiological responses during subthreshold high-frequency rTMS of the primary sensorimotor cortex (M1/S1) were visualised within distinct cortical motor regions, comprising PMd, SMA, and contralateral M1/S1, while no significant responses were evidenced in the area of stimulation.

Repetitive TMS during or before motor behaviour illustrated the context-dependence of rTMS-induced activity changes.

The first demonstration of TMS-fMRI at 3 Tesla provided evidence that subthreshold rTMS can activate distinct networks including subcortical motor regions. The subthreshold nature of rTMS was confirmed by simultaneous electromyographic recordings from the target muscle.

Stimulation of the dorsal premotor cortex provided evidence that rTMS-evoked local activity changes depend on the input function. The capability of TMS to target distinct networks in the human brain was confirmed.

TMS targets a set of cortical and subcortical structures. Local responses may not invariably be elicited, indicating that low levels of synaptic activity, as occurring at low-intensity stimulation, do not necessarily evoke corresponding changes in cortical haemodynamics. It is concluded that combined TMS-fMRI offers a means to assess the mechanism of action of TMS at high spatial and temporal resolution.

# Acknowledgements

I am deeply grateful to my supervisors John Rothwell and Jens Frahm for their continuous supervision, enduring encouragement, intellectual challenge and stimulating education. Their constant enthusiasm regarding all aspects of this thesis has supported me throughout the last years. I am particularly grateful for John's sedulous commitment on the administrative organisation of this thesis.

I would especially like to thank Walter Paulus for his organisation of the European graduate programme through which I was funded and his persistent enthusiasm for making this 'european thingie' happen.

My gratitude and thank goes to Jürgen Baudewig for all the collaboration, education, and patience which provided the backbone of my work.

I am very thankful to Hartwig Siebner for his generous support, fruitful ideas and enriching discussions.

None of the work presented here could have been conducted without the continuous administrative and technical support by Peter Asselman and Kelly Parsons in London, and Kurt Böhm and Christine Crozier in Göttingen. I am furthermore indebted to Anthony Thomas and Stefan Cohrs for providing essential equipment to me.

Furthermore, many thanks go to my colleagues, fellow-students, and friends Jürgen Baudewig, Lars Christensen, Brian Day, Peter Dechent, Patrick Fallskämper, Willibald Gerschlager, Catherine Harmer, Estelle Himmelbach, Stefan Kalla, Lucy Lee, Simone Klinge, John Marsden, Antonio Oliviero, Christian Rochford, Raymond Reynolds, Kai Thilo, Martin Voss, Martin Wienisch Jr., Frank Wiesel, Kielan Yarrow, and all colleagues at the Biomedizinische NMR Forschungs GmbH for their scientific advice, being my subjects, helping me set up experiments and for socialising outside of work.

For constant guidance and accompaniment, starting back during my university years, I am much obliged to John R. Hernshey and Anders A. Baumann.

The financial support of the Deutsche Forschungsgemeinschaft (DFG) is gratefully acknowledged.

Lastly, I especially would like to thank my mother for her support, encouragement and enduring love.

# Table of Contents

# Publications

The following publications have emerged from this thesis:

* Bestmann S, Baudewig J, Siebner HR, Rothwell JC, Frahm J (2004). Functional MRI of the immediate impact of transcranial magnetic stimulation on cortical and subcortical motor circuits. *Eur. J. Neurosci.* **19:**1-13 *(in press).*

Bestmann S, Siebner HR, Modugno N, Amassian VE, Rothwell JC (2004). Inhibitory interactions between pairs of subthreshold conditioning stimuli in the human motor cortex. *Clin. Neurophysiol. (in press*).

* Bestmann S, Baudewig J, Frahm J (2003). On the synchronization of transcranial magnetic stimulation and functional magnetic resonance imaging. *J. Magn. Reson. Imaging* **17:**309-316.

* Bestmann S, Baudewig J, Siebner HR, Rothwell JC, Frahm J (2003). Subthreshold high-frequency TMS of human primary motor cortex modulates interconnected frontal motor areas as detected by interleaved fMRI-TMS. *Neuroimage* **20:**1685-1696.

* Bestmann S, Baudewig J, Siebner HR, Rothwell JC, Frahm J (2003). Is functional magnetic resonance imaging capable of mapping transcranial magnetic cortex stimulation? *Clin. Neurophysiol. Suppl.* **56:**55-62.

* Siebner HR, Lee L, Bestmann S (2003). Interleaving TMS with functional MRI: now that it is technically feasible how should it be used? *Clin. Neurophysiol.* **114:**1997-1999.

Gerschlager W, Christensen LO, Bestmann S, Rothwell JC (2002). rTMS over the cerebellum can increase corticospinal excitability through a spinal mechanism involving activation of peripheral nerve fibres. *Clin. Neurophysiol.* **113:**1279-1285.

Fisher RJ, Nakamura Y, Bestmann S, Rothwell JC, Bostock H (2002). Two phases of intracortical inhibition explored by transcranial magnetic threshold tracking. *Exp. Brain Res.* **143:**240-248.

Modugno N, Nakamura Y, Bestmann S, Curra A, Berardelli A, Rothwell JC (2002). Neurophysiological investigations in patients with primary writing tremor. *Mov. Disord.* **17:**1336-1340.

Baudewig J, Siebner HR, Bestmann S, Tergau F, Tings T, Paulus W, Frahm J (2001). Functional MRI of cortical activations induced by transcranial magnetic stimulation (TMS). *Neuroreport* **12:**3543-3548.

* Incorporated into the thesis.

# List of Tables

# List of Figures

# Abbreviations

| | |
|---|---|
| AC | anterior commissure |
| AMT | active motor threshold |
| AP | action potential |
| AUD | auditory cortex |
| BOLD | blood oxygenation level dependent |
| CMA | cingulate motor area |
| CS | conditioning stimulus |
| CSN | corticospinal neurons |
| EEG | electroencephalography |
| EMG | electromyography |
| EPI | echo-planar imaging |
| EPSP | excitatory post-synaptic potential |
| FEF | frontal eye field |
| FDI | first dorsal interosseous |
| fMRI | functional magnetic resonance imaging |
| GLM | general linear model |
| GPe | globus pallidus pars externa |
| GPi | globus pallidus pars interna |
| ICI | intracortical inhibition |
| ICF | intracortical facilitation |
| IPSP | inhibitory post-synaptic potential |
| ISI | inter-stimulus interval |
| LFP | local field potential |
| LPMC | lateral premotor cortex |
| M1 | primary motor cortex |
| M1/S1 | primary sensorimotor cortex |
| MEP | motor evoked potential |
| MRI | magnetic resonance imaging |
| NIRS | near-infrared spectroscopy |
| NMR | nuclear magnetic resonance |

| | |
|---|---|
| PC | posterior commissure |
| PET | positron emission tomography |
| PMd | dorsal premotor cortex |
| PMv | ventral premotor cortex |
| rCBF | regional cerebral blood flow |
| RF | radiofrequency |
| RMT | resting motor threshold |
| rTMS | repetitive transcranial magnetic stimulation |
| ROI | region of interest |
| SMA | supplementary motor area |
| TES | transcranial electric stimulation |
| TMS | transcranial magnetic stimulation |
| TE | echo time |
| TR | repetition time |
| TTG | transverse temporal gyrus |
| VA | ventral anterior part of the thalamus |
| VL | ventral anterior part of the thalamus |
| VLo | nucleus ventralis lateralis pars oralis |
| VPLo | nucleus ventroposterioris lateralis pars oralis |

# 1 Introduction

”How can we know the dancer from the dance?” (*Among school children*, W.B. Yeats). This quote elegantly illustrates one of the fundamental limitations of modern brain research: every component of a behaviour that we may investigate is inextricably intertwined and interacting with other components of the behaving agent and is subserving a broader scope which often will be inaccessible to our insight. We, however, are relying on the observation of fractions of a system to infer about general principles that may direct the entity of the brain.

While this poses a fundamental epistemological problem, within the modern neurosciences an enlargement of the often constricted insight provided by a single method would already ameliorate our situation. Without doubt many methods have contributed to the understanding of cortical function, yet obvious limitations are inherent to every single methodology. As one example, functional brain imaging enables us to visualise brain activity directly or indirectly at high spatial resolution, but it does not provide sufficient information regarding causality between brain activation states and behaviour. By contrast, transcranial magnetic stimulation (TMS) allows one to derive causal relationships between behaviour and a stimulated brain region, yet the localisation is comparatively poor and no information is provided regarding brain regions remote from the site of stimulation. The traditional way of overcoming the discrepancy between causation and correlation has been the investigation of focal lesions in patients. Little is known however about functional compensation following brain damage, and although lesions may appear to be focal, their impact on remote brain regions can be substantial. This inevitably prevents us from transferring our observations from the lesioned to the healthy brain.

One of the paramount challenges to modern neuroscience therefore seems to be the integration of different yet complementary methods that have been established for the investigation of the brain. With respect to the above

example, the combination of functional brain imaging, in particular non-invasive functional magnetic resonance imaging (fMRI), and TMS promises to derive information regarding both causation and correlation between brain function and behaviour in healthy humans. In the present thesis, all experiments are concerned with the implementation of combined TMS-fMRI and the physiological characterisation of TMS-evoked activity changes in the human brain. Apart from contributing to our understanding of the physiology of TMS, such a characterisation needs to precede the much more complex application of TMS-fMRI to cognitive experiments.

Over the last two decades, TMS has evolved from a tool applied to test the integrity of corticospinal pathways to a widely used research method for both basic neuroscientists and cognitive scientists to probe the function of many areas of the cerebral cortex (as reviewed by WALSH & COWEY, 2000; ZIEMANN & ROTHWELL, 2000; COWEY & WALSH, 2001; SIEBNER & ROTHWELL, 2003). Support for the idea of combined TMS-fMRI studies stems from earlier investigations that combined other neuroimaging techniques with TMS. Cracco and Amassian, for example, first combined electroencephalography (EEG) and TMS to explore transcallosal (CRACCO ET AL., 1989) and frontocerebellar (AMASSIAN ET AL., 1992a) circuits. This approach was perfected in a series of studies (ILMONIEMI ET AL., 1997; TIITINEN ET AL., 1999; NIKOULINE ET AL., 1999) that now enable the investigation of TMS-induced changes in spontaneous electric activity at high temporal resolution. OLIVIERO ET AL. (1999) combined near-infrared spectroscopy (NIRS) and TMS to investigate the coupling between cortical haemodynamics and TMS-induced activity, and reported TMS-induced metabolic increases concomitant with increases in cerebral blood flow. Measures of cerebral blood flow by single-photon emission computed tomography (SPECT) have recently provided evidence for TMS-induced changes of blood flow remote from the site of stimulation (OKABE ET AL., 2003).

The combination of positron emission tomography (PET) and TMS provides the most compelling evidence that the combination of TMS and neuroimaging opens insight into cortical function otherwise not accessible. In

the pioneering work by Tomas Paus and collaborators, TMS-induced changes in regional cerebral blood flow (rCBF) were demonstrated using both low and high stimulation frequencies (PAUS ET AL., 1997, 1998, 2001). In the meantime, activity patterns were found to be modulated beyond the site of stimulation, for example following TMS of the primary motor cortex (PAUS ET AL., 1998; SIEBNER ET AL., 1998; 2000, 2001a,b; CHOUINARD ET AL., 2003; SPEER ET AL., 2003a; STRAFELLA ET AL., 2003), the frontal eye-field (FEF) (PAUS ET AL., 1997), the mid-dorsolateral prefrontal cortex (PAUS ET AL., 2001; SPEER ET AL., 2003b), and the lateral premotor-prefrontal cortex (SIEBNER ET AL., 2001a; STRAFELLA & PAUS, 2001; LEE ET AL., 2003; SIEBNER ET AL., 2003a).

While EEG and NIRS essentially are restricted to the outer convexity of the brain, the invasive properties and in particular the low temporal resolution of PET impose a major constraint on its applicability to the investigation of human brain function. These constraints favour the use of non-invasive and unrestricted brain imaging tools such as fMRI, which furthermore offers a high spatial and temporal resolution. Until recently, however, a combination of TMS and fMRI has been regarded as technically impossible. In a seminal study, BOHNING ET AL. (1997) were the first to successfully combine both methods directly and, subsequently, record functional brain images based on blood-oxygenation-level-dependent (BOLD) contrast during TMS (BOHNING ET AL., 1998, 1999, 2000a,b). The combination with neuroimaging offers a more direct and immediate visualisation of TMS-induced brain activity changes, while previous techniques have provided indirect measures of cortical function, as for example reaction times or motor evoked potentials (SIEBNER & ROTHWELL, 2003).

The present thesis focuses on the investigation of the motor system. This was motivated by the abundance of TMS studies in the motor system providing a solid ground for the interpretation of the present experiments. Furthermore, most studies combining TMS and neuroimaging have focused on the motor system as the direct effects of stimulation can be easily monitored, and, finally, the motor system is easily accessible to TMS. In the following, the motor system will briefly be reviewed and a short introduction into the

methods of fMRI and TMS will be provided to set grounds for the subsequent experimental chapters and to illustrate the motivation for the presented methodological approach.

## 1.1 The motor system

The motor system represents the only way by which we can interact with our environment. The control of motor output, both during postural control and voluntary movement, requires a hierarchical organisation that allows to integrate incoming sensory information and outgoing motor commands. In this thesis, experiments were focused on the motor cortices of the frontal lobe. Nevertheless, with respect to the results discussed in the subsequent chapters it seems pertinent to provide a broader overview of the organisation and structure of the motor system. Clearly, an exhaustive overview on all brain regions, particularly those involved in hand movement, hand co-ordination and visuomotor transformations is beyond the scope of this work. Hence, the basic organisation, anatomy and function of the motor system shall be reviewed in the following sections. Additional information regarding other systems or brain regions shall be given in the respective chapters when necessary.

### 1.1.1 Anatomy of the motor cortex

Although the microscopic structure of the neocortex in man follows an organisation that displays little variations within different brain structures, the motor areas of the frontal cortex exhibit certain features that make them relatively easy to distinguish from non-motor regions. The cortex is organised in a layered fashion, with each layer displaying a specific intracortical organisation that can be identified on grounds of cell structure, connectivity, transmitter density, and function. In principle, the cortex is comprised of six layers:

Layer I is termed the molecular or zonal layer and adjacent to the pia mater. It mainly contains fibres and the horizontal cells of Cajal, with their long axis

running parallel to the gyral surface. These fibres are densely organised in a running plexus.

Layer II is termed the external granular layer. It is packed with small cells with pyramidal, round or stellar shapes. Another feature are the vertically directed apices of the pyramidal cells.

Layer III is termed the pyramidal layer. It contains large pyramidal cells in the deeper parts while medium sized pyramidal cells predominate at the superior aspect of this layer.

Layer IV is termed internal granular layer. It predominantly contains small and densely packed cells of both stellar and pyramidal shape and furthermore contains rich horizontally directed fibres.

Layer V is termed ganglionic layer and predominantly houses medium and large pyramidal cells, with their apical dendrites directed towards the molecular layer. In addition, abundant horizontally projections are formed by the basal dendrites. All cortical areas have layer V output directed to lower brain structures.

Layer VI is termed the multiform layer. Its spindle-shaped cells can be further subdivided into a superficial and deep part, the latter of which fuses with the adjacent white matter.

In primates, the motor areas of the frontal cortex are situated in Brodmann areas (BA) 4 and 6 at the lateral surface, and areas 23 and 24 as well as the medio-dorsal part of area 6. These gross anatomical subdivisions can be distinguished from their adjacent structures by their relatively large pyramidal neurons in layer V and their comparatively small internal granular layer. Area 4 can be distinguished from area 6 by the giant Betz cells. This distinction, however, is a gradual one, with the size of the Betz cells progressively decreasing towards the lateral arm area of the precentral gyrus. Area 6 can be subdivided into at least three distinct regions. On the lateral surface, a superior and an inferior part can be distinguished; both of them are separated from the mesial part of area 6. Area 6 lies dorsal of the agranular cingulate cortex (areas 23 and 24). Here, three motor regions have been identified: the

rostral cingulate motor area (rCMA) is situated on the dorsal surface of the cingulate gyrus, the caudal CMA on the ventral bank of the cingulate sulcus, and a caudal area on the dorsal bank of this sulcus.

While area 4 is also termed the primary motor area (M1), the adjacent areas 6, 23 and 24 are commonly termed secondary motor regions. Apart from their cytoarchitectural difference with regions from the prefrontal cortex, they can be identified as motor areas based on their corticospinal pyramidal projections and their reciprocal corticocortical connections to the primary motor cortex (JONES, 1987; DUM & STRICK, 1991; HE ET AL., 1993, 1995).

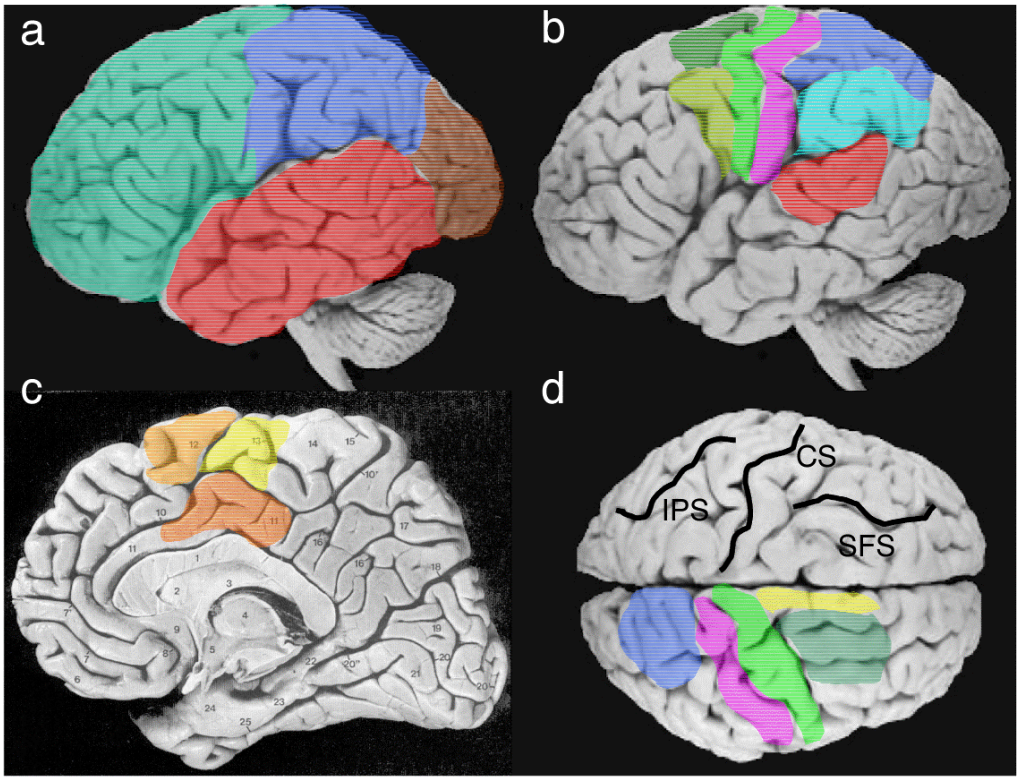


**Figure 1.1.** Motor structures of the cerebral cortex. **(a)** The cerebral cortex can be divided into a frontal (green), temporal (red), parietal (blue), occipital (brown), and insular part (not shown). **(b)** On the lateral convexity, the dorsal premotor cortex (dark green), ventral premotor cortex (PMv, yellow-green), primary motor cortex M1 (area 4, green), primary somatosensory cortex (S1; area 1, 2, 3; pink), superior parietal lobule (SPL; blue), inferior parietal lobule (IPL; light blue), and primary auditory cortex (AUD, red) can be distinguished by gross anatomical landmarks. **(c)** On the mesial surface, the supplementary motor area (SMA; yellow), pre-SMA (orange) and cingulate motor area (dark orange) can be identified. **(d)** On the dorsal surface, the SMA (yellow) and dorsal premotor cortex (PMd, green) can be identified anterior to M1 (light green). SFS: superior frontal sulcus; CS: central sulcus; IPS: intraparietal sulcus.

### 1.1.2 The primary motor cortex

**The architecture of the primary motor cortex.** The primary motor cortex is a pre-eminent structure among neocortical brain regions both in terms of its location and structure (Figure 1.1). Its position within the anatomical hierarchy makes it unique as a recipient of multifarious integrated inputs from various brain regions that are processed to brain stem structures and the spinal cord. Here, these inputs become translated into meaningful actions, such as voluntary movement.

Remarkable features of the primary motor cortex are the giant pyramidal or Betz cells in layer V, the sparseness of neuronal cells, the poor lamination, and the absence of layer IV. Furthermore, area 4 reveals the greatest cortical thickness, being about 1.6 times thicker than the primary visual cortex (ROCKEL ET AL., 1980). Based on neurotransmitter binding sites and cytoarchitecture, it has recently been subdivided into two distinct subregions 4a and 4p (GEYER ET AL., 1996). Two distinct cell types characterise M1: the pyramidal cells and non-pyramidal cells.

The pyramidal cells form the primary output of the motor cortex. As mentioned above, the internal granular layer is poorly developed while layers III and V exhibit a richness of pyramidal cells. The size of pyramidal cells shows remarkable variation. The giant Betz cells have diameters of up to 120 µm (MEYER, 1987) with a cell density of only 20-25 cells per 100 $\mu m^3$ of layer V (HUMPHREY & CORRIE, 1978), and are often grouped into 2-6 cells situated in the upper margin of layer V. The dendrites of the pyramidal cells receive massive synaptic inputs and are covered with spines, with each pyramidal cell receiving input from approximately 60.000 synapses (CRAGG, 1975). While the apical dendrites ascend into the superficial cortical layers, they remain clustered. As suggested by PORTER & LEMON (1993), this forms the basis of a rich communication network between clustered neurons. Pyramidal cells in layers II and III give rise to the majority of corticocortical afferents (GHOSH ET AL., 1987), terminating in all six layers of the cortex and forming connections with dendritic spines of pyramidal cells and non-pyramidal cells (SLOPER &

POWELL, 1979). Collaterals of pyramidal neurons in layer V (GHOSH ET AL., 1988) but also layer II and III (LANDRY ET AL., 1980) form long horizontal connections of up to 2 mm. These collaterals target both distal and proximal neurons (KELLER, 1993) which can provide both excitatory and inhibitory drive to remote pyramidal neurons. The majority of synaptic input to pyramidal and non-pyramidal cells stems from local sources (GATTER & POWELL, 1978), which are predominantly inhibitory (JONES, 1983). For example, they are formed by pyramidal neurons in more superficial layers of the cortex with their short collaterals terminating in layer V, where they synapse with dendritic spines of pyramidal cells (KELLER & ASANUMA, 1993). This complex columnar and intralaminar organisation emphasises the notion that M1 cannot simply be regarded as an 'upper motoneuron' but as an area forming a substrate for the temporal co-ordination of movement segments that constitute multijoint movement sequences.

The stellate or basket cells form the most abundant non-pyramidal cell group in the motor cortex (MEYER, 1987) and are predominantly located in layers III to V, with their myelinated axons oriented horizontally. They form inhibitory GABAergic connections with pyramidal neurons, thus mediating inhibitory effects exerted by collaterals or corticofugal neurons (JONES, 1983).

**Afferents to the motor cortex.** The topographic organisation of afferent projections into area 4 shows significant degrees of segregation and separation, thus reflecting the complex organisation of the motor system with regard to both afferent and efferent projections, and contrasting the orderly topography in the primary visual (HUBEL & WIESEL, 1962) and sensory cortices (MOUNTCASTLE, 1957). In conjunction with information from joint and cutaneous receptors, muscle afferents provide information about proprioception and kinaesthesia (GANDEVIA ET AL., 1992). Primary, secondary, and Golgi tendon organ afferent fibres enter the spinal cord through the dorsal roots and branch over several segments. They synapse on interneurons within the intermediate and ventral grey matter of the spinal cord. Information regarding limb position, muscle stretch, and muscle tension are transmitted to higher levels of the central nervous system. Information from

large-diameter afferents crosses the midline of the medulla and ascends in the medial lemniscus. These afferents terminate in ventral posterolateral nucleus of the dorsal thalamus, from which the information is processed to the primary and secondary somatosensory cortex in the postcentral gyrus. Principally, there appears to be a complete segregation of afferent inputs to area 4 and area 1, 2, and 3a,b (JONES, 1987). Axons project from the somatosensory cortex to higher-order somatosensory cortices as well as to areas of the motor cortex. The latter originate from the postcentral areas 1, 2, 3a and from the thalamus (GHOSH ET AL., 1987). Short-latency peripheral inputs, especially from muscles, reach the motor cortex via connections from area 3a (GHOSH ET AL., 1987). As such, peripheral input as for example from light touch, taps and manipulation of the fingers can drive unit responses in the motor cortex of the anaesthetised monkey (ROSEN & ASANUMA, 1972), demonstrating the importance of re-afferent somatosensory input to motor cortex activity. It has been hypothesised that the large population of subcortically projecting pyramidal cells in area 4 may also be monosynaptically influenced by projections from the thalamus (JONES, 1987).

Furthermore, extensive projections to M1 originate in the dorsolateral part of area 6 including the SMA (MUAKKASSA & STRICK, 1979; GHOSH ET AL., 1987). While the forelimb area of M1 receives topographically organised projections from the premotor cortex and area 5 of the parietal cortex, the inputs from the SMA and cingulate motor regions reveal only a coarse topographical order (TOKUNO & TANJI, 1993), possibly reflecting anatomical substrates of different functional roles of these areas in the co-ordination of motor behaviour. Callosal afferents originate in layer III of the homotopic M1 and modest heterotopic callosal afferents reach M1 from the SMA, premotor cortex, and the cingulate motor areas (ROUILLER ET AL., 1994).

**Topography of M1.** The inner walls of the central sulcus interdigitate into a complex gyral arrangement in the depth of the central sulcus approximately halfway between the midline and the lateral fissure (WHITE ET AL., 1997). The border to the caudally adjoining somatosensory cortex lies in the fundus in the depth of the central sulcus, while the dorso-medial border of area 4 is

demarcated by the cortical surface on the vertex of the precentral gyrus. Medially, M1 extends to the paracentral lobule. As already described eloquently and in astonishing detail by CUNNINGHAM (1892), CAMPBELL (1905) and SYMINGTON & CRYMBLE (1913), the walls of the central sulcus build interlocking protrusions in the depth of the central sulcus that result in an elevated bridge between the corresponding gyri. This complex arrangement has been implicated as the digit and hand representation based on neuroimaging studies. As pointed out by White and colleagues (WHITE ET AL., 1997), almost every brain imaging study inspecting finger or digit movement presents localised activity in the depth of the central sulcus near the interdigitation of the pre- and postcentral gyrus. The authors proposed this to be an anatomical landmark for the proximal extremity (WHITE ET AL., 1997), corresponding to electrophysiological identification of the hand representation about midway between the central and lateral fissure (PENFIELD & RASMUSSEN, 1950; WOOLSEY ET AL., 1979). Recent brain imaging studies confirm that the hand area can be identified macroanatomically by a knob-like structure in the precentral gyrus that is often resembling an omega or epsilon in the axial plane and is located in the middle portion of the central sulcus (YOUSRY ET AL., 1997; DECHENT & FRAHM, 2003). This conforms to the notion that the motor cortex is somatotopically organised, with the leg being represented on the mesial cortical surface and the trunk, arm, hand, face and throat in medio-lateral order on the cortical convexity. However, this representation is not a one-to-one mapping of body parts. Within M1, a distributed and overlapping network of movement representations can be found (SANES & SCHIEBER, 2001). Furthermore, there is considerable convergence of output from a wide M1 territory to the motor neuron pool (ANDERSEN ET AL., 1975), as well as substantial divergence of output from single cortical neurons to multiple motor neuron pools (SHINODA ET AL., 1981). In line with this, recent functional MRI studies have revealed that the somatotopic organisation of individual fingers is reflected in multiple and spatially overlapping activation sites rather than in a separated clustering of different digits (SANES ET AL., 1995; DECHENT & FRAHM, 2003).

### 1.1.3 The secondary motor (premotor) cortices

The premotor regions of the frontal lobe modulate motor output both via their connections with the primary motor cortex (Figure 1.2) and the spinal cord (DUM & STRICK, 1991). At least six well-defined motor areas have been identified in the monkey, most of them having analogous representations in the human (for example, as being identified by neuroimaging).

**The dorsal premotor cortex (PMd).** On grounds of both anatomical and functional studies, the premotor cortex on the lateral surface of the brain can be subdivided into a dorsal and a ventral region. The dorsal premotor cortex is located at the lateral surface of the frontal cortex within the rostral portion of the precentral gyrus and the caudal superior frontal gyrus (RIZZOLATTI ET AL., 1998). It can be further subdivided into a caudal and rostral subdivision (BARBAS & PANDYA, 1987). The caudal portion is directly connected to M1 and the spinal cord (MUAKKASSA & STRICK, 1979; DUM & STRICK, 1991), without revealing substantial connections to the prefrontal cortex (LU ET AL., 1994). This area (area F2 in the monkey) receives heterotopic projections from the rostral PMd (F7), the ventral premotor cortex (PMv) (F4, F5), the SMA-proper (F3), and the primary motor cortex. In contrast, the rostral aspect of the PMd does not project to the primary motor cortex or the spinal cord (MUAKKASSA & STRICK, 1979; DUM & STRICK, 1991) but connects to the prefrontal cortex (LU ET AL., 1994; MARCONI ET AL., 2003) and the pre-SMA (MARCONI ET AL., 2003). In this regard, the PMd exhibits a similar rostro-caudal organisation as the SMA (see below; Figure 1.2). The predominant parietal input to PMd comprises the medial intraparietal sulcus, the occipito-parietal region, ventral intraparietal area, and area 7a and 7b (TANNE-GARIEPY ET AL., 2002). Both compartments of the PMd receive their predominant callosal projections from the homotopic counterpart (MARCONI ET AL., 2003).

The rostral PMd has been implicated with the linkage of eye-hand actions to the cognitive aspects required for the successful processing of movement-related information while the caudal part of PMd is more closely linked to the processing of movement-related information *per se* (PICARD & STRICK, 2001).

A clear distinction can be made between activity in M1 and PMd: there is a rostro-caudal gradient in which neurons encoding visuospatial aspects of movements are preferentially located in PMd and neurons encoding movement are located in M1 (SHEN & ALEXANDER, 1997a,b; JOHNSON ET AL., 1999). Therefore, the PMd seems to be more concerned with various aspects of action planning, movement preparation, response selection, and visual guidance of responses, and plays a preferential role in generating a representation of the extrinsic visuospatial objectives of a task and stimulus-response associations involved in appropriate motor response selection (SHEN & ALEXANDER, 1997a,b). For example, the PMd is implicated in conditional motor behaviour in which actions must be selected on the basis of arbitrary stimulus-response mappings (PASSINGHAM ET AL., 1988; WISE ET AL., 1996). It appears to be most important when motor instructions arise from a source other than the object to be manipulated (MURRAY ET AL., 2000).

**The ventral premotor cortex (PMv).** The PMv in area 6 is densely interconnected with M1 (Figure 1.2) and contains direct projections to the spinal cord (DUM & STRICK, 1991; HE ET AL., 1993). It is situated ventral to the PMd, at the mesial rostral portion of the precentral gyrus and the caudal portion of the middle frontal gyrus, and in humans it lies ventral to the FEF. However, its precise location in humans is not as well established as in the monkey (GREZES & DECETY, 2001). Both somatosensory and visual input is projected to the PMv via the anterior intraparietal area (AIP), area 7b, and somatosensory regions (GODSCHALK ET AL., 1984; RIZZOLATTI ET AL., 1998; TANNE-GARIEPY ET AL., 2002). Its linkage with visuomotor transformations for grasping is emphasised by the strong projections from the anterior intraparietal cortex (LUPPINO ET AL., 1999). The more caudal F4 subdivision, on the other hand, is primarily linked with the ventral intraparietal region, which is possibly involved in peripersonal space coding for movement (LUPPINO ET AL., 1999). The dorsal and ventral parts of the premotor cortex seem to receive segregated input from the parietal cortex. Based on present imaging data, a definite correspondence in humans to the functional subdivisions of the PMv in monkeys cannot be claimed (PICARD & STRICK, 2001).

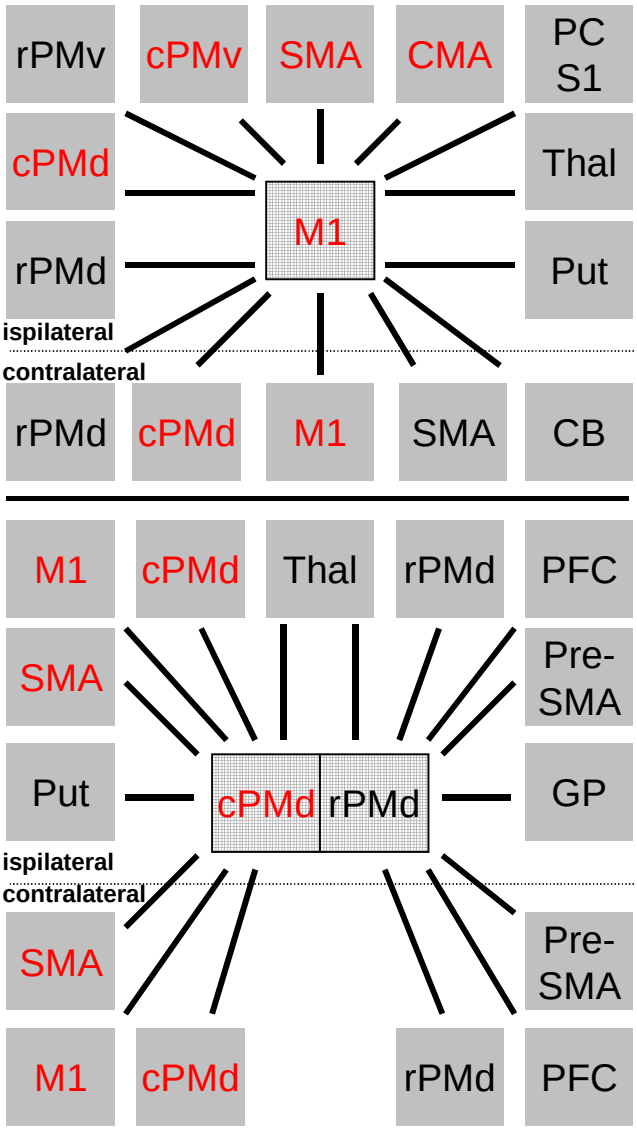


**Figure 1.2.** Schematic drawing of assumed connections from the human primary motor cortex **(top)** and dorsal premotor cortex **(bottom)**. No indication of the strength of connections is given. Regions in red contain corticospinal projections. For details, see text. M1: primary motor cortex, cPMd: caudal part of the dorsal premotor cortex, rPMd: rostral PMd, cPMv: caudal part of the ventral premotor cortex, rPMv: rostral PMv, SMA: supplementary motor area, CMA: cingulate motor area, PC: parietal cortex, S1: somatosensory cortex, Thal: thalamus, Put: putamen, CB: cerebellum

**The supplementary motor area (SMA).** The SMA is located at the medial wall of the frontal lobe in area 6. At least two distinct subdivisions have been identified in monkeys. The SMA (SMA-proper) lies in the caudal portion of area 6, while the pre-SMA is located rostrally to it (PICARD & STRICK, 1996). In humans, their border is presumably located at the level of the anterior commissure (AC). This location corresponds to areas F3 and F6, respectively, in the monkey, and areas 6aα and 6aβ of VOGT & VOGT (1919). Recently, a

further subdivision of the postcommissural portion of the SMA into a rostral and a caudal sector has been proposed in humans (VOROBIEV ET AL., 1998). The border between the mesial portion of M1 and the SMA is approximately given by the level of the posterior commissure (PC). The SMA is directly connected with the primary motor cortex and the spinal cord (MUAKKASSA & STRICK, 1979; HE ET AL., 1995; DUM & STRICK, 1996), while the pre-SMA is connected to the prefrontal cortex and lacks significant projections to M1 or the spinal cord (LUPPINO ET AL., 1993; LU ET AL., 1994; LIU ET AL., 2002). The hand representation of the SMA receives most of its input (42-65%) from dense callosal projections of its homotopic counterpart (LIU ET AL., 2002), as well as input from the contralateral rostral and caudal cingulate motor areas, the lateral premotor cortex, and M1 (ROUILLER ET AL., 1994). In the pre-SMA callosal input from the homotopic counterpart also predominates and is complemented by input from the rostral parts of the PMd, PMv and cingulate motor areas (LIU ET AL., 2002).

Originally, the SMA has been implicated to complexly organised motor tasks, especially with regard to the programming of complex voluntary movements. Mounting evidence exists, however, that the SMA is also linked to simple motor behaviour (TANJI, 1985, 1996; PICARD & STRICK, 2001). For example, movement-related activity and sensitivity to passive joint or muscle manipulation are frequently found in the SMA-proper (MATSUZAKA & TANJI, 1996). The much weaker cortico-motoneuronal projections from the SMA in comparison to those arising from M1 opt for a more modulatory and preparatory function rather than substituting the role of M1 corticospinal control (LEMON ET AL., 2002). While the SMA is believed to be more concerned with externally triggered movements, development of automatic movements, simple motor preparation, and execution of movements (PICARD & STRICK, 1996; DEIBER ET AL., 1999), the pre-SMA is more linked to the preparation and acquisition of higher-order spatiotemporal movement patterns, especially in relation to context changes in the environment (SHIMA ET AL., 1996; TANJI, 1996; PICARD & STRICK, 2001).

### 1.1.4 The corticospinal tract

The corticospinal tract is the dominant output pathway of the motor cortices. It is comprised by the pyramidal cell axons of layer Vb. The giant Betz cells of M1 (Brodmann areas 4 and 6) provide the largest and hence most rapidly conducting fibres, however, accounting only for 3-5% of the fibres of the corticospinal tract (GRAF VON KEYSERLINGK & SCHRAMM, 1984). The descending axons pass through the centrum semiovale and project via the internal capsule. They then form the cerebral peduncle, projecting to the base of the pons. The axons are bundled to form the medullary pyramid from which about 70-90% of the axons cross to the contralateral spinal cord, while about 10-30% remain ipsilateral and traverse caudally as the ventral or anterior corticospinal tract (NATHAN & SMITH, 1955; THACH, 1999). Crossed fibres run into the lateral and anterior column of the spinal cord (THACH, 1999). This crossing decussation explains why the musculature of the body is controlled by the motor cortex of the contralateral hemisphere.

The corticospinal tracts are concerned with different parts of the musculature: the lateral tract is linked to the limbs, and the anterior tract to the axial and girdle-to-limb musculature (NATHAN ET AL., 1990). Anatomical evidence exists that descending axons from M1 in the lateral corticospinal tract terminate in the spinal motoneuron pools (KUYPERS, 1960; SHINODA ET AL., 1981). Depending on their target muscles, the corticospinal axons ramify into all layers of the spinal grey matter and synapse onto spinal interneurons and, to a smaller extent, directly onto motor neurons. Of the latter, the corresponding somata are situated in the anterior bank of the central sulcus, particularly from the hand and feet representations of the motor cortex. It has been suggested that the corticospinal neurons (CSN), in particular the direct corticomotoneuronal projections, convey dextrous movements, e.g. in precision grip (MUIR & LEMON, 1983).

Several non-primary motor areas of the frontal cortex that are reciprocally connected to M1 contain substantial corticospinal projections and the number of CSNs from secondary motor areas exceeds the number of CSNs in

M1 (DUM & STRICK, 1991; HE ET AL., 1993, 1995). Hence, a substantial, and maybe the largest portion of corticospinal fibres originate in areas 1, 2, 3, 4, 5, and 6 (KUYPERS, 1987). This idea is complemented by the observation that following ablation of area 4, only 30-40% of the pyramidal tract degenerates (LASSEK, 1942). The predominant termination of corticospinal projections from the SMA and the dorsal and ventral cingulate motor area is in the intermediate zone of the spinal cord (BRINKMAN, 1982), which is rich in interneurons projecting to motoneurons and indicates the capability of secondary motor areas to influence spinal activity. These projections presumably regulate sensory inflow rather than control motor function (SCHIEBER, 1999), although their precise function is less well elucidated as for the projections arising from M1.

The cerebral cortex also projects to the spinal cord indirectly via brainstem structures, namely the pontine nuclei and lower brainstem structures (CARPENTER, 1978). Important tracts from subcortical structures to the spinal cord are the tectospinal tract from the superior colliculus, the vestibulospinal tract from vestibular nuclei, the reticulospinal tract from the pons, and the rubrospinal tract from the red nucleus, respectively.

### 1.1.5 The thalamus, basal ganglia, and cerebellum

Not all of the output of cortical motor areas is directed to the spinal cord. Substantial information is relayed to the subcortical structures of the thalamus, basal ganglia, and the cerebellum. These structures have a major contribution in the fine-tuning of motor behaviour, relaying corticocortical information and processing of afferent and efferent information.

**The thalamus.** Almost all information that reaches the cortex is relayed via the thalamus, and as such the thalamus is in an unparalleled position to control information flow to the cortex. Furthermore, the thalamus plays a decisive role in corticocortical communication by controlling information that is directed from one cortical area to another (SHERMAN & GUILLERY, 2002). Efferents from the thalamus project into almost every region and all layers of the neocortex. These projections are organised in a corticotopic manner. The

precentral gyrus and central sulcus receive input from subdivisions of the ventrolateral thalamus. The nucleus ventroposterioris lateralis pars oralis (VPLo) and area X receive input predominantly from the deep cerebellar nuclei (ASANUMA ET AL., 1983; HOLSAPPLE ET AL., 1991) and from ascending somatosensory pathways in the spinal cord (LEMON & VAN DER BURG, 1979). On the other hand, the outputs from the internal part of the globus pallidus (GPi) are relayed via the nucleus ventralis lateralis pars oralis (VLo) and medialis (VLm). Only recently, direct evidence has been established that both cerebellar and basal ganglia outputs project via the thalamus into the hand representation of M1 (HOLSAPPLE ET AL., 1991). The separation of these outputs at the thalamic level is preserved in M1: the strongest input to the rostral aspects of area 4 at the crest of the precentral gyrus originates from the VPLo (JONES ET AL., 1979; HOLSAPPLE ET AL., 1991), while the strongest projections to the hand representation located in the rostral bank of the central sulcus originate in VLo (JONES ET AL., 1979; HOLSAPPLE ET AL., 1991), which also projects to the SMA (WIESENDANGER & WIESENDANGER, 1985).

**The basal ganglia.** The principle components of the basal ganglia are the striatum (caudate nucleus and putamen), the subthalamic nucleus (STN), the globus pallidus (internal, GPi and external, GPe) and the substantia nigra (pars compacta, SNc, and pars reticulata, SNr). This complex arrangement of subcortical structures is involved in a closed cortico-basal ganglia-thalamo-cortical loop in which the basal ganglia do not contain direct peripheral input or output to somatosensory or motor systems. A substantial portion of layer V neurons project to the corpus striatum and globus pallidus, where cortical input terminates in a roughly topographical manner, with somatosensory and motor regions projecting to the putamen and association cortices projecting mainly to the caudate nucleus (JONES ET AL., 1977; PARENT, 1990). Virtually all cortical regions project to the striatum at varying degrees, with somatosensory input being most extensive (GERFEN, 1984; RAGSDALE & GRAYBIEL, 1990). Further input to the striatum stems from the thalamus and STN (PARENT, 1990). The STN, located ventral to the thalamus and rostro-lateral to the red nucleus receives glutamatergic input exclusively from motor

areas M1, PMd, SMA, FEF, and GABAergic input from the GPe (PARENT & HAZRATI, 1995a). The STN and the striatum project to the GPi and SNr, which constitute the predominant output from the basal ganglia. Information is processed in segregated parallel channels in the GPi, while it appears to be intermingled in the SNr (PARENT & HAZRATI, 1995b). Both structures direct GABAergic output to the thalamic relay nuclei, ventral anterior (VA) and ventral lateral (VL), and the brainstem (PARENT & HAZRATI, 1995a). The coarse segregation is still maintained at the thalamic level (ILINSKY & KULTAS-ILINSKY, 1987). These thalamic nuclei in turn project back to distinct frontal premotor cortical areas (ALEXANDER ET AL., 1986), whereas those innervated by cerebellar fibres project back to the motor cortex (ALEXANDER ET AL., 1986; ALEXANDER & CRUTCHER, 1990).

**The cerebellum.** The cerebellum can be divided into three lobes: The floccunodular lobe, located on the inferior surface, the posterior lobe, and the anterior lobe. The latter two are separated by the primary fissure. Information from the cortex, including primary motor, premotor, cingulate, posterior parietal, and prefrontal cortex enters the cerebellum via corticopontocerebellar pathways, comprising excitatory mossy and climbing fibres projecting from the basal pontine nuclei of the pons and the inferior olivary nuclear complex, respectively. The basal pontine nuclei receive information from virtually the entire cerebral cortex, but primarily from cortical somato-motor regions (ALLEN & TSUKAHARA, 1974). The cerebellar three-layered cortex surrounds the deep cerebellar nuclei, which form the output structures of the cerebellum. Each nucleus has a separate somatotopic representation of the body and receives modularly organised input from the cerebellar cortex (VOOGD & GLICKSTEIN, 1998). The deep cerebellar nuclei exert excitatory glutamatergic control over movement of ipsilateral body segments by projecting to the spinal cord, the vestibular, reticular, and red nuclei, the superior colliculus, and inter alia, via the thalamus, the motor cortices and prefrontal area 46. More recent studies furthermore indicate that the dentate regions project to different cortical areas with little overlap, suggesting that each cortical target region receives input from a distinct

dentate output region (MIDDLETON & STRICK, 1998; DUM & STRICK, 2003). As proposed recently, distinct cerebrocerebellar circuits for motor as well as cognitive processing exist (KELLY & STRICK, 2003). The motor circuit predominantly involves cerebellar lobules IV-VI, while for example area 46 of the prefrontal cortex mainly projects to and receives input from crus II of the ansiform lobule.

## 1.2 Functional magnetic resonance imaging

The advent of functional neuroimaging has opened unprecedented opportunities to study the brain *in vivo* and repeatedly. Basically, all functional neuroimaging techniques capitalise on the coupling between cerebral blood flow, neuronal activity and energy utilisation. The discovery of deoxyhaemoglobin as an endogenous contrast agent (OGAWA ET AL., 1990) has proven to be a sensitive indirect marker of neuronal activity. In order to understand the technical problems arising from the combination of TMS and fMRI, as well as the possible mechanisms of TMS-induced changes in cortical haemodynamics, the following section summarises the principles of nuclear magnetic resonance (NMR) and MR imaging. On grounds of parsimony, this will only include the basic concepts and methodology. Several excellent reviews provide an in-depth coverage of the basic mechanisms of NMR (e.g., DE GRAAF, 1998; HAACKE ET AL., 1999; STARK & BRADLEY, 1999).

### 1.2.1 Nuclear magnetic resonance

Nuclei with an odd number of protons and/or neutrons possess an angular momentum or nuclear spin. Therefore, they can be viewed as dipoles, or small magnets, in which the vector representation is termed magnetic dipole moment. These randomly oriented dipoles will line up and precess around the direction of a static magnetic field ($B_0$). Here, using a classical vector model of rotating spins provides a good approximation for the understanding of the basic principles of NMR. Despite the widespread use of this model it should be emphasised that quantum theory is required for full explanation of the topic. The rate of precession is linearly dependent on the external magnetic field strength. This relationship can be expressed in the so-called Larmor-equation:

$$\omega_0 = \gamma B_0$$

$\omega_0$ = resonance frequency in MHz

$\gamma$ = gyromagnetic ratio

$B_0$ = external magnetic field strength (Tesla)

For hydrogen in water molecules, $\gamma 2\pi$ is 42.58 MHz/T, resulting in precession frequencies $\upsilon$ of ~84 MHz at 2.0T and ~127 MHz at 3.0T, respectively.

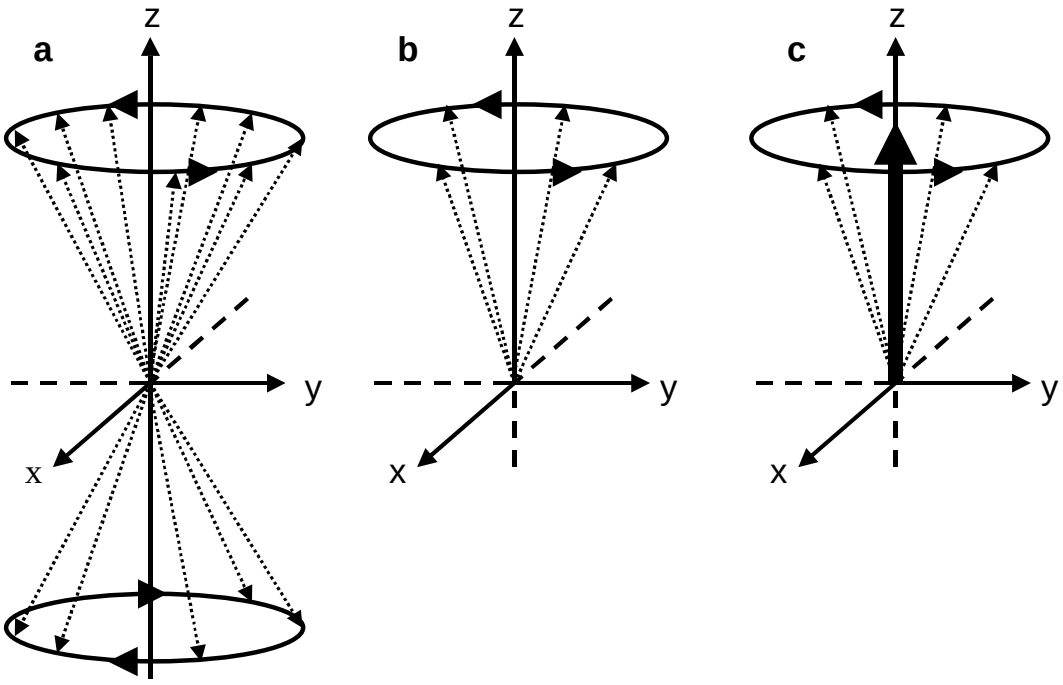


**Figure 1.3.** Principle of longitudinal magnetisation. Within a static magnetic field, the number of parallel oriented protons exceeds the number of anti-parallel oriented protons. **(a)** The fractional excess of parallel protons **(b)** exert also a magnetic moment along the *xy*-dimension. As their precession is incoherent, only a component oriented with the static magnetic field remains, termed longitudinal magnetisation **(c)**.

The most abundant isotope $^{1}H$, which is the most important for MRI, has a spin $I=\frac{1}{2}$. Within a static magnetic field, there are two states of rotating spin vectors: a parallel (lower energy level) and an antiparallel (higher energy level) orientation to the static field, also referred to as Kern-Zeeman-levels. In addition, there are magnetic forces along the *x* and *y* direction. Because all protons precess at different phases, these forces cancel out each other so that only the component aligned with $B_0$ remains, the so-called longitudinal magnetisation. NMR cashes in on the fractional excess of the population in the lower energy level (which is about 1/100 000 at 1.5T) and reflects the frequency-specific excitation produced by transitions between the two energy states (Figure 1.3). As can be seen from Figure 1.4, this ratio is changed when

energy is transmitted into the system: more protons will now be oriented in anti-parallel direction.

For MR-imaging, a radiofrequency (RF) pulse at the Larmor frequency and orthogonal to $B_0$ (i.e. in *xy*-direction) is applied to excite the nuclear spins that precess at the same frequency along $B_0$ and are phase-coherent with the RF-pulse. Formally this process can be described as

$$\mathbf{B_{RF} = 2B_1 \cos(\omega t)}$$

$B_1$ = electromagnetic field amplitude

$t$ = time

Furthermore, magnetisation is passed into the transverse ($B_{xy}$) plane as a result of synchronisation of precessing spin moments following RF-pulse application (Figure 1.4). In general, the magnetisation can be rotated by any angle $\alpha$, which is dependent on the duration $\tau_P$ and amplitude $B_1$ of the RF pulse and can be expressed as

$$\alpha = \gamma \int_0^{\tau_P} \mathbf{B_1(t)\, t}$$

As such, a 90° excitation pulse refers to the complete transition of longitudinal magnetisation into the transverse (*xy*) plane.

The energy emitted at return into equilibrium in form of a rotating vector reflects an RF-signal which can be received by an antenna. This signal contains a constant frequency, because the vector rotates at the precession frequency and decreases over time as the transversal magnetisation decays.

### 1.2.2 Relaxation and image contrast

In principle, NMR relaxation measures the return of perturbed nuclear spins into thermal equilibrium after RF energy transmission (HOWSEMAN & BOWTELL, 1999). Upon termination of the RF pulse, the return into equilibrium involves two processes: return of longitudinal magnetisation and disappearance of transverse magnetisation. Although both processes occur at the same time, they reflect independent mechanisms and hence exhibit different time

constants, termed longitudinal or spin-lattice relaxation time ($T_1$) and transversal or spin-spin relaxation time ($T_2$).

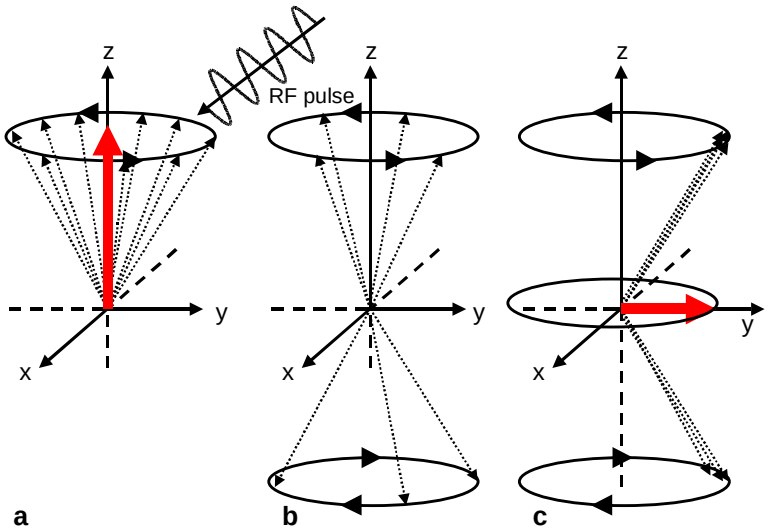


**Figure 1.4.** Principle of transverse magnetisation. Energy transmission via an RF pulse at the resonance frequency **(a)** leads to energy absorption, transferring more protons into an anti-parallel orientation **(b)**. At the same time, precessing spins synchronise to the phase of the RF-pulse, inducing a magnetisation in the *xy*-direction **(c)**.

These contrasts are important in biological tissue as the number of spins that contribute to the transverse magnetisation within a probe determine the proton spin density. Because water is the most abundant molecule in biological tissue, the proton spin density is primarily determined by the water concentration.

The $T_1$-relaxation falls off exponentially within the return of the longitudinal *z*-magnetisation $M_z(t)$, which is directed along the static $B_0$ field. Spin-lattice relaxation occurs as a consequence of interactions of the excited nuclear-spin dipoles and random fluctuating magnetic fields in surrounding tissue. The source of these fields is movement of surrounding dipoles in the lattice fluctuating at the resonance frequency. As such, the spin-lattice $T_1$-relaxation is defined as the time constant

$$\mathbf{M_z(t) = M_0 - (M_0 - M_z(0)) \exp\left(-\frac{t}{T_1}\right)}$$

that describes the return of equilibrium magnetisation $M_0$, where $M_z(0)$ describes the magnetisation along the *z*–axis immediately following excitation. The degree of this relaxation is determined by the proximity

between the frequency of this fluctuation and the Larmor frequency. $T_1$ relaxation involves energy transmission between Kern-Zeeman-levels and therefore the energy state of the spin system is changed. Medium-sized molecules, e.g. lipids, are closer to the Larmor frequency of most static fields used in neuroimaging and hence relax relatively fast. Depending on their composition, different tissues differ in their $T_1$-values, providing the basis for $T_1$-weighted imaging.

The $T_2$ relaxation reflects the spin dephasing in the *xy*-plane and is mediated by interactions of the moving spins (Figure 1.5). In this process, energy is transferred within the spin system. As any energy transition of a nucleus induces local field changes at neighbouring nuclei, the frequency of the proton precession is altered, leading to a loss of RF-induced phase coherence and finally in transverse magnetisation. $T_2$ is defined by

$$\mathbf{M_{x,y}(t) = M_{x,y}(0) \exp(-\frac{1}{T_2})}$$

as the time constant describing the loss of transverse magnetisation ($M_{x,y}$).

$T_2$ is long for small and short for larger molecules. Consequently, the $T_2$ contrast in most biological tissues is almost inverted to the $T_1$ contrast: while the white matter is brighter than grey matter in $T_1$-weighted imaging, the opposite is the case for $T_2$-weighted imaging.

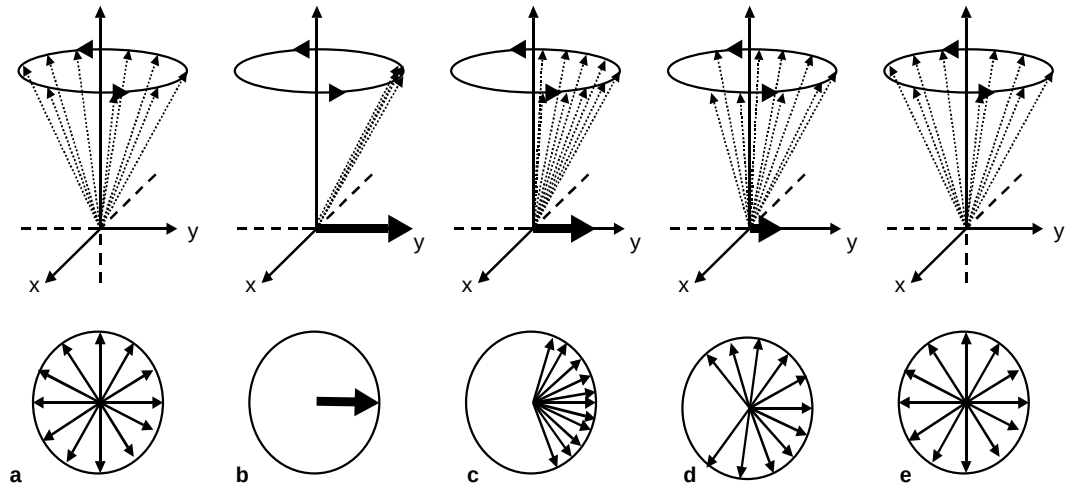


**Figure 1.5.** Transverse relaxation. The gradual loss of phase coherence **(a-e)** is explained by energy transmission between protons. While the energy of the system remains constant, the phase coherence between protons is gradually destroyed.

In biological probes, the $T_2$ relaxation is faster than expected from theoretical considerations. This is constituted by the lack of completely homogenous magnetic fields in experimental settings. Here, the occurrence of local magnetic field inhomogeneities and inhomogeneities due to the application of field gradients required for imaging inevitably leads to additional dephasing of magnetisation. The empirical $T_2^*$ time is therefore faster than the theoretical $T_2$ time and can be expressed as

$$\frac{1}{T_2^*} = \frac{1}{T_2} + \frac{1}{2T_1} + \gamma \Delta B_o + K$$

Typical $T_1$ relaxation times for protons in the brain at 2T are in the order of 1500 ms. By contrast, $T_2$ relaxation times are between 140-400 ms, and $T_2^*$ relaxation times are in the order of 50-100 ms.

### 1.2.3 Basic principles of functional MR-imaging

The use of linear-field gradients on the main static field allows reconstruction of the projections of an object. It is imperative for so-called Fourier imaging that $B_0$ is modulated rapidly and precisely in all three dimensions by these gradients. A gradient refers to the dynamic change of the magnetic field along a specific dimension. These gradients determine a range of Larmor frequencies which in turn provide accurate spatial information. For MRI, the spatial information is encoded by slice-selecting gradients ($G_{ss}$), frequency-encoding gradients ($G_{fe}$) and phase-encoding gradients ($G_{pe}$), respectively. Along the direction of each gradient, the resonance frequency of respective spins is increased, extending the Larmor equation to

$$\omega_0(x) = \gamma B_0 + x \gamma G_s$$

For the selection of a desired compartment of a probe (slice), a frequency-selective RF pulse (usually an amplitude-modulated RF pulse with a sinc function) is applied in conjunction with a field gradient perpendicular to the desired slice. The RF pulse of the bandwidth $\Delta\omega$ will excite only spins precessing at the frequencies within the frequency range of the RF pulse. Thus, the RF pulse is used to excite the biological tissue within this slice (Figure 1.6), i.e. perpendicular to the slice selection gradient.

The slice thickness Δr is determined by

$$\Delta r = \frac{\Delta\omega}{\gamma G_{ss}}$$

As sketched in Figure 1.6, the position and thickness of a slice can be determined by $G_{ss}$ and the bandwidth of the RF pulse, respectively.

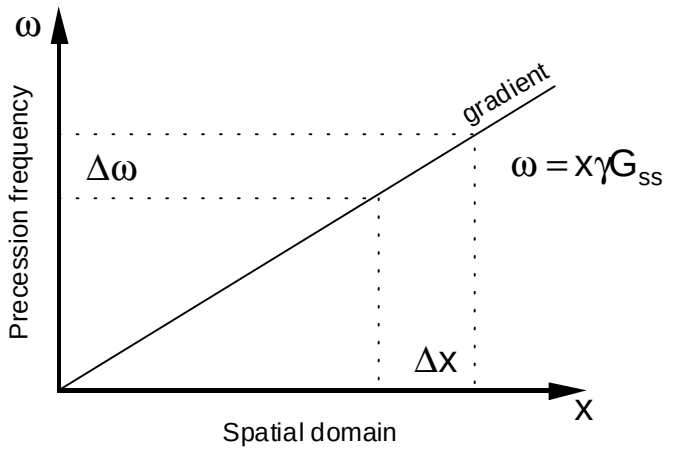


**Figure 1.6.** Schematic of the principle of slice-selective excitation. The application of the slice-selective gradient $G_{ss}$ makes an RF pulse of a defined frequency and bandwidth Δω spatially selective to excitation of a slice Δx.

The other orthogonal gradients are used to extract spatial information from within that slice. The readout gradient ($G_{fe}$) is applied when the MR data is acquired, while the phase-encoding gradient ($G_{pe}$) is used to encode the second spatial dimension in the picture plane. To acquire an image of $N_{fe}$ x $N_{pe}$ picture elements (pixels), $N_{fe}$ points will be sampled with the same read-out gradient $G_{fe}$, and $N_{pe}$ increments of the phase-encoding gradient $G_{pe}$ will be conducted. During each readout iteration, the acquired signal is comprised of the same frequencies which differ in their phase, as determined by the phase-encoding gradient. The $N_{fe}$ x $N_{pe}$ data matrix, which is commonly termed *k*-space, represents the desired image in the inverse spatial domain. Using Fourier transform to extract the amplitudes of each row of the data matrix and the phase angles of the frequency components for every column finally results in the desired image.

Volume coverage is acquired by repetition of the image acquisition process at different slice positions. The acquisition time is determined by the product

of the number of brain sections and the time between slice excitations (usually reflecting the time needed to record a single section). The time between repeated acquisitions of the same slice is termed repetition time (TR). This time also determines the effect of $T_1$ relaxation on image intensity. Short TR values result in a reduced signal and furthermore increase the likelihood of occurrence of in-flow effects related to $T_1$-relaxation.

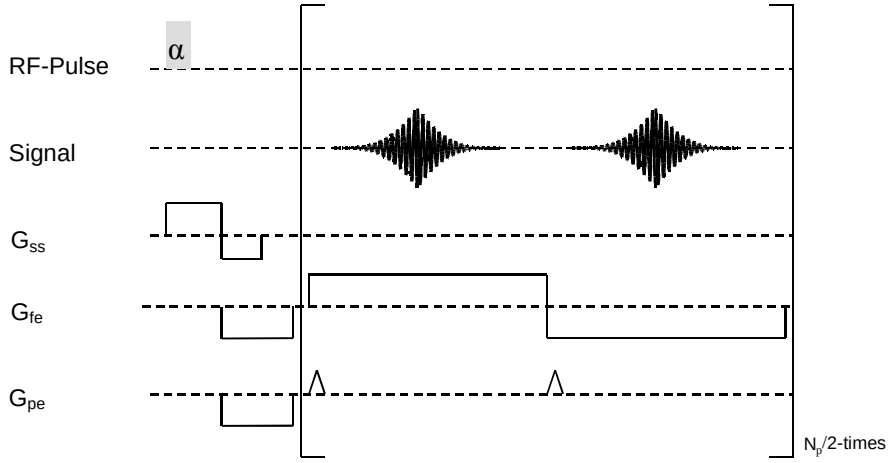


**Figure 1.7.** Schematic of a echo-planar imaging (EPI) gradient-echo sequence. For details see text.

The most common technique for functional MRI is echo-planar imaging (EPI), as originally proposed by PETER MANSFIELD (1977). With EPI, an entire image can be obtained using a single excitatory RF pulse (Figure 1.7). This is because EPI collects a complete data set within the short time during which the FID can be measured, which is normally limited by $T_2$*. As dephased spins are refocused with use of a sign-reversed magnetic gradient rather than by additional RF pulses, it is also called gradient-echo EPI. An oscillating gradient along the readout direction generates a train of echoes of the NMR signal, which are progressively phase-encoded by application of an additional orthogonal gradient. The latter gradient reflects a series of so-called 'blips' which coincide with the zero crossings of the switched gradient. Along the phase-encoding direction, the short 'blips' advance the encoding to the next *k*-space line. A bidirectional scheme is most commonly applied, i.e. scanning even and odd lines from left to right and vice versa (Figure 1.8). Within this scheme the effective echo-time (TE) is defined from the slice excitation pulse

to the acquisition of the *k*-space centre. The magnitude of the data from the center of *k*-space constitutes the image contrast while the data obtained from the periphery of *k*-space mainly defines the high-frequency domains of an image, i.e. the contours.

Using EPI, images may be acquired within 50 ms or less, mainly depending on the desired resolution, the gradient system, and the requirement to avoid peripheral nerve stimulation. In comparison to conventional fast gradient-echo techniques, EPI offers an increased signal-to-noise ratio (SNR) and a high temporal resolution as more time is provided for recovery of longitudinal magnetisation, which diminishes signal saturation and increases SNR. In addition, the intrinsic $T_2$*-weighting of gradient echo EPI images automatically reveals the required sensitivity to blood oxygenation changes.

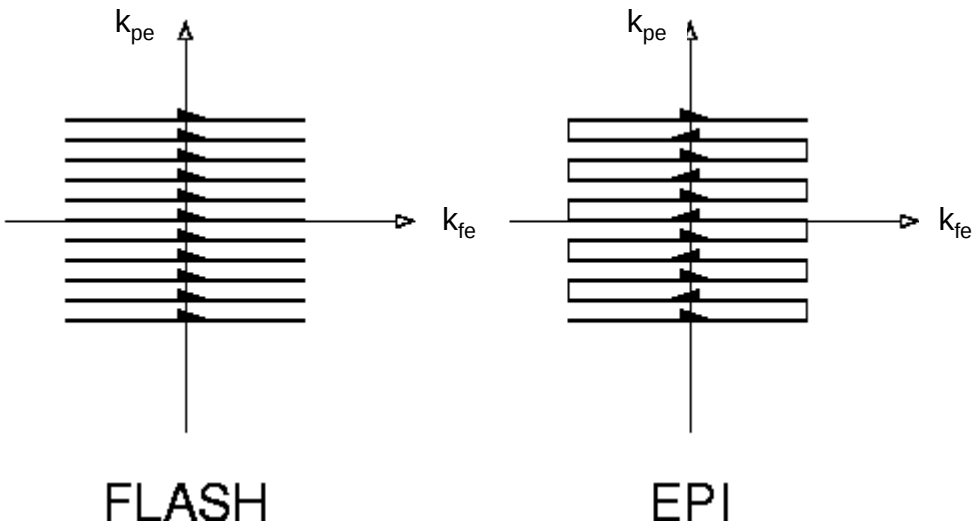


**Figure 1.8.** Pictorial comparison of the acquisition trajectories in *k*-space of FLASH and EPI techniques. In FLASH imaging which is commonly used for anatomical imaging, one line in *k*-space is sampled after each RF-excitation (gradient echo). By generating multiple gradient echoes with incremented phase-encoding gradients, EPI allows for sampling of several lines in *k*-space following a single RF-excitation. $K_{fe}$: frequency-encoding direction in *k*-space, $k_{pe}$: phase-encoding direction in *k*-space.

Evidently, detection of relevant physiological signal depends on SNR and contrast-to-noise ratio (CNR). Both are determined by the relaxation times, flip angle, repetition time, and number of repetitions. In addition, technical factors such as the RF coil, receiver noise levels, gradient switches, and resonant input circuits influence the measurement.

### 1.2.4 The BOLD contrast

The elegance of fMRI undoubtedly stems from its capability to capitalise on a contrast agent inherent to all endothermal animals: the microscopic magnetic local field inhomogeneities induced by the endogenous haemoglobin of red blood cells.

The major part of blood oxygen is bound to haemoglobin (Hb). This macromolecule is composed by two polypeptide chains, each of which is bound to an iron-protoporphyrin complex. As the blood is transported from the oxygen-rich arterial side to the oxygen-low venous side of the capillary bed, oxygen dissociates from Hb and supplies the surrounding tissue. Functional MRI utilises $T_2$*-sensitive imaging sequences which are susceptible to changes in blood oxygenation levels. Oxygenated haemoglobin ($Hb_{ox}$) is diamagnetic and has little impact on an external magnetic field and therefore on the phase coherence of proton spins. This low-spin state of the iron molecule ($Fe^{2+}$) is precipitated by donation of the oxygen's electrons. On the other side, susceptibility changes in the neighbourhood of paramagnetic deoxyhaemoglobin ($Hb_{deox}$) cause local magnetic field variations, which in turn result in increased spin-dephasing and a decreased MR signal (OGAWA ET AL., 1990; TURNER ET AL., 1991). This is because the paramagnetic high-spin state of $Hb_{deox}$, which is due to the four unpaired outer electrons of $Fe^{2+}$ functions as a paramagnetic agent. The so-called blood-oxygenation-level-dependent fMRI exploits this endogenous imaging contrast that renders the use of external contrast agents obsolete and allows for an unlimited number of measurements in a single subject.

Figure 1.9 summarises the hypothesised relationship between cerebral blood volume, cerebral blood flow, perfusion and BOLD contrast. In the resting state, the energy demand of the brain is predominantly provided by oxidative metabolism and regional CBF: the cerebral metabolic rate of glucose utilisation and the cerebral metabolic rate of oxygen are intimately coupled (SOKOLOFF, 1978; YAROWSKY & INGVAR, 1981). It is assumed that changes in neuronal activity lead to a higher rate of energy metabolism in the

corresponding tissue. A concomitant increase in vasodilatation of the capillary bed supports this increased energy demand, hence providing glucose and oxygen to the area of increased activity and, consequently, an increase in rCBF and regional cerebral blood volume (rCBV). However, the very much pronounced increase in rCBF overcompensates the elevated oxygen consumption and therefore results in an excess $Hb_{ox}$ concentration on the venous side of the capillary bed, which decreases the $Hb_{deox}$ content in the surrounding tissue. Since a reduced $Hb_{deox}$ concentration attenuates local susceptibility effects, the respective regions reveal increased signal intensity in $T_2$*-weighted MR images.

A caveat is given by the inevitable contribution of draining veins, which can be centimetres away from the neuronal site of activity (FRAHM ET AL., 1994; KIM ET AL., 1996) and the fact that the close relationship between neuronal activity and blood flow tends to diverge during mental activity (e.g., VAFAEE ET AL., 1998, 1999; VAFAEE & GJEDDE, 2000). Empirical data suggests that the increase in oxygen use may depend on the specific context under which neurons are active, and that stimuli imposed on brain tissue have to exceed a certain threshold before glycolysis is augmented by increased oxidative metabolism (VAFAEE ET AL., 1999).

The measurement of the BOLD effect is relatively straightforward when using common gradient echo sequences, yet the quantitative interrelation between signal changes and haemodynamic and metabolic parameters is a complex one. Because many voxels contain rather heterogeneous distributions of vessels, the underlying vascular geometry and distribution of $Hb_{deox}$ is not easily modelled and therefore the BOLD contrast provides a more qualitative rather than quantitative measure of cortical activity (HOWSEMAN & BOWTELL, 1999; LOGOTHETIS, 2003). For example, typical fMRI experiments utilise linear voxel resolutions of 2-3 mm, which inevitably contain small capillaries (5 µm diameter), venules (up to 30 µm), and pial veins (up to 400 µm), and even larger draining veins. Moreover, it is important to note that the observed signal changes are relative to the background task in that any inferred activation needs to be described relative to the cognitive background level.

Several authors have argued that large signal changes in $T_2$*-weighted images may occur when a substantial fraction of a voxel contains large vessel components. This in turn results in bulk phase changes occurring in the vessel during activation (FRAHM ET AL., 1994; HOWSEMAN ET AL., 1999). Although several strategies exist to discriminate signal contributions from larger vessels (BOXERMAN ET AL., 1995; LEE ET AL., 1995), they still represent a major confound of functional MRI.

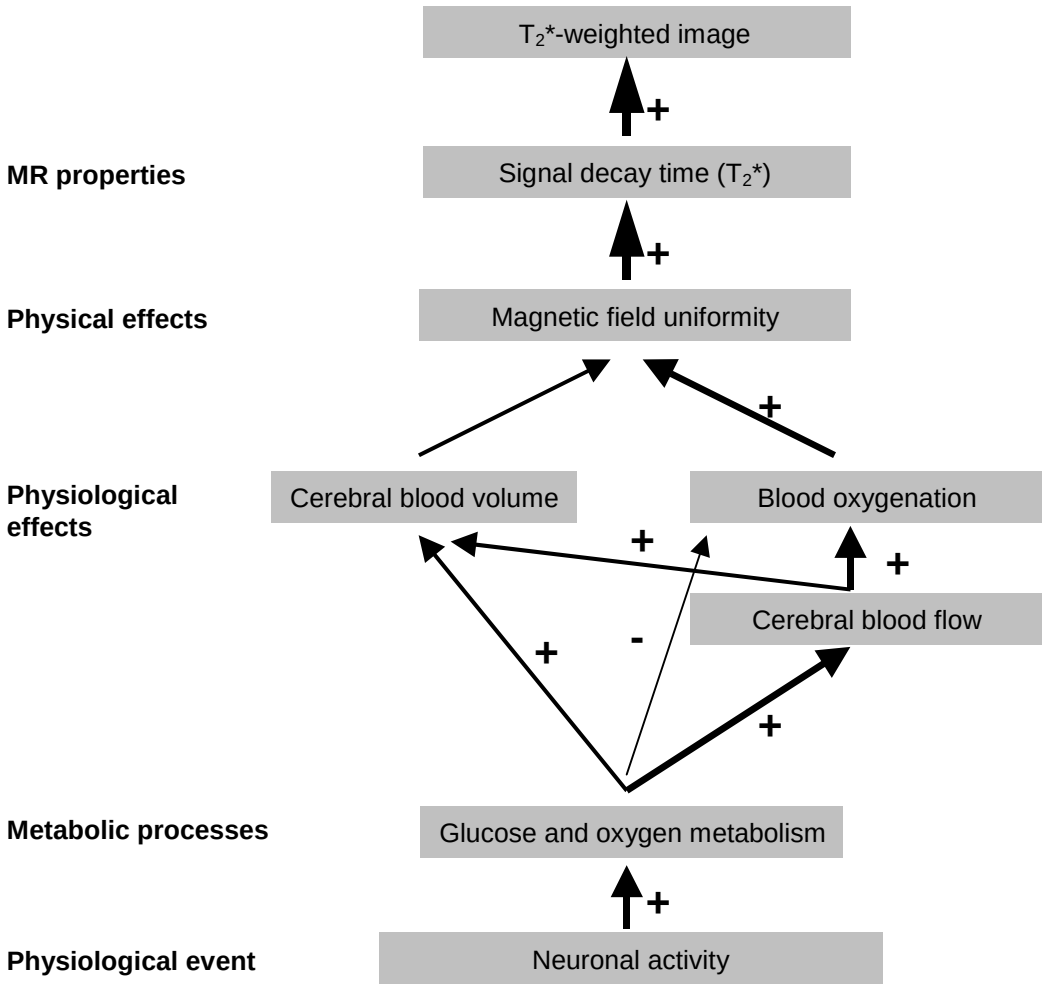


**Figure 1.9.** Illustration of the hypothesised neuro-vascular coupling in the brain. Plus signs indicate positive influence, minus signs indicate negative influence on subsequent stages. The importance of the relationship between two components is expressed by the thickness of the arrows. For details, see text.

**The physiological basis of the BOLD signal.** In functional MRI, regional changes in brain activity are inferred from the obtained changes in local haemodynamics. In most studies, this relationship is simply accepted and often BOLD signal changes are even regarded as a direct measure of cortical

activity. However, there are considerable lacunae in our knowledge regarding the exact coupling between neuronal activity and the subsequent haemodynamic response. Several studies have convincingly shown that the relative importance of neuronal firing and synaptic activity is profoundly different. For example, when simultaneously recording single-unit activity in the rat cerebellar cortex, an increase of both local field potentials (LFP) and CBF during electrical stimulation of parallel fibres known to inhibit the spontaneous firing rate of Purkinje cells can be observed (MATHIESEN ET AL., 1998). The local field potential is a weighted average of dendrosomatic pre- and postsynaptic currents, which contains dendritic spikes or activity of small interneurons and hence predominantly reflects the input to and the local processing in, rather than the output from a given area. The strong correlation between the summed field potential and increased CBF implies that postsynaptic activity is the driving force for changes in cortical haemodynamics and hence the BOLD signal (MATHIESEN ET AL., 1998, 2000; LAURITZEN, 2001; NIELSEN & LAURITZEN, 2001; LAURITZEN & GOLD, 2003).

Earlier high-field fMRI studies of the rat have already indicated that regional CBF changes preferably occur in layer IV of the cortex and thus presumably are co-localised with the neuronal assemblies associated with the input signal processing (YANG ET AL., 1996). Electrophysiological recordings from the visual cortex of the monkey *during* fMRI support the above results. Here, the local field potential provided a better estimate of the BOLD response to visual stimulation than multiunit activity. The latter only transiently increased after stimulation onset while the former was sustained during the whole stimulation period (LOGOTHETIS ET AL., 2001).

The dominant source for BOLD MRI signal changes is presumably stemming from excitatory neuronal activity. At present, the contribution of inhibitory neurons is less well elucidated. Inhibitory activity requires energy, and thus predicts a BOLD response. However, only about 10-20% of cortical neurons are inhibitory (ARTHURS & BONIFACE, 2002), and these make far fewer synapses than excitatory neurons that furthermore have a lower metabolic

demand for restoration of post-synaptic currents (LAURITZEN, 2001; ARTHURS & BONIFACE, 2002; ATTWELL & LAUGHLIN, 2001).

There is less consensus regarding the mediators of the neurovascular response. It is generally accepted that nitric oxide (NO) has an important role in triggering haemodynamic responses (AKGOREN ET AL., 1996; ATTWELL & IADECOLA, 2002). Recent data suggests, however, that stimulation of different afferent inputs even within the same brain region may utilise different mediators of vasodilation (AKGOREN ET AL., 1997), and the direct involvement of neurotransmitters, astrocytes, or ion-flux is also believed to contribute to the control of haemodynamics in the brain (MAGISTRETTI & PELLERIN, 1999; SOKOLOFF, 1999; LAURITZEN, 2001).

### 1.2.5 Spatial and temporal resolution

Functional MRI commonly utilises a spatial resolution of 1-8 mm in either dimension, depending on the desired slice thickness, the number of phase and frequency-encoding steps, and the imaged field-of-view (FOV). As the expected signal changes in fMRI are relatively small (1-5% at 1.5T), a high SNR is required for reliable signal detection. When spatial resolution is increased (and voxel size decreases), the MR signal in each voxel decreases while the electronic noise in each voxel remains relatively constant, and consequently SNR is reduced. At low spatial resolution, the convoluted structure of brain tissue can introduce so-called partial volume effects into functional data. Although large voxel sizes provide an excellent SNR, they are likely to contain both active and inactive brain tissue which reduces the relevant physiological signal significantly. By increasing the scanning time per section, an increase in spatial resolution is at the expense of temporal resolution and spatial volume coverage.

Although the temporal characteristics of the BOLD response may not be ubiquitous throughout the brain, some general features can be described. A short initial (and controversially debated) decrease of approximately 1 s (MENON ET AL., 1995; HU ET AL., 1997) is followed by a BOLD MRI signal increase peaking between 4-8 s after onset of stimulation (MENON ET AL.,

1995; FRANSSON ET AL., 1998b, 1999a) and finally results in a modest undershoot before return to baseline (FRANSSON ET AL., 1998a; FRANSSON ET AL., 1999b). Therefore, the delay of the haemodynamic response is in the range of several seconds and significantly longer than the tens to hundreds of milliseconds of actual neuronal activity. Following the peak of the haemodynamic response, a return to baseline levels is achieved after 10-60 seconds, depending on the stimulation period. Consequently, the BOLD response is an indirect measure of neuronal activity that furthermore has a temporal and spatial resolution several times lower than the underlying neuronal event.

Although an uncoupling of flow and metabolism has been proposed following prolonged stimulation periods (FRAHM ET AL., 1996; KRUGER ET AL., 1996), this has not invariably been confirmed (BANDETTINI ET AL., 1997; HOWSEMAN ET AL., 1998). This incongruity presumably relates to the fact that transient responses are found in large vessels while sustained responses appear to occur in cortical grey matter (CHEN ET AL., 1998). In general, there is consensus that a model of the expected activity can be generated by convolution of a haemodynamic response function and the experimental design, despite apparent non-linear components of the response at very low or high levels of stimulation (FRISTON ET AL., 1998). Assuming an ubiquitous haemodynamic response, a temporal resolution below the sluggish haemodynamic response can be achieved by convolution with the expected haemodynamic response function. However, non-linearities of that response increase variability in the haemodynamic response latency, and are the main limiting factor rather than the haemodynamic response delay itself.

### 1.2.6 Artefacts of functional MR images

One of the most derogating problems of $T_2$*-weighted imaging is the sensitivity to macroscopic field inhomogeneities as found at the air, tissue and bone interfaces. The problems occur since different media occupy differences in magnetic susceptibility. All anatomical structures of the head are "contaminated" by these resulting localised magnetic field gradients. The air-

filled sinuses near the frontal pole, the complex structures at the inferior temporal lobes, the petrous bone, and the air passages located near the cerebellum and the ear pose particular problems. As a result of localised field gradients, spin dephasing and consequently an unwanted relocation of signal due to the additional magnetic field gradient occurs. An additional source of profound image distortions is the long read-out time of EPI images after each single RF excitation. In this connexion, the shape of the image distortion is dependent on the orientation of the phase-encoding gradient of the acquired images.

A further image artefact inherent to EPI is the so-called Nyquist ghosting that appears as a low intensity image halfway across the image field of view. This artefact arises because the odd and even echoes need to be reversed with respect to each other as a result of the polarity reversal of the imaging gradients. Several factors contribute to this reversal: imperfect timing, eddy currents, nonlinearities in the receiver filters, and field inhomogeneities (SCHMITT ET AL., 1998). The generation of very large currents through the system's gradient coils which are likely to lead to substantial image distortions is considered one of the biggest disadvantages of EPI.

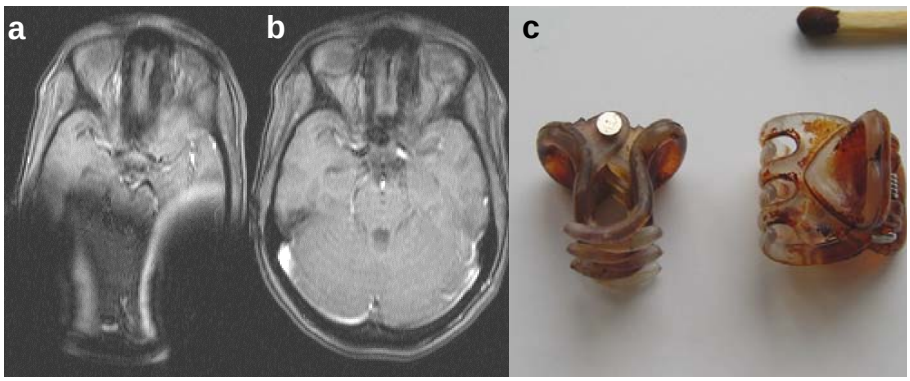


**Figure 1.10. (a)** T1-weighted anatomical image exhibiting severe distortions and **(b)** the same image section without distortions. Imaging artefacts were caused by ferromagnetic bolts of hair-clips of the subject **(c)**. This example illustrates the necessity for non-ferromagnetic TMS probes in order to allow for unperturbed MR-imaging.

Severe image distortions occur due to increased inhomogeneity of the static field by large probes, e.g. the human head. Taking safety issues aside, ferro-

magnetic materials within the MR environment generally foreclose successful imaging (Figure 1.10).

Motion artefacts have bedevilled fMRI from early on and occur when the subject moves during the data acquisition period. Even head motions of a fraction of a pixel during data acquisition can produce substantial signal fluctuations in the signal time course (HAJNAL ET AL., 1994). This artefact is often elevated at pixel boundaries, in particular when occurring in synchrony with the experimental paradigm, where signal intensities are drastically different and are often congregated around the edge of the brain, because here the contrast borders are much stronger than between grey and white matter and cerebrospinal fluid (CSF) within the brain. Although movement correction algorithms can partly adjust for motion artefacts, they may fail to detect signal changes related to stimulus-correlated movement. For example, they cannot account for movements across slices that may result in double excitation, or omission of excitation of brain sections. In-plane movement may lead to phase-shifts that become translated into false image reconstructions. These movements can lead to entirely false-positive activations as signal intensity changes will be highly correlated with the respective comparison specified in the analysis (HOWSEMAN & BOWTELL, 1999). Therefore, images should be inspected for activations at sharp image boundaries, which often indicate such confounding activations.

## 1.3 Transcranial magnetic stimulation

The advent of a variety of new non-invasive brain mapping techniques have yielded new insights into the functional organisation of the human brain. As one of these techniques, TMS has been successfully used to study cortical excitability, plasticity, connectivity and functional organisation of the human brain (PASCUAL-LEONE ET AL., 1999; ZIEMANN & ROTHWELL, 2000; COWEY & WALSH, 2001; WALSH & COWEY, 2000; SIEBNER & ROTHWELL, 2003). The main advantage of TMS, which distinguishes it from all other neuroimaging techniques, is its capability to non-invasively stimulate the cortex via the intact scalp at high temporal resolution (~1 ms). It therefore allows for an active modulation of neuronal activity and excitability in defined cortical networks (ROTHWELL, 1999). In the following section, the basic principles of TMS as well as important experimental findings relevant to the present work will be reviewed.

### 1.3.1 Basic principles

TMS is based on the principle of electromagnetic induction which was originally discovered by Michael Faraday at the Royal Institution in 1831 and later applied to neuroscience research by Barker and colleagues (BARKER ET AL., 1985). The method utilises a time-varying magnetic field to induce electrical currents in conducting tissue (JALINOUS, 1991). It is the magnetic field used to induce a current which distinguishes TMS from transcranial electrical stimulation (TES). This has coined the name transcranial *magnetic* stimulation, despite the fact that it is the induced current that stimulates cortical tissue and not the magnetic field. The magnetic field is generated by passing a very brief (approximately 250 µs) and high-current electrical pulse (up to 8000A) through a wired coil placed over the scalp. This field can reach up to 2.5T under the surface of the coil but decays by the square of the distance from the coil (Figure 1.11). The field is oriented perpendicular to the coil and in turn induces an electrical current parallel to the plane of the coil in any conductive medium (Figure 1.11). An apparent advantage of TMS is the

low impedance of the skull to the penetration of the magnetic field because it allows painless induction of eddy currents in the brain. Following Lenz's law, the induced current will flow in opposite direction to the current in the stimulating coil. The rate of change of the induced magnetic field determines the size of the induced current: it is proportional to the rate of change of the magnetic field, which again is directly proportional to the rate of change of the electrical current passed through the coil (Figure 1.11). Given that appropriate stimulation parameters are chosen, the induced electrical currents are capable to depolarise cortical neurons and generate action potentials (APs) (ROTHWELL ET AL., 1999).

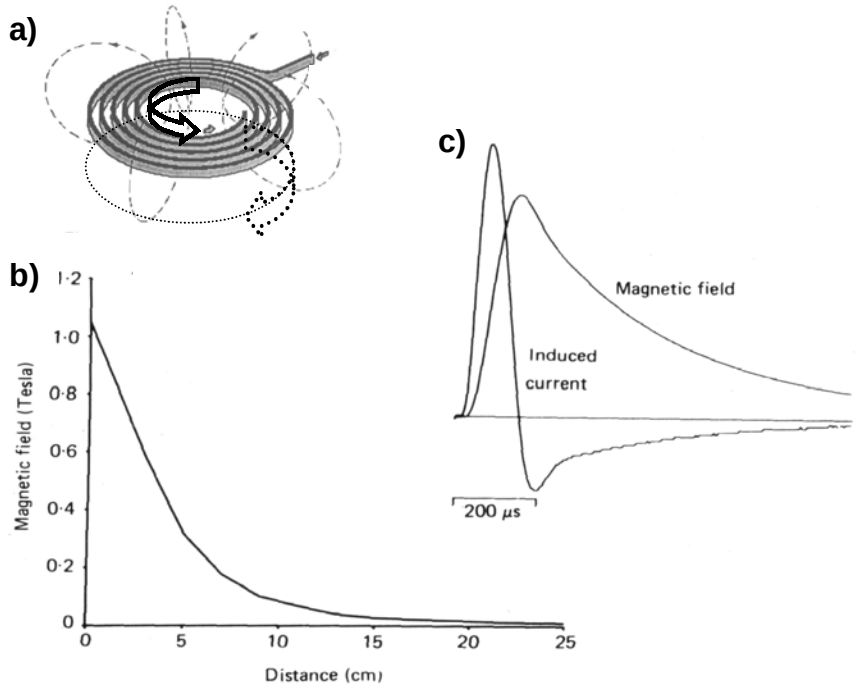


**Figure 1.11.** Principle of TMS. **(a)** A high electrical current (up to 8000 A) is passed through a stimulating coil, inducing a perpendicular magnetic field that in turn induces an electrical current in a conductive medium with an opposite direction of current flow. The induced magnetic field falls off almost exponentially with the distance from the coil **(b)**. The induced current in a conductive medium is dependent on the rate of change and amplitude of the magnetic field **(c)**.

While round coils induce a circular magnetic field under their surface, which in turn generates a perpendicular electric current of the same geometry in conductive tissue (Figure 1.11), the so-called figure-of-eight coil has a more complex magnetic field geometry (Figure 1.12). In general, these coils consist of two round coils with an overlapping intersection in the middle. They are

wound in such a manner that the currents in the two loops circulate in opposite directions and therefore sum up at the intersection. The induced magnetic field is approximately twice as strong at the intersection as compared to the outer wings of the coil and therefore allows more focal stimulation. With a standard figure-of-eight coil, the stimulated region covers approximately 4 cm and therefore is likely to stimulate a corresponding region in the brain. It is important to note that while the induced magnetic field can be easily calculated using the Biot-Svart law, the complex conductivity profile of the human brain does not allow for an accurate calculation of the induced electric field (THIELSCHER & KAMMER, 2002). However, inferences can be made regarding the "functional" effectiveness of stimulation even without detailed knowledge of the exact induced current.

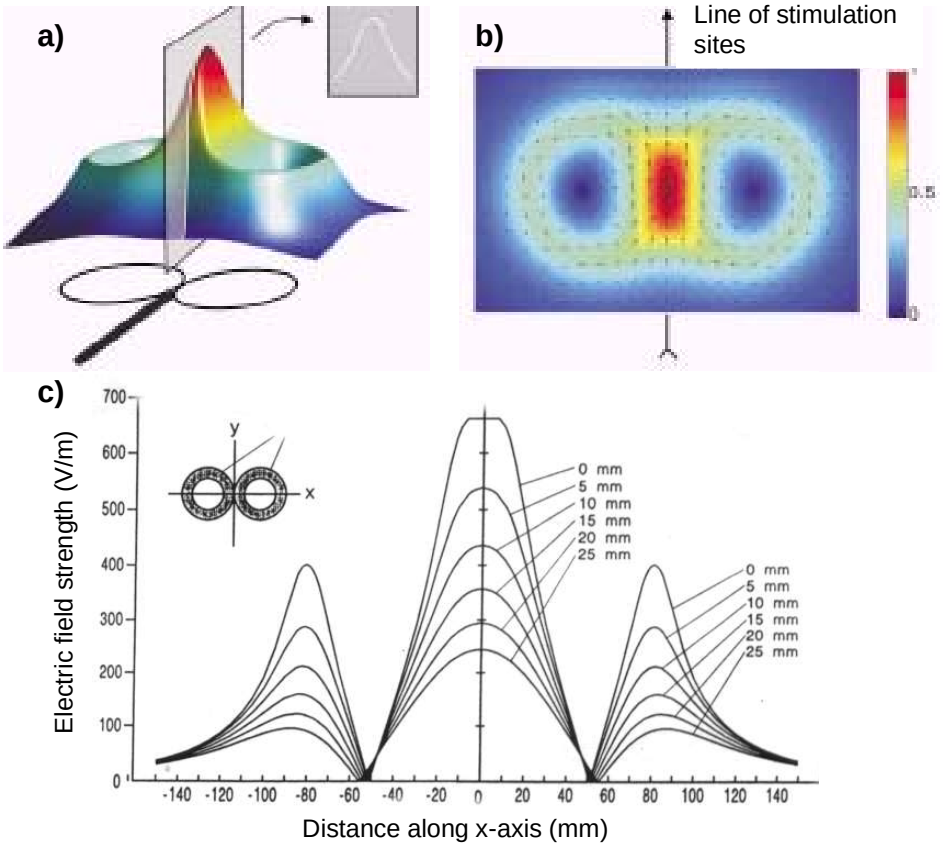


**Figure 1.12. (a)** Spatial characteristic of an induced magnetic field of a standard figure-of-eight coil (The Magstim Company) calculated on a plane 1 cm above the coil plane. The induced field strength is coded as both colour and height. The highest intensity occurs at the intersection of the two round coil wings. **(b)** Two-dimensional depiction of the magnetic field strength in the same plane as the TMS coil. Adapted from *Thielscher A & Kammer T (2002) Neuroimage* ***17:****1117-1130.* **(c)** Induced electric field profile for a standard figure-of-eight coil. Adapted from *Jalinous R (1991) J. Clin. Neurophysiol.* ***8:****10-25.*

### 1.3.2 Stimulation characteristics

The effects of TMS on the cortex are dependent on a number of factors. These critically influence the efficacy, the localisation and the physiological modulation exerted by the stimulation. These parameters are constituted by the pulse intensity, pulse amplitude, pulse waveform and duration, and pulse frequency (JALINOUS, 1991; BRASIL-NETO ET AL., 1992). In addition, the induced magnetic field, and hence the induced electrical field is influenced by the geometry, size and orientation of the coil (JALINOUS, 1991; BRASIL-NETO ET AL., 1992; TROMPETTO ET AL., 1999; DI LAZZARO ET AL., 2002), skull shape and skull thickness, cortical anatomy, especially the orientation of the stimulated neurons (ROTHWELL, 1997), the coil-tissue distance (JALINOUS, 1991), and the temperature of the conducting medium (MACCABEE ET AL., 1998).

In principle, stimulation of cortical and subcortical tissue can be achieved approximately 2-3 cm away from the coil, although larger coils and high intensities may be even more effective (HARMER ET AL., 2001). This also illustrates that effective stimulation under the coil wings may occur under certain circumstances, thus rendering some forms of supposed sham-stimulation ambiguous (LOO ET AL., 2000; LISANBY ET AL., 2001). Furthermore, possible activation of adjacent brain regions at high stimulation intensities have to be taken into account and carefully monitored.

The spatial resolution of TMS has been estimated in the range of 1 cm. It is important to stress that this does not imply exclusive stimulation of the cortex within a 1 cm region; it rather indicates that differential effects of stimulation can occur within coil position changes of 0.5-1 cm (BRASIL-NETO ET AL., 1992; WASSERMANN ET AL., 1992). Under most circumstances, however, TMS is likely to target a range of tissue decidedly larger than 1 cm. While the magnetic field is strongest in the middle of the coil, the spatial derivative of the magnetic field is strongest at the two bifurcation points of the wings of the coil. Fibres oriented parallel to the junction of the coil will therefore be stimulated best at the bifurcation points (MACCABEE ET AL., 1993). This illustrates that, while the magnetic field distribution of TMS is practically

identical at different positions of the conductive medium (BARKER ET AL., 1985), the distribution of the induced electric field is determined by the local geometry and conductive properties of the brain.

### 1.3.3 Transcranial magnetic stimulation of the motor cortex

The following section will focus on the physiological effects of TMS over the motor cortical system. The aforementioned characteristics of the giant Betz cells make stimulation of these fibres particularly easy and the motor cortex has been investigated extensively because electromyographic recordings can be measured from peripheral muscles contralateral to the site of stimulation to assess the effects exerted by TMS. In contrast to TES, which predominantly activates vertical corticospinal axons directly (ROTHWELL, 1997), TMS modulates CSNs primarily via activation of their horizontally oriented afferents. Direct stimulation of CSN only occurs at very high stimulation intensities (NAKAMURA ET AL., 1996; ROTHWELL, 1997). This is explained by the direction of the cortically induced currents with respect to the orientation of the cortical neurons. Stimulation is maximal in those neuronal elements located in the plane of the coil. In these elements, stimulation occurs when they are in the plane of the virtual anode (+) and cathode (-).

Effective stimulation of the motor cortex is prone to induce compound motor action potentials in the contralateral limb (Figure 1.13). Furthermore, TMS of the motor cortex elicits a series of descending positive waves with a periodicity of approximately 600 Hz and 10 ms duration. Given their order of occurrence, the first wave is termed D (direct) wave, followed by the subsequent indirect or I waves (PATTON & AMASSIAN, 1954, 1960; AMASSIAN ET AL., 1987). Vahe Amassian and his pals have provided evidence that the initial descending volley is produced by direct excitation of corticospinal fibres, presumably at the axon hillock or first or second internode, while the later I waves are generated by interposed synapses within intact grey matter (but also additional recruitment of corticospinal neurons). For example, ablation or anaesthesia of the grey matter abolishes I waves while keeping the D wave unchanged (PATTON & AMASSIAN, 1954, 1960). Additional evidence for a

cortical origin of I waves stems from thalamocortical lesion studies in the cat that revealed unchanged I wave occurrence despite the degeneration of the thalamocortical fibres exciting pyramidal tract neurons monosynaptically (AMASSIAN & WEINER, 1966). The differences in latency of the motor evoked potential (MEP) between electrical stimulation and TMS of about 1-2 ms further indicate predominant cortical transsynaptical excitation by TMS (DAY ET AL., 1989; WERHAHN ET AL., 1994). This difference is presumably explained by differences in the direction of the induced currents: a TMS coil placed tangentially over the scalp will predominantly induce a current parallel to the plane of the coil (ROTH ET AL., 1991). While electrical stimulation will generate both vertical and horizontal current flow, at threshold and with an antero-posterior coil orientation, TMS will mainly excite neuronal elements oriented horizontally to the induced electrical field (AMASSIAN ET AL., 1992b), as for example interneurons or cortico-cortical projections that run in an antero-posterior direction. As a consequence, CSNs will be excited transsynaptically and descending volleys will have slightly prolonged latencies. At medio-lateral coil orientations and high stimulation intensities these latency differences between TMS and TES tend to disappear.

Studies by AMASSIAN and colleagues (AMASSIAN ET AL., 1992b) have furthermore emphasised the importance of bends in nerve fibres. While fibres running strictly parallel to a uniform electrical field will experience virtually no stimulation, an outward current flow out of the nerve fibre can occur where fibres bend away from the plane of the electrical field, thus resulting in excitation of the fibre. Here, the spatial derivative of the outward current determines the efficacy of stimulation of a nerve (MACCABEE ET AL., 1993). This is important when considering the anatomy of the motor cortex: fibres that follow the gyral surface will bend through the induced electrical fields and therefore will be preferentially excited. This also explains why varying current orientations will target different cortical circuits, depending on their localisation and fibre orientation.

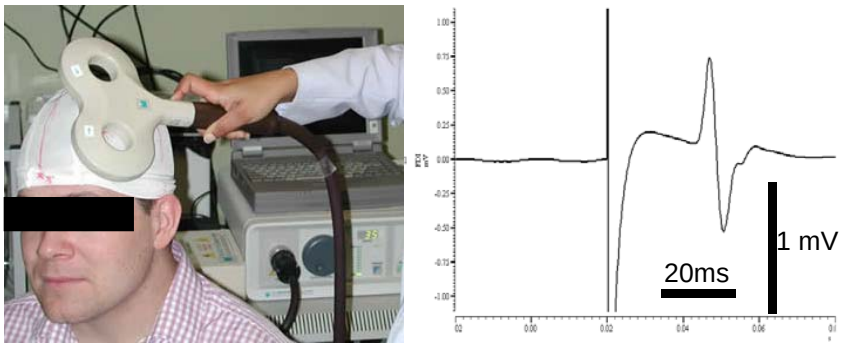


**Figure 1.13.** A single TMS pulse applied to the primary motor cortex (left) applied at the right intensity elicits a motor evoked potential in a contralateral hand muscle (right) as recorded with electromyography.

The MEP exhibits substantial intraindividual variability, which is reduced at high intensities and during pre-innervation (KIERS ET AL., 1993). These are likely to stem from mechanisms intrinsic to the motor system, as neither slight changes in coil position, background voluntary contraction, nor influence by cardiac or respiratory cycles can fully explain these variations (AMASSIAN ET AL., 1989). As shown in a comparison of stimulation conducted manually or by frameless stereotaxy, variations in coil position do not alter MEP variability of (GUGINO ET AL., 2001), suggesting that these variations are inherent properties of the resting corticospinal system and caused by alterations in cortical excitability over time (KIERS ET AL., 1993).

**Intracortical inhibition and facilitation.** TMS activates intracortical circuitry as well as corticofugal projections. The so-called paired-pulse stimulation technique (FERBERT ET AL., 1992; KUJIRAI ET AL., 1993) has become the gold standard to investigate the intracortical processes in the human motor cortex non-invasively. In this technique, two magnetic pulses are applied through the same stimulation coil placed over the motor cortex. The first stimulus is a low intensity and usually subthreshold pulse (i.e. not depolarising descending fibres directly) followed by a stronger and usually suprathreshold pulse, which on its own produces a clear electromyographic response in a contralateral muscle. This allows investigation of the effect of the first, the conditioning stimulus (CS), on the size of the myographic response of the second, the test stimulus (TS). At an inter-stimulus interval (ISI) of 1-6 ms, the response of the TS will be inhibited, while the response will be facilitated at longer intervals of

7-15 ms. In the macaque, the latencies measured from the lumbrosacral axonal responses to TMS are consistent with a cortical origin of action (EDGLEY ET AL., 1997). Moreover, the CS does not affect the size of the H-reflex (KUJIRAI ET AL., 1993), but its effects are altered in cortical myoclonus (BROWN ET AL., 1996), indicating that the conditioning effect on the TS arises at the cortical level. Epidural recordings from the cervical spinal cord in intractable pain patients provide additional evidence for a cortical origin of the effects of the CS (DI LAZZARO ET AL., 1998, 1999, 2002). Because there is increasing evidence that these effects are mediated by intracortical circuits (KUJIRAI ET AL., 1993; ZIEMANN ET AL., 1996a; DI LAZZARO ET AL., 1998, 1999, 2000; FISHER ET AL., 2002; HANAJIMA ET AL., 2003), they have been termed intracortical inhibition (ICI) and intracortical facilitation (ICF), respectively. The different dynamics between ICI and ICF imply that separate intracortical structures in the motor cortex mediate these processes (ZIEMANN ET AL., 1996a; NAKAMURA ET AL., 1997; ABBRUZZESE ET AL., 1999; SANGER ET AL., 2001; FISHER ET AL., 2002; HANAJIMA ET AL., 2003). The neurons responsible for ICI do not inhibit CSNs directly. As TMS is assumed to activate CSNs indirectly via excitatory synaptic inputs evoking I waves, ICI is thought to be an indirect inhibitory modulation of these interneurons.

Given the size of the coil and the induced magnetic field, it has intuitive appeal to regard the stimulation as non-selective to any underlying structure. However, both mono- and biphasic TMS can be used to target the motor cortex in highly specific manners that allow detailed inferences about motor cortex physiology. As mentioned above, several studies have shown, that distinct cortical systems can be targeted by TMS (KUJIRAI ET AL., 1993; ZIEMANN ET AL., 1996a; FISHER ET AL., 2002; BESTMANN ET AL., 2004). For example, ICI can be observed selectively at lower intensities of CS than ICF (ZIEMANN ET AL., 1996a; NAKAMURA ET AL., 1997) and ICI and ICF furthermore seem to be generated at spatially distinct sites (ASHBY ET AL., 1999). Furthermore, pairs of conditioning stimuli at low intensity interact in an inhibitory fashion, whereas no facilitatory interaction seems to exist at these low intensities (BESTMANN ET AL., 2004). Importantly, even when a single CS is

applied below an effective intensity for either ICI or ICF, pairs of CS at this intensity are prone to induce ICI much before any facilitatory interaction occurs. The different thresholds for ICI and ICF thus indicate mediation by different subsets of interneurons.

The physiological activation patterns become more complex after biphasic TMS, which is commonly used for repetitive stimulation. This is mirrored by the observation that the optimal coil orientation to mediate cortical activity are different to those used for monophasic TMS. Although direct comparisons of the effectiveness of mono- and biphasic pulses have been attempted (SOMMER ET AL., 2002), they suffer from the disability to match input-output relationships, and observed physiological differences are likely to originate from stimulation of different subsets of neurons, or different doses of induced current.

**The effect of voluntary contraction.** A further observation relevant to the presented experiments is the increased excitability of both corticospinal- and motoneurons during voluntary contraction. Depending on the pattern of motor unit recruitment in different muscles, MEPs increase markedly during pre-innervation. The increases are partially mediated by increased output from the motor cortex in response to the stimulus (MAZZOCHIO ET AL., 1994; UGAWA ET AL., 1995; DI LAZZARO ET AL., 1998), while others are due to intracortical processes (RIDDING ET AL., 1995; WASSERMANN ET AL., 1996). Recent studies provide evidence that the reduction of paired-pulse inhibition during muscle activity is, at least in part, due to effects on late I-waves (ZOGHI ET AL., 2003). The differential modulation of ICI during voluntary muscle activity is presumed to mediate the generation of fractionated activity of intrinsic hand muscles required for dextrous behaviour (ZOGHI ET AL., 2003). The findings illustrate the context-dependence of TMS: varying levels of synaptic activity in the stimulated brain region influence the efficacy of stimulation.

In summary, TMS can selectively target inhibitory and facilitatory processes in the motor cortex and furthermore allows for the investigation of dynamic changes in cortical excitability during motor behaviour or pharmacological

intervention. Despite the size of the stimulating coil, focal changes originating from the motor cortex may be targeted and hence provide a tool to separate intracortical, corticospinal and spinal information processing in man. In that, TMS has contributed substantially to the understanding of motor behaviour and physiology.

### 1.3.4 Motor thresholds

In most TMS studies, the cortical motor threshold is defined as the minimum intensity producing an MEP in a target muscle on 50% of trials (ROTHWELL ET AL., 1999). Due to the contribution of both the cortex and the spinal cord in the generation of the MEP, however, cortical excitability is not well defined at rest (SIEBNER & ROTHWELL, 2003). There is uncertainty of how far CSNs are away from firing threshold: inactive neurons could be close to firing threshold or far away from it. In addition, changes in spinal excitability might be responsible for the occurrence of a muscle discharge. As a consequence, the estimation of motor thresholds during active muscle contraction, when synaptic activity is better defined, provides a more accurate measure of cortical excitability. At first glance, the MEP offers an adequate measure to explore the effects of TMS onto the human brain, yet the site of stimulation will be at least two synapses away from the peripheral muscle recording. The MEP is produced by repetitive discharge in the cortex that generates a series of descending volleys in large diameter corticospinal axons. While the descending volleys evoked by TMS depend on stimulus intensity and the excitability of cortical cells, the response in peripheral muscles depends on transmission through implicated excitatory and inhibitory interneurons and on the excitability of the motoneuron pool. Temporal dispersion of descending volleys, combined activity in central and peripheral motor neurons, and the fluctuating levels of excitability of involved synapses contribute to the MEP and thus make it a complex and variable phenomenon to interpret (KIERS ET AL., 1993).

In a series of studies, Ziemann and colleagues (ZIEMANN ET AL., 1995, 1996b,c,d) have shown that the administration of drugs acting on the

neuronal membrane excitability affect corticomotor thresholds, while drugs that influence synaptic neurotransmission have little influence. For example, anti-epileptic drugs with prominent sodium and calcium channel blocking capacity but limited or absent neurotransmitter interaction influence motor thresholds significantly (ZIEMANN ET AL., 1996b,c,d). These studies lend credence to the idea that the motor threshold is primarily influenced by membrane properties of the cortico-spinal system.

### 1.3.5 Repetitive transcranial magnetic stimulation

TMS pulses applied in rapid succession at a frequency of 1 Hz or more can produce changes in cortical excitability outlasting the stimulation period, depending on intensity, duration and frequency of the stimulation (PASCUAL-LEONE ET AL., 1994; CHEN ET AL., 1997; MUELLBACHER ET AL., 2000; ROMEO ET AL., 2000; FIERRO ET AL., 2001; MODUGNO ET AL., 2001; TSUJI & ROTHWELL, 2002; GILIO ET AL., 2003; SCHAMBRA ET AL., 2003). Set out in this manner, TMS has been used as a model to provoke and investigate acute cortical plasticity in the intact human brain (see SIEBNER AND ROTHWELL, 2003, for review). Repetitive TMS typically induces decreases or increases in MEP amplitude after low-frequency (1 Hz) and high frequency (> 1 Hz) stimulation, respectively.

Low-frequency stimulation of M1 at intensities above motor threshold reduces corticospinal excitability, as reflected in increased corticomotor resting thresholds and decreased MEP size (CHEN ET AL., 1997; MUELLBACHER ET AL., 2000; GILIO ET AL., 2003). When applying intensities below resting motor thresholds these effects become attenuated and longer stimulation series are required (MAEDA ET AL., 2000b) while intensities below active motor thresholds require even more prolonged stimulation periods for inducing after effects (CHEN ET AL., 1997; GERSCHLAGER ET AL., 2001; MUNCHAU ET AL., 2002; SCHAMBRA ET AL., 2003). The dose-dependency is further illustrated by the fact that fifteen minutes of 1Hz rTMS at 105% of resting motor threshold (RMT), for instance, evoke subtle changes in contralateral corticospinal excitability (WASSERMANN ET AL., 1998), while prolonged stimulation of 30 minutes and

higher intensities (110-150% RMT) increases contralateral MEPs for up to 15 minutes after stimulation (SCHAMBRA ET AL., 2003).

Facilitatory after effects are regularly induced by high-frequency protocols. When applied at suprathreshold intensities, even relatively short trains of 500 ms at 150% motor threshold increase the MEP size for about 3 min after the stimulation (PASCUAL-LEONE ET AL., 1994). At intensities below resting motor thresholds stimulation periods generally have to be longer to induce lasting changes in corticospinal excitability (MAEDA ET AL., 2000a,b).

As pointed out by SIEBNER & ROTHWELL (2003), the administration of short TMS trains (~ 20 pulses) allows to assess the factors mediating inhibition and facilitation and their interaction. For example, transient inhibition of the MEP for up to 1 s can already be observed after 4 pulses at 20 Hz and 150% of resting motor threshold (MODUGNO ET AL., 2001). Interestingly, the prolongation of stimulation trains leads to facilitation of the MEP (MODUGNO ET AL., 2001), indicating a separation between the threshold for inhibitory and facilitatory effects (MODUGNO ET AL., 2001; FITZGERALD ET AL., 2002). While short TMS trains induce transient inhibition, longer trains, especially at higher intensities and frequencies promote facilitatory effects. Depending on the stimulation dose, the effects of rTMS can outlast the stimulation by up to 30 minutes (PEINEMANN ET AL., 2000; MUELLBACHER ET AL., 2000; GERSCHLAGER ET AL., 2001). After effects occur even following subthreshold stimulation (e.g. PEINEMANN ET AL., 2000). Given their predominant cortical site of action (Di LAZZARO ET AL., 1998) they are at least partially generated at the cortical level.

One interesting feature of rTMS is the induction of effects remote from the site of stimulation. In a recent elegant study, GILIO ET AL. (2003) have revealed that TMS (1 Hz, 15 min) over one hemisphere reduced interhemispherical inhibition in the contralateral side with a concomitant increase in corticospinal excitability. Using a series of control experiments, the authors were able to conclude that these effects were predominantly, if not exclusively, mediated by cortico-cortical projections, and not by afferent feedback or spinal mechanisms. Similarly, 30 minute trains of suprathreshold

1 Hz rTMS of the motor cortex increase contralateral excitability for about 15 minutes (SCHAMBRA ET AL., 2003).

Repetitive TMS over other brain regions can produce after effects in the motor cortex. For instance, 1 Hz rTMS of the PMd decreases corticospinal excitability of the motor cortex and alters the time course of corticocortical ICI and ICF (GERSCHLAGER ET AL., 2001; MUNCHAU ET AL., 2002). Stimulation at 5 Hz and below active motor threshold of the SMA induces a deterioration of inter-limb co-ordination accompanied by a decreased coupling between motor cortices (SERRIEN ET AL., 2002). Finally, high-frequency stimulation (10 Hz) of the prefrontal cortex can lead to a temporary increase in cortico-cortical coherence and an increase in EEG amplitude and frequency (JING & TAKIGAWA, 2000; OKAMURA ET AL., 2001).

Since the after effects of rTMS tend to disappear when tested during actively contracted muscles, they are presumably mediated by changes in excitability of the resting corticospinal system, rather than by changes in effective neurotransmission at cortical synapses (TOUGE ET AL., 2001). Despite the profound electrophysiological changes following various rTMS protocols, the behavioural consequences are, at best, only modest. Several authors have failed to demonstrate changes in simple motor behaviour following rTMS in healthy subjects (CHEN ET AL., 1997; MUELLBACHER ET AL., 2000; ROSSI ET AL., 2000; SCHAMBRA ET AL., 2003), or reported only modest behavioural effects (SCHLAGHECKEN ET AL., 2003), despite the occurrence of both corticospinal and cortical excitability changes. The absence of pronounced behavioural effects might be explained by compensation of the contralateral M1 (i.e. ipsilateral to the movement). Indeed, bilateral rTMS results in substantial decreases of motor performance (STRENS ET AL., 2003).

### 1.3.6 TMS and cognitive neuroscience

TMS may elicit positive phenomena which can be observed after stimulation of the primary motor cortex, e.g. leading to muscle twitches in the contralateral hand, or the primary visual cortex, e.g. leading to the perception of phosphenes. Negative phenomena, referring to the manipulation of

behavioural performance, e.g. increases in reaction times or error rates, can also be observed. These effects have also been coined "virtual lesions" (WALSH & COWEY, 1998) because the disruptive behavioural effects of TMS are transient and reversible. The short-lived effect on brain function after single TMS pulses allows to obtain information regarding the temporal involvement of a given cortical region in a specific behaviour, i.e. its "causal chronometry" (DAY ET AL., 1989; PASCUAL-LEONE ET AL., 2000).

Set out in this manner, BESTMANN ET AL. (2002) investigated the involvement of the superior parietal cortex in a visuo-motor mental rotation task. In comparison to control stimulation over the vertex, rTMS over left or right superior parietal cortex led to an increased reaction time, at increased processing demands. Moreover, the effects occurred only when stimulation was applied relatively early during the task. A further example is the investigation of cortical excitability during action observation (FADIGA ET AL., 1995; GANGITANO ET AL., 2001) or motor imagery (ABBRUZZESE ET AL., 1999; FADIGA ET AL., 1999; HASHIMOTO & ROTHWELL, 1999; ROSSINI ET AL., 1999; FACCHINI ET AL., 2002). These studies have convincingly shown that mental processes such as motor imagery can exert dynamic effects on the excitability of the motor cortex that resemble those exerted by actual movements. The increases in cortical excitability are furthermore confined to the prime-mover muscle for the mentally simulated movement (ROSSINI ET AL., 1999) and mostly mediated at the cortical, and not at the spinal level (FADIGA ET AL., 1995, 1999; HASHIMOTO & ROTHWELL, 1999). The fact that degraded task performance occurs only during increased facilitation, e.g. in motor mental rotation tasks (GANIS ET AL., 2000), suggests that these observations are not merely artificial.

The abundant number of studies applying TMS in such an interfering manner have provided important knowledge regarding the causal relationship between behaviour and brain function (as reviewed by PASCUAL-LEONE ET AL., 1999, 2000; WALSH & RUSHWORTH, 1999; JAHANSHAHI & ROTHWELL, 2000). Clearly, a tenable linkage between cortical stimulation and behaviour favours a better understanding of the basic physiology in order to overcome the

limitations of patient studies, in which no detailed information regarding the extent and physiology of brain damage is usually available. As shall be shown later, this understanding can at best be considered modest, and asks for a more copious understanding of TMS.

### 1.3.7 Safety considerations

While the safety of single pulse TMS is well established, the application of rTMS bears several potential risks that should be accounted for. The discharge noise of the TMS coil can cause temporary elevations in auditory thresholds (PASCUAL-LEONE ET AL., 1993), and hence the use of ear-plugs or headphones is recommended. A more serious concern is the capability of rTMS to induce seizures. Several cases of TMS-induced seizures have been reported, and therefore any subject revealing a family history of epilepsy or other neuropsychiatric conditions should be excluded from partaking in experiments. Several studies have proposed stimulation guidelines (PASCUAL-LEONE ET AL., 1993; JAHANSHAHI ET AL., 1997; WASSERMANN, 1998). Although not exhaustive in extent, these studies provide conservative guidelines regarding the applicable stimulation protocols.

The knowledge concerning the long-term effects of TMS is even more limited. Because of the dose-dependency of the physiological effects of rTMS on the motor cortex (MODUGNO ET AL., 2001), it can be assumed that extended stimulation protocols bear the risk of long-term changes. Several animal studies have reported such changes in monoamine transmitter systems (BEN-SHACHAR ET AL., 1997; KECK ET AL., 2000) and brain-derived neurotrophic factor (MULLER ET AL., 2000). On the other hand, daily administration of 1000 TMS pulses was not found to change astrocytic or microglial reaction nor to alter brain metabolites as measured by proton magnetic resonance spectroscopy (LIEBETANZ ET AL., 2003). Only one study to date has explored long-term changes in cortical excitability following prolonged subthreshold stimulation series at 1 Hz (1200 stimuli) in man, and demonstrated cumulative plastic changes in motor cortical excitability lasting more than a day but less than a week (BAUMER ET AL., 2003). The ongoing debate of potential treatment

effects of stimulation in major depression automatically implies that effects outlasting the stimulation can be induced. These effects cannot always be assumed beneficial rather than deleterious, and it is recommended to minimise stimulation periods and the number of experiments.

## 1.4 Combined TMS and fMRI

The introduction of combined TMS and neuroimaging techniques presents a powerful tool to characterise TMS-related changes in cortical processing at a systems level. One attractiveness of using functional brain imaging in conjunction with TMS originates from the more direct measures regarding the physiological effect of TMS. Furthermore, rather than using peripheral measures such as MEPs, or even more complex variables, such as reaction times and error rates in neuropsychological experiments, functional brain imaging obtains measures of cortical activity changes that are more directly related to the stimulation. Since TMS offers the capability of modulating neuronal activity, it facilitates causal inferences regarding the structure – function correlations obtained by fMRI. When used simultaneously, the potential arises to transiently manipulate brain function and at the same time investigate changes in cortical activity related to this intervention. One would hope to overcome the problem of neuroimaging to making inferences between biochemical changes associated with neuronal activity and a particular cognitive function, which are not necessarily unidirectional. Brain regions activated during a specific task might in fact be epiphenomenal or reflect processing of task-unrelated behaviour, however, standard experimental approaches do not provide sufficient information regarding this issue.

There are three conceivable ways of combining TMS and neuroimaging (as summarised in PAUS, 2002). Stimulation might be applied before, after, or during functional imaging. The temporal separation of TMS and fMRI is not hampered by technological burdens and long lasting stimulation protocols might be applied in order to change cortical excitability for up to 30 minutes, during which functional imaging may be conducted (WARD, 2003). In this

approach, long-lasting effects of stimulation on brain activity patterns can be visualised, thus providing an insight into cortical plasticity (SIEBNER ET AL., 2000; LEE ET AL., 2003). The simultaneous combination of TMS and neuroimaging on the other hand, especially fMRI, is technically more demanding, yet it offers the unique opportunity to immediately record changes in brain activity as a result of stimulation in both the stimulated and remote brain regions.

Based on these ideas, Daryl Bohning and his co-workers in Charleston, USA, were the first to overcome the technical burdens of simultaneous TMS-fMRI to record MR images during TMS (BOHNING ET AL., 1997) and, subsequently, obtain the first functional brain images during administration of single TMS pulses (BOHNING ET AL., 1998). In a series of studies that were catalysed by the technological advances concerning the successful combination of TMS and fMRI (SHASTRI ET AL., 1999), the effects of TMS over the motor cortex (BOHNING ET AL., 1999, 2000a,b, 2003b) and the prefrontal cortex (NAHAS ET AL., 2001) on brain activity have been explored. This approach further profits from being unpainful, especially in comparison with combined TES and fMRI (BRANDT ET AL., 2001), and therefore reduces complications regarding subjects compliance as well as the interpretation of functional data. Despite striking similarities between BOLD MRI signal changes following volitional hand movement and suprathreshold TMS of the motor cortex (BOHNING ET AL., 1999, 2000a,b; BAUDEWIG ET AL., 2001; KEMNA & GEMBRIS, 2003), a positive BOLD response to subthreshold TMS or TMS over the prefrontal cortex is not invariably found (BOHNING ET AL., 1999; BAUDEWIG ET AL., 2001; NAHAS ET AL., 2001; KEMNA & GEMBRIS, 2003). These results have led BAUDEWIG ET AL. (2001) to emphasise the possibility that BOLD MRI signal changes following suprathreshold stimulation might be, at least partially, mediated by re-afferent processing from somatosensory afferents. Although the exact factors mediating TMS-induced changes in cortical haemodynamics remain obscure, amounting evidence exists that these do not unequivocally occur after all stimulation protocols.

Despite the growing number of combined TMS-fMRI studies, several issues still impose major problems when stimulating inside an MR scanner. First, application of TMS pulses inducing maximal field strengths of approximately 2T within an MR environment dramatically increases forces and torques exerted onto the stimulation coil. While the TMS coil might be strengthened to withstand these torques, the discharge will nevertheless result in profound amplification of the characteristic 'click' sound of the TMS coil. Second, the mere presence of the TMS coil can introduce significant susceptibility MR-artefacts. These can be reduced by homogeneous and non-ferromagnetic stimulation coils and appropriate orientation of the EPI section orientation with respect to the plane of the coil (BAUDEWIG ET AL., 2000). Third, the stimulator as well as the connecting cable may provide sources for RF contamination. Fourth, the restricted space within the head coil of the MR environment effectively limits the regions accessible to the TMS coil and furthermore make accurate placement of the coil a major problem. It has been proposed that the induction of eddy currents can potentially perturb MR images for up to 100 ms after a single TMS pulse (SHASTRI ET AL., 1999). Finally, barring these immanent technical problems, we are far from understanding the physiological coupling between cortical stimulation as exerted by TMS and neurovascular mechanisms.

## 1.5 Aims of the thesis

Since the first description of combined TMS-fMRI, only a handful of studies have been published using this approach to explore the mechanisms of action of TMS (BOHNING ET AL., 1998, 1999, 2000a,b, 2001; BAUDEWIG ET AL., 2000, 2001; KEMNA & GEMBRIS, 2003). Careful inspection of MR-image quality in some of these studies points towards considerable technical burdens that hamper the interpretation of earlier publications. Previous data indicates the requirement to dovetail synchronous TMS-fMRI application in order to allow for robust and replicable investigations. Only limited information exists regarding the technical solutions to combine TMS and fMRI without significant loss in data quality (SHASTRI ET AL., 1999). In fact, few attempts have been made to systematically investigate changes in cortical haemodynamics and activity for a wide range of stimulation protocols or even develop strategies to do so, and the profound technical challenges still existing most likely explain the sparseness of combined TMS-fMRI studies.

The initial aim of this thesis was to develop technical and experimental strategies to successfully interleave TMS with fMRI and to systematically characterise the factors that constitute unperturbed MR imaging in the presence of a TMS coil and during TMS pulse application. Given the increasing number of higher field MR systems, it was further aimed to assign the results to both 2T and 3T MR systems (Chapter 3).

Previous studies have concentrated on low-frequency stimulation of the motor cortex but information regarding the immediate impact of high-frequency rTMS protocols is less certain. Initial experiments carried out throughout this thesis have pointed towards the possibility to use rTMS at higher frequencies (BAUDEWIG ET AL., 2001). The discordant information regarding the occurrence of TMS-induced BOLD MRI signal changes in the directly stimulated cortex motivated several experiments investigating the extent to which BOLD MRI signal changes during TMS are related to the stimulation per se or to re-afferent somatosensory processing induced by peripheral muscle movements. Furthermore, a more detailed inspection of

TMS-evoked activity changes in areas beyond the site of stimulation was conducted. These issues will be addressed in Chapter 4. Repetitive TMS was applied to the left primary motor cortex for 10 s at a rate of 4 Hz while imaging the primary and secondary motor cortices. The contribution of re-afferent somatosensory processing was investigated by applying stimulation intensities above and below thresholds for peripheral muscle movements, but always above intensities know to effectively target the cortex.

The context-dependence of TMS-evoked activity changes was investigated by application of TMS during simple motor behaviour. It is known that TMS affects the cortex differently during rest or during motor behaviour, and it was aimed to visualise these changes with fMRI. Chapter 5 presents the investigation of cortical activity changes during an isometric voluntary tonic contraction task while rTMS of the left sensorimotor cortex was applied either alone, during or before voluntary contraction periods, respectively.

Subsequently, the obtained technical solutions to interleave TMS and fMRI at frequencies beyond 1 Hz were transferred to a higher field system of 3 Tesla. This experiment aimed to profit from the proposed increases in BOLD sensitivity at higher fields and thus to detect subtle activity changes in local and remote brain regions. In particular, it was aimed to visualise subcortical activity changes during rTMS. Chapter 6 presents the results of rTMS of the left motor cortex at 3 Hz over 9.9 s at intensities above and below motor thresholds and simultaneous monitoring of electromyographic activity.

Finally, TMS was applied to the dorsal premotor cortex to investigate the capability of TMS to act on distinct cortical networks other than M1/S1 (Chapter 7), using the same protocol as in Chapter 6.

# 2 Experimental Methods

This chapter describes the methods and procedures applied throughout the different experimental chapters. Additional information, whenever required, will be given in the respective chapters.

## 2.1 Subjects

A total number of 41 subjects was investigated in the experiments reported in this thesis (Table 2.1). All subjects were healthy at the time of the experiments and reported no previous personal or family neuropsychiatric or neurological history. Subjects were consistent right-handers according to the Edinburgh handedness inventory (OLDFIELD, 1971). When subjects participated in more than one experiment, these were separated by at least one month. Prior to each experiment, subjects were informed about the procedure and potential risks of the study. Each subject received the equivalent of 10 £ / hour for participation. Written informed consent was obtained prior to the experiment. All studies were conducted with local ethics approval and according to the standards laid down by the Declaration of Helsinki.

## 2.2 Structural magnetic resonance imaging

For experiments at 2.0 Tesla (Siemens Vision, Erlangen) a standard transmit-receive head-coil was used. Anatomical images were acquired using a short-echo time 3D FLASH sequence (TR / TE = 15 / 4 ms, flip angle 20°, 1 x 1 $mm^2$ resolution, 2 mm section thickness) covering the whole head.

For experiments at 3 Tesla (Siemens Trio, Erlangen, effective field strength 2.89T; resonance frequency 123.234 MHz) a transmit-receive head-coil was used. Anatomical images were acquired using a short-echo time 3D FLASH sequence (TR / TE = 11 / 4.92 ms, flip angle 15°, 1 x 1 $mm^2$ resolution, 1 mm section thickness) covering the whole head.

Table 2.1. List of subjects

| ID | Age | Gender | Handedness | Comments |
|---|---|---|---|---|
| **Chapter 3** | | | | |
| Vol_1535 | 40 | m | R | - |
| Vol_3148 | 26 | m | R | - |
| **Chapter 4** | | | | |
| Vol_2992 | 41 | m | R | - |
| Vol_3002 | 21 | f | R | - |
| Vol_3003 | 23 | f | R | - |
| Vol_3009 | 28 | m | R | - |
| Vol_3014 | 23 | f | R | - |
| Vol_3015 | 27 | m | R | - |
| Vol_3030 | 26 | f | R | - |
| Vol_3038 | 30 | m | R | excluded |
| Vol_3040 | 40 | m | R | - |
| **Chapter 5** | | | | |
| Vol_3067 | 28 | m | R | - |
| Vol_3075 | 22 | f | R | - |
| Vol_3076 | 31 | m | R | - |
| Vol_3078 | 28 | m | R | - |
| Vol_3079 | 23 | f | R | - |
| Vol_3081 | 41 | m | R | - |
| Vol_3082 | 23 | f | L | - |
| Vol_3085 | 26 | f | R | - |
| Vol_3086 | 27 | m | R | - |
| **Chapter 6** | | | | |
| Vol_3199 | 42 | m | R | - |
| Vol_3202 | 24 | f | L | - |
| Vol_3206 | 26 | f | R | - |
| Vol_3208 | 31 | m | R | - |
| Vol_3209 | 28 | f | R | - |
| Vol_3210 | 26 | m | R | - |
| Vol_3211 | 29 | f | R | - |
| Vol_3214 | 25 | f | R | - |
| Vol_3218 | 28 | m | R | - |
| Vol_3248 | 26 | m | R | excluded |
| Vol_3250 | 21 | f | R | - |
| Vol_3255 | 25 | f | R | - |
| **Chapter 7** | | | | |
| Vol_3234 | 28 | m | R | |
| Vol_3236 | 25 | f | R | |
| Vol_3254 | 26 | f | R | |
| Vol_3259 | 29 | f | R | |
| Vol_3260 | 25 | f | R | |
| Vol_3285 | 28 | m | R | No EMG |
| Vol_3299 | 29 | f | R | |
| Vol_3316 | 42 | m | R | |
| Vol_3320 | 25 | f | R | |

m: male, f: female, R: right, L: left

## 2.3 Functional magnetic resonance imaging

Functional MRI at 2.0 Tesla was conducted using a $T_2$*-weighted single-shot gradient-echo EPI sequence (frequency-selective fat suppression, TR / TE = 2000 / 53 ms, flip angle 70°, 128 x 128 matrix, 2 x 2 $mm^2$ resolution, 4 mm section thickness). Eight brain sections covering the primary and secondary motor cortex were acquired. Each fMRI session lasted 5 min 15 s.

Functional MRI at 3 Tesla was conducted using a $T_2$*-weighted single-shot gradient-echo EPI sequence (frequency-selective fat suppression, TR / TE = 3320 / 36 ms, flip angle 70°, 128 x 128 matrix, 2 x 2 $mm^2$ resolution, 4 mm section thickness). Twenty oblique brain sections covering the primary and secondary motor cortex, the dorsal part of the cerebellum, the basal ganglia and the thalamus were acquired. Each fMRI session lasted 4 min 58 sec.

The first four volumes of each data set were later discarded to allow for T1-equilibration effects. 3D-shimming was carried out in all experiments until no significant changes in the shim-values occurred.

## 2.4 MR data analysis

In all experiments, raw and unfiltered EPI data sets were inspected for TMS-related signal perturbations, static inhomogeneity artefacts and RF noise.

Single-subject raw data was initially analysed by correlation analysis following previously proposed iterative thresholding (BAUDEWIG ET AL., 2003) on individual unfiltered EPI images. This allowed for a careful inspection of activation patterns and image quality, as the corresponding unthresholded correlation maps enable for sensitive identification of stimulus-correlated movements or image degradations. Correlation coefficients were re-scaled as percentile ranks of the noise distribution, based on the noise distribution of the histogram of each correlation coefficient map (adapted from BAUDEWIG ET AL., 2003). Pixels above the 99.99 percentile rank of the individual noise distribution were identified as activated (corresponding to a type-one error probability of $p < 0.0001$). This was complemented by appending directly neighbouring pixels exceeding a 95 percentile rank of the noise distribution (corresponding to a type-one error probability of $p < 0.05$). The analysis was based on a boxcar reference function matching the behavioural protocol and shifted by two images (4 s at a TR of 2000 ms) or 1 image (3.32 s at a TR of 3320 ms), respectively. For individual analysis, activation maps were superimposed onto the individual functional images ($T_2$*-weighted EPI) to

circumvent spatial inaccuracies from the alignment between functional and anatomical data sets.

Further imaging data analysis and visualisation was performed using the BrainVoyager 4.8 or 2000 software package (Brain Innovation, Maastricht, The Netherlands). 3D anatomical datasets were transformed into Talairach space (TALAIRACH & TOURNOUX, 1988) following previously published procedures (GOEBEL ET AL., 1998; LINDEN ET AL., 1999; TROJANO ET AL., 2000). First, the points of the AC and PC, providing two rotation parameters for mid-sagittal alignment, as well as the outer borders of the cerebrum were specified. Subsequently, 3D sets were scaled into the dimension of the Talairach atlas by a piecewise affine and continuous transformation for each of the 12 defined subvolumes. Temporal filtering (low frequency drift removal), interslice time correction, and motion correction with an exclusion criterion of > 2 mm in either translation or rotation was performed. Subsequently, functional time series were interpolated into 3 x 3 x 3 $mm^2$ (nominal) spatial resolution and co-registered and normalised into Talairach space. Co-registration between EPI data sets and 3D structural data sets were computed from the slice position parameters of the respective recording session and visually inspected to facilitate appropriate alignment, given the fact that $T_2$*-weighted EPI images often exhibit geometrical distortions that might lead to inaccurate alignment with anatomical data sets. Consequently, this provided four-dimensional functional datasets co-registered with three-dimensional anatomical images. To facilitate visualisation of results, activation maps were projected onto a standard reference brain (Montreal Neurological Institute, MNI) in stereotaxic Talairach space.

A general linear model (GLM) that modelled the time course of experimental conditions convolved with a haemodynamic response function (BOYNTON ET AL., 1996) was calculated from the fMRI sessions of the respective experiment (given by the number of sessions per subjects). In all cases, stimulation or movement epochs, respectively, were considered as the effects of interest. Fixed-effects models were used to make statistical inferences at a group level. A fixed-effect model enables inferences about the presence of an effect

within the subjects of this study, but precludes inferences about the average size of the effect within the population from which the present subject sample was selected. Three-dimensional group statistical maps were generated by associating each voxel with the F-value corresponding to the specified predictor and calculated on the basis of the least squares solution of the GLM. After specification of the GLM, differences between experimental conditions were assessed using appropriately weighted linear contrasts. First, the BOLD MRI signal was compared during each experimental condition with the respective baseline condition (rest). Second, more complex contrasts were specified which tested for differences in BOLD MRI signal changes between experimental conditions. Significance values were corrected for multiple comparisons.

As this analysis requires the unbiased determination of volumes, BOLD MRI signal time courses were obtained from *a priori* anatomically defined regions-of-interest (ROI). Detailed description of the ROIs will be given in the respective experimental chapters. Mean signal time courses were expressed as percentage change with reference to the last three time points of each experimental cycle. Signal time courses were time-locked averaged for each ROI. Mean signal intensities were calculated for each functional image in each ROI and *t*-tests were used to compare the percent signal change during stimulation or movement epochs with baseline epochs.

## 2.5 Transcranial magnetic stimulation

TMS was conducted using non-ferromagnetic figure-of-eight coils (70 mm outer wing diameter) connected to a Magstim Rapid stimulator (The Magstim Company, Wales, UK). Each coil was a custom product by the Magstim company adjusted to the requirements of fMRI at 2T and 3T, respectively. In all experiments, biphasic electrical pulses of approximately 250 µs duration and 50 µs rise time were applied. The initial direction of induced current flow was posteroanterior – anteroposterior (PA-AP) in all experiments. At active motor threshold intensities, PA-AP stimulation evokes an I1 wave at latencies comparable to I1 or I3 latencies evoked by PA monophasic stimulation, and

at higher intensities, additional I wave recruitment takes place (DI LAZZARO ET AL., 2003).

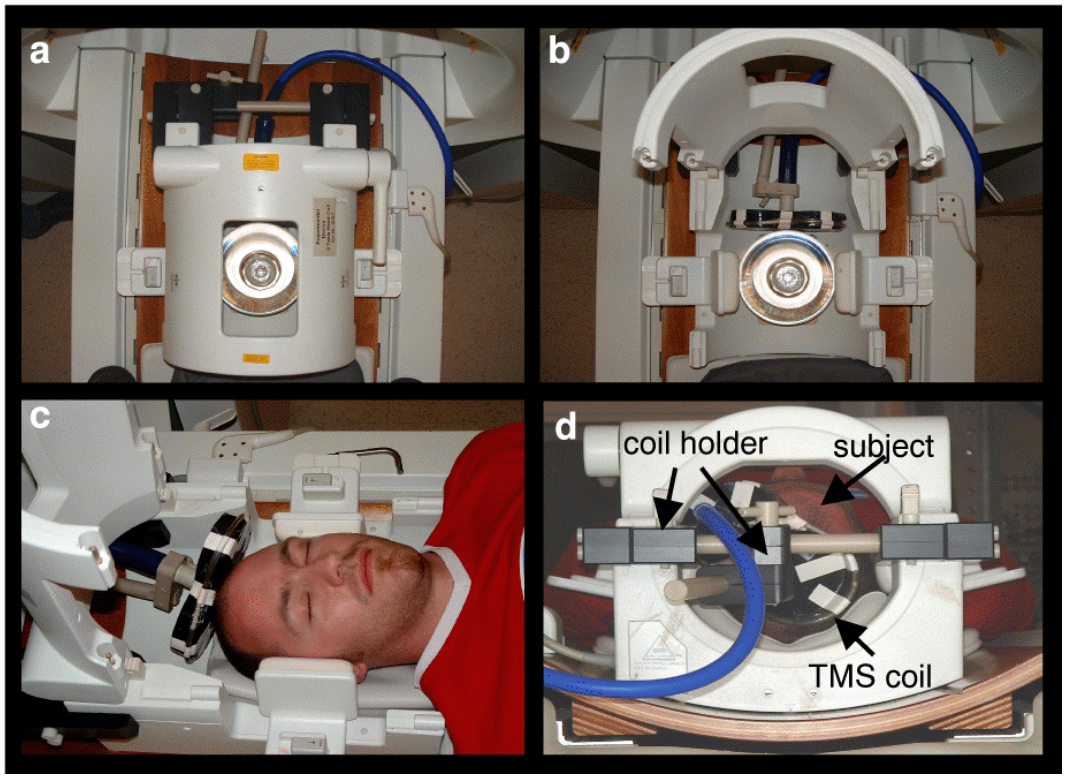


**Figure 2.1.** Experimental set-up at 2.0T. **(a)** Top view of 2T head coil with attached coil holder. The TMS coil is placed perpendicular to the $B_0$ axis and adjacent to a water-phantom, as used for the characterisation of static and dynamic artefacts in Chapter 3. **(b)** Open MR head coil showing the spatial configuration of the TMS coil and the phantom inside MR head coil. **(c)** Open MR head coil showing the spatial configuration of the TMS coil placed atop the left M1/S1 of the author of the present thesis **(d)** Rear view of the MRI head coil inside the magnet. Subjects lay supine with the TMS coil fixed by the coil holder over the left sensorimotor cortex.

Identification of the position of the TMS coil by structural MRI was accomplished either by a water-filled plastic hose attached along the outer surface of the coil or Vitamin E capsules fixed to the coil. The TMS coil was connected to the TMS stimulator outside the RF shielded cabin via an 8 m cable through an RF filter tube. Due to the resistive properties of the cable, TMS output intensities were attenuated by approximately 20%.

For the motor cortex, stimulation sites were centered over the optimal scalp site to elicit muscle twitches in the right first dorsal interosseous (FDI) muscle. For stimulation of the PMd, a point 2 cm anterior and 1 cm medial to the motor cortex hot spot was selected (SCHLUTER ET AL., 1998, 1999; JOHANSEN-

BERG ET AL., 2002). The intersection of the coil was oriented perpendicular to the presumed line of the central sulcus and laterally oriented at a 45° angle away from the midline.

Fixation and placement of the TMS coil was achieved by custom-made adjustable plastic coil holder attached to the MRI headcoil (Figures 2.1 and 2.2). The coil holder was developed in-house, using Polyetheretherketon (PEEK) reinforced plastic to withstand the vibrations of the TMS coil. In order to avoid mechanical damage to the MRI headcoil, direct contact with the TMS coil was strictly avoided, and the induced magnetic field of the TMS coil was never directed directly onto the frame of the headcoil.

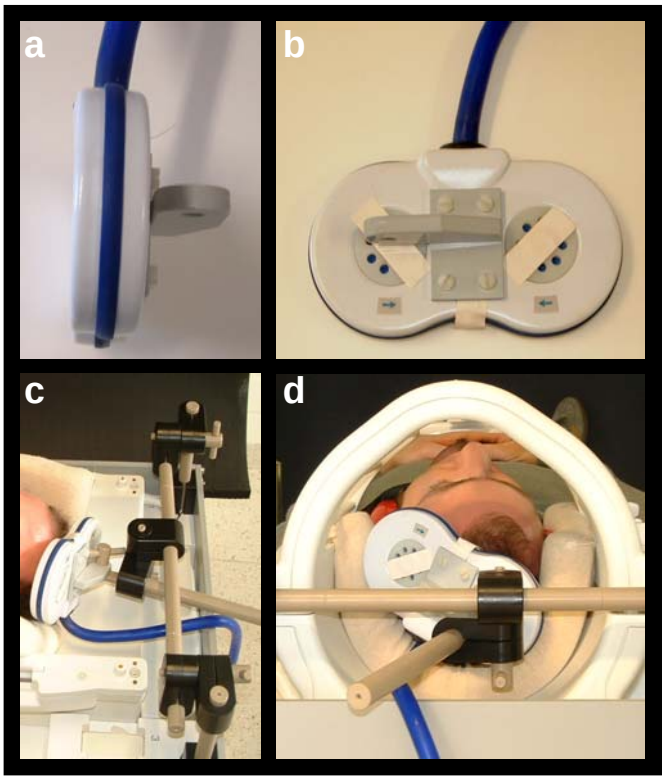


**Figure 2.2.** Experimental set-up at 3T. Side **(a)** and top **(b)** view of the TMS coil suitable for 3T. The coil was developed in collaboration with Magstim Company. **(c)** Open MR head coil showing the spatial configuration of the coil holder, and the TMS coil inside of the MR head coil. **(d)** Coil holder with TMS coil placed atop the left M1/S1 of the author of the present thesis. In order to provide accurate placement of the TMS coil, the head of the subject was slightly tilted.

At each RF excitation, a simultaneous 5V TTL pulse was delivered by the MR scanner. This signal was fed into the parallel port of a personal computer (DOS operating system) and accurate synchronisation of fMRI and TMS was

achieved using an in-house developed C program or Presentation 0.51 software (Neurobehavioral Systems, Inc., San Francisco, USA).

The position for stimulation and motor thresholds were determined prior to scanning with the subjects outside the MR environment. In a first step, single-pulse TMS was used to identify the optimal scalp position for eliciting a muscle twitch in the right FDI muscle. An initial estimation of the threshold was obtained by changing stimulus intensities in 5% steps of stimulator output. Following this, an accurate estimation was conducted by changing stimulator output intensities in 1% steps. The resting motor threshold (RMT) was first defined as observable muscle response in the contralateral FDI in 50% of trials. Subsequently, the individual RMT was defined as the minimum output of the stimulator that induced observable muscle movements in the target muscle in 2 out of 4 rTMS trains that would later be given in the respective experiment. The active motor threshold (AMT) was taken as the minimum intensity that led to an observable muscle twitch in the right FDI during a pincer grip at 10% maximum voluntary contraction (MVC) in 2 out of 4 rTMS trains. This procedure took into account a possible increase in excitability during the repeated administration of suprathreshold rTMS trains (PASCUAL-LEONE ET AL., 1994). Furthermore, when subjects had to perform a motor task, stimulation intensities were appropriately adjusted in order to not evoke any movements during the motor behaviour. Although the threshold estimation based on the observation of muscle twitches is less accurate than using electromyography, it was favoured on grounds of parsimony within the experimental procedure, especially for the control of thresholds within the MR environment. Thresholds and coil positions were checked after positioning the subject within the MRI scanner as well as after each experimental session.

## 2.6 Electromyographic recordings

Surface electromyographic recordings reported in Chapters 6 and 7 were made from the right FDI in a belly-tendon montage using non-ferromagnetic sintered Ag/AgCl surface electrodes (9 mm diameter). The electrodes were

connected to BrainAmp MR-compatible EEG amplifier (Brain Products, Munich, Germany) placed at the entrance of the bore of the magnet. The amplifier was connected to a personal computer via a fibre optic cable. Data was recorded on disc for later off-line analysis using Brain Vision 1.0 software (Brain Products, Munich, Germany) at a sample rate of 2000 Hz.

The onset and offset of recordings with imaging artefacts were marked interactively and time-locked averaged to the onset of stimulation epochs. EMG recordings were rectified and low-pass filtered at 50 Hz. For MR imaging gradient removal, a frequency extraction between 7-25 Hz was conducted. The resulting frequency spectra preserve temporal information, although some of the quantitative information is lost. Therefore only the occurrence of electromyographic activity during stimulation and movement epochs was inspected, rather than the strength of the electromyographic responses between TMS conditions. Recordings from each session were normalised to the mean EMG amplitude. Paired *t*-tests were used to compare normalised mean EMG levels during TMS and resting epochs. Unless otherwise instructed, subjects were asked to relax their hands throughout the experiment. Apart from the experiment reported in Chapter 5, subjects were instructed to keep their eyes closed during scanning.

## 2.7 Safety

Prior to the experiments, the corresponding TMS coils were intensively tested within the MR environment. At least 3000 TMS pulses were discharged at 100% of stimulator output with each TMS coil in a perpendicular orientation to $B_0$. Following this, the coils were inspected by Magstim Company to ensure that no invisible cracks had occurred. The TMS coils were further checked for damage after each experiment.

During scanning subjects wore ear-plugs and head-phones with the head cushioned by foam pads to restrict head movements. This effectively attenuated the discharge noise of the TMS coil. Vibrations of the TMS coil

were largely reduced by the rigid coil holder. In some subjects, the orientation of the TMS coil was changed to minimise vibrations.

In order to avoid carry-over effects of cortical stimulation, and to comply to recommended safety margins (JAHANSHAHI ET AL., 1997; WASSERMANN, 1998), stimulation blocks were separated by 5-10 minutes. None of the subjects received more than 1200 TMS pulses per experiment, with only a maximum of one third being above motor thresholds.

# 3 Artefact characterisation and synchronisation strategies for simultaneous transcranial magnetic stimulation and functional MRI

## 3.1 Introduction

Despite the increasing interest in combined MRI-TMS studies, there is only limited information about the static and dynamic artefacts related to the TMS coil and magnetic pulse applications, respectively (SHASTRI ET AL., 1999). The mere presence of a TMS coil may lead to image artefacts when using MRI sequences (such as EPI) that are susceptible to magnetic field inhomogeneities. Recently, corresponding signal losses and geometric distortions were shown to depend on the orientation and distance of the imaging section studied with respect to the TMS coil (BAUDEWIG ET AL., 2000). While disturbances due to sparse TMS pulses could be minimised by sufficiently large waiting periods before imaging (BOHNING ET AL., 2000, NAHAS ET AL., 2001), TMS applications with higher stimulation frequencies still require a more detailed description of potential pitfalls. The aim of the present chapter was to provide a comprehensive analysis of TMS-related EPI artefacts, and to develop a strategy for synchronising high-frequency TMS with serial multi-slice EPI as commonly applied for mapping human brain function. It was furthermore aimed to transfer the obtained results onto higher magnetic field strengths (3T), which are becoming more commonly used for the investigation of human brain function.

## 3.2 Materials and methods

### 3.2.1 Subjects

Two male subjects (26 and 40 years) participated in the study after giving informed written consent before all examinations.

### 3.2.2 Transcranial Magnetic Stimulation

TMS with biphasic pulses was performed using a Magstim Rapid stimulator and a figure-of-eight coil with a long axis of 190 mm and a diameter of 100 mm (The Magstim Company, Wales, UK). The coil was specially designed for MRI at 2T and did not contain any ferromagnetic materials. For experiments at 3T, a similar coil with 170 mm diameter was used. Both coils were prototypes especially designed to withstand the mechanical perturbations and torques provoked by the opposition of the static magnetic and TMS-induced magnetic field (see below).

### 3.2.3 Echo-Planar Imaging

Structural and functional MR images were acquired as described in Chapter 2. Initially, studies were conducted at 2T (Siemens Magnetom Vision, Erlangen, Germany). Phantom studies involved a water-filled spherical glass container. Additional experiments were performed with use of a 15% Agar solution to exclude vibration-related fluid movements as a putative source of MRI signal alteration. Subsequently, the experiments were transferred to 3T (Siemens Trio, Erlangen, Germany). In both cases, the MRI head coil had an inner diameter of 32 cm, which provided sufficient space for the placement and fixation of the TMS coil.

All phantom studies were analysed with in-house software. Signal intensities of each image were calculated without spatial or temporal filtering in a Region-of-Interest covering the object center. Determination of the coil position was achieved by 3D surface reconstruction of $T_1$-weighted images using BRAIN VOYAGER 3.0 (Brain Innovation BV, The Netherlands).

### 3.2.4 Combined TMS and EPI

Extending a previous study (BAUDEWIG ET AL., 2000), the static effects of a TMS coil on the quality of gradient-echo EPI were systematically tested for different orientations of the TMS coil (transversal, coronal) and imaging gradients (slice selection, phase encoding, frequency encoding), excluding only those EPI

combinations that are beyond human safety recommendations. Subsequently, the dynamic effects associated with the application of TMS pulses were investigated as a function of time before and during EPI.

The study comprised four different parts, each carried out at both 2T and 3T:

**TMS before EPI:** as previous work suggests that images may be affected even 100 ms after a TMS pulse (SHASTRI ET AL., 1999), the effect of a single TMS pulse on a single EPI section oriented parallel to the TMS coil was studied as a function of time (1-ms steps) for various coil-section distances (2 cm, 4 cm, and 6 cm) and TMS pulse intensities (50% and 100% of stimulator output). In addition, to assess induced eddy currents as a potential source of image degradation (SHASTRI ET AL., 1999), a magnetic resonance gradient pick-up coil recorded field fluctuations after TMS at 2T.

**TMS during fat-suppression pulses:** The different precessional frequencies of lipid and water protons is used to selectively suppress the signal from one or the other. This is commonly achieved by a frequency-selective 90° excitation pulse centered around the maximum proton resonance of either water or lipid and with a narrow bandwidth that spares excitation of one or the other. Using a spoiler gradient, the excited respective transverse magnetisation is lost, and during the subsequent imaging sequence it remains without signal as no longitudinal magnetisation has yet recovered. Generally, a large volume is used for fat-suppression rather than a single section because selective excitation of lipid protons in a single section would also excite water protons in adjacent sections at the low end of the gradient. This in turn could affect subsequent imaging of that section. A single TMS pulse was applied approximately at the peak of the fat-suppression pulse of an EPI sequence, and changes in EPI signal intensity of subsequent images were examined.

**TMS during data acquisition:** high-frequency TMS in conjunction with multi-slice EPI aggravate the difficulty of embedding repetitive TMS pulses within serial EPI acquisitions. Although it has been reported that reasonable image quality may be achieved with TMS pulses applied shortly after the mean TE (SHASTRI ET AL., 1999), a more comprehensive examination addressed the

effects of a single TMS pulse at variable times (1-ms steps) during data readout, i.e. as a function of the affected high and low spatial frequencies and for different coil-slice distances (2 cm, 4 cm, and 6 cm).

**TMS during RF excitation:** although a disturbance of the slice-selective RF excitation by a simultaneous TMS pulse will likely be expected, its translation into longitudinal magnetisation may cause persistent alterations extending the acquisition of the directly affected image. Therefore, a single TMS pulse was applied approximately at the peak of the RF excitation pulse (pulse width 9.6 ms at 2T, 2.5 ms at 3T, sinc profile) of an EPI sequence, and changes in EPI signal intensity of subsequent images were examined as a function of time for various repetition times and flip angles.

**TMS during functional brain mapping:** to demonstrate the confounding effects of TMS onto functional EPI of human brain activation, a single TMS pulse was applied to the left-hemispheric M1/S1 of a right-handed male subject during functional mapping (TR = 2000 ms, 2 x 2 x 4 $mm^3$ spatial resolution, eight sections covering the primary and secondary motor cortex) of BOLD responses to a sequential finger-to-thumb opposition task of the dominant hand (visually cued tapping of individual fingers against the thumb at 2 Hz). The paradigm consisted of eight cycles of 10-second tapping epochs followed by 20-second rest epochs. The position of the TMS coil atop M1 was determined inside the scanner, but without imaging, by applying suprathreshold TMS pulses. During functional EPI, a single subthreshold TMS pulse (39% stimulator output, AMT 45%) was synchronised to coincide with a single RF pulse exciting only one of the sections at the start of each finger-tapping epoch. The validity of the mapping procedure was tested by repeating the task without TMS. Task-related EPI signal changes were identified by cross-correlation with a boxcar reference function matching the finger-tapping protocol with a shift by one image (2 seconds) to account for hemodynamic response delays. Quantitative activation maps were obtained by automated user-independent statistical procedures as described in Chapter 2.

Set out in this manner, suprathreshold rTMS at 120% RMT was conducted over the left motor cortex at 3T in a different subject. This initial experiment was performed subsequent to the characterisation of static and dynamic imaging artefacts to prepare the ground for the functional experiments described in Chapters 6 and 7 and explore the feasibility of fMRI at higher field strength.

It has intuitive appeal to call for the use of RF filters that prevent interspersion of noise via the connecting cable of the TMS coil. However, these were not found to be essential for successful TMS-fMRI combination, which is at variance with previous studies at lower field of 1.5T (SHASTRI ET AL., 1999; BOHNING ET AL., 1998, 1999). These studies reported the need of RF filters for the reduction of noise emission into the scanner room, asking for the close attention to RF noise when combining TMS and fMRI at this lower field strength. Therefore, a comparison of RF noise emission from the Magstim RapidStim used throughout this thesis was performed at 1.5T and 3T.

## 3.3 Results

Figure 3.1 summarises the key findings for EPI effects introduced by the presence of a TMS coil. For the coil-phantom arrangement chosen here, strong artefacts were obtained whenever the frequency-encoding gradient was pointing through the plane of the TMS coil. These distortions occurred regardless of whether the image section was cutting through the TMS coil plane or not. For coronal sections, a switch of the frequency-and phase-encoding gradient largely reduced the ghosting artefacts. Similarly, transverse sections at some distance apart from the coil, and with phase-encoding gradients in a posterior-anterior direction, revealed only negligible distortions. On the other hand, and in line with previous observations (BAUDEWIG ET AL., 2000), a distance of only 2 cm was insufficient to avoid severe artefacts (not shown). Although similar results were observed for a coronal orientation of the TMS coil as shown in Figure 3.1b, direct susceptibility artefacts were significantly more pronounced. In general, best results were obtained if both the section orientation and the frequency-encoding gradient were parallel to

the plane of the TMS coil. Under such optimised conditions, the left-hand side of Figure 3.2 shows signal intensity changes from transverse sections of the same phantom as in Figure 3.1 that are induced by the application of a single TMS pulse at variable times before the EPI sequence. The data reveal signal alterations for waiting periods after TMS of less than about 100 ms, which decrease in amplitude with increasing section distance from the TMS coil. It should be noted that such intensity variations are difficult to detect by inspection of individual images because visible image distortions only occurred for TMS pulses at 30–50 ms or less before the RF pulse.

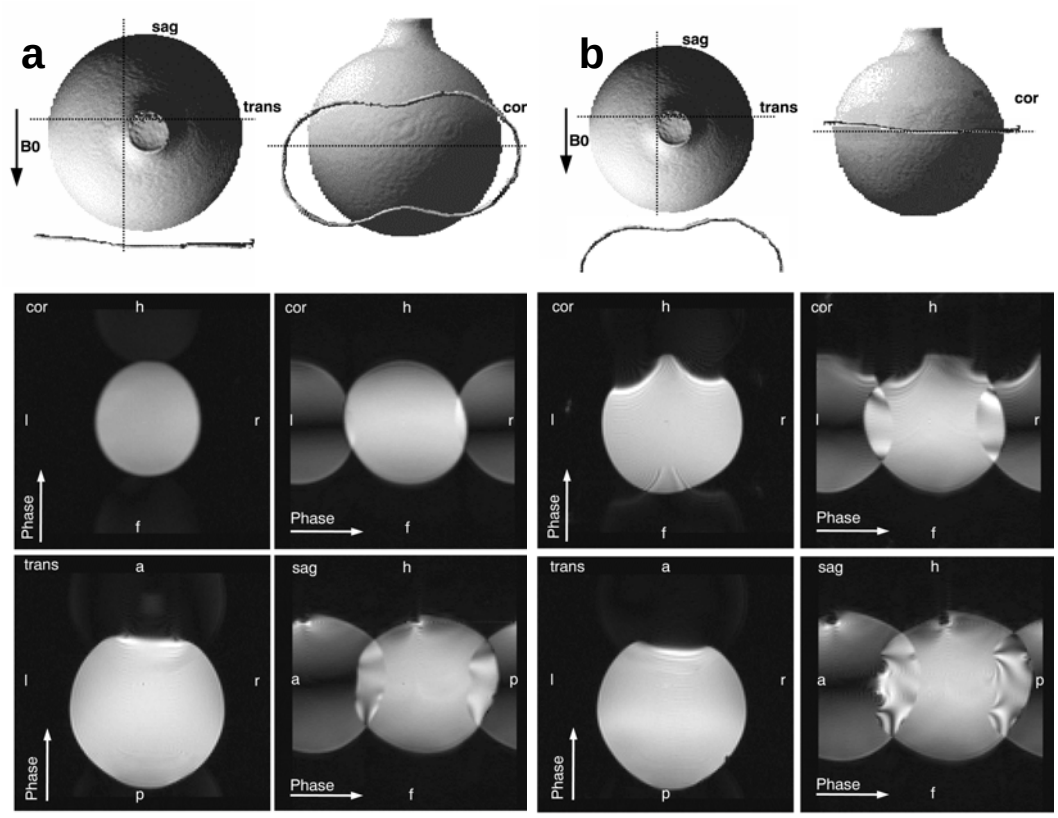


**Figure 3.1. (a) (top)** Top and frontal view of a spherical water phantom (surface reconstruction, 3D FLASH) with a transverse orientation of the figure-of-eight TMS coil (long axis 190 mm) highlighted by a water-filled plastic hose (arrow: static magnetic field, broken lines: EPI sections). With this coil configuration, the static magnetic field and TMS-induced magnetic field oppose each other. **(middle)** In coronal sections a switch of the frequency- and phase-encoding gradient largely reduces ghosting artefacts. **(bottom)** Transverse section at 6cm distance from the TMS coil and sagittal. **(b) (top)** Top and frontal view of a spherical water phantom with a coronal orientation of the TMS coil. At this orientation, the induced magnetic field runs perpendicular to the static magnetic field. **(middle)** Coronal section as well as **(bottom)** transverse section at 6 cm distance from the TMS coil and sagittal section. a: anterior, cor: coronal, f: foot, h: head, l: left, r: right, sag: sagittal, trans: transverse, Phase: phase-encoding gradient axis, p: posterior.

Complementary to these imaging results, a magnetic field gradient pick-up coil 2 cm underneath the TMS coil detected transient magnetic fields that lasted for up to 35 ms. These fields were attenuated when the distance of the pick-up coil from the TMS coil was increased to 4 cm or 6 cm, and enhanced for TMS coil orientations which resulted in magnetic fields opposing the static field of the MRI system and thus larger torques. In general, both the EPI artefacts and transient magnetic fields decreased in amplitude when the TMS intensity was reduced from 100% to 50% of maximum stimulator output.

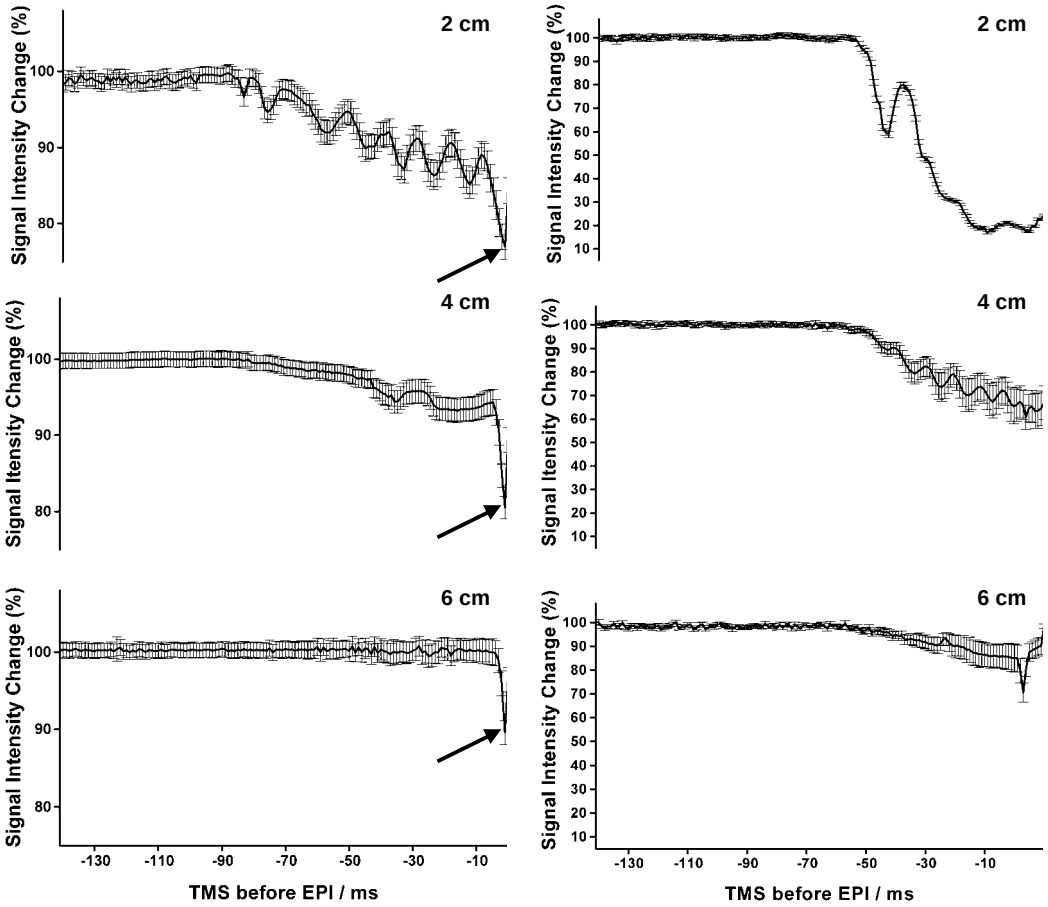


**Figure 3.2. (left)** EPI signal intensity changes (mean ± SD) from a central Region-of-Interest of transverse sections through the spherical phantom shown in Fig. 3.1 at 2 cm, 4 cm, and 6 cm distance from the TMS coil as a function of time (1 ms steps) between a single TMS pulse (100% stimulator output) and the EPI RF excitation pulse at 2T. For waiting periods of less than about 100 ms the data reveals signal fluctuations of up to 20% for the closest section which decrease with increasing distance. The arrows indicate the time of the fat-suppression pulse. **(right)** The same experiment at 3T. Compared to 2T, signal fluctuations increase dramatically as the TMS pulse approaches RF excitation for waiting periods of less than 50 ms. These signal fluctuations become evident approximately 70 ms prior to RF excitation. Note the near complete loss of signal directly underneath the coil for a 2 cm distance.

Similar results were observed at 3T. As depicted in the right-hand side of Figure 3.2, signal fluctuations and reductions are increased at 3T, resulting in near-complete signal loss in the direct proximity of the TMS coil when pulses are applied approximately 50 ms or less before RF excitation. These signal degradations attenuate with increasing distance between the TMS coil and EPI section, however, still being in the order of 20% at 6 cm distance (Figure 3.2 bottom right). As indicated by the arrows of Figure 3.2, direct interference with fat-suppression pulses leads to a frequency shift that translates into unwanted suppression of water protons and signal intensity dropouts. Noteworthy, as fat-suppression pulses are spatially non-selective, this in general affects the entire volume (not shown).

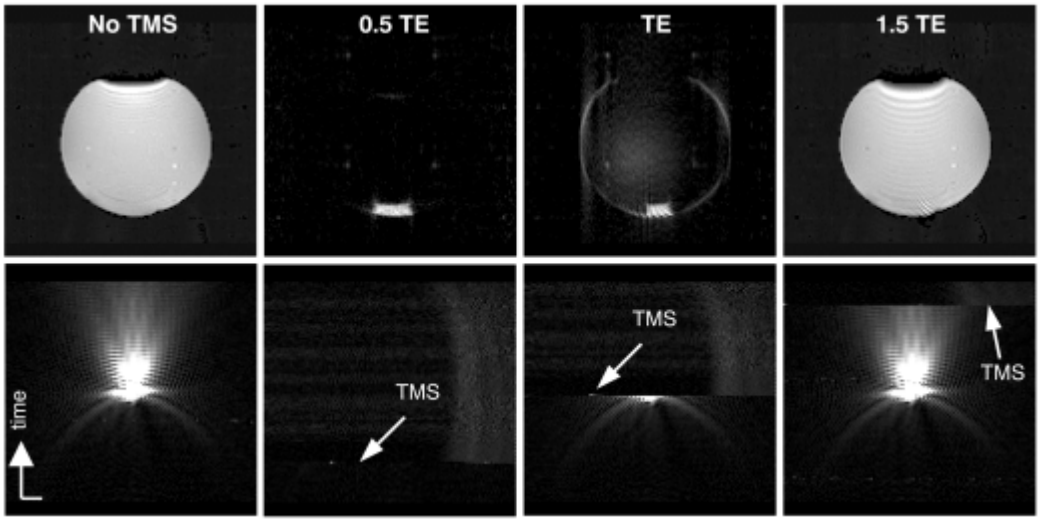


**Figure 3.3.** Effects of a single TMS pulse on **(top)** EPI and **(bottom)** corresponding raw data sets when applied at different times during data acquisition (mean TE = 53 ms, echo train length 113 ms) for a transverse section at 6 cm distance from the TMS coil at 2T (other parameters as in Fig. 3.2). Whereas TMS pulses cause dramatic signal losses during the acquisition of the first half of *k*-space, reasonable images may be obtained at later periods after scanning about 3/4 of *k*-space (1.5 TE).

The degrading effect of a TMS pulse during EPI is demonstrated in Figure 3.3 and Figure 3.4. Almost independent of the distance from the coil, the application of a TMS pulse during the first half of data acquisition, i.e. before the acquisition of the low spatial frequencies, causes a complete loss of signal. As evident from the raw data sets, the physical reason is an effective spoiling of all transverse magnetisations, i.e. gradient echoes, after the TMS

pulse. With increasing waiting periods after the onset of data acquisition, the resulting image quality gradually recovers to that obtainable without a TMS pulse. This holds true particularly for TMS pulses applied after recording about 3/4 of *k*-space at echo times greater than the mean TE. Although such TMS pulses still eliminate all residual gradient echoes, the images present with only minor high-frequency distortions.

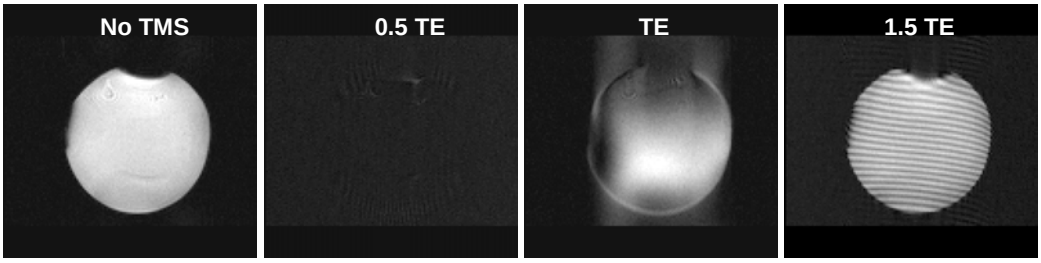


**Figure 3.4.** Effects of a single TMS pulse on EPI images when applied at different times during data acquisition (mean TE = 36 ms, echo train length 91 ms) for a transverse section at 6 cm distance from the TMS coil at 3T (other parameters as in Fig. 3.2). Images obtained at later periods after scanning about 3/4 of *k*-space (1.5 TE) still exhibit artefacts related to loss of the high frequency components of the image.

The direct interference of a TMS pulse with the RF excitation process not only corrupts the affected image, but also increases the signal intensity in subsequent acquisitions. As shown in Figure 3.5 and Figure 3.6, the duration and magnitude of respective EPI signal changes in successive images are dependent on the repetition time and flip angle, i.e. the degree of T1 saturation imposed onto the steady-state magnetization. They may reach amplitudes of up to 15% at 2T and last for up to 8 seconds for pronounced T1 saturation, e.g. TR = 1000 ms and 90°, and only about 1 second for spin-density weighted EPI, e.g. TR = 125 ms and 10°. Although quantitatively different, the signal changes display similar time-constants at 3T. It is important to emphasise that these effects are not necessarily visible as geometric distortions in individual images.

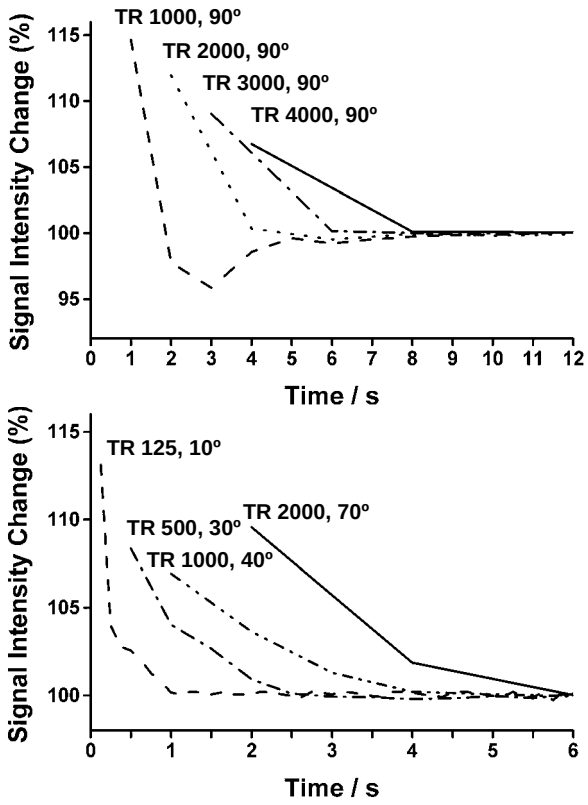


**Figure 3.5.** EPI signal intensity changes in successive acquisitions at 2T after application of a single TMS pulse during RF excitation of the first image (omitted) as a function of time for various repetition times TR **(top)** and flip angles **(bottom)** in a transverse section at 6 cm distance from the TMS coil (other parameters as in Fig. 3.2). Depending on the degree of T1 saturation the data reveal long-lasting signal fluctuations due to a disturbance of the steady-state longitudinal magnetization.

The persistent signal changes associated with TMS pulses synchronised to the beginning of an EPI sequence, i.e. close to RF excitation, pose a major problem for combinations with functional brain mapping. An example is shown in Figure 3.7 which compares activation maps obtained with and without TMS. In the absence of TMS, the finger-to-thumb opposition task activates M1 and the SMA in the sections shown. A single TMS pulse applied during RF excitation of the middle section in Figure 3.7 at the start of each finger-tapping epoch results in marked false-positive activations even when the single corrupted image is eliminated from the analysis. Pertinent effects mainly occur at contrast borders with cerebrospinal fluid (long T1).

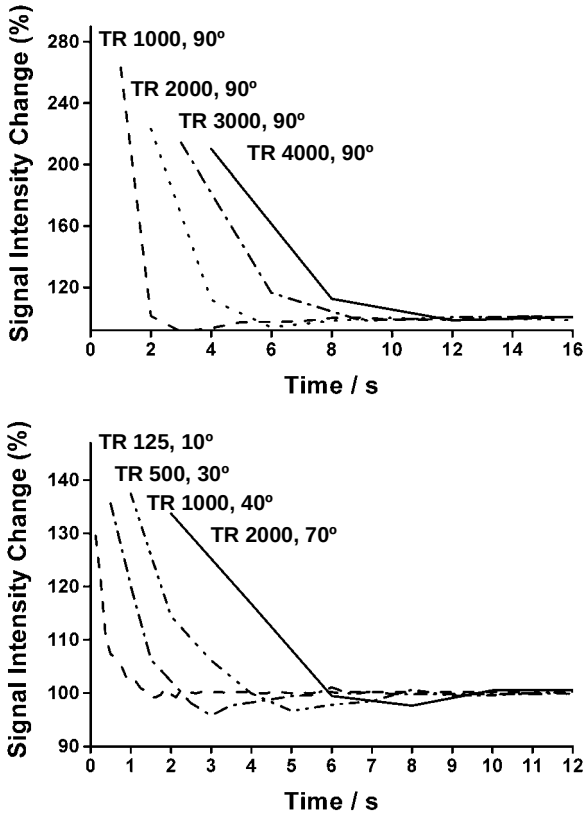


**Figure 3.6.** EPI signal intensity changes in successive acquisitions at 3T after application of a single TMS pulse during RF excitation of the first image (omitted) as a function of time for various repetition times TR **(top)** and flip angles **(bottom)** in a transverse section at 6 cm distance from the TMS coil (other parameters as in Fig. 3.2). Depending on the degree of T1 saturation the data reveal long-lasting signal fluctuations due to a disturbance of the steady-state longitudinal magnetization.

The fact that spatially, but not temporally, adjacent sections reveal similar false-positive activations supports the notion that the underlying mechanism is not due to the TMS pulse itself, but represents a longer-lasting disturbance of the steady-state magnetization concurrent with task performance.

As seen in Figure 3.8, an initial experiment carried out to assess the feasibility of interleaved fMRI and TMS at 3T revealed localised activity increases within the motor system similar to results obtained previously at 2T (BAUDEWIG ET AL., 2001). Here, special care was taken to not interfere with RF excitation or data acquisition. This illustrates for the first time that TMS can successfully be applied within higher field MR systems when taking the aforementioned precautions regarding imaging artefacts. At 3T, similar false-positive

activations were evoked when a single TMS pulse was applied during RF excitation (not shown).

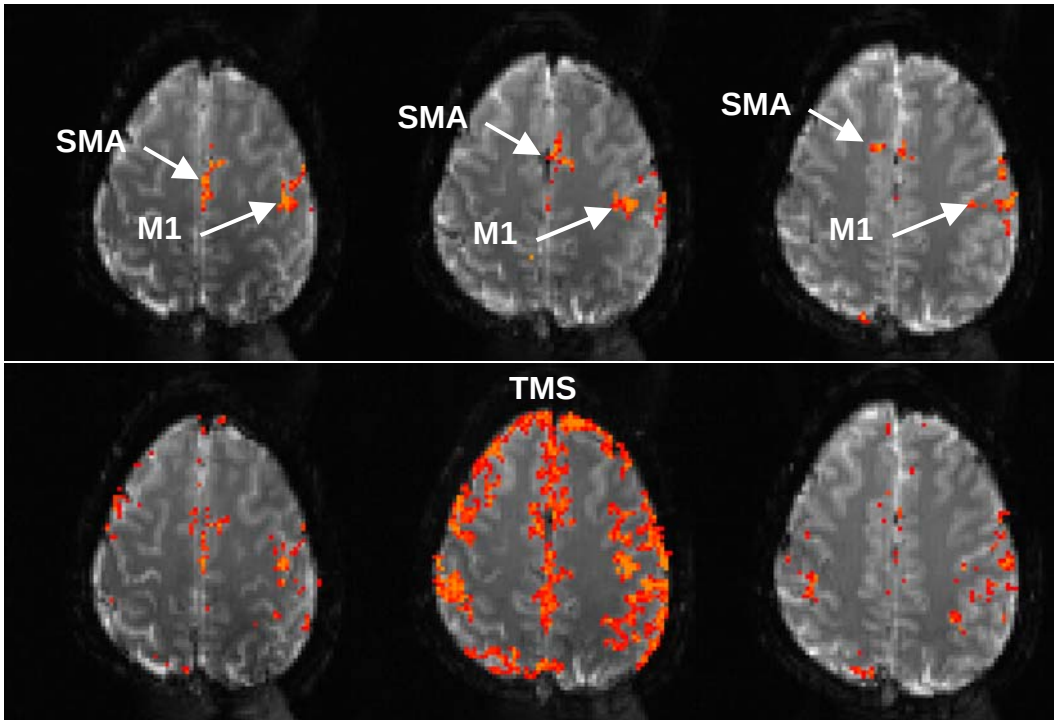


**Figure 3.7.** Functional activation maps (3/8 neighbouring sections) for a sequential finger-to-thumb opposition task obtained **(top)** without and **(bottom)** with TMS. A single TMS pulse during RF excitation of the first set of multi-slice images in each finger-tapping epoch (affecting the middle section only) causes a task-related perturbation of the steady-state longitudinal magnetization which translates into false-positive activations. Due to imperfect slice excitation profiles, spatially adjacent image sections reveal more subtle biases.

The SNR (mean of ROI/ SD of background noise) was compared in the left and right M1/S1 as well as a frontomedial and a posteromedial ROI. Each ROI comprised 125 pixels from a slice cutting through the hand knob of M1/S1. In each ROI, SNR was measured from three image during stimulation periods (120% RMT) and during rest. For example, in ten subjects that participated in the study reported in Chapter 6, the SNR was slightly larger at rest as compared to stimulation epochs in all four ROIs (mean ± SD left M1/S1: 96.87 ± 4.19 vs. 91.22 ± 3.62; right M1/S1: 88.71 ± 4,89 vs. 82.26 ± 4.34; frontomedial: 96.38 ± 4.26 vs. 92.25 ± 3.21; posteromedial: 95.11 ± 4.23 vs. 89.01 ± 4.15. This indicates that slight decreases in signal-to-noise levels of approximately 6% occurred during rTMS, yet were not necessarily most pronounced in the area of stimulation.

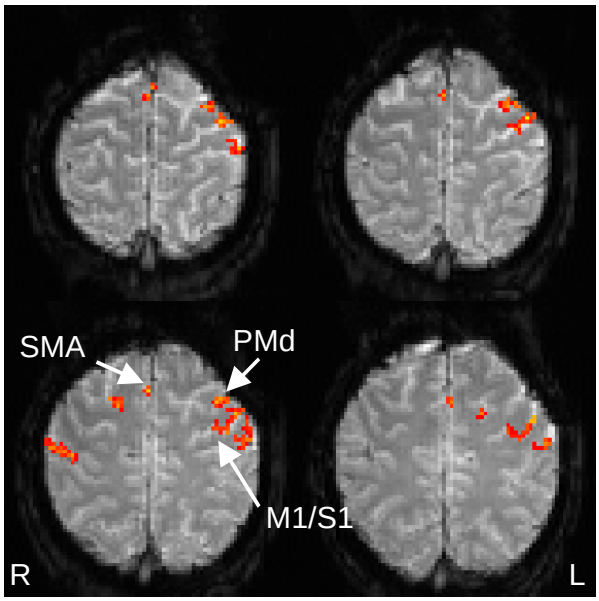


**Figure 3.8.** Combined TMS-fMRI at 3T (2 x 2 x 4 $mm^3$ spatial resolution). Four adjacent brain sections of a single subject showing activation obtained for suprathreshold rTMS (120% resting motor threshold, 2 Hz, 10 s) over the left M1 hand area (control period 20 s). Suprathreshold TMS evoked responses in M1, SMA and PMd in agreement with the results obtained by BAUDEWIG ET AL., 2001. The results provided the first demonstration that combined TMS and fMRI is feasible at 3T. R: right, L: left.

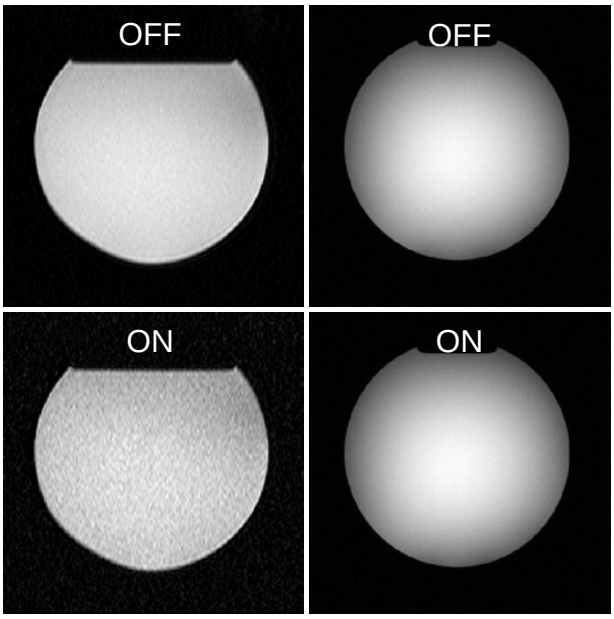


**Figure 3.9.** Comparison of static imaging artefacts resulting from the antenna properties of the connecting cable of the TMS coil and the RF noise emission of the TMS machine at 1.5T **(left)** and 3T **(right)**. With the machine switched off, RF interference can be seen at 1.5T, revealed as grainy structures in the MR image. At 3T, no interference is evidenced, indicating that RF noise transmitted into the scanner via the connecting cable is unlikely to interfere with the resonance frequency at 3T (center frequency 123.234 MHz). RF interference is even worse at 1.5T with the TMS machine switched on, while no such artefacts are prominent at 3T.

The comparison of RF noise interference at 1.5T and 3T revealed profound signal distortions at 1.5T, indicating the transmission of RF at the resonance frequency (~84 MHz) into the scanner room via the antenna-like properties of the connecting cable (Figure 3.9). At 3T, however, no such interference was observed, regardless of the TMS machine being switched on or off.

## 3.4 Discussion

This chapter provides a detailed analysis of TMS-related MRI artefacts that leads to solutions for a successful combination of both methods in a simultaneous approach. The chapter therefore extends previous work (SHASTRI ET AL., 1999; BAUDEWIG ET AL., 2000) and, in addition, transfers the acquired knowledge to higher field strength by providing the first functional images at 3T.

In particular, it was confirmed that combinations of TMS and EPI benefit from a parallel arrangement of the TMS coil plane with both the MRI section orientation and the frequency-encoding gradient. Because such ideal geometric conditions are seldom applicable for successful stimulation of the cortex, the use of oblique TMS coil orientations is expected to enhance image distortions. In general, such considerations together with EPI safety restraints and the need for multi-slice volume coverage seem to limit the degrees of freedom for a placement of the TMS coil.

The comparison of static image artefacts at 2T and 3T suggests that improvements in coil design carried out to accommodate the increasing mechanical forces at 3T strongly improve imaging quality. Furthermore, the results indicate that the shorter echo-times and stronger read-out gradients at 3T outweigh the increased susceptibility to magnetic field distortions, and even allow for oblique slice orientations without additional image degradation. Whether further technical improvements such as better coil designs, more tolerable imaging sequences, or even faster imaging techniques will enhance the flexibility of combined TMS and MRI studies remains to be seen. The basic problem of all TMS and MRI combinations is

that the TMS pulse itself represents an extremely efficient spoiler gradient that eliminates all transverse magnetisations and asks for a complete separation of imaging sequences and TMS pulses.

A TMS pulse generates magnetic field fluctuations for up to 100 ms that originate from eddy currents in the TMS coil. The underlying mechanism is based on the torque a TMS coil experiences in response to a pulse discharge when the generated magnetic field and the $B_0$ field interact. This generates a rapid mechanical vibration of the coil easily noted as a "click" sound. The torque and therefore also the loudness of the sound increase in the static magnetic field of the MRI scanner, and in particular for orientations opposing the MRI ($B_0$) field. The following oscillating vibrations induce currents in the TMS coil by electromagnetic induction which, in turn, cause weak magnetic fields perpendicular to the TMS coil plane. This is also suggested by the periodicity of the signal fluctuations also shown in Figure 3.2. Without sufficiently long waiting periods, these transient fields modulate the imaging gradients of subsequent EPI sequences. The aforementioned explanation is in contrast to a previous suggestion that TMS-induced image degradations are due to eddy currents induced in the conducting structures of the MRI system (SHASTRI ET AL., 1999). In fact, the present understanding is strongly supported by the observation that both the strength of the transient magnetic fields measured directly by a pick-up coil and the image artefacts detected in subsequent EPI acquisitions decreased with increasing distance from the TMS coil. On the other hand, eddy currents in the scanner elements should affect the entire volume within the magnet bore, which is in contrast to the experimental behaviour observed here. It may be argued that the directly detected magnetic field fluctuations lasted for only 35 ms and therefore cannot account for all of the EPI impairments. However, this apparent conflict has to be ascribed to the limited sensitivity of the pick-up coil in comparison with the susceptibility of imaging gradients to even weak magnetic gradient fields. As revealed by Figure 3.2, signal fluctuations and degradations were substantially stronger at 3T, while the onset of their occurrence seemed to be slightly later (approximately 70 ms before RF excitation). This is attributable to

the expected stronger mechanical vibrations at higher field strength and indirectly strengthens the notion that vibrating oscillations of the TMS coil are responsible for the observed signal distortions. However, the application of a different TMS coil, TMS coil holder and different imaging sequences makes a direct comparison difficult. Nevertheless, the data emphasise the requirement to provide waiting periods of around 70-100 ms (when using maximal stimulation intensity of 100% stimulator output) in order to avoid the affliction of subsequent images.

With respect to the temporal relationship between TMS and EPI, either the TMS pulse itself or its accompanying magnetic field fluctuations will have different consequences. First, while waiting periods after TMS and before EPI of 50–100 ms may alter EPI signal intensities, periods of less than 30–50 ms cause geometric distortions. These values are dependent on stimulation intensity and TMS coil orientation, and will generally be large for high intensities and oblique TMS coil configurations. Second, during EPI, TMS pulses operate as efficient spoiler gradients that completely dephase transverse magnetisations and thus eliminate the residual echo train. Depending on which parts of the *k*-space acquisition are affected, the artefacts in Fourier space range from complete image corruption to complex modulations of the point-spread-function and the presence of mild blurring. Third, when affecting RF excitation, TMS pulses alter the steady-state longitudinal magnetization with severe consequences for serial imaging as used in functional brain mapping.

In conclusion, in order to minimise image artefacts, any direct interference of TMS and EPI should be avoided. Alternatively, the experimental design must allow for an unambiguous identification and elimination of perturbed images, as inappropriate timing of TMS pulses may not only degrade the quality of individual images but also cause dynamic signal fluctuations in serial acquisitions. Provided that proper synchronisation ensures a sufficient temporal decoupling, interleaved high-frequency TMS and multi-slice EPI will further develop into a useful tool for clinical and cognitive neuroscience.

The results depicted in Figure 3.9 furthermore point out the requirement for effective filtering of RF noise caused by the TMS probe at 1.5T. As initially addressed by SHASTRI and colleagues (SHASTRI ET AL., 1999), the insertion of a cable into the MR room can introduce RF-induced artefacts due to the antenna-like properties of the connecting cable. Upon careful inspection of their results, a relatively poor image quality is revealed, as evidenced by the *t*-maps or unprocessed images. This may result from the aforementioned problems (SHASTRI ET AL., 1999; BOHNING ET AL., 1999). Following this problem, filters were introduced to prevent transmission of RF noise into the MR environment. The disadvantage of such RF filters is the potential of further TMS pulse strength attenuation and TMS pulse shape distortion. It is important to emphasise that in the initial phase of this thesis these problems were not apparent, which is attributed to the utilisation of field strengths above 1.5T that make RF interference less likely. Indeed, a direct comparison of signal quality at 1.5T and 3T yielded no sign of image distortions in the presence of the TMS coil at 3T. This was true whether the TMS pulse generator was turned on or off. In contrast, MR images were significantly distorted at 1.5T as soon as the TMS coil was introduced into the MR environment and connected to the stimulator outside (Figure 3.9), thus indicating the requirement of appropriate RF filtering. Therefore, the data suggests that higher field strength might be favoured for combined TMS and fMRI with respect to static and dynamic imaging artefacts. On the other hand, the increased mechanical perturbations of the TMS probe and corresponding acoustic noise at higher field strength have to be taken into account with respect to the subjects compliance and possible confounding brain activations.

### 3.4.1 fMRI strategies for mapping TMS-induced cortical hemodynamics

The static image distortions resulting from susceptibility artefacts introduced by the TMS coil can lead to signal dropouts of up to 2 cm underneath the coil (BAUDEWIG ET AL., 2000). In human studies, these problems can be largely

avoided as the distance between the TMS coil which is placed tangentially to the scalp and the cortical target area usually exceeds 2 cm (BAUDEWIG ET AL., 2000).

Dynamic image distortions reflect the interference of TMS pulses with MRI signal excitation and detection during BOLD-sensitive echo-planar imaging. Using EPI, coverage of the entire brain is accomplished within a TR of typically 2 to 4 seconds. To avoid confounding effects of TMS on image quality, it is necessary to prevent the application of TMS pulses during imaging. An impressive example are the massive false-positive activations emerging when TMS pulses are applied during slice-selective RF excitation as shown in Figure 3.7. In order to accommodate the requirements of both rTMS and fMRI, three basic strategies emerge as feasible technical solutions:

A first approach employs the use of short trains of rTMS at high frequencies such as 10 Hz, while deliberately sacrificing those images that are acquired during the administration of the rTMS train. This strategy is demonstrated in Figure 3.10 and was originally chosen by BAUDEWIG and colleagues (2001). It benefits from the fact that BOLD responses exhibit a delayed maximum effect after about 4-6 seconds, so that perturbed images may be discarded from the analysis without afflicting images with relevant physiological information. The technique allows for high-frequency rTMS at the expense of restricted pulse train duration and/or MRI volume coverage.

Second, rTMS and fMRI may be completely separated in time (Figure 3.11). Here, the whole volume is acquired before applying TMS pulses. For example, within a given TR, a submaximal number of sections is imaged without any temporal gaps. The remaining time of the TR can be used for TMS pulse application. This approach completely avoids TMS pulse – MR image interference and therefore reduces the risk of artefact induction while allowing high-frequency stimulation. However, this is at the expense of pulse train duration and / or MRI volume coverage.

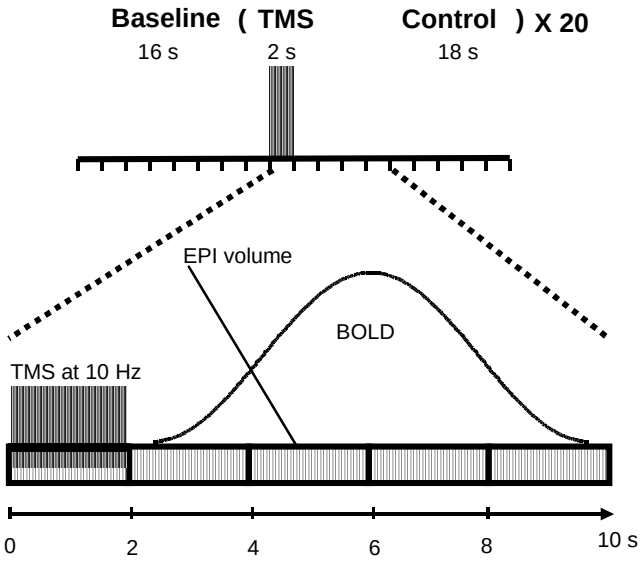


**Figure 3.10.** Schematic outline of an event-related TMS-fMRI protocol using rTMS epochs of 2 s duration (10 Hz, 20 pulses) and control periods of 18 s in conjunction with multi-slice single-shot EPI (TR = 2000). Although TMS results in image destruction of a whole EPI volume, subsequent volumes remain unperturbed, so that TMS-induced BOLD responses are fully detected because of their hemodynamic delay.

Finally, TMS and fMRI may be interleaved and synchronised. Though technically more difficult to implement, this offers stimulation over longer periods while minimising imaging artefacts (e.g. ~10 seconds, see Chapters 4-7). Because of the requirement to separate TMS pulses from MR image acquisitions for up to 100 ms, this approach is limited to rTMS at frequencies on the order of 1-5 Hz. For example, as shown in Figure 3.12, TMS pulses may be applied every 500 ms for 12 s. Thus, the maximum stimulation frequency is limited by the number of sections required for coverage of the respective brain region.

Summarising the technical requirements, there is a trade-off between optimal fMRI and rTMS protocols. High-frequency TMS requires to decrease the spatial resolution, increase the TR, or introduce spatial gaps between sections in order to achieve sufficient brain coverage. Furthermore, stimulation epochs are limited in time in order to avoid substantial loss of data, thus imposing the use of an event-related TMS-fMRI design for this approach. On the other hand, if high spatial resolution and large brain coverage is important, or longer stimulation epochs are desired, rTMS can only be applied at relatively

low frequencies of approximately 4 Hz. Consequently, this approach is suitable for application of the block design.

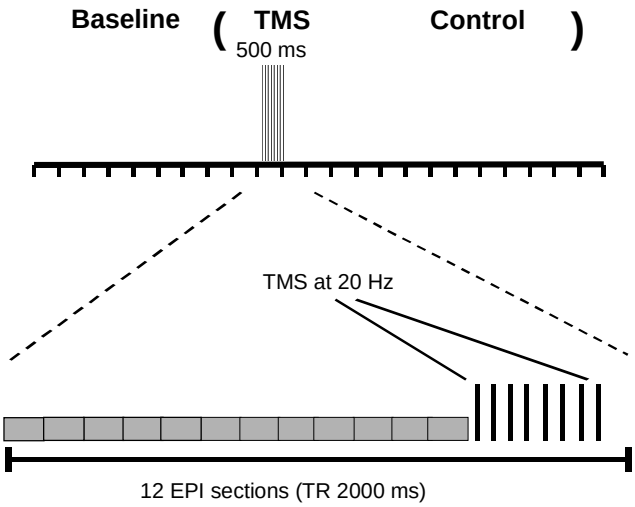


**Figure 3.11.** Schematic outline of an TMS-fMRI protocol using short trains of high-frequency TMS over a period of 500 ms (20Hz) following EPI volume acquisition (TR = 2000, 12 sections). This protocol completely separates TMS and EPI, however, only allows for application of short stimulation trains.

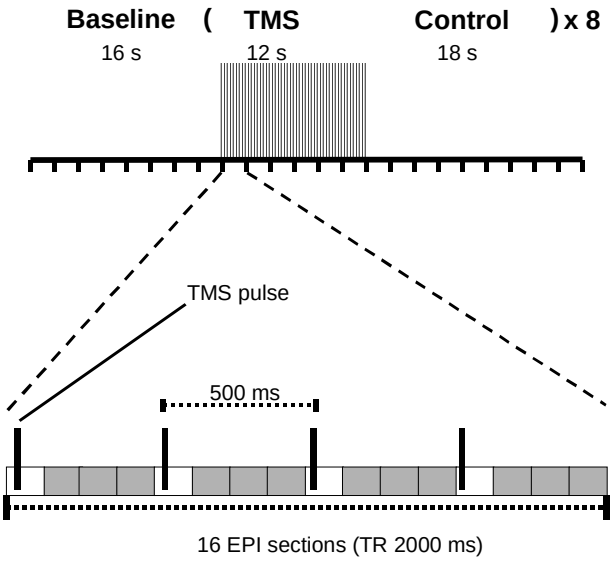


**Figure 3.12.** Schematic outline of an interleaved TMS-fMRI protocol using single TMS pulses for a period of 12 s (2 Hz, 24 pulses) synchronised to EPI (TR = 2000, 16 sections). The protocol perturbs every fourth section and therefore restricts TMS applications to low frequencies.

### 3.4.2 Other considerations

Since the initial reports of BOHNING ET AL. (1997, 1998), a number of combined TMS-fMRI studies have demonstrated the technical feasibility of

applying rTMS during functional MRI. Although cortical stimulation protocols need to be adapted to the scanning parameters and vice versa, event-related or interleaved strategies ensure successful brain imaging at the expense of some flexibility of the experimental procedures, e.g. with respect to volume coverage. Several technical issues remain to be optimised.

One of the strongest limitations for combined TMS-fMRI is imposed by the limited space in the MR scanner. This requires the design of smaller MR-compatible TMS coils. These would increase the accessibility of cortical areas to be stimulated within the restricting geometry of an MRI head coil. At present, certain brain regions, such as the frontal and posterior parietal lobe, remain difficult to access with TMS during fMRI. This holds especially true for head-scanners that generally have smaller head coils than whole-body systems.

There is some controversy regarding the generation of torques upon firing TMS pulses in the MR environment. Shastri and collaborators (SHASTRI ET AL., 1999) previously mentioned that torques are generated when an imbalance in magnetic field strength around the lobes of the TMS coil occurs, and that only figure-of-eight coils might be used due to a supposed cancellation or balancing of torques. From the data presented here and the experience and observations obtained through the development of the method, it seems clear that neither is a sufficient explanation. In principal, the torques are generated due to the opposing magnetic fields of the scanner and the TMS coil.

As illustrated in Figure 3.13, the resulting torques are nearly zero when the coil is held in the isocenter of the magnet with perfectly symmetrical orientation of the coil perpendicular to $B_0$ (assuming a perfect TMS coil design which does not introduce inhomogeneities of the induced magnetic field). When the TMS coil is tilted, a static magnetic field gradient will be present along the TMS coil, and therefore a gradient $\delta t$ in the induced torque will be generated along the TMS coil. This is reflected in the increased discharge noise when using oblique TMS coil orientations. Finally, when placing the TMS coil parallel to the $B_0$ field, the induced torque gradient will

be maximal, as being reflected in profoundly amplified discharge noise and even stronger TMS coil movements. It should be noted that this holds true irrespective of the design of the TMS coil as long as coils are strengthened to withstand any possible torques. With regard to the subjects compliance, TMS coil orientations should be used that minimise the occurrence of torques.

Although a proper fixation of the TMS is advisable, it can be counterproductive in the case of coil holder vibrations following TMS pulse applications. When the coil is connected to a lever, TMS-induced mechanical vibrations and related eddy currents are likely to be amplified. Furthermore, the acoustic noise resulting from the discharge of the TMS coil is significantly amplified in a static magnetic field. At 3T, this noise becomes fairly uncomfortable and likely to induce temporary auditory threshold shifts. However, the high-frequency nature of the TMS pulse allows effective filtering and dampening by head-phones or ear-plugs and their use is strongly recommended. Following these precautions, all subjects participated in the experiments without major problems.

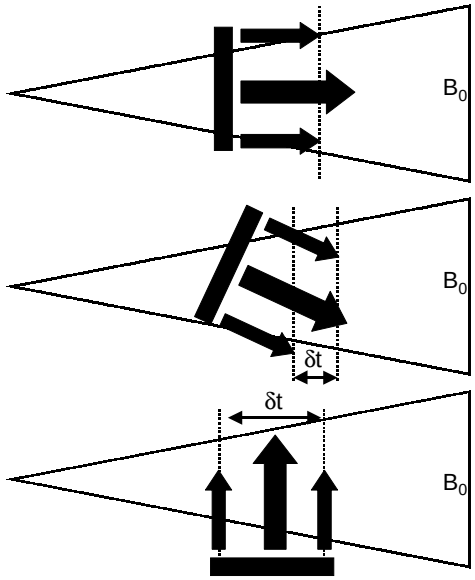


**Figure 3.13.** Schematic drawing of the interaction between the TMS-induced magnetic field and the static magnetic field ($B_0$). The figure-of-eight coil is indicated by the black bar, whereas the induced magnetic field is indicated by black arrows. **(top)** With coil orientations perpendicular to $B_0$, the torques imposed onto the TMS coil are relatively symmetrical. **(middle)** When using oblique TMS coil orientations, the opposing magnetic fields are not equally strong along the surface of the coil, thus increasing torques δt. **(bottom)** Parallel TMS coil orientations further increase δt, resulting in significantly amplified discharge noise and even visible TMS coil movements.

# 4 Subthreshold high-frequency TMS of human primary motor cortex interleaved with fMRI

## 4.1 Introduction

Since the original studies of Bohning and colleagues (BOHNING ET AL., 1997, 1998), an increasing number of studies have aimed to elucidate the cortical underpinnings of TMS by means of fMRI. Most of these studies have utilised low-frequency stimulation protocols of 1 Hz or less, and despite the widespread use of high-frequency rTMS to interfere with brain function, few studies have attempted to apply these protocols to MRI.

The advantage of low-frequency rTMS protocols lies in the relatively unperturbed acquisition of MR images (BOHNING ET AL., 1998, 1999, 2000a,b; NAHAS ET AL., 2001). On the other hand, high-frequency rTMS ( >1 Hz) has been widely used to induce a temporary functional lesion (PASCUAL-LEONE ET AL., 2000) or short-term plasticity (SIEBNER & ROTHWELL, 2003). Hence, a more detailed description of functional changes in the cortex as indexed by the BOLD MRI signal might reveal important insights into the underpinnings that mediate the interfering and conditioning effects of high-frequency rTMS. In an initial study during the early phase of this thesis, high-frequency rTMS (1 s, 10 Hz) was interleaved with fMRI by discarding perturbed images from the analysis (BAUDEWIG ET AL., 2001). However, as shown in Chapter 3, this increases the risk of direct TMS pulse-MRI sequence interference that may lead to long-lasting alterations of the longitudinal magnetisation and false-positive activations. Furthermore, it requires omission of images acquired during the stimulation period, therefore limiting this approach to relatively short stimulation epochs.

Evidence from TMS-PET studies reveals changes in rCBF following high-frequency rTMS in local and remote brain regions. For example, short trains of 10 Hz stimulation of the FEF not only elicits activity changes in the area of stimulation but even in superior parietal and medial parieto-occipital regions

know to be anatomically connected to the FEF (PAUS ET AL., 1997). Stimulation of the left dorsolateral prefrontal cortex at 10 Hz has been shown to reduce [$^{11}$C]Raclopride binding in the ipsilateral caudate nucleus selectively (STRAFELLA ET AL., 2001). Furthermore, several 10 Hz trains to the left medio-dorsolateral frontal cortex modulate brain activity in distinct fronto-cingulate circuits (PAUS ET AL., 2001), which is paralleled by changes in field-potential recordings in the rat following electrical stimulation (PAUS ET AL., 2001).

While combinations of TMS with fMRI have reported robust fMRI signal changes in the directly stimulated motor cortex after high-intensity stimulation exceeding individual motor thresholds (BOHNING ET AL., 1998, 1999, 2000a,b; BAUDEWIG ET AL., 2001), under these circumstances, neuronal processing of re-afferent feedback from activated hand muscles contralateral to the stimulated motor cortex yields substantial contributions to BOLD MRI signal changes (BAUDEWIG ET AL., 2001).

The primary aim of this study was therefore (i) to establish a strategy for performing high-frequency rTMS during BOLD-sensitive single-shot echo-planar imaging (EPI) which allows for a distortion-free and unrestricted visualisation of rTMS-induced changes in cortical haemodynamics, and (ii) to map the cortical activation patterns elicited by short trains of subthreshold high-frequency rTMS to the left M1/S1. To enable a better comparison with both previous rTMS-fMRI studies (BOHNING ET AL., 1998, 1999, 2000a,b; BAUDEWIG ET AL., 2001) and experimental conditions causing actual hand movements, the paradigms comprised suprathreshold rTMS and voluntary finger tapping as controls.

## 4.2 Materials and Methods

### 4.2.1 Subjects

Nine healthy subjects without any previous neuropsychiatric history (mean age 28 years, range 21-41 years; four females) participated in the study.

### 4.2.2 Experimental protocol

Each participant underwent four fMRI sessions in a counterbalanced order. Sessions were conducted in a block design comprising eight alternating cycles of an experimental condition (10 s) followed by a baseline condition (20 s). Three fMRI sessions applied rTMS at 110% of individual RMT, 110% of individual AMT, or 90% AMT, respectively. Motor thresholds were determined outside the magnet and again validated after the subject were positioned into the scanner. Whereas suprathreshold rTMS at 110% RMT leads to muscle twitches in the contralateral hand, the latter two intensities predominantly act on intracortical circuits (DI LAZZARO ET AL., 1998, 2002) without evoking myographic activity in peripheral hand muscles. To avoid carry-over effects caused by lasting changes in excitability of the stimulated left primary sensorimotor hand area, sessions were separated by approximately 10 min. In a fourth session, a sequential finger tapping task of the right dominant hand was performed to reliably identify M1/S1 and adjacent secondary motor areas. The task required sequential opposition of the thumb against the index, middle, ring, and little finger at a rate of 2 Hz. Movement epochs and speed were triggered by the discharging noise of TMS pulses at 15% of stimulator output, which is far below the lowest stimulation intensities reported to effectively target the motor cortex (FISHER ET AL., 2002). Otherwise, subjects were instructed to keep their eyes closed and keep their limbs relaxed throughout the experiment.

### 4.2.3 Magnetic resonance imaging

MRI was performed at 2.0 Tesla (Siemens Vision, Erlangen) using the parameters described in the experimental methods chapter.

### 4.2.4 Transcranial magnetic stimulation

TMS was applied following the details specified in the experimental methods chapter. No electromyographic activity from intrinsic hand muscles was recorded during scanning.

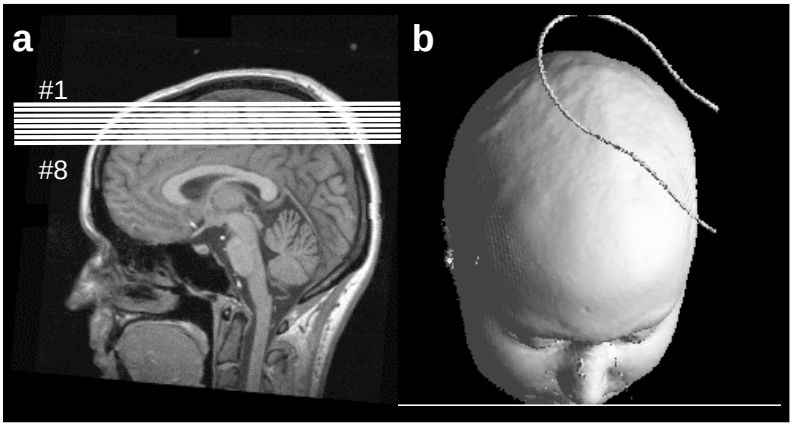


**Figure 4.1.** Experimental set-up. **(a)** Sagittal T1-weighted MR image indicating the sections selected or functional MRI of the primary sensorimotor cortex and adjacent secondary motor areas. **(b)** Surface reconstruction of the subject's head from a three-dimensional anatomical data set. The position of the TMS coil with respect to the skull is indicated by the contours of a water-filled plastic-hose attached to the TMS coil.

### 4.2.5 Interleaved rTMS–fMRI

The section orientation and TMS coil position is shown in Figure 4.1 and the basic experimental protocol followed a block design as illustrated in Figure 4.2. After acquisition of an initial baseline of 16 s (8 EPI volumes each representing the acquisition of 8 sections within 2 s), the protocol comprised 8 cycles of a rTMS or finger tapping epoch of 10 s duration (5 volumes) followed by a 20 s period of motor rest (10 volumes). As previous studies reported that recording of distortion-free images requires waiting periods of at least 100 ms after each TMS pulse (SHASTRI ET AL., 1999; CHAPTER 3), a stimulation frequency of 4 Hz was chosen, so that unperturbed images could be acquired every 250 ms. TMS pulses were applied immediately after the end of each image acquisition (EPI duration 113 ms) yielding an effective waiting period between TMS pulses and subsequent image acquisition of 137 ms. In cases where a suboptimal relative orientation of the TMS coil plane to the EPI slice-selective and frequency-encoding gradients caused local field distortions (BAUDEWIG ET AL., 2000; CHAPTER 3), the MRI section orientation was slightly re-adjusted until a reasonable image quality was obtained.

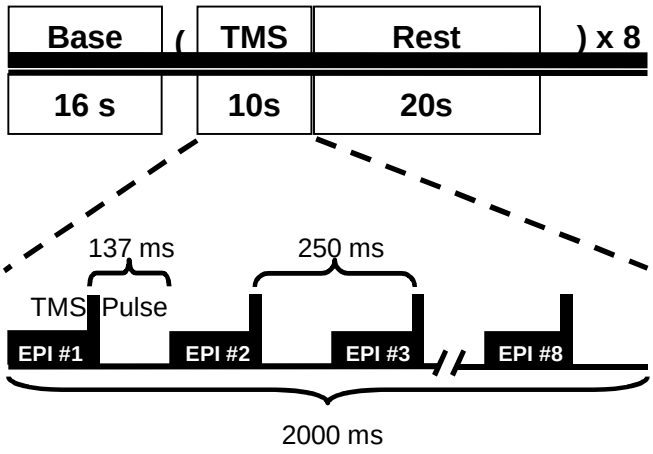


**Figure 4.2.** TMS-fMRI protocol. Repetitive TMS was conducted in a block design (8 cycles) alternating rTMS epochs (4 Hz, 10 s) with periods of motor rest (20 s). Repetitive TMS intensities investigated were 110% RMT, 110% AMT, and 90% AMT. Individual EPI acquisitions lasted for 113 ms, while images were acquired every 250 ms. With TMS pulses applied directly after termination of an EPI sequence, the procedure yielded 137 ms waiting periods prior to a subsequent image acquisition.

### 4.2.6 Data analysis

In the present study, we employed a descriptive analysis of individual BOLD MRI signal changes. This approach allowed us to assess between-subjects variability in cortical activity patterns and to detect subtle changes in BOLD MRI signal at high spatial resolution.

EPI raw images were carefully inspected for signal distortions due to inadequately timed TMS pulses. Data preprocessing included 2D motion correction across scans by spatially realigning functional images to the first image of a serial acquisition (BrainVoyager 4.8, Brain Innovation, Maastricht, The Netherlands) followed by linear drift removal. Individual task-related BOLD responses were analysed as described in the general methods section, using a correlation analysis approach (BAUDEWIG ET AL., 2003).

For group level analysis, the mean number of activated pixels averaged across subjects was obtained in *a priori* anatomically defined regions-of-interest (ROI) for all conditions (see below). The same ROI definitions were used to elucidate mean BOLD MRI signal intensity time courses. To facilitate the procedure, the EPI-derived activation maps at 2 x 2 x 4 $mm^3$ resolution were spatially filtered to isotropic 3 mm resolution and co-registered with the

individual 3D anatomical scans. The ROI for M1/S1 was positioned around the central sulcus at the location of the identified landmark of the hand area (YOUSRY ET AL., 1997) at which primary motor and primary sensory cortex interdigitate (WHITE ET AL., 1997). The anterior and posterior borders extended from the centre of the lateral surface of the precentral gyrus to the centre of the lateral surface of the postcentral gyrus.

The location of the SMA at the dorsal medial wall was divided into a posterior part, commonly referred to as SMA-proper, and an anterior part, described as pre-SMA (PICARD & STRICK, 1996, 2001). The border between pre-SMA and SMA-proper was defined by a plane perpendicular to the AC-PC line at the level of the AC and the posterior border was defined by the paracentral lobule (PICARD & STRICK, 1996). The anterior border of the pre-SMA was located at the level of the genu of the corpus callosum. The inferior border of both SMA-proper and pre-SMA was marked by the cingulate gyrus. For the ROI analysis, a single midline region was selected for SMA-proper and pre-SMA, as activations from right and left SMA often overlapped at the chosen spatial resolution.

The rostral border of the lateral premotor cortex (LPMC) was defined by the coronal plane perpendicular to the most rostral part of the genu of the corpus callosum. The posterior limit of LPMC was marked by the centre of the lateral surface of the precentral gyrus, directly adjacent to the ROI of the M1/S1. While the medial extent was limited by the ROI of the SMA, its lateral extent was arbitrarily restricted by the ROI of M1/S1.

Values of percent signal change were averaged across subjects and based on the mean difference of MRI signal in each experimental and baseline condition for each subject. Identification of significant changes in MRI signal time courses were computed using one-way analysis of variance (ANOVA) and post-hoc pairwise comparisons with the experimental condition as within-group factor and correction for multiple comparison.

## 4.3 Results

No adverse effects were reported by any of the subjects. One subject was excluded from data analysis because of pronounced EPI ghosting artefacts that extended into anterior motor areas. Stimulation thresholds varied between 56% and 89% of stimulator output. On average, repetitive TMS motor thresholds were 3.5% lower than thresholds obtained for the application of single TMS pulses.

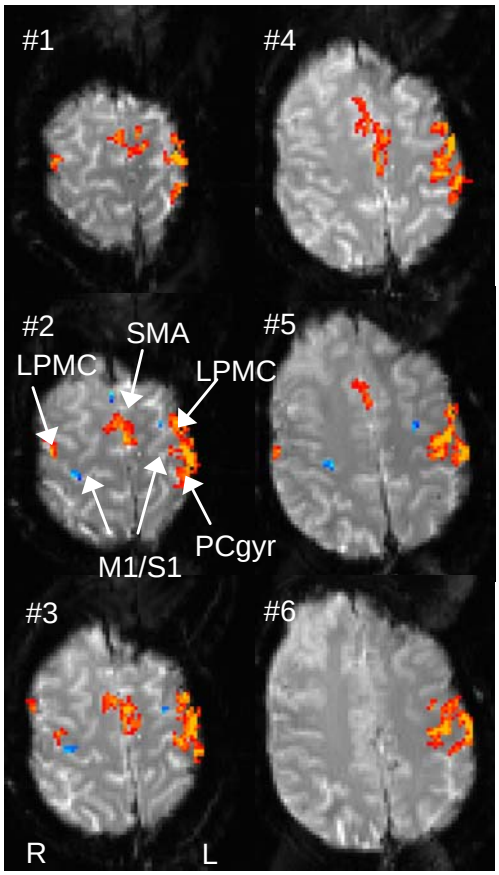


Figure 4.3

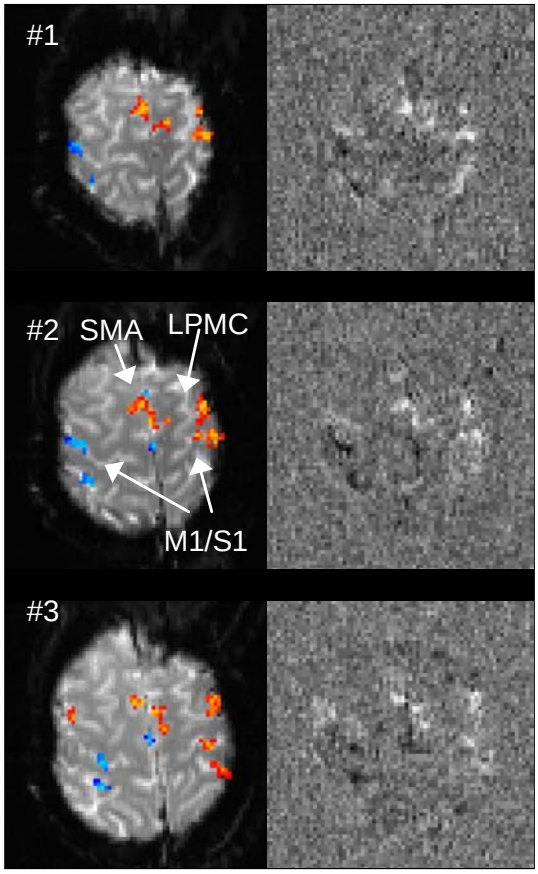


Figure 4.4

**Figure 4.3.** Activation maps (6 sections) of a representative subject obtained for right-hand finger tapping. Positive and negative BOLD MRI signal changes are coded in red-yellow and blue, respectively. Finger tapping at a rate of 2 Hz was cued by discharging the TMS coil at 15% of stimulator output. LPMC: lateral premotor cortex, SMA: supplementary motor cortex, M1/S1: primary sensorimotor cortex, PCgyr: postcentral gyrus, L: left, R: right.

**Figure 4.4. (left)** Activation maps (3 sections, same subject as in Fig. 4.3) and **(right)** corresponding unthresholded maps of correlation coefficients obtained for suprathreshold rTMS (110% RMT) over the left M1/S1. For other parameters see Fig. 4.3.

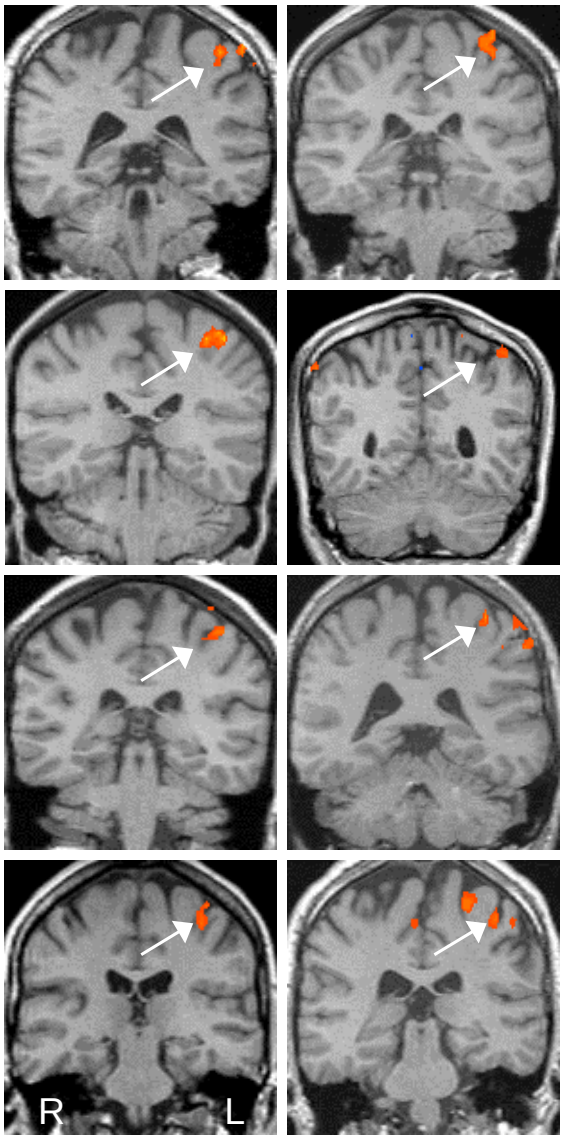


Figure 4.5

**Figure 4.5.** Individual activation maps (coronal sections, 8 subjects) obtained for suprathreshold rTMS (110% RMT) over the left M1/S1. Image sections were selected to cover the respective activation centres within the left M1/S1 after retransformation of the maps to 3 mm isotropic resolution in accordance with the individual three-dimensional anatomy. Except for one subject, activations were located within the hand region of the central sulcus. For other details see Figs. 4.2 and 4.3.

### 4.3.1 Finger tapping

Sequential right-hand finger tapping led to pronounced activations in bilateral M1/S1, LPMC and SMA in 8/8 subjects. As shown for a representative subject in Figure 4.3, activation maps of task-related BOLD MRI signal increases (coded in red-yellow) corresponded to previously reported activity patterns induced by similar finger tapping tasks (BOECKER ET AL., 1994;

KLEINSCHMIDT ET AL., 1997; BAUDEWIG ET AL., 2001; DECHENT & FRAHM, 2003). The observation of BOLD MRI signal decreases in ipsilateral M1/S1 (coded in blue) is in agreement with a recent fMRI study of phasic finger movements with the right dominant hand (HAMZEI ET AL., 2002). Quantitative results in terms of mean numbers of activated pixels averaged across subjects are summarised in Table 4.1 and Table 4.2 in comparison with corresponding data for rTMS conditions.

Table 4.1: Cortical activation volumes

| | rTMS over left M1/S1 at | | | | | | Finger Tapping | |
|---|---|---|---|---|---|---|---|---|
| | 110% RMT | | 110% AMT | | 90% AMT | | | |
| Region of Interest | POS | NEG | POS | NEG | POS | NEG | POS | NEG |
| Left M1/S1 | 90±27 | – | – | – | – | – | 294±31 | – |
| Right M1/S1 | – | 43±19 | – | 40±16 | – | 38±10 | 94±22 | 34±12 |
| Left LPMC | 39±17 | – | 20±5 | – | 22±6 | – | 109±28 | 10±8 |
| Right LPMC | 57±23 | – | 17±4 | 14±7 | 23±13 | – | 117±40 | – |
| SMA-proper | 172±63 | – | 38±20 | 13±7 | 61±15 | 18±9 | 374±70 | – |
| Pre-SMA | 18±9 | – | – | – | – | – | 32±15 | 12±5 |

Values are given as number of activated pixels (mean ± SD; averaged across subjects, *n*=8) representing BOLD MRI signal increases (POS) and decreases (NEG). Activations in two or less subjects with mean pixel numbers below 10 are not listed. M1/S1: primary sensorimotor cortex, LPMC: lateral premotor cortex, SMA: supplementary motor area, RMT: resting motor threshold, AMT: active motor threshold

Table 4.2: Number of subjects showing activity

| | rTMS over left M1/S1 at | | | | | | Finger Tapping | |
|---|---|---|---|---|---|---|---|---|
| | 110% RMT | | 110% AMT | | 90% AMT | | | |
| Region of Interest | POS | NEG | POS | NEG | POS | NEG | POS | NEG |
| Left M1/S1 | 7/8 | – | – | – | – | – | 8/8 | – |
| Right M1/S1 | – | 5/8 | – | 6/8 | – | 6/8 | 8/8 | 6/8 |
| Left LPMC | 4/8 | – | 5/8 | – | 5/8 | – | 8/8 | 2/8 |
| Right LPMC | 5/8 | – | 4/8 | 3/8 | 4/8 | – | 8/8 | – |
| SMA-proper | 7/8 | – | 3/8 | 4/8 | 5/8 | 3/8 | 8/8 | – |
| Pre-SMA | 2/8 | – | – | – | – | – | 3/8 | 2/8 |

Values represent number of subjects displaying activity in the respective experimental conditions shown in Table 4.1. For details see Table 4.1.

### 4.3.2 Suprathreshold rTMS

Activation maps that represent BOLD responses to interleaved TMS pulses were largely free from TMS-related artefacts (Figure 4.4, left column). This is even better demonstrated in the corresponding unthresholded maps of correlation coefficients shown in the right column. As the largest image distortions are to be expected for suprathreshold stimulation (Chapter 3), these maps prove that the experimental strategies developed for synchronising rTMS to multi-slice EPI resulted in reasonable image quality in all conditions.

Figure 4.5 summarises the central activations in M1/S1 obtained for suprathreshold rTMS for individual subjects. All subjects reported finger movements during stimulation. Coronal sections cutting through the activation centre in M1/S1 show that in 7/8 subjects suprathreshold rTMS evoked activations in left M1/S1 which extended into the depth of the central sulcus or were even exclusively located to it. Only in one case activations were centered in areas directly under the TMS coil. Additional activations were detected in SMA-proper, and, to a lesser extent, in left and right LPMC. Quantitative results for all regions and conditions are given in Table 4.1 and Table 4.2.

### 4.3.3 Subthreshold rTMS

Subthreshold rTMS was conducted at two different intensities, that is 110% AMT and 90% AMT. Neither intensity resulted in overt movements during rTMS and subjects noted no contractions in their right hand. In contrast to suprathreshold 4 Hz rTMS, no change in the BOLD MRI signal could be detected in the stimulated left M1/S1 during subthreshold 4 Hz rTMS (Figure 4.6, Table 4.1 and 4.2). However, as shown in Figure 4.6, subthreshold rTMS induced activations in the region of the SMA-proper in 5/8 subjects. In terms of number of activated pixels, subthreshold rTMS-induced activations in SMA were only about 29% and 13% of those obtained during suprathreshold rTMS at 110% of RMT and finger tapping, respectively (Table 4.1 and 4.2).

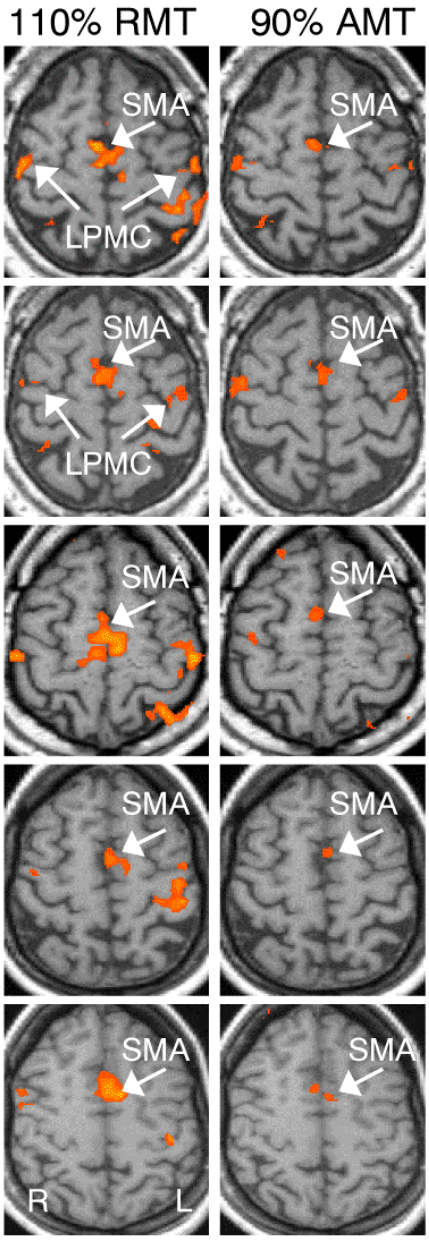


Figure 4.6

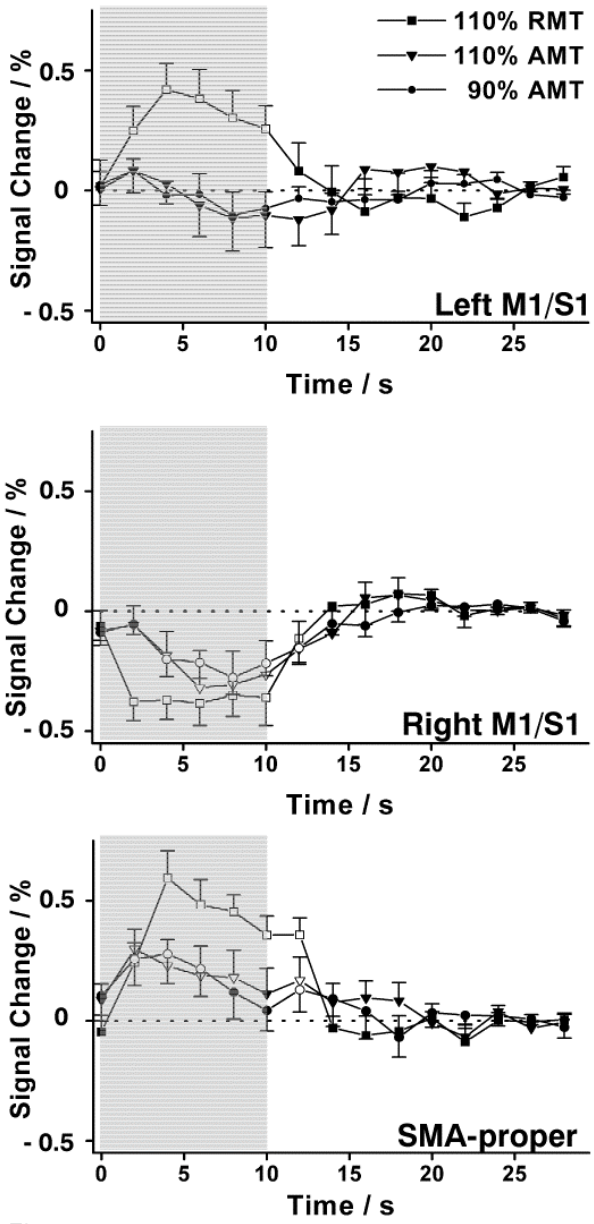


Figure 4.7

**Figure 4.6.** Individual activation maps (transverse sections, 5 subjects) obtained for **(left)** suprathreshold rTMS (110% RMT) and **(right)** subthreshold rTMS (90% AMT) over the left M1/S1. While suprathreshold rTMS evoked activations in M1/S1, SMA, and lateral premotor cortex, subthreshold rTMS elicited responses in SMA but not in the stimulated (left) M1/S1. Two subjects revealed additional responses in lateral premotor cortex. For other details see Figs. 4.2 and 4.3.

**Figure 4.7.** Mean time courses of BOLD MRI signal intensities averaged across subjects within anatomical regions-of-interest in left and right M1/S1 and posterior supplementary motor area (SMA-proper). Shaded areas mark stimulation periods with rTMS. Open symbols indicate significant difference from baseline ($P \leq 0.05$). Suprathreshold rTMS resulted in significant signal increases in left M1/S1 and SMA-proper. Subthreshold rTMS revealed no activations in the stimulated left M1/S1 but prominent signal increases in SMA-proper. Both sub- and suprathreshold rTMS evoked significant signal decreases in right M1/S1.

Furthermore, subthreshold rTMS led to a decrease in BOLD MRI signal in contralateral (right) M1/S1 in 6/8 subjects (Table 4.2). While the magnitude of this negative BOLD response was comparable across all rTMS conditions (Table 4.1 and 4.2), the onset of the decreases induced by subthreshold rTMS at 110 % and 90 % AMT was slightly delayed (Figure 4.7).

### 4.3.4 Time-resolved BOLD responses

Figure 4.7 illustrates the time courses of BOLD responses to sub- and suprathreshold rTMS in anatomically defined ROIs averaged across all subjects. In general, neither positive nor negative BOLD responses to rTMS resulted in temporal response patterns that deviated from the haemodynamic characteristics commonly associated with the cortical processing of other motor tasks or visual stimuli of similar duration.

Confirming the pattern revealed by the activation maps (Figures 4.3–4.6) and quantitative activation volumes (Table 4.1, 4.2), suprathreshold rTMS elicited significant increases in the BOLD MRI signal in left M1/S1 and SMA-proper as well as decreases in contralateral (right) M1/S1. In contrast, subthreshold rTMS evoked significant BOLD responses only in SMA-proper (i.e., signal increases) and contralateral M1/S1 (i.e., signal decreases) but not in the stimulated M1/S1.

## 4.4 Discussion

Using an effective strategy for synchronising TMS pulses with multi-slice EPI, the present study demonstrates the feasibility of artefact-free fMRI recordings of cortical haemodynamics that reflect high-frequency TMS-induced activations in distinct cortical areas of the motor system. A key finding was the modulation of BOLD responses remote from the site of stimulation in a cortical motor network comprising SMA-proper, LPMC and contralateral M1/S1 even at subthreshold stimulation intensities. Without provoked finger movements, this modulation could not have been due to afferent feedback from peripheral muscle twitches. Conversely, BOLD responses to

suprathreshold rTMS over the left M1/S1 predominantly represent cortical processing of re-afferent feedback from activated peripheral hand muscles.

Neuronavigational studies have demonstrated a good spatial correspondence between the cortical area activated in fMRI by a simple motor task and the area of magnetically evoked motor potentials (BOROOJERDI ET AL., 1999; MACDONELL ET AL., 1999). The spatial congruence of M1/S1 activations obtained for voluntary finger tapping and suprathreshold rTMS-induced finger movements therefore indicates that the experimental set-up successfully targeted the M1/S1 hand region during TMS.

### 4.4.1 Changes in BOLD MRI signal during subthreshold rTMS

The most important observation is the occurrence of subthreshold rTMS-induced BOLD MRI signal increases in LPMC and SMA-proper in 5/8 subjects as these responses cannot be explained by re-afferent feedback loops in the absence of evoked movements. The observed signal changes in LPMC are in accordance with previous studies that pointed towards effective modulation of premotor-primary motor cortical circuits by rTMS (SIEBNER ET AL., 2001a; CIVARDI ET AL., 2001; MUNCHAU ET AL., 2002). They are also in line with the known anatomical connectivity between LPMC and M1 (GEYER ET AL., 2000). The proximity of the LPMC to the site of stimulation raises the possibility that some of the observed effects could be caused by spread of the TMS excitation from M1/S1. However, previous studies suggest that this is highly unlikely at intensities around or below active motor thresholds (GERSCHLAGER ET AL., 2001; MUNCHAU ET AL., 2002).

The SMA-proper is densely interconnected with M1 (GEYER ET AL., 2000) which complements its functional involvement in the processing of relatively simple movement behaviour (TANJI ET AL., 1996). Here it is shown that subthreshold 4 Hz rTMS to the left M1/S1 can alter neuronal activity in the SMA-proper, presumably due to an activation of functional connections between M1 and SMA-proper. This notion would be consistent with the lack of remote BOLD MRI signal changes in the pre-SMA (Table 1) which is

densely connected with prefrontal regions but does not have strong connections to M1/S1 (RIZZOLATTI ET AL., 1996).

Despite the fact that projections from LPMC to M1 (MUNCHAU ET AL., 2002) and SMA-proper to M1 (SERRIEN ET AL., 2002) can be successfully targeted with low-intensity rTMS, it is not clear which circuits are responsible for the cortical changes distant from the site of M1/S1 stimulation. One possibility would be the activation of connecting fibres from M1 to SMA-proper (GEYER ET AL., 2000) and M1 to LPMC (STEPNIEWSKA ET AL., 1993). This implies direct stimulation of axons that anti/orthodromically produce synaptic activity at the distant sites. Given the low stimulation intensity, it may well be that subthreshold rTMS is below the threshold for direct stimulation of cortico-cortical connections. Alternatively, the effects of rTMS over the motor cortex are known to influence local activity, for example by altering the excitability in motor cortical circuits by changing membrane potentials (TOUGE ET AL., 2001), that in turn modulate ongoing activity in these connections.

The absence of significant signal changes in M1/S1 after subthreshold rTMS has been noted previously (BOHNING ET AL., 1999; BAUDEWIG ET AL., 2001). TMS at intensities above active motor thresholds excites corticospinal neurons by producing repetitive activity in excitatory intracortical neurons that result in high-frequency discharges (so-called indirect or I waves) in the pyramidal tract (for review see ZIEMANN & ROTHWELL, 2000). Intensities below AMT, however, do not evoke this type of activity (DI LAZZARO ET AL., 1998). Moreover, physiological studies suggest these intensities to affect low-threshold inhibitory elements that do not discharge repetitively (FISHER ET AL., 2002). Activation of these neurons should produce inhibitory synaptic activity within the primary motor cortex. However, recent studies have suggested a sigmoid relationship between synaptic activity and rCBF, indicating that low levels of synaptic activity are not necessarily accompanied by a corresponding increase in rCBF (MATHIESEN ET AL., 1998; NIELSEN & LAURITZEN, 2001; LAURITZEN & GOLD, 2003). Thus, the resulting net activity to low-intensity stimulation is possibly close to physiological background levels and not eliciting significant changes in BOLD MRI signal in the area underneath

the TMS coil. Because the effects of rTMS are strongly dependent on frequency, intensity, and duration of stimulation (MODUGNO ET AL., 2001), it is supposed that net changes in neuronal activity in the stimulated M1/S1 reported in previous PET studies most likely accrued from the application of prolonged trains of TMS pulses (>50 s).

Recent studies have demonstrated that in the rat cerebellar cortex up to 95 % of the blood flow increase depends on postsynaptic activity (MATHIESEN ET AL., 2000) and that the BOLD MRI signal is slightly better correlated to synaptically evoked local field potentials than to the spiking output of the area (LOGOTHETIS ET AL., 2001). These recent findings might help to explain the observed remote BOLD MRI signal changes by modulation of postsynaptic activity via direct activation of projecting fibres or indirect secondary modulation of interconnected brain regions, which would also be in line with observations that the absence of rCBF increases does not rule out significant neuronal activity (NIELSEN & LAURITZEN, 2001).

Taken together, the results support the notion that subthreshold rTMS is capable to modulate activity in directly connected brain regions, whereas areas not directly connected with the stimulated area are less likely targeted by subthreshold stimulation.

### 4.4.2 Changes in BOLD MRI signal during suprathreshold rTMS

The present findings are in accordance with previous TMS-PET and TMS-fMRI investigations of suprathreshold rTMS over M1/S1 revealing strong signal changes in M1/S1 and SMA-proper and at least in part of the subjects also in LPMC (PAUS ET AL., 1998; BOHNING ET AL., 1999, 2000a, 2001; SIEBNER ET AL., 2000, 2001a; KEMNA & GEMBRIS, 2003). In particular, activations in M1/S1 after suprathreshold rTMS were primarily found in the depth of the central sulcus or extended into its fundus concordant to activations induced by volitional finger movement. Because the magnetic field of the TMS pulse decays exponentially with distance from the TMS coil (JALINOUS, 1991), the strongest stimulation is to be expected directly under the coil. Thus, localised activity in the M1/S1 hand region cannot be attributed to a direct stimulation

of large vessels located on the outer convexity of the brain but reflects rTMS-induced modulation of cortical activity both due to direct excitation of cortical neurons and re-afferent feedback activation.

### 4.4.3 Negative BOLD responses in contralateral M1/S1

The detection of BOLD MRI signal decreases in right M1/S1 in all experimental conditions is a novel observation as far as subthreshold rTMS is concerned. Similar fMRI changes have only been noted after short trains (1 s) of suprathreshold rTMS (KEMNA & GEMBRIS, 2003). Using PET, decreases in rCBF contralateral to the stimulated M1 have been reported during inhibitory paired-pulse TMS (PAUS ET AL., 2001) and prolonged 1 Hz rTMS at suprathreshold intensity (FOX ET AL., 1997). It is tempting to speculate whether negative BOLD responses indeed reflect decreased neural activity, for example, originating from transcallosal projections of the stimulated M1/S1 to its contralateral homotopic part. Although little attention has been drawn on the origin of negatively correlated BOLD MRI signals, recent high-field fMRI studies strongly suggest that a decrease in BOLD MRI signal is due to active cortical inhibition (SHMUEL ET AL., 2002). On the other hand, inhibitory processes have also been reported to result in increased blood flow (LAURITZEN, 2001). Hence, the resulting activity changes after subthreshold stimulation might result from a net effect of modulated cortical activity patterns in secondary motor areas that lead to increases in blood flow and associated BOLD MRI signal in SMA-proper and LPMC, in conjunction with decreased blood flow and BOLD MRI signal in contralateral (right) M1/S1. The results underscore the capability of rTMS to modulate synaptic activity in interconnected regions even at intensities below corticomotor thresholds. Combined TMS-fMRI may provide a powerful tool to visualise TMS-induced cortical connectivity at high spatiotemporal resolution and help unravelling the physiological processes underlying TMS of the cortex.

# 5 Investigation of the context-dependence of responses evoked by transcranial magnetic stimulation in frontal motor areas

## 5.1 Introduction

Transcranial magnetic stimulation can interfere with the normal pattern of neuronal activity subserving perception, motor execution, or higher-level cognitive processes (JAHANSHAHI & ROTHWELL, 2000). This disruptive effect of TMS on cortical function is often referred to as a "temporary lesion" (PASCUAL-LEONE ET AL., 1999) and in recent years, the TMS lesion approach has become a prime tool to modern neuroscience for the investigation of causal relationships between behaviour and its underlying brain function (WALSH & RUSHWORTH, 1999).

Experiments that make use of this temporary lesion effect assume that if activity in a cortical area is essential for a task, then an appropriately timed magnetic stimulus will impair task performance. Sometimes it will be necessary to disrupt cortical activity for a longer period in order to provoke a temporary lesion. This can be achieved by applying a short train of rTMS at frequencies of 5 Hz or more. Despite its increasing use, the neuronal mechanisms that mediate the lesion effect of TMS are largely unknown. Possible mechanisms include (i) a transient synchronisation of neuronal activity of a large proportion of neurons under the coil, (ii) the induction of an activation of intracortical inhibitory circuits for 50-200 ms depending on stimulus intensity, and / or (iii) impaired functional cross-talk with interconnected areas by activation of cortico-cortical or cortico-subcortical interneurons (SIEBNER & ROTHWELL, 2003).

Several groups have demonstrated the feasibility of interleaving TMS with BOLD fMRI (BOHNING ET AL., 1998, 1999, 2000a,b; BAUDEWIG ET AL., 2001; KEMNA & GEMBRIS, 2003; MCCONNELL ET AL., 2003). Since the BOLD MRI

signal provides a sensitive means to detect changes in regional neuronal activity both in the stimulated area and interconnected brain regions, online fMRI during TMS holds great promise to advance our knowledge of how TMS interacts with ongoing neuronal activity in the intact human brain.

Previous interleaved TMS-fMRI studies have been concerned with TMS induced changes in cortical neuronal activity at rest, but fMRI has not yet been used to explore how TMS interacts with neuronal activity subserving a distinct cerebral function. This, however, is of considerable interest given the widespread use of TMS as a tool to induce a temporal lesion. Following up on previous work (BAUDEWIG ET AL., 2000, 2001; CHAPTERS 3-4), rTMS to the left M1/S1 was interleaved with fMRI to investigate task-related changes in regional neuronal activity during simple motor behaviour. A tonic precision grip task was chosen to provoke a constant level of voluntary pre-activation of the left M1/S1. Participants were required to perform a precision grip with their right hand and to maintain a pre-defined force level using visual feedback. A 10 second train of subthreshold 4 Hz rTMS was given either before or during the task and fMRI was used to visualise the impact of rTMS on motor activity. It was hypothesised that rTMS over M1/S1 would modulate activity patterns in primary and frontal motor areas generated by such a motor behaviour even in the absence of changes in task performance.

## 5.2 Materials and Methods

### 5.2.1 Subjects

Nine healthy subjects without any previous neuropsychiatric history (mean age 27 years, range 22-42 years; four females) participated in the study.

### 5.2.2 Experimental protocol

The study design consisted of four experimental conditions (Figure 5.1): (1) Tonic contraction (TC) alone, (2) subthreshold rTMS alone, (3) subthreshold rTMS during TC, and (4) subthreshold rTMS before TC. Using a block design, each condition was studied in separate fMRI sessions. Each experimental

condition was repeated eight times per session, and the order of experimental conditions was counterbalanced among subjects. In conditions 1-3, 10-second epochs of the respective experimental condition alternated with 20-second epochs of baseline (i.e. resting condition). In condition 4, 10-second epochs alternated between rTMS, tonic contraction, and rest in a fixed order. In condition 2-4, 320 TMS pulses were administered at 4 Hz and 90% of AMT. In condition (1), rTMS was applied at 15% of stimulator output only to match the auditory stimulation among conditions. At this intensity, the noise associated with the discharge of the coil was clearly audible without effective excitation of cortical neurons (FISHER ET AL., 2002; BESTMANN ET AL., 2004).

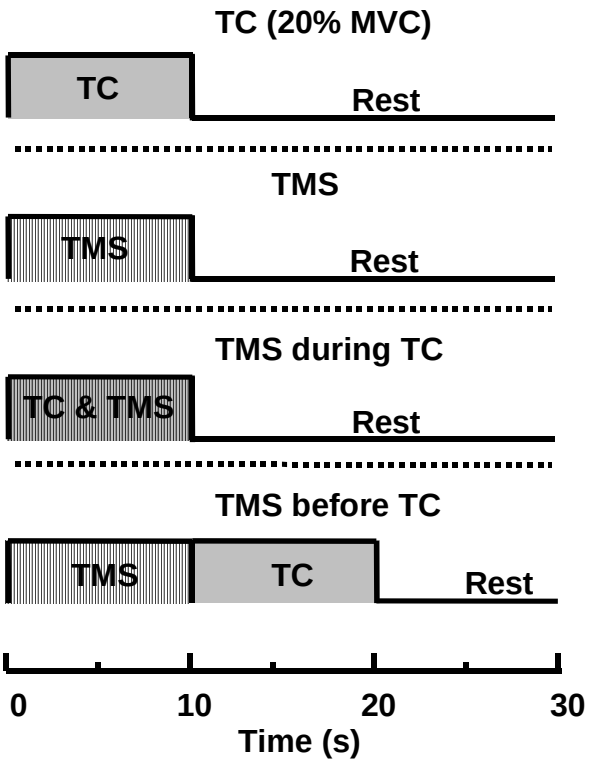


**Figure 5.1.** Schematic drawing of experimental protocol. Four imaging sessions were conducted in counterbalanced order. TC: tonic contraction at 20% of maximum voluntary contraction (MVC) using the right thumb and index finger, TMS: transcranial magnetic stimulation at 4 Hz and 90% AMT, TMS during TC: rTMS during tonic contraction, TMS before TC: rTMS prior to tonic contraction. For details of stimulation see text.

### 5.2.3 Magnetic resonance imaging

MRI was performed at 2.0 Tesla (Siemens Vision, Erlangen) using the parameters described in the experimental methods chapter.

### 5.2.4 Transcranial magnetic stimulation

TMS was applied following the details specified in the general methods chapter. No electromyographic activity from intrinsic hand muscles was recorded during scanning.

### 5.2.5 Interleaved rTMS-fMRI

TMS and fMRI was interleaved and synchronised in the same way as reported in Chapter 4.

### 5.2.6 Tonic contraction task

The motor paradigm was a tonic contraction task. Participants were required to squeeze an air-filled elastic plastic bulb with their right thumb and index finger for 10 s. The remaining digits of the right hand were immobilised by adhesive tape to restrict concomitant finger movements. Maximum grip force was assessed prior to the experiment and defined as the average force level during five 10 s periods of MVC. During the tonic contraction task, participants were required to maintain 20% of maximum grip force for 10 seconds. Special care was taken that rTMS did not evoke muscle twitches during contraction periods. The task started and ended with the appearance and disappearance of a horizontal line which was presented in the center of the subjects visual field. The horizontal line corresponded to 20% of individual maximum grip force. Participants received continuous visual feedback of the exerted force level (Figure 5.2, left panel). The force level was given as a moving vertical bar and subjects were asked to match the height of the bar to the horizontal line. Subjects were instructed to perform the task as accurate as possible. Participants were trained on the tonic contraction task outside the scanner until they could perform the task without difficulties.

Inside the scanner, subjects lay supine with their arms rested comfortably onto their sides, with near extension of elbows. A video beamer projected the visual stimuli onto a frosted screen mounted atop the head coil. Unrestricted view of the screen was achieved by an adjustable mirror system overlaying the subjects eyes.

### 5.2.7 Motor performance analysis

The plastic bulb which was squeezed by the subjects was connected to a DMP 343 force-transducer (DMT Druckmesstechnik GmbH, Welver, Germany) via an air-filled plastic hose (1 mm diameter). The force signal was digitised (LTC1290, LINEAR Technology, USA) at a sample rate of 10 Hz. For each contraction epoch, the mean force level and the coefficient of variation (SD / mean) of grip force were measured off-line and the correlation between force profiles and the stimulation protocol were calculated using Pearson's correlation coefficients. Grip force was normalised to the required force level.

### 5.2.8 Data analysis

Data analysis was conducted following the details specified in the experimental methods chapter.

For each of the 32 fMRI sessions (eight subjects, four sessions per subject), a GLM was computed that modelled the time course of experimental conditions convolved with a haemodynamic response function (BOYNTON ET AL., 1996). For statistical inferences at a group level a fixed-effects model was used. Three-dimensional group statistical maps were generated by associating each voxel with the F-value corresponding to the specified predictor and calculated on the basis of the least squares solution of the GLM. After specification of the GLM, differences between experimental conditions were assessed using appropriately weighted linear contrasts. BOLD MRI signals were compared during each experimental condition with the respective baseline condition (rest). Furthermore, more complex contrasts were specified which tested for differences in BOLD MRI signal changes between

experimental conditions. Corrected P values of < 0.01 were considered statistically significant.

In addition, signal time courses were obtained from *a priori* anatomically defined ROIs following the procedure described in Chapter 4. Three lateral ROIs were defined in each hemisphere: M1/S1, PMd, and the anterior portion of the IPS. Furthermore, two medio-dorsal ROIs were determined: SMA-proper and pre-SMA.

ROIs were determined following previously published demarcations of respective frontal motor regions. The M1/S1 hand area was defined around the central sulcus (WHITE ET AL., 1997; YOUSRY ET AL., 1997), and the PMd was defined as the region directly adjacent to M1/S1 (FINK ET AL., 1997; PICARD & STRICK, 1996, 2001; HLUSTIK ET AL., 2002). The SMA and pre-SMA reside at the medial wall of the prefrontal cortex (MUAKKASSA & STRICK, 1979) and were demarcated by a line perpendicular to the anterior commissure-posterior commissure (PICARD & STRICK, 1996, 2001). The ventral border was constituted by the cingulate or the paracingulate gyrus (PAUS ET AL., 1996), respectively. As activation centers in SMA often overlap at the chosen spatial resolution, the medial ROIs were collapsed into single midline ROIs.

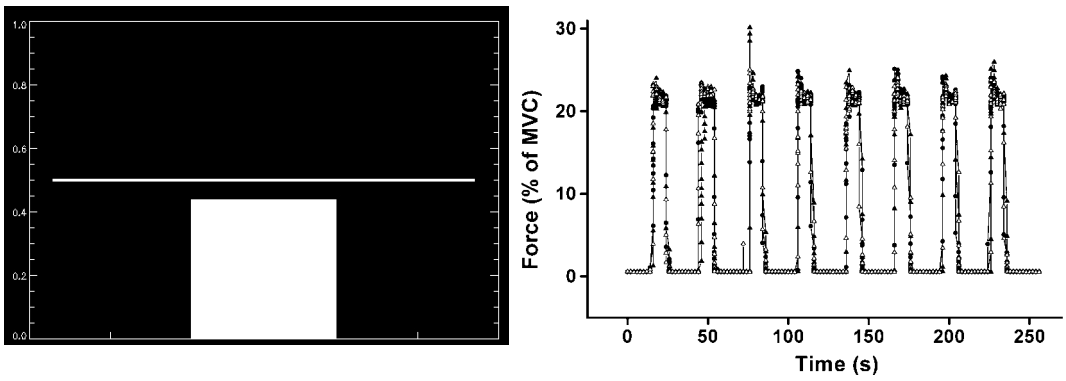


**Figure 5.2.** Visual stimulus and behavioural performance. **(left)** Example of the visual screen. Subjects were instructed to match a white column reflecting the force output with a horizontal line indicating the required force level. **(right)** Behavioural performance of a single subject. No differences in force profiles were found between tonic contraction (TC, black circle), TMS during TC (black triangle), and TMS before TC (white triangle).

## 5.3 Results

None of the subjects experienced any adverse side effects from stimulation. All but one subjects reported no overt muscle twitches during rTMS. This subject was excluded from the analysis. Stimulation intensities ranged from 58-79% of maximum stimulator output.

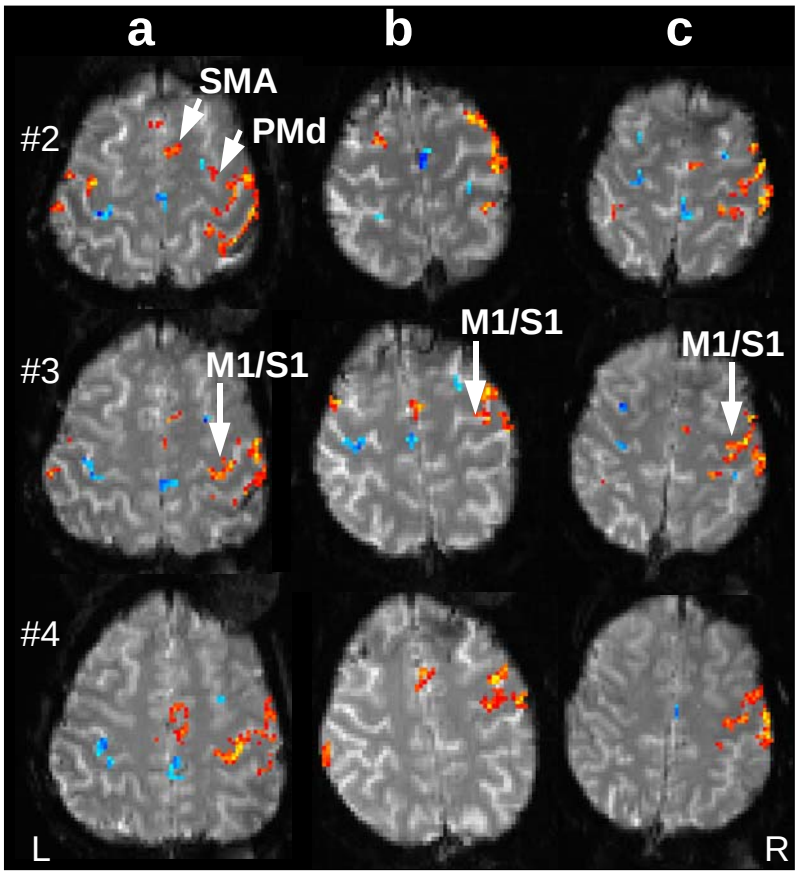


**Figure 5.3.** Three selected raw EPI axial sections from three subjects **(a-c)** showing activity changes subthreshold rTMS (4 Hz, 10 s) over the left M1/S1 during tonic contraction. Localised activity in response to contraction and rTMS was found within primary and secondary frontal motor regions. No indication of image perturbations in the regions of interest resulting from rTMS application are evident. M1/S1: primary sensorimotor cortex, SMA: supplementary motor area, PMd: dorsal premotor cortex, L: left, R: right.

### 5.3.1 Behavioural results

All subjects performed the task without any difficulties. Figure 5.2 illustrates grip force profiles in a representative subject. The mean grip force was 22.3 ± 4.3 % of maximal grip force across all sessions. Mean grip forces in the respective experimental conditions were: 21.6 ± 4.8 % MVC (TC alone), 22.3

± 3.7 % (TMS during TC), and 23.1 ± 2.9 % MVC (TMS before TC). The force profiles were highly correlated with the behavioural paradigm (from $r$ = 0.84 to $r$ = 0.93) and motor performance yielded similar coefficients of variation of motor behaviour (TC: 0.222, TMS during TC: 0.166, TMS before TC: 0.126). Differences among the three experimental conditions were excluded by pair-wise comparisons.

### 5.3.2 Magnetic resonance imaging

The brain images of three representative subjects shown in Figure 5.3 indicate that the quality of fMRI images was not affected by TMS pulses or static inhomogeneity artefacts caused by the transducing coil.

### 5.3.3 Neuronal activity during tonic contraction

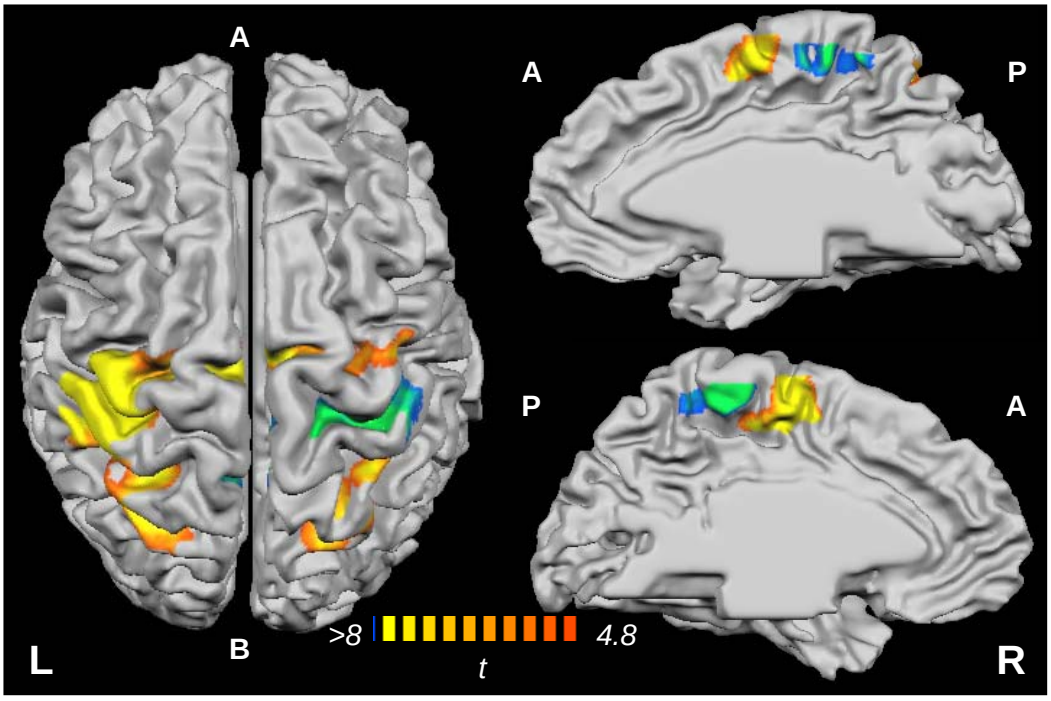


**Figure 5.4.** Main effect of tonic contraction of eight subjects. Colour scaling indicates significant regions showing activation (yellow-red) or deactivation (blue-green) when the tonic contraction task was compared to the baseline condition (P<0.01, corrected). The results are projected onto a 3D-template brain (MNI) in stereotaxic space. Force generation was associated with activity increases in left M1/S1, bilateral PMd, left anterior intraparietal region, bilateral superior parietal cortex, and bilateral SMA. Deactivations were found in right M1/S1 and bilateral posterior SMA. A: anterior, P: posterior, L: left, R: right.

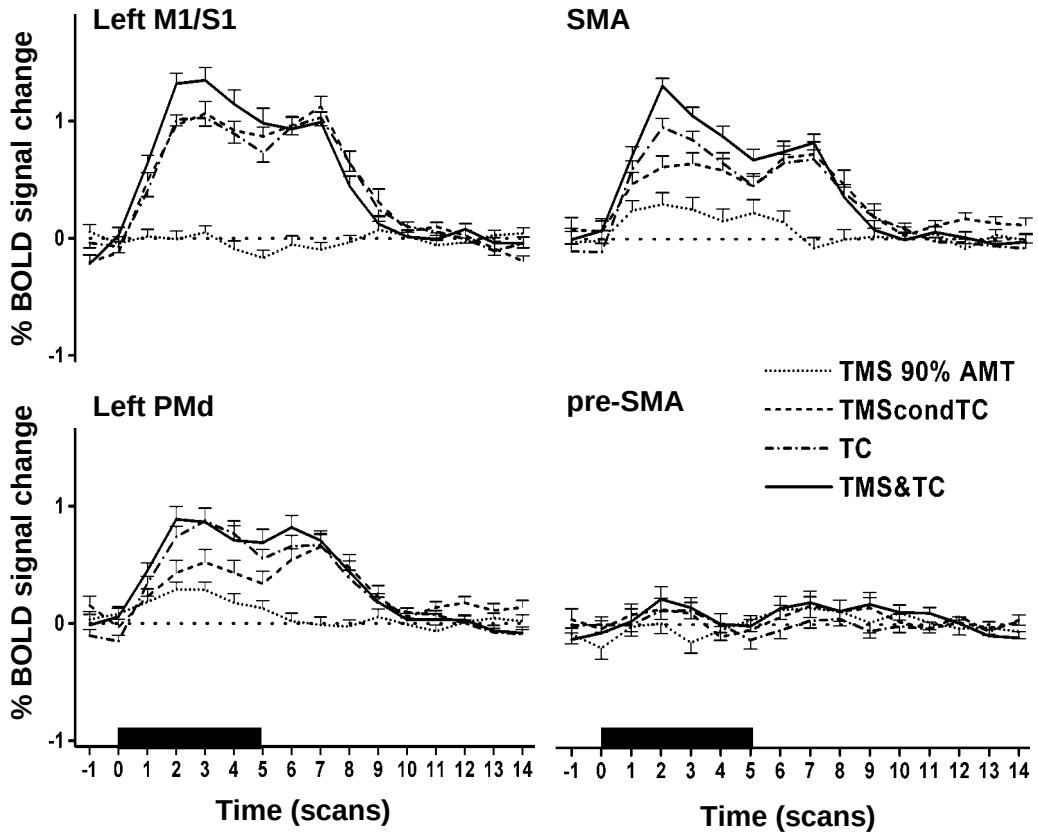


**Figure 5.5.** Mean time courses of BOLD MRI signal changes in *a priori* anatomically defined ROIs for all experimental conditions showing the percentage of signal changes (mean ± s.e.m.; n=8). Time-courses of rTMS before TC are aligned to the onset of movement epochs. Black bars indicate movement or stimulation periods, respectively. M1/S1: sensorimotor cortex, SMA: supplementary motor area, PMd: dorsal premotor cortex.

In all subjects, TC at 20% of maximum force increased neuronal activity (as indexed by the BOLD MRI signal) in a set of frontoparietal motor cortical areas (Figure 5.4, Table 5.1). In the left hemisphere, foci in the M1/S1, PMd, the anterior part of IPS, and the postcentral sulcus showed an increase in the BOLD MRI signal during TC. A less consistent increase in BOLD MRI signal was observed in the right PMd and the anterior part of IPS. The main cluster of activated voxels in M1/S1 extended anteriorly into the PMd and posteriorly into the anterior part of the IPS, ranging from *y= -9 mm* to *y= -40 mm* in MNI space. Activation clusters in the left and right IPS extended from the anterior portion of the IPS medially into the postcentral gyrus and the superior parietal lobe. In the right PMd, the cluster of activated voxels extended from *y= -19* mm to *y= -7 mm*. In the medial portion of the frontal lobe, there was a bilateral increase in activity in the SMA. The cluster in the

SMA was located in SMA proper, extending from *y= -19 mm* to *y= -3 mm*. A task-related decrease in BOLD MRI signal was detected in the homologous right M1/S1 and in the paracentral lobule (i.e. the primary motor leg area). The ipsilateral decrease in activity in the homologous M1/S1 was mostly confined to the central sulcus, with little spread towards the dorsal surface of the precentral or postcentral gyrus. This pattern of cortical activation and deactivation was highly consistent among the three conditions that involved the TC task (Table 5.2).

Table 5.1: Brain activity during rTMS and tonic contraction (TC)

| | Talairach Coordinates[1] | | | |
|---|---|---|---|---|
| Anatomical/functional location | *x* | *y* | *z* | t-value[2] |
| **Contrast TMS – Rest** | | | | |
| L premotor (PMd) | -40 | -14 | 60 | 5.17 |
| R central sulcus (M1/S1) | 30 | -30 | 57 | -4.72 |
| R precentral gyrus (PMd) | 21 | -8 | 52 | 4.78 |
| BL superior frontal gyrus (SMA)[3] | 6 | -3 | 56 | 5.27 |
| BL paracentral lobule (putative leg area) | 1 | -31 | 59 | -5.91 |
| **Contrast TC – Rest** | | | | |
| L central sulcus (M1/S1) | -36 | -26 | 55 | 12.43 |
| L precentral gyrus (PMd) | -24 | -14 | 57 | 10.83 |
| L postcentral gyrus | -36 | -32 | 54 | 10.81 |
| L superior parietal lobe | -24 | -61 | 53 | 8.69 |
| L intraparietal sulcus (anterior part) | -38 | -38 | 51 | 10.53 |
| R central sulcus (M1/S1) | 35 | -27 | 54 | -10.88 |
| R precentral gyrus (PMd) | 27 | -11 | 57 | 7.23 |
| R superior parietal lobe | 23 | -62 | 53 | 9.14 |
| R intraparietal sulcus (anterior part) | 34 | -45 | 54 | 9.3 |
| BL superior frontal gyrus (SMA) [3] | 0 | -12 | 57 | 11.66 |
| BL paracentral lobule (putative leg area) | 0 | -36 | 56 | -10.18 |

[1]Coordinates correspond to center of gravity of respective activation clusters. [2]Peak activation within cluster with $P < 0.01$, corrected. [3]The activation was located on the ventro-medial part of the superior frontal gyrus. L: left, R: right, BL: bilateral.

### 5.3.4 Changes in BOLD MRI signal provoked by TMS alone

Replicating the results reported in the previous chapter, subthreshold rTMS induced well-defined increases in the BOLD MRI signal in the caudal SMA and the PMd bilaterally (Table 5.1). There was also a decrease in BOLD MRI

signal in the contralateral homologous M1/S1 and paracentral lobule (i.e. the primary motor leg area) (Table 5.1). In all subjects, the area and magnitude of BOLD MRI signal changes were significantly smaller than those evoked by voluntary tonic contraction.

There were also some notable differences in terms of the localisation of regional maxima in the premotor cortex: In the caudal SMA, the peak activity associated with TC was located in the posterior portion of the caudal SMA (*x, y, z* coordinates = *0, -12, 57*) compared to peak activity induced by TMS (*x, y, z = 6, -3, 56*). In left PMd, two distinct sub-regions increased its neuronal activity during the TC task: a lateral focus with peak activity at *x, y, z= -32, -17, 57* and a medial focus with peak activity (*x, y, z= -17, -16, 59*). Only the lateral focus (peak activity at *x, y, z= -40, -14, 60*) also demonstrated an increase in activity during TMS. In none of the subjects a significant change in BOLD MRI signal in the stimulated M1/S1 was found.

Table 5.2: Conjunction analysis

| | Talairach Coordinates[1] | | | |
|---|---|---|---|---|
| Anatomical/functional location | *x* | *y* | *z* | t-value[2] |
| **Conjunction analysis TC + (TMS during TC) + (TMS before TC) – Rest** | | | | |
| L central sulcus (M1/S1) | -35 | -24 | 55 | 11.86 |
| L precentral gyrus (PMd) | -32 | -17 | 57 | 8.67 |
| L precentral gyrus (PMd) | -17 | -16 | 59 | 8.52 |
| L intraparietal sulcus (putative BA 40) | -37 | -48 | 51 | 6.24 |
| L postcentral sulcus | -39 | -37 | 55 | 10.85 |
| L intraparietal sulcus (anterior part) | -29 | -53 | 53 | 10.68 |
| R central sulcus (M1/S1) | 41 | -32 | 56 | -5.33 |
| R precentral gyrus (PMd) | 40 | -10 | 56 | 7.29 |
| R precentral gyrus (PMd) | 22 | -13 | 58 | 7.63 |
| R superior parietal lobe | 23 | -61 | 53 | 6.7 |
| R intraparietal sulcus (anterior part) | 38 | -43 | 54 | 4.78 |
| R postcentral gyrus | 33 | -44 | 54 | 7.43 |
| BL superior frontal gyrus (SMA) | 0 | -12 | 56 | 11.87 |
| BL paracentral lobule (putative leg area) | 1 | -33 | 57 | -6.37 |

[1]Coordinates correspond to center of gravity of respective activation clusters. [2]Peak activation within cluster with $P < 0.01$, corrected. [3]Rescaled to voxel size 1 x 1 x 1 mm. [4]Including transverse temporal gyrus, superior temporal gyrus, ventral part of parietal operculum and planum temporale. L: left, R: right, BL: bilateral.

### 5.3.5 Effects of TMS on motor activity

Table 5.3: Differences in brain activity

| Anatomical/functional location | Talairach Coordinates[1] x | y | z | t-value[2] |
|---|---|---|---|---|
| **Contrast (TC during TMS) – TC** | | | | |
| L central sulcus (M1/S1) | -31 | -23 | 52 | 5.03 |
| R central sulcus (M1/S1) | 21 | -31 | 58 | -5.51 |
| BL superior frontal gyrus (SMA) | -3 | 0 | 56 | 5.47 |
| BL paracentral lobule (putative leg area) | 0 | -40 | 56 | -4.99 |
| **Contrast (TC during TMS) – (TMS before TC)** | | | | |
| L central sulcus (M1/S1) | -39 | -20 | 51 | 6.69 |
| L premotor (PMd) | -35 | -12 | 63 | 6.02 |
| R central sulcus (M1/S1) | 35 | -26 | 52 | -4.45 |
| R precentral gyrus (PMd) | 43 | -6 | 54 | 5.89 |
| BL superior frontal gyrus (SMA) | 2 | -2 | 58 | 4.99 |
| BL paracentral lobule (putative leg area) | 2 | -32 | 60 | 5.54 |
| **Contrast TC – (TMS before TC)** | | | | |
| L precentral gyrus (PMd) | -21 | -11 | 56 | 4.60 |
| R central sulcus (M1/S1) | 37 | -28 | 54 | -5.38 |
| BL superior frontal gyrus (SMA) | -7 | -11 | 58 | 5.14 |
| BL paracentral lobule (putative leg area) | 2 | -36 | 59 | -5.92 |

[1]Coordinates correspond to center of gravity of respective activation clusters. [2]Peak activation within cluster with $P < 0.01$, corrected. [3]Rescaled to voxel size 1 x 1 x 1 mm. [4]Including transverse temporal gyrus, superior temporal gyrus, ventral part of parietal operculum and planum temporale. MGN: medial geniculate nucleus. L: left, R: right, BL: bilateral.

Though TC was associated with a similar pattern of motor activity regardless of the experimental condition (Table 5.2), rTMS to left M1/S1 shaped motor activity in frontal motor and premotor areas induced by the TC task. When TMS was given during the TC task, neuronal activity increased in the stimulated M1/S1 and the caudal SMA (Figure 5.6, Table 5.3). In the left M1/S1, a TMS-induced increase in task-related activity (peak activity at *x, y, z= -31, -23, 52*) occurred in the same region of the M1 that showed maximal neuronal activity during the TC task (*x, y, z= -36, -26, 55*). By contrast, simultaneous TMS increased neuronal activity in a part of the SMA that was spatially distinct from the area of peak activation during TC. While neuronal activity during TC was most pronounced in the posterior portion of the SMA (*x, y, z=0, -12, 57*), TMS during TC increased task-related activity in the anterior part of the caudal SMA (*x, y, z= -3, 0, 56*).

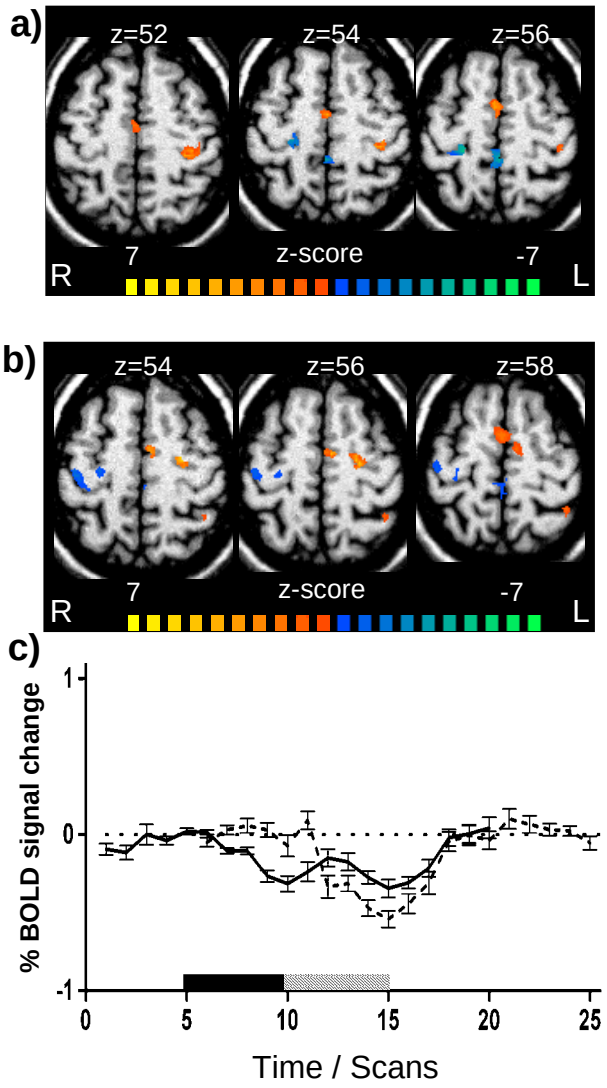


**Figure 5.6. (a)** TMS during tonic contraction (rTMS during TC) is contrasted with tonic contraction (TC). Repetitive TMS during TC evokes increases activity in the bilateral SMA and left M1/S1, as well as further decreases in the contralateral M1/S1. **(b)** TMS before tonic contraction is contrasted with tonic contraction (TC). Activity in SMA and left PMd was elevated during TC. When TMS was applied before TC, the task-related decrease in right M1/S1 was attenuated. Colour scaling indicates all significant voxels showing increased activity for TC (yellow-red) or TMS before TC (blue) ($P<0.01$, corrected). Activations are superimposed onto a 3D-template brain (MNI). L: left, R: right. **(c)** Averaged signal time course in the right M1/S1 for TC (solid line), and TMS before TC (broken line) (mean ± SEM; n=8). The whole time courses are displayed with overlapping TC periods. The data illustrates that task-related activity decreases are attenuated when TMS is applied prior to movement epochs.

A different pattern emerged when the rTMS train was given immediately before the TC task. A preceding rTMS train caused a relative reduction in task-related neuronal activity in the left PMd and the SMA compared to TC alone or simultaneous TMS / TC (Table 5.3). In addition to a reduction of task-related activity, rTMS also attenuated the task-related decrease of the

BOLD MRI signal in the right homologous M1/S1 (Figure 5.6). The voxels showing the strongest attenuation of task-related neuronal activity in the caudal SMA (*x, y, z= -7, -11, 58*) and in left PMd (*x, y, z= -21, -11, 56*) corresponded to those voxels in SMA and PMd that showed the most prominent increase in BOLD MRI signal during TC (SMA: *x, y, z=0, -12, 57*; PMd: *x, y, z= -17, -16, 59*; Table 5.1 and 5.3).

However, these voxels were spatially distinct from those voxels that showed a maximum increase in BOLD MRI signal during TMS (SMA: *x, y, z=6, -3, 56*; PMd: *x, y, z= -40, -14, 60*; Table 5.1 and 5.3). Inspection of the time course of the mean BOLD MRI signal in the caudal SMA and left PMd revealed that only the initial component of the task-related BOLD MRI signal increase was attenuated (Figure 5.6).

## 5.4 Discussion

The present work is, to my best knowledge, the first study to use fMRI to explore the immediate impact of rTMS on regional neuronal activity during a simple motor task. It was found that a short train of rTMS below AMT can induce acute changes in task-related activity in frontal motor areas without affecting motor behaviour. The effects of rTMS were critically dependent on the timing of rTMS relative to the TC task. The main new findings can be summarised as follows: (1) In the stimulated M1/S1, rTMS increased task-related neuronal activity when rTMS was given during but not before the TC task. (2) In caudal SMA, the anterior portion increased task-related activity during the administration of rTMS. Conversely, a posterior portion of caudal SMA exhibited a reduction in task-related activity when rTMS was given just prior to TC. (3) Task-related activity was also attenuated in the medial part of the left PMd when rTMS preceded TC. (4) rTMS had also an attenuating effect on task-related decrease in activity in the right homologous M1/S1.The implications of these data will be discussed in terms of the present understanding of rTMS effects in three sections: 1) the effects of rTMS on neuronal activity in the motor system at rest, 2) the modulatory effects of

rTMS on motor activity in the stimulated left M1/S1, and 3) rTMS-induced changes in motor activity in remote frontal motor areas.

### 5.4.1 The effects of rTMS on motor neuronal activity at rest

The observation of TMS-induced remote activity changes at rest is congruent with the increasing evidence that subthreshold rTMS is able to modulate activity beyond the site of stimulation (GERSCHLAGER ET AL., 2001; MUNCHAU ET AL., 2002; STRENS ET AL., 2002; CHEN ET AL., 2003; LEE ET AL., 2003; OKABE ET AL., 2003; OLIVIERO ET AL., 2003; SIEBNER ET AL., 2003a; RIZZO ET AL., 2004). In frontal motor regions these changes can even be observed during short trains of subthreshold rTMS (OKABE ET AL., 2003; CHAPTER 4). In general, the subthreshold nature of rTMS renders remote activity changes unlikely to accrue from direct excitation of corticocortical (FERBERT ET AL., 1992) or corticospinal (DI LAZZARO ET AL., 1998) projecting fibres or lasting changes in synaptic neurotransmission. Studies in patients with callosal agenesis suggest that decreased BOLD responses subsequent to motor behaviour are not critically dependent on callosal connections (REDDY ET AL., 2000), suggesting that changes in excitability of local circuits shape the ongoing activity pattern and these changes in turn influence activity in interconnected cortical and subcortical brain regions. In line with recent observations (BOHNING ET AL., 1998; BAUDEWIG ET AL., 2001; OKABE ET AL., 2003), no significant activity changes were observed at the site of stimulation during subthreshold rTMS at rest. There is some uncertainty regarding the lack of local response modulations. As it is known that subthreshold TMS excites circuits involved in the generation of I waves in the motor cortex (ZIEMANN & ROTHWELL, 2000), in the present experiments local synaptic activity seems to have been dissociated from a corresponding BOLD MRI signal increase.

### 5.4.2 The modulatory influence of TMS on motor activity in M1/S1

In principle, TC evoked activity changes in a set of primary and frontal motor regions that corresponded with previous observations (EHRSSON ET AL., 2001; KUHTZ-BUSCHBECK ET AL., 2001; WARD & FRACKOWIAK, 2003) and are presumed

to reflect both generation of muscular force and the fine-control of dexterous manipulation (EHRSSON ET AL., 2001; KUHTZ-BUSCHBECK ET AL., 2001). Congruent with electrophysiological studies (RIDDING ET AL., 1995; TOUGE ET AL., 2001; ZOGHI ET AL., 2003), TMS applied during motor behaviour evoked an increase of local activity as compared to TC alone. This provides the first demonstration of a shaping of local activity even by short subthreshold TMS trains.

Assuming that corticospinal excitability was elevated during motor behaviour, TMS was presumably more effective to interact with ongoing neural activity. An alternative view holds that rTMS amplified task-related activity by interacting with those circuits already involved in the generation of motor output.

A recent study provides evidence that the effects of rTMS are context-dependent: while subthreshold 5 Hz rTMS of the primary motor cortex impaired ongoing dextrous force manipulation and decreased corticospinal excitability, none of these effects were observed when rTMS was applied at rest (STRENS ET AL., 2003). Compared to the more complex motor task of STRENS ET AL. (2003), TMS did not seem to change ongoing motor activity significantly to perturb the simple nature of the motor task applied in the present experiment. In the future, more complex motor tasks may help to elucidate how functional consequences of rTMS are mirrored in cortical activity changes, assuming that complex behaviour is more easily perturbed by rTMS.

The lack of a significant response modulation in the left M1/S1 when TMS was applied prior to motor behaviour further emphasises that the resting and the active brain exhibit different haemodynamical susceptibilities to subthreshold rTMS. This case rests upon previous observations that rTMS-induced changes in corticospinal and intracortical excitability measured at rest evoke either no (CHEN ET AL., 1997; MUELLBACHER ET AL., 2000; ROSSI ET AL., 2000; SCHAMBRA ET AL., 2003) or little changes (SCHLAGHECKEN ET AL., 2003) in subsequent motor behaviour. This shows that tonic motor drive 'washes away' changes in cortical excitability evoked at rest.

### 5.4.3 The modulatory influence of TMS on motor activity in frontal motor areas

An important observation is that TMS resulted in either decreased (right M1/S1), increased (SMA, PMd, left M1/S1) or spatially shifted (SMA, PMd) activity, depending on the context of TMS application. At present, there is little knowledge regarding the exact mechanisms leading to such differential effects. However, the mere observation of a redistribution of activity is important in terms of our understanding of the focality of rTMS. Most importantly, the different distribution of activity between conditions indicates that the context directs the quality and localisation of TMS. In the homologous M1/S1, for example, this might reflect a redistribution of the task-related decreased response. In the SMA, the pattern of activity was slightly changed depending on the context.

In the caudal SMA, the change in activity might reflect interaction with basic movement components. This would be concurrent with the observation that prolonged voluntary motor drive normalised the initial influence of rTMS on cortical activity. In contrast, the rostral SMA has been linked to slightly more complex components of dextrous movements and activity changes observed during precision grip may reflect compensatory processes to the interference of rTMS with such basic movement components (VOROBIEV ET AL., 1998). The fact that no elevated response in the left PMd was observed might be due to a ceiling effect that obscured any further signal increase in this region.

It furthermore seems that rTMS prior to motor behaviour decreased the task-related responsiveness of SMA and PMd. This initial attenuation normalised during movement epochs, providing further support to the notion that the effects of TMS at rest and activation are profoundly different.

The regions of activation in the present study are in keeping with the known intimate anatomical connectivity of the frontal motor areas (MUAKKASSA & STRICK, 1979; ROUILLER ET AL., 1994; GEYER ET AL., 2000) and previous demonstrations of changes in the functional coupling between frontal motor regions and M1 following subthreshold rTMS (SIEBNER ET AL., 2000, 2001b;

SERRIEN ET AL., 2002; CHEN ET AL., 2003; OLIVIERO ET AL., 2003; STRENS ET AL., 2003; RIZZO ET AL., 2004). This suggests that the reshaping of cortical activity in one subregion by means of rTMS mediates activity changes in neighbouring subregions. Regions targeted by rTMS at rest are likely to influence activity in spatially distinct but interconnected regions that are involved during motor behaviour.

The observed redistribution of cortical activity even after short stimulation protocols is not likely to result from direct excitation of monosynaptic connections between frontal motor regions. Whether remote activity changes point towards cortical connectivity between brain regions or reflect cortical plasticity in terms of an active short-term compensation to the perturbation of ongoing activity can not be resolved on grounds of the present data. However, a similar redistribution of cortical activity has been reported in a combined TMS-PET investigation of subthreshold rTMS of the motor cortex (LEE ET AL., 2003). Here, functional connectivity analysis elegantly revealed a remodelling of motor function during motor behaviour. This was attributed to the lack of behavioural changes to the occurrence of acute motor plasticity in response to temporarily induced lesions.

In most regions, BOLD MRI signal changes followed the dynamic components of the motor task, namely the onset of contraction periods and the termination. It should be noted, however, that time courses were obtained from anatomically defined ROIs that were considerably larger than the activated clusters. For example, the transient response in left PMd during TMS presumably results from an attenuation due to the averaging in the respective anatomical ROI. Evidence from electrophysiological studies indicates that neuronal firing rates in the primary motor cortex increase during the dynamic phases of a grasp-and-release task (PICARD & SMITH, 1992; SALIMI ET AL., 1999). This is mirrored by increased BOLD responses in M1/S1 and SMA following muscle relaxation (TOMA ET AL., 1999; KUHTZ-BUSCHBECK ET AL., 2001). In the present study, camel-back shaped response profiles following the dynamic components of the motor task were found in frontal motor regions and the IPS. In both areas, this might reflect some aspect of

visuomotor integration in which the dynamic aspects (i.e. its onset and termination) of the visual feedback during contraction periods influenced BOLD responses in a similar fashion as the dynamic components of TC itself.

Decreased BOLD responses were observed in the M1/S1 ipsilateral to the tonic contraction. Similar responses have been reported during power grasp (FOLTYS ET AL., 2003), sequential finger tapping (ALLISON ET AL., 2000), and precision grip at low force (HAMZEI ET AL., 2002) and are presumably related to active suppression of movement, as reflected by corticospinal inhibition on the side ipsilateral to the movement (LEOCANI ET AL., 2000). Although there is less consensus regarding the mechanisms underlying negative BOLD responses, it has recently been argued that the negative BOLD response indeed reflects active synaptic inhibition (SHMUEL ET AL., 2002). In the case of subthreshold rTMS this is unlikely to be evoked by direct transcallosal inhibition but more likely mediated indirectly via corticocortical pathways.

The results have particular implications for the interpretation of cognitive TMS studies. They show that subthreshold rTMS is capable of both a *pre-shaping* and a *re-shaping* of cortical activity patterns subsequent or concurrent, respectively, to motor behaviour. As a consequence, significant changes in cortical activity may only become detectable during active performance of a task. Moreover, the results emphasise that a lack of TMS-evoked behavioural changes does not imply ineffective targeting of cortical neurons. On the other hand, in the case of an absence of behavioural consequences following stimulation of brain regions that do not exhibit so-called positive phenomena, as for example the prefrontal or parietal cortex, one can not be certain to have targeted the cortex successfully at all.

### 5.4.4 Further considerations

Following muscle contraction, changes in corticospinal excitability occur that result from altered membrane properties of corticospinal tract neurons, altered synaptic transmission of inhibitory and/or excitatory neurons, excitability changes in motor cortical interneurons, or excitability changes in inputs to the motor cortex (TAYLOR & GANDAVIA, 2001). Since TC was

conducted at low force levels (20% MVC) over short periods (10 s) every 20 seconds, it seems reasonable to assume that fatigue did not play a significant role during the course of the experiment.

Peri-Rolandic activation foci in simple motor tasks often cover both pre- and postcentral gyrus (CRAMER ET AL., 2002) and are not easily separated with common spatial resolutions of EPI. A central sensorimotor ROI was therefore defined, covering both pre- and postcentral gyrus at the level of the primary motor hand area. Given the fact that neurons in the postcentral gyrus also exhibit force level-related firing patterns (SALIMI ET AL., 1999), contribution from both precentral and postcentral regions may have influenced changes in cortical activity patterns.

# 6 Functional MRI of the immediate impact of TMS on cortical and subcortical motor circuits

## 6.1 Introduction

While TMS has evolved to a widely used research tool for probing the function of a variety of areas of the cerebral cortex (for recent reviews see WALSH & COWEY, 2000; ZIEMANN & ROTHWELL, 2000; COWEY & WALSH, 2001; SIEBNER & ROTHWELL, 2003), this is contrasted by the lacunae in our knowledge regarding its mechanisms of action. In the past many studies relied on the assumption that the major impact of TMS on brain activity is focal to the site of stimulation, yet increasing evidence suggests that TMS can also modulate neural circuits in remote brain regions. Such distant activations within a particular brain system hamper the interpretation of behavioural TMS studies unless the extent of possible TMS effects on brain function is known in sufficient detail. Furthermore, confounds that are barely recognisable without neuroimaging may result in unwanted activations caused by stimulation of brain systems other than the target system, for example involving the auditory, tactile, cutaneous or somatosensory cortex (PAUS, 1999; SIEBNER ET AL., 1999a,b, 2003c). In addition, such confounds may lead to cross-modality suppression (PAUS, 2000).

Catalysed by recent technical developments in combined TMS-fMRI (SHASTRI ET AL., 1999; BAUDEWIG ET AL., 2000; CHAPTER 3), rTMS was synchronised to BOLD-sensitive EPI in order to investigate cortical and particularly subcortical motor structures during both supra- and subthreshold stimulation of the left M1/S1 hand area. Extending the work at lower field in Chapters 3-5, this high-resolution 3T study further advances the technical aspects of combined TMS-fMRI and addresses not only cortical motor regions but also putative modulations in the basal ganglia and thalamus. Moreover, simultaneous recordings of electromyographic activity in the contralateral hand monitored the supra- or subthreshold nature of the used TMS pulses.

## 6.2 Methods

### 6.2.1 Subjects

Twelve healthy subjects (21-41 years, mean age 27.5 years, seven female) participated in the study.

### 6.2.2 Experimental protocol

Each study comprised three successive experimental conditions the order of which was randomised between subjects: (i) rTMS at 3 Hz and 110% of RMT, (ii) rTMS at 3 Hz and 90% of individual AMT, and (iii) voluntary finger movements requiring dorsi-flexion of the right index finger to functionally locate respective motor regions. Finger movements were acoustically triggered by discharging the TMS coil at the same frequency as during stimulation conditions (3 Hz) but at only 15% of stimulator output. This intensity is too low to stimulate the cortex (FISHER ET AL., 2002; BESTMANN ET AL., 2004) but still audible during scanning.

After an initial equilibration period (33.2 s duration corresponding to the acquisition of 10 brain volumes) experimental protocols comprised 8 epochs of stimulation and rest, that is either rTMS (30 pulses) or voluntary finger movement (9.96 s duration corresponding to 3 volumes) followed by a period of rest (23.24 s duration corresponding to 7 volumes). Accordingly, the total measuring time per paradigm was 4 min 59 s. Experimental conditions were separated by five minutes to avoid carry-over effects of the stimulation. Throughout the experiments, subjects were instructed to keep their eyes closed and to relax their hands, unless movement periods were indicated. None of the subjects received more than 800 effective TMS pulses per day, half of them at subthreshold intensity. The study therefore conformed to previously recommended safety guidelines (WASSERMANN, 1998).

### 6.2.3 Magnetic resonance imaging

MRI was performed at 3.0 Tesla (Siemens Trio, Erlangen) using the parameters described in the experimental methods chapter.

### 6.2.4 Transcranial magnetic stimulation

TMS was applied to the left M1/S1 following the details specified in the experimental methods chapter.

### 6.2.5 Electromyographic recordings

Electromyographic recordings were obtained following the details specified in the experimental methods chapter.

### 6.2.6 Combined TMS and fMRI

In all participants, it was possible to place the coil at the previously identified position over the left primary motor cortex. In some cases, it was necessary that subjects slightly tilted their head in order to allow accurate placement of the TMS coil. Head movement was restricted by foam-padded cushions and subjects wore ear-plugs and noise reducing head-phones throughout the entire experiment. Subjects lay supine with their arms rested comfortably onto their sides and near extension of the elbows. The good correspondence between the optimal coil position for eliciting a motor evoked potential in contralateral hand muscles and the site of activation within the sensorimotor cortex during voluntary finger tapping (MACDONELL ET AL., 1999; HERWIG ET AL., 2002) suggests that the primary sensorimotor hand area was successfully targeted. TMS coil position and motor thresholds were briefly evaluated after each experiment by applying single TMS pulses.

Functional images were acquired every 166 ms with each image acquisition lasting for 91 ms. TMS pulses were applied every 332 ms (3.001 Hz), starting immediately after acquisition of a single image, so that the minimum waiting period between a TMS pulse and a subsequent EPI acquisitions was 75 ms. This slightly shorter value than previously recommended for TMS-fMRI at 1.5

and 2.0T (SHASTRI ET AL., 1999; CHAPTER 3) was attributed to the improved design and better fixation of the TMS coil, which reduced mechanical vibrations known to induce distorting electromagnetic fields. Because of intersubject anatomical variability of M1, the corresponding variation of the TMS coil with respect to the $B_0$ field makes it difficult to fully predict and control for torque interactions. In fact, in one subject EPI images following TMS pulse application were significantly distorted. Noteworthy, this subject had a relatively high motor threshold (88 % of stimulator output), so that the corresponding mechanical vibrations may have resulted in electromagnetically induced local field variations lasting longer than the 69 ms allowed for in the EPI protocol. Hence, the subject was excluded from the study.

### 6.2.7 Data analysis

Data analysis was conducted following the details specified in the experimental methods chapter.

In addition, signal time courses were obtained from a priori anatomically defined ROIs. These included left (stimulated) and right M1/S1, SMA, left and right PMd, left and right ventro-lateral nucleus (VLN) of the thalamus, and auditory cortex (AUD). Each ROI was demarcated with a rectangular cube on the respective individual anatomical region without overlapping with adjacent ROIs.

M1/S1 was located by the presumed anatomical landmark of the primary motor hand area (YOUSRY ET AL., 1997) and extended to the fundus of the central sulcus at which primary motor and sensory cortex interdigitate (WHITE ET AL., 1997). The antero-posterior extent of M1/S1 was designated by the lateral convexity of the pre- and postcentral gyrus, respectively. The medio-lateral borders were defined by the level of the superior frontal sulcus and the inferior frontal sulcus, respectively. The caudal part of the superior frontal gyrus directly adjacent and at the level of the motor hand area housed the PMd (FINK ET AL., 1997). Its rostral dimension was confined by the plane perpendicular to the rostral part of the genu of the corpus callosum. The

medial extent of PMd was delineated by the lateral surface of the superior frontal gyrus. The border between dorsal and ventral premotor cortex is not clearly defined (GREZES & DECETY, 2001) and was marked by the lateral extent of the M1/S1 ROI (HLUSTIK ET AL., 2002).

The SMA resides at the medial wall of the prefrontal cortex (PICARD & STRICK, 2001) with its extent at the lateral surface being confined by the middle of the superior frontal gyrus. The rostral border of the SMA, which separates it from the anteriorly situated pre-SMA was defined by a line perpendicular to the AC-PC line at the level of the AC (PICARD & STRICK, 1996, 2001). The caudal extent of the SMA was restricted by the paracentral lobule (PICARD & STRICK, 1996) and the ventral border was constituted by the cingulate or the paracingulate gyrus (PAUS ET AL., 1996), respectively. The medial ROI (SMA) was collapsed into a single midline ROI not including the pre-SMA or cingulate motor area (CMA). The auditory cortex comprised the transverse temporal gyrus (TTG) and the mid-dorsal surface of the superior temporal gyrus. Medially, its extent was restricted by the medial border of the insula. The caudal border was marked by the extent of the TTG, while the rostral extent was arbitrarily confined by the level of the central sulcus. The ventro-lateral nucleus cannot easily be distinguished from other thalamic nuclei on T1-weighted images. Therefore, a region starting at the posterior commissure level and extending rostrally halfway to the anterior commissure was demarcated. In a similar fashion, the ROI extended from the lateral border of the thalamus to halfway its medial border.

Mean signal time courses were expressed as percentage change with reference to the last three time points of each experimental cycle. Signal time courses were time-locked averaged for each ROI. Mean signal intensities were calculated for each functional image in each ROI and *t*-tests were used to compare the percent signal change during stimulation or movement epochs with baseline epochs.

## 6.3 Results

None of the subjects reported any side effects from the experimental procedure apart in some cases from slight discomfort on the head resulting from the pressure of the TMS coil. In one subject, no electromyographic responses could be recorded due to computer problems. However, as recordings from all other subjects confirmed the presence or absence of EMG responses to supra- and subthreshold stimulation, respectively, the data from this subject was not excluded from the final analysis. One subject was excluded due to insufficient MRI quality.

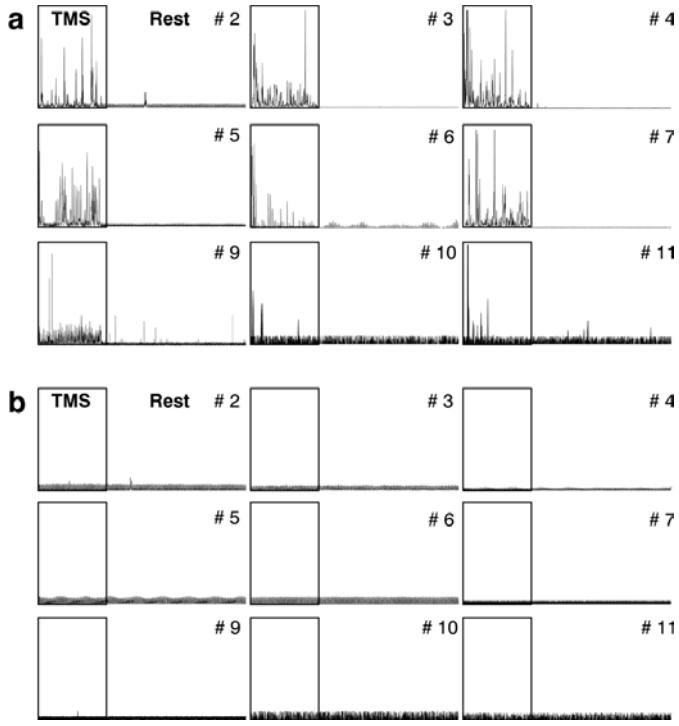


**Figure 6.1**. Electromyographic recordings of **(a)** suprathreshold and **(b)** subthreshold rTMS from nine subjects during fMRI. Stimulation epochs (boxes) were time-locked averaged to the onset of stimulation. Frequency extraction (7-25 Hz) was performed to reduce MRI gradient artefacts. Suprathreshold rTMS evoked clear myographic activity in the contralateral FDI muscle, whereas no such activity was observed during subthreshold rTMS

### 6.3.1 Motor system

As can be seen in Figure 6.1, suprathreshold rTMS evoked clear electromyographic activity in the right FDI muscle when compared to resting epochs (*t*-test, $p<0.01$) similar to voluntary finger dorsi-flexion (not shown). By contrast, no differences in EMG activity during subthreshold rTMS and

baseline epochs was found (*t*-test, p=0.22), thus confirming its subthreshold nature.

Individual activation maps superimposed onto EPI raw images together with the corresponding unthresholded correlation maps are shown in Figure 6.2 for a representative subject and two brain sections. The examples refer to voluntary finger movement as well as rTMS at supra- and subthreshold intensity. These images clearly demonstrate the absence of image artefacts related to simultaneous rTMS, confirming that we had allowed for sufficient waiting periods between TMS pulses and MR image acquisition.

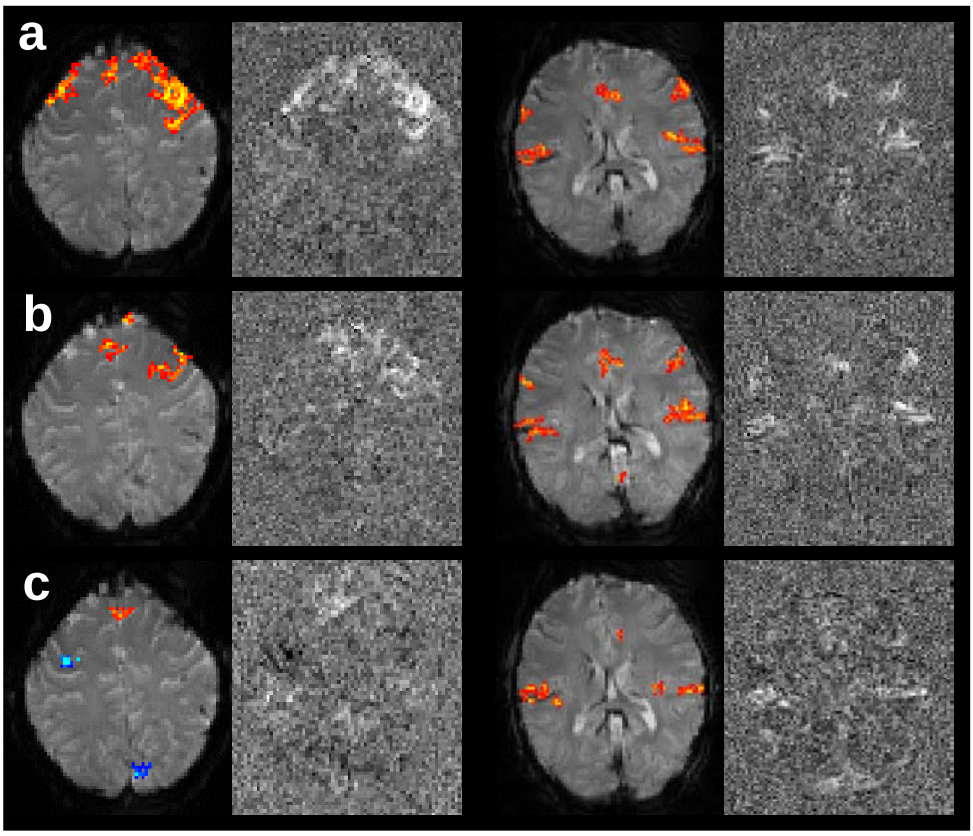


**Figure 6.2.** Individual activation maps superimposed onto EPI raw images and corresponding unthresholded correlation maps from a representative subject obtained for **(a)** an acoustically cued voluntary finger movement, **(b)** suprathreshold rTMS at 110% RMT, and **(c)** subthreshold rTMS at 90% AMT in oblique sections cutting through (left) the M1/S1 and (right) the auditory cortex. While activations, that is positive BOLD responses or signal increases, are coded in red-yellow, BOLD MRI signal decreases are coded in blue. No image degradation was revealed during rTMS at any intensity.

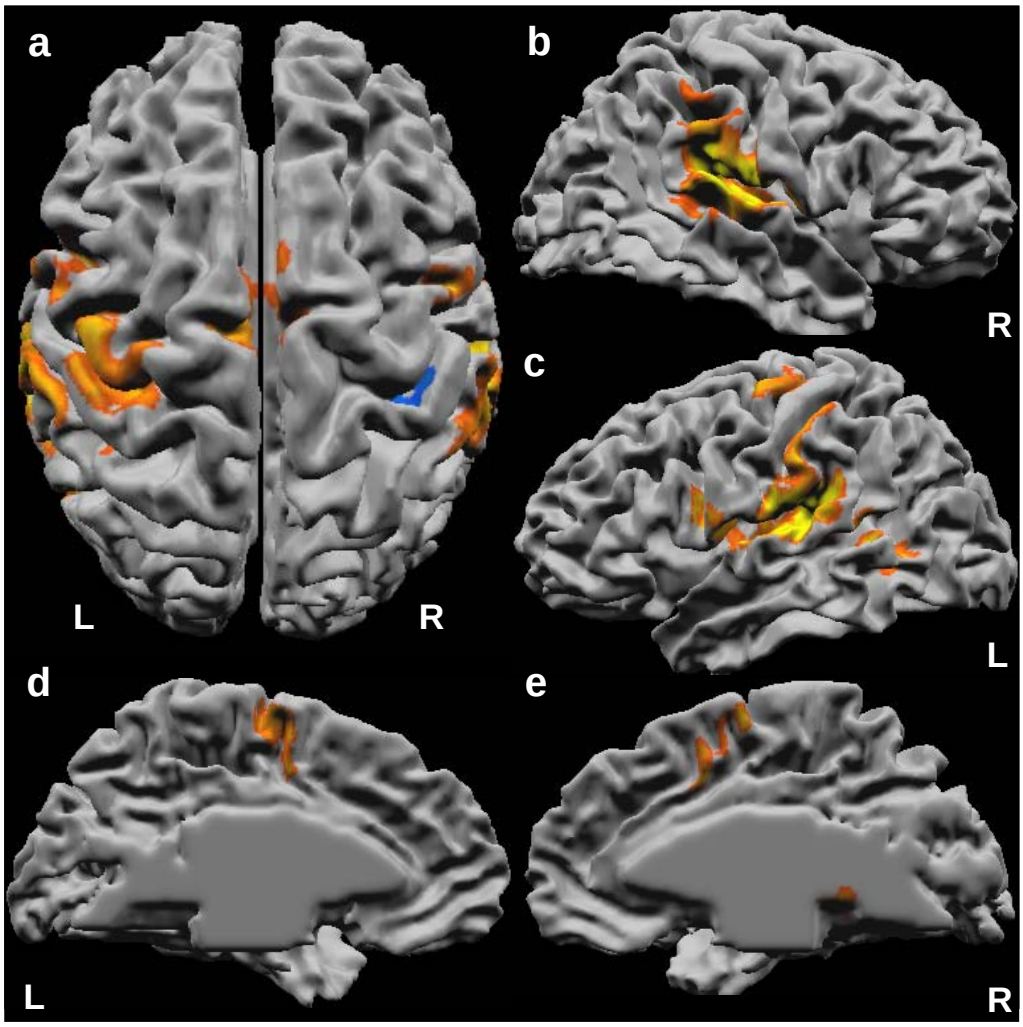


**Figure 6.3.** Cortical activations obtained for a group analysis (11 subjects, P < 0.01, corrected) of responses to suprathreshold rTMS. The maps represent **(a)** dorsal, **(b,c)** lateral, and **(d,e)** medial views of significant activations projected onto a 3D surface reconstruction of a template brain (Montreal Neurological Institute, MNI). Increased activity (red-yellow) was found in left M1/S1, PMd, bilateral SMA and auditory cortices, S1 and S2, and left ventral posterior middle temporal gyrus. In the left hemisphere, additional activity was found along the inferior precentral sulcus. Activations in the putamen and thalamus are not shown on these 3D views. Decreased BOLD MRI signal intensities (blue) were found in the right M1/S1 hand region and the occipital cortex (not shown). L: left, R: right.

Figure 6.3 illustrates the results of a group analysis by showing statistically significant activations evoked by suprathreshold rTMS as projections onto a segmented reference brain (MNI). Quantitative information about respective centers of gravity (in Talairach coordinates), t-values, and cluster volumes are summarised in Table 6.1. At a group level, focal increases in synaptic activity (as indexed by an increase in BOLD MRI signal) was detected in the stimulated left M1/S1 hand area, PMd and the inferior part of the precentral gyrus (putative PMv), bilateral SMA and CMA, and to a lesser extent, the right

PMd. The left cortical motor-related activation on the lateral surface extended from *y= -9* mm to *-29* mm. In the midline region, activation in the SMA spanned from *y= -16* mm to *14* mm. Furthermore, there was localised activity in the region around left ventral posterior middle temporal gyrus (mean coordinates *x= -49, y= -51, z=7*). The homologous of the right M1/S1 contralateral to the site of stimulation showed a significantly decreased BOLD MRI signal. Activity in the ipsilateral (right) antero-dorsal cerebellar lobule was evidenced in 8 subjects (mean coordinates *x=8, y= -50, z= -12*).

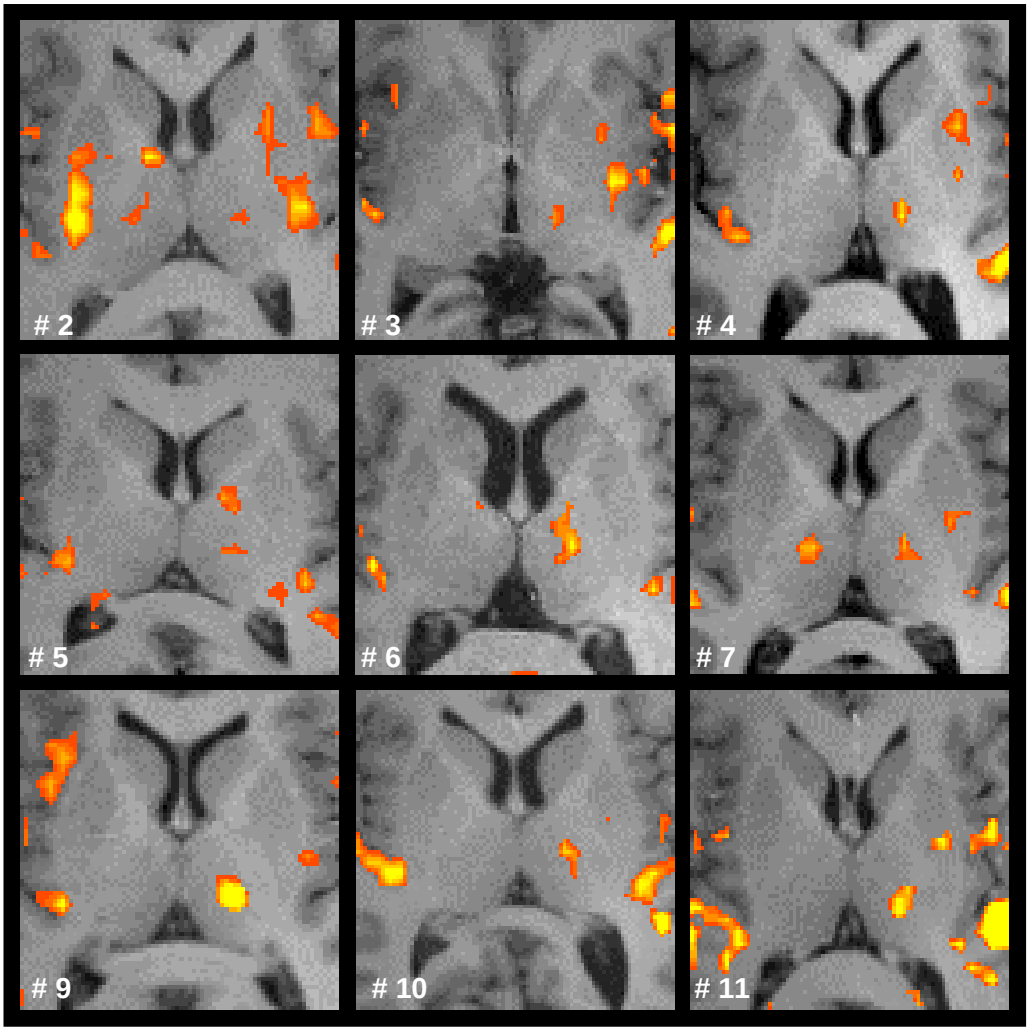


**Figure 6.4.** Individual activation maps of the nine subjects who presented with left-hemispheric thalamic activity in response to suprathreshold rTMS ($P < 0.0001$, uncorrected) superimposed onto individual anatomical images in stereotaxic space (*z=9*). Several subjects showed additional activity in the putamen and/or right thalamus (not always visible in the selected sections).

At the subcortical level, Figure 6.4 shows selected individual activation maps of all nine subjects with thalamic activations in response to suprathreshold

rTMS. In all cases, the center of gravity was located at the presumed coordinates of the left VLN. Less consistent and much smaller activity was located in the right VLN. Activity of the lentiform nucleus was primarily located in the ventro-medial postcommissural portion of the putamen, although such findings were characterised by considerable inter-individual variability. A corresponding group analysis is shown in Figure 6.5 depicting enlarged views in all three orientations.

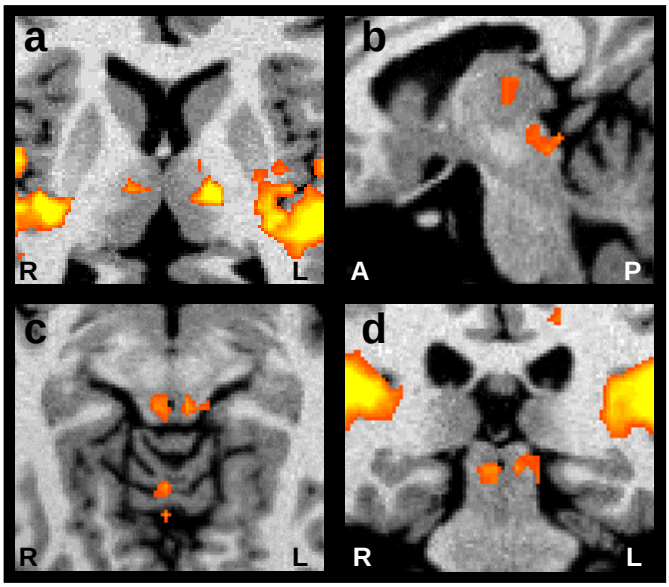


**Figure 6.5.** Subcortical activations obtained for a group analysis (11 subjects, P < 0.01, corrected) of responses to suprathreshold rTMS. **(a)** Enlarged view of a transverse section (*z*=9) of a standard reference brain (MNI) with pronounced activation of the postero-commissural left ventro-lateral thalamus and putamen as well as smaller activations in the right thalamus contralateral to the stimulation. **(b)** Sagittal section (*x*= -5) demonstrating distinct activations in the motor and auditory regions of the thalamus. **(c)** Transverse section (*z*= -5) with bilateral activation of the inferior colliculi. **(d)** Coronal section (*y*= -26) showing bilateral activation of the inferior colliculi. Note also the pronounced activation in the entire auditory cortex. L: left, R: right.

### 6.3.2 Auditory system

In addition to motor activity, Figure 6.3 shows widespread bilateral activity within the primary and secondary auditory cortex, the superior and dorsal part of the middle temporal gyrus, the planum temporale, and the depth of the Sylvian fissure covering the entire TTG. Again, Talairach coordinates of centers of gravity and activation volumes are given in Table 6.1. There was considerable overlap in antero-posterior extent (left: *y*=5 mm to -45 mm; right:

*y*=*-12* mm to *-41* mm) and medio-lateral extent of activated regions in the temporal lobe (left: *x*= *-64* mm to *-29* mm, right: *x*= *-64* mm to *31* mm). As shown in Figure 6.3c, the left-sided temporal cluster extended more rostrally and fused with a cluster in the inferior part of the precentral sulcal region. At the subcortical level shown in Figures 6.4 and 6.5, bilateral activation was found in the inferior colliculi and the medial geniculate nucleus, which tended to be lateralised to the left.

### 6.3.3 Subthreshold rTMS versus suprathreshold rTMS

Subthreshold rTMS did not yield significant activations in the stimulated M1/S1, but caused marked BOLD MRI signal changes in the SMA, CMA, and left PMd. Additional activations were seen in the left and right ventro-lateral thalamus. No consistent activity changes were detected in the striatum. These findings are visualised in Figure 6.6 comparing subthreshold rTMS with suprathreshold rTMS, while quantitative data for subthreshold rTMS are given in Table 6.2. In the auditory cortex, subthreshold rTMS elicited widespread activations similar to those found for suprathreshold rTMS, ranging from*y*=*-18* mm to *-42* mm (left) and *y*=*-9* mm to *-40* mm (right). In the group analysis, significant activation in the inferior colliculus was only detected in the left hemisphere. Figure 6.6 further demonstrates that BOLD MRI signal decreases were found for both TMS conditions not only in the right M1/S1 contralateral to the site of stimulation and the medial paracentral lobule, but also in the occipital and posterior parietal cortex, with a right-hemispheric preponderance. These latter decreases were located in the medial occipital cortex (putative V1), right transverse occipital sulcus (putative V5), and posterior parietal cortex.

Figure 6.7 summarises BOLD MRI signal intensity time courses obtained from six regions-of-interest and for all three experimental conditions, that is voluntary finger movement as well as supra- and subthreshold rTMS. With the exception of the stimulated M1/S1, all pre-defined regions-of-interest showed a significant modulation of the regional BOLD MRI signal in response to subthreshold rTMS. In the stimulated M1/S1, a modulation of the BOLD MRI

signal occurred only during suprathreshold rTMS. No differences in signal intensity were seen in the auditory cortices and left thalamus.

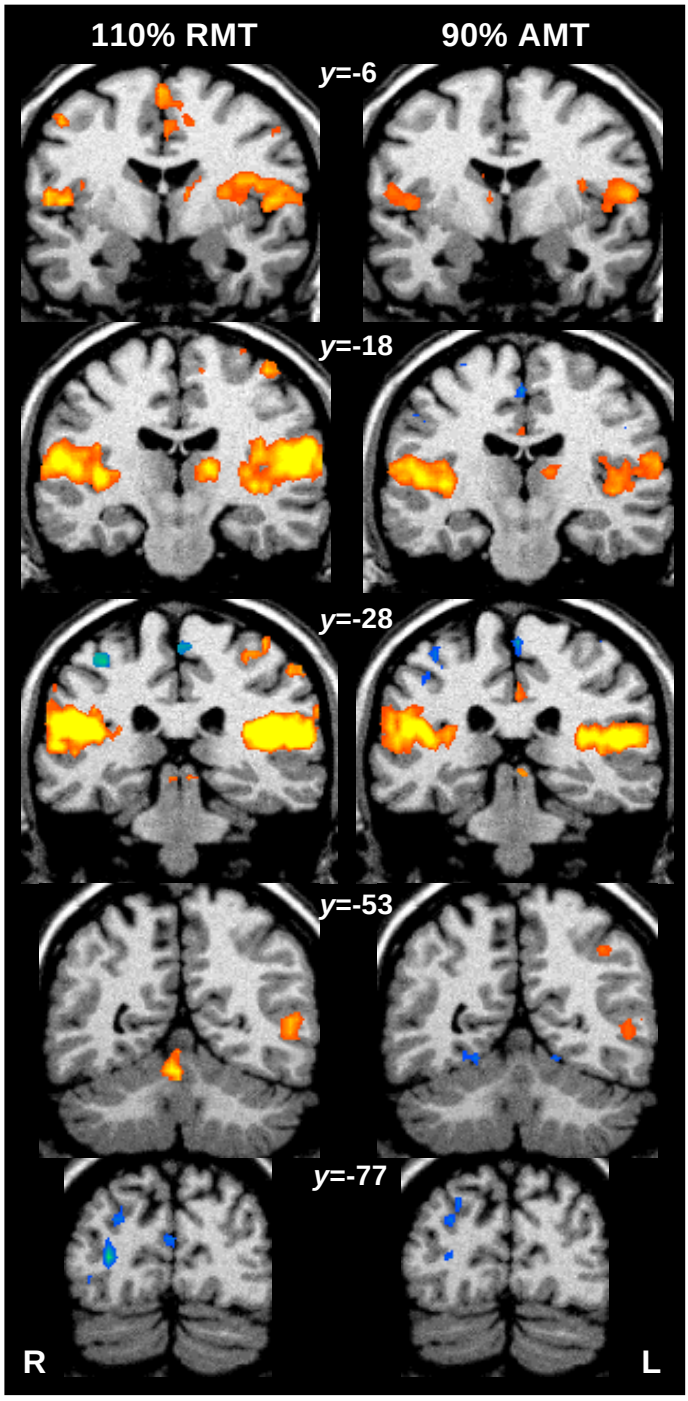


**Figure 6.6.** Activations obtained for a group analysis (11 subjects, P < 0.01, corrected) of responses to (left) suprathreshold rTMS at 110% RMT, and (right) subthreshold rTMS at 90% AMT projected onto 5 coronal sections of a standard reference brain (MNI, Talairach coordinates indicated). Apart from pronounced auditory activation, suprathreshold rTMS induced activations (red-yellow) in the left M1/S1, the medial SMA and CMA, the lateral postcentral region (putative S1 and S2) and the left thalamus. BOLD MRI signal decreases (blue) were observed in the right M1/S1 and occipital cortex. Except for the stimulated left M1/S1, subthreshold rTMS evoked similar but smaller activations.

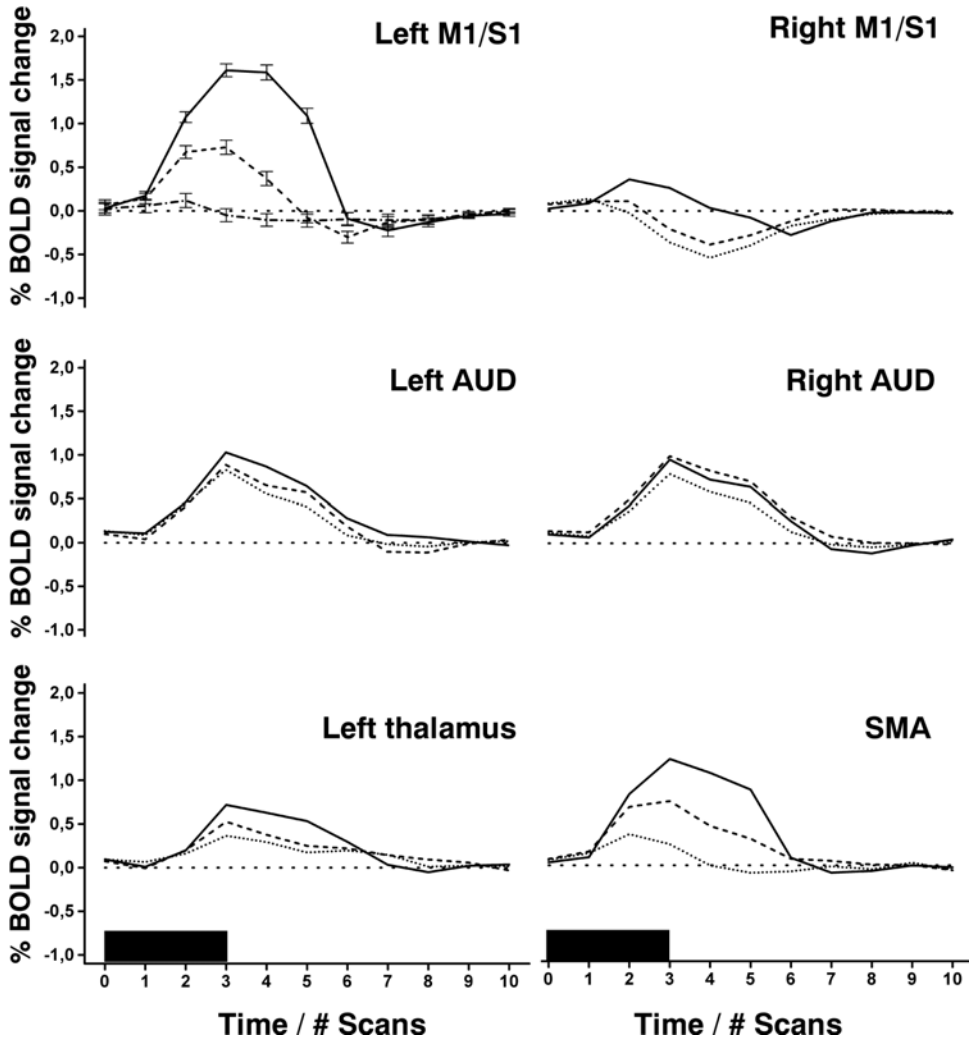


**Figure 6.7.** BOLD MRI signal intensity time courses (mean ± SEM, only indicated in the upper left graph for the sake of visibility) from 6 regions-of-interest for voluntary finger movement (solid line), suprathreshold rTMS at 110% RMT (dashed line), and subthreshold rTMS at 90% AMT (dotted line). Stimulation periods are indicated by black bars. M1/S1: sensorimotor cortex, PMd: dorsal premotor cortex, SMA: supplementary motor area, AUD: auditory cortex.

As shown in Figure 6.8 and summarised in Table 6.3, a direct comparison of activations evoked by supra- and subthreshold rTMS yielded significant differences in several cortical motor regions, while no differences were found in auditory cortical or subcortical areas. In more detail, suprathreshold rTMS led to stronger activations in the medial cortical regions of the left M1/S1 hand area, the SMA and CMA, the left PMd, and left parietal operculum. Furthermore, no significant difference in auditory activity was detected when rTMS was contrasted with voluntary finger movement (not shown). Voluntary

finger movement elicited significantly stronger responses in all motor regions when compared to either supra- or subthreshold rTMS.

Table 6.1: Activity evoked by suprathreshold rTMS (110% RMT)

| | Talairach Coordinates[1] | | | | |
|---|---|---|---|---|---|
| Anatomical/functional location | x | y | z | t-value[2] | Volume[3] |
| L sensorimotor (M1/S1) | -36 | -22 | 56 | 7.86 | 1600 |
| L precentral sulcus (PMd) | -28 | -15 | 65 | 6.04 | 267 |
| L inferior part of precentral gyrus (PMv) | -52 | 0 | 17 | 10.52 | 1806 |
| L postcentral sulcus | -56 | -25 | 43 | 7.80 | 997 |
| L auditory cortex (AUD) | -47 | -29 | 17 | 16.28 | 7346 |
| L insular cortex | -35 | -1 | 15 | 10.36 | 964 |
| L ventral posterior middle temp. Gyrus | -49 | -51 | 7 | 6.42 | 493 |
| L ventro-lateral thalamus (VLN) | -11 | -14 | 11 | 9.33 | 966 |
| L putamen | -27 | -7 | 12 | 7.61 | 590 |
| L inferior colliculus / MGN | -6 | -26 | -2 | 6.35 | 185 |
| SMA | 1 | -10 | 60 | 9.58 | 1327 |
| Cingulate motor area (CMA) | 1 | 1 | 41 | 9.14 | 1365 |
| Posterior SMA | 1 | -36 | 56 | -7.13 | 245 |
| R sensorimotor (M1/S1) | 39 | -29 | 54 | -5.86 | 276 |
| R auditory cortex (AUD) | 49 | -29 | 16 | 12.97 | 6883 |
| R ventro-lateral thalamus (VLN) | 11 | -12 | 10 | 6.86 | 188 |
| R inferior colliculus (IC) | 4 | -26 | -6 | 6.30 | 119 |
| R posterior parietal cortex | 17 | -83 | 24 | -5.31 | 386 |
| R transverse occipital sulcus | 29 | -82 | 13 | -5.77 | 189 |
| R cerebellar hemisphere | 12 | -46 | -12 | 11.97 | 1122 |

[1]Coordinates correspond to center of gravity of respective activation clusters. [2]Peak activation within cluster with $P < 0.01$, corrected. [3]Rescaled to voxel size 1 x 1 x 1 mm.

## 6.4 Discussion

The present results for the first time demonstrate that activations of distinct motor networks by short periods of focal rTMS of the sensorimotor cortex can be detected with BOLD-sensitive fMRI at a field strength of 3T. In particular, the underlying changes of the BOLD MRI signal were not localised to the area stimulated by TMS but involved a range of cortical and subcortical motor pathways and, furthermore, cover major parts of the auditory system. While the activations of multiple motor areas illustrate the capability of TMS to act on functionally and anatomically connected circuits remote to the

stimulated brain region, the occurrence of auditory activations emphasise the requirement to carefully control for the confounding influences on regional synaptic activity due to concomitant sensory stimulation.

Table 6.2: Activity evoked by subthreshold rTMS (90% AMT)

| | Talairach Coordinates[1] | | | | |
|---|---|---|---|---|---|
| Anatomical/functional location | x | y | z | t-value[2] | Volume[3] |
| L precentral sulcus (PMd) | -26 | -14 | 62 | 5.04 | 108 |
| L auditory cortex (AUD) | -46 | -24 | 13 | 13.82 | 6039 |
| L ventro-lateral thalamus (VLN) | -10 | -14 | 11 | 6.74 | 599 |
| L inferior part of precentral gyrus (PMv) | -52 | -2 | 14 | 8.49 | 1157 |
| L inferior colliculus IC / MGN | -5 | -25 | -3 | 4.51 | 82 |
| SMA | 5 | -5 | 59 | 5.68 | 284 |
| Cingulate motor area (CMA) | 2 | 8 | 42 | 5.60 | 515 |
| Posterior SMA | 0 | -30 | 57 | -7.15 | 450 |
| Medial occipital cortex | 1 | -82 | 14 | -6.32 | 440 |
| R sensorimotor (M1/S1) | 35 | -30 | 53 | -7.26 | 321 |
| R auditory cortex (AUD) | 49 | -21 | 14 | 12.09 | 5280 |
| R ventro-lateral thalamus (VLN) | 11 | -11 | 11 | 6.86 | 159 |
| R posterior parietal cortex | 14 | -84 | 29 | -7.30 | 199 |
| R transverse occipital sulcus | 30 | -79 | 9 | -7.77 | 310 |

[1]Coordinates correspond to center of gravity of respective activation clusters. [2]Peak activation within cluster with $P < 0.01$, corrected. [3]Rescaled to voxel size 1 x 1 x 1 mm.

Table 6.3: Contrast supra- vs subthreshold rTMS

| | Talairach Coordinates[1] | | | | |
|---|---|---|---|---|---|
| Anatomical/functional location | x | y | z | t-value[2] | Volume[3] |
| L sensorimotor (M1/S1) | -36 | -26 | 58 | 8.79 | 1371 |
| L precentral sulcus (PMd) | -28 | -14 | 65 | 4.88 | 158 |
| L postcentral gyrus | -51 | -29 | 47 | 6.57 | 1153 |
| SMA | 0 | -11 | 57 | 6.42 | 669 |
| Cingulate motor area (CMA) | -3 | -9 | 47 | 6.43 | 887 |
| Right Cerebellum | 11 | -45 | -13 | 6.12 | 166 |

[1]Coordinates correspond to center of gravity of respective activation clusters. [2]Peak difference with $P < 0.01$ corrected. [3]Rescaled to voxel size 1 x 1 x 1 mm. L: left, R: right

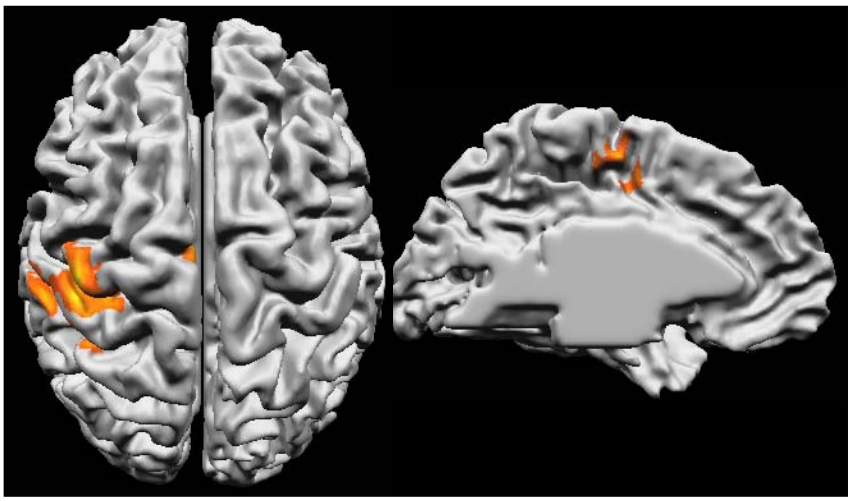

**Figure 6.8.** Brain regions with significantly stronger activations (11, subjects, $P < 0.01$, corrected) evoked by suprathreshold rTMS as compared to subthreshold rTMS. When projected onto the dorso-lateral surface of a reference brain (MNI), more pronounced suprathreshold rTMS effects were detected in the left M1/S1, PMd, and postcentral sulcus. Medially, stronger activations were found in the SMA and dorsal cingulate gyrus. No significant differences were detected in the auditory cortical and subcortical regions. L: left, R: right.

### 6.4.1 Motor system

The extent of TMS-induced activity changes within cortical and subcortical motor networks was similar to that observed previously using PET (PAUS ET AL., 1997, 1998; SIEBNER ET AL., 2000; 2001a,b, 2003a; LEE ET AL., 2003) or fMRI (NAHAS ET AL., 2001; CHAPTER 3). Apart from the contralateral M1/S1, pertinent areas include the left dorsal premotor area together with bilateral posterior SMA and CMA. Subcortical activations were seen in ipsilateral cerebellum, ventrolateral thalamus and ventro-medial putamen. Because similar activation patterns are elicited in response to voluntary finger movements, much of this activity presumably reflects the anatomical connectivity of the stimulated M1/S1 known to possess direct monosynaptic connections with all of the aforementioned areas. This understanding is also consistent with the fact that TMS activated the posterior part of the SMA rather than the pre-SMA. Whereas the former is intimately linked with M1 (GEYER ET AL., 2000), the latter predominantly projects to the prefrontal cortex and does not have any direct connections with M1/S1 (RIZZOLATTI ET AL., 1996).

In general, the pattern of changes in activity within the motor system was similar during suprathreshold and subthreshold rTMS except for the directly stimulated M1/S1, which was only activated during suprathreshold stimulation. As suggested previously, the most likely explanation for this difference is due to the fact that much of the suprathreshold M1/S1 activation represents the afferent feedback from the actual muscle movements induced by the TMS pulses (BAUDEWIG ET AL., 2001; CHAPTER 4). Nevertheless, the complete absence of any BOLD MRI signal changes in M1/S1 during subthreshold TMS is surprising for two reasons. First, there is good electrophysiological evidence that subthreshold stimulation activates the cortical circuitry even if it fails to elicit the corticospinal output necessary for a muscle twitch (DI LAZZARO ET AL., 1998, FISHER ET AL., 2002). Recordings from implanted spinal epidural electrodes probing descending motor activity indeed demonstrated that little if any activity is evoked by TMS below active motor threshold (DI LAZZARO ET AL., 1998, 2002). On the other hand, paired pulse experiments in which a small initial stimulus is used to condition the response to a larger test stimulus clearly show that a subthreshold TMS pulse can affect the excitability of cortical circuits (KUJIRAI ET AL., 1993; FISHER ET AL., 2002; BESTMANN ET AL., 2004). Pharmacological evidence suggests that much of this altered excitability is synaptically mediated via local GABAergic synapses (ZIEMANN ET AL., 1996b, 1998; DI LAZZARO ET AL., 2000). Thus, if subthreshold pulses induces a transsynaptic excitation of cortical neurons, then why is this not reflected in a BOLD response?

At present, one can only speculate on the possible answers to the above question. Explanations proposed so far range from insufficient sensitivity for the detection of subtle BOLD MRI signal changes at the site of stimulation to a cancellation of inhibitory and excitatory processes that lead to a negligible net synaptic activity with no haemodynamic output, and the occurrence of altered haemodynamic response characteristics that may not be detected by using common response functions (SIEBNER ET AL., 2003b). Although no test for alternative haemodynamic responses in the stimulated M1/S1 was conducted, the temporal profile of BOLD MRI signal increases in remote

motor regions was in excellent agreement with a large number of preceding fMRI motor studies. At present, a model in which the local haemodynamic changes that are evoked at the site of stimulation by subthreshold rTMS do not exceed the background physiological `noise' level seems favourable. Similar ideas were recently reported in a combined SPECT-TMS study (OKABE ET AL., 2003). Despite widespread activity changes in remote motor regions, no evidence was found for local responses during 1 Hz rTMS just above AMT. It is also interesting to note that a similar lack of BOLD MRI activations at the site of stimulation was reported after TMS over the lateral premotor cortex (BAUDEWIG ET AL., 2001; KEMNA & GEMBRIS, 2003) and the postcentral region (KEMNA & GEMBRIS, 2003). In addition, small but non-significant activity increases in M1 were reported in a recent PET-TMS study despite widespread activations in other connected areas (CHOUINARD ET AL., 2003).

A second question related to subthreshold rTMS concerns the mechanism that activates areas distant from the site of stimulation. In the previous chapters it was already argued that such activations are likely to reflect changes in synaptic input from M1/S1, at least for motor-related areas. However, if a subthreshold stimulus does not evoke activity in the corticospinal output from M1, it remains questionable if it can directly activate cortico-cortical or cortico-subcortical pathways. The fact that the presumed transcallosal output from one motor cortex to the other usually has a higher threshold than the corticospinal output (FERBERT ET AL., 1992) suggests that the answer is negative. Another possibility holds that remote motor activations result from a change in the general pattern of ongoing physiological activity in the motor system which is initiated by a TMS-induced alteration of the cortical excitability within M1/S1. This would be consistent with previous findings of remote excitability changes in response to subthreshold rTMS of the premotor cortex (GERSCHLAGER ET AL., 2001; MUNCHAU ET AL., 2002; RIZZO ET AL., 2004). At low stimulation intensities and short pulse trains the expected small change in the overall neural activity is probably unable to reach the threshold for local haemodynamic increases which would also be in line with suggested nonlinearities of neurovascular

coupling (MATHIESEN ET AL., 1998; LAURITZEN, 2001). Nevertheless, rTMS at subthreshold intensity might still be able to alter the efferent function of M1 to such a degree that it induces changes in blood flow or BOLD MRI signal strength in directly connected brain regions.

It should be noted that previous PET-TMS studies have reported strong effects at the site of stimulation when using longer stimulation periods of up to 30 min (SIEBNER ET AL., 2000, 2001a,b, 2003a,c; LEE ET AL., 2003). Thus, the absence of a BOLD effect to a brief period of subthreshold rTMS seems to indicate a dose-dependency which leads to rather different cortical (and haemodynamic) effects for prolonged stimulation as compared to a short series of stimuli. Further work is needed to address this problem.

Extending previous PET and fMRI studies, both supra- and subthreshold rTMS of the motor cortex evoked localised activity changes in subcortical structures such as the ipsilateral ventro-lateral thalamus and postcommissural portion of the putamen. Less consistent activity was found in the contralateral thalamus and putamen. These subcortical structures are known to be intimately linked to the sensorimotor cortex (PARENT & HAZRATI, 1995a,b). The location of thalamic activity corresponded well with previously described motor activity of the thalamus (LEHERICY ET AL., 1998). Consistent activation was found in the ventro-lateral nucleus, with some degree of overlap with the ventral posterolateral (VPL) and posteromedial (VPM) nucleus. A possible explanation may result from the fact that rTMS not only activates thalamocortical motor regions related to limb movement (VPL), but also leads to processing of somatosensory information evoked by the stimulated sensation of both the limbs (VPL) and head (VPM). Activity in the basal ganglia was predominantly found in the postcommissural part of the putamen again known to receive strong sensorimotor projections (PARENT & HAZRATI, 1995b). Involvement of this location is largely in agreement with previous fMRI investigations on basal ganglia activity (LEHERICY ET AL., 1998; SCHOLZ ET AL., 2000; GERARDIN ET AL., 2003).

During suprathreshold rTMS, several subjects reported some degree of discomfort from the pressure of the vibrating TMS coil on the head.

Activations in the anterior insula were only seen during suprathreshold stimulation and may represent neural processing of this unpleasant input. This interpretation is in accordance with SIEBNER ET AL. (2001b) who found a linear activity increase in the anterior insular cortex with the frequency of rTMS of the left M1/S1.

### 6.4.2 Auditory system

Pronounced activations in the superior temporal gyrus and sulcus and TTG bilaterally were found in all conditions, similar to previous reports using either PET (SIEBNER ET AL., 1999b) or fMRI (BOHNING ET AL., 1999, 2000b; BAUDEWIG ET AL., 2001; NAHAS ET AL., 2001). They were primarily located in the upper posterior section of the TTG and superior temporal gyrus in agreement with other recent studies (BILECEN ET AL., 2002; BRECHMANN ET AL., 2002; HUGDAHL ET AL., 2003). The activations extended into the planum temporale and inferior frontal gyrus (putative PMv) as observed for processing of loud stimuli (BILECEN ET AL., 2002; BRECHMANN ET AL., 2002).

Despite a lack of statistical significance, activations in the auditory system tended to be stronger during acoustically triggered finger movements than during sub- or suprathreshold rTMS. In view of studies reporting an intensity-dependent BOLD response to sound in the auditory cortex (JANCKE ET AL., 1998; LASOTA ET AL., 2003; BILECEN ET AL., 2002; BRECHMANN ET AL., 2002), this result is surprising given the substantial differences in sound pressure between the two rTMS conditions and the low-level stimulation used for acoustic triggering. However, inside the static magnetic field of a 3T MRI system, the much enhanced noise of a coil discharge may lead to a ceiling effect in terms of the BOLD response. Thus, a more likely possibility is that auditory activations during voluntary movement were boosted by attentional factors as subjects had to attend to stimulation epochs in order to identify the acoustic trigger and carry out the task, whereas during rTMS subjects were only instructed not to move. In fact, several reports observed substantial attentional modulation of cortical auditory activity. For example, activity along the middle temporal gyri and superior temporal gyrus increased during

attention to sounds and words as compared to passive listening (HUGDAHL ET AL., 2003). Attention also modulated the auditory activity as reflected in the early and late components of event-related potentials and magnetic fields (ARTHUR ET AL., 1991; RIF ET AL., 1991). In addition, foreground-background decomposition of different auditory patterns, as presumably also required for a distinction of the TMS clicks from the background noise of the scanner, has been reported to evoke stronger auditory activations than the mere listening to sound patterns above background noise (BRECHMANN ET AL., 2002).

Stimulation of the auditory cortex was accompanied by increased synaptic activity in the bilateral inferior colliculi and MGN. These activations within the auditory system are convincingly explained by the click sounds of the discharging TMS coil, which were substantially amplified within the scanner. The MGN reflects the auditory thalamic relay and projects into the primary auditory cortex via the auditory radiation. Although the location and spatial extent of the MGN can vary considerably in stereotaxic space (RADEMACHER ET AL., 2002), it was clearly distinguishable from the motor nuclei of the thalamus. There was some degree of inter-individual variability between subjects and often the activations in the inferior colliculus and MGN formed into one cluster. This is presumably due to the relatively low spatial resolution in comparison to the small size of these structures.

### 6.4.3 Technical considerations

Although EMG activity was monitored during MRI, this was only accomplished for the primary target muscle of the contralateral hand. One therefore cannot fully exclude the occurrence of myographic activity in adjacent hand or limb muscles that may have contributed to the observed results. Given the relatively low stimulation intensity for subthreshold rTMS, however, it seems unlikely that spread of activation to other hand muscles or even proximal limb muscles took place. This is supported by the absence of significant signal changes in the stimulated M1/S1 during subthreshold rTMS. Processing of the EMG for a reduction of EPI-related artefacts preserved the temporal resolution of the tracings and therefore allowed for a reliable

detection of peripheral muscle responses but also precluded a quantitative analysis of the amplitude information.

Similar to the previous chapters, it seems reasonable to assume the given set-up for combined TMS-fMRI properly targeted the left M1/S1 even though no stereotaxic positioning devices were used. In fact, previous work demonstrated a good correspondence of the optimal scalp position for TMS of the contralateral hand with respective activation clusters for hand movements (MACDONELL ET AL., 1999; SIEBNER ET AL., 2001a; HERWIG ET AL., 2002). In the future, the use of recently introduced MR-guided coil-positioning devices (BOHNING ET AL., 2003) will facilitate accurate coil placement. This will be even more important for brain regions other than M1/S1, for example the prefrontal cortex, that cannot easily be located using TMS.

# 7 Combined rTMS and fMRI of the dorsal premotor cortex

## 7.1 Introduction

The previous chapters have demonstrated the capability of interleaved TMS-fMRI to investigate the motor cortical system at high spatial and temporal resolution and visualise a distinct network of primary and secondary cortical and subcortical motor regions activated by short trains rTMS. In the following chapter, rTMS was applied to the left dorsal premotor cortex to investigate the specificity of rTMS-evoked BOLD responses with regard to the targeted cortical system.

The PMd is concerned with various aspects of action planning, movement preparation, and response selection (MURRAY ET AL., 2000; RUSHWORTH ET AL., 2003), while M1 then transforms this information into direct movement signals. Compelling evidence for the functional implication of the PMd in motor attention and selection has repeatedly been offered by reversible lesion studies in healthy humans using TMS (RUSHWORTH ET AL., 2003). For example, short trains of rTMS applied during movement preparation impairs subsequent task performance, with a left-hemispheric preponderance (SCHLUTER ET AL., 1998, 1999; JOHANSEN-BERG ET AL., 2002).

Recent evidence portends, however, that rTMS over the putative PMd also influences excitability of the primary motor cortex (CIVARDI ET AL., 2001; GERSCHLAGER ET AL., 2001; MUNCHAU ET AL., 2002; CHOUINARD ET AL., 2003; SIEBNER ET AL., 2003a; RIZZO ET AL., 2004). Furthermore, TMS does not tell us whether stimulation activates additional cortical or subcortical brain regions that in turn may contribute to the functional consequences of stimulation. In this regard, the use of complementary neuroimaging techniques allows for the delineation of brain activity in regions not directly accessible to TMS alone. For example, evidence from combined TMS and PET studies indicates

that rTMS of the PMd influences activity in a distinct network of anatomically linked motor regions (CHOUINARD ET AL., 2003). However, whereas prolonged PMd stimulation of 15-30 minutes induces widespread cortical and subcortical activity changes (CHOUINARD ET AL., 2003; SIEBNER ET AL., 2003a), there is less knowledge regarding the pattern of activity evoked by short trains of rTMS to the PMd.

This chapter took advantage of interleaved rTMS and fMRI to investigate local and remote activity changes subsequent to stimulation over 10 second periods of the left PMd. This method allows for the investigation of the mechanism of action of TMS at high temporal and spatial resolution (BOHNING ET AL., 1998, 1999, 2000; SHASTRI ET AL., 1999; BAUDEWIG ET AL., 2001; NAHAS ET AL., 2001; CHAPTER 4). An apparent advantage of this procedure is the visualisation of the physiological impact of short and transient rTMS at a high temporal and spatial resolution. Previous studies on the PMd have used stimulation epochs of one second and failed to detect significant BOLD MRI signal changes at the site of stimulation (BAUDEWIG ET AL., 2001; KEMNA & GEMBRIS, 2003). It was thus hypothesised that slightly longer stimulation periods may be more efficient in tackling a haemodynamic response. In comparison to previous TMS-fMRI studies (BOHNING ET AL., 1999; 2000; CHAPTER 4), stimulation of the PMd circumvents the problem of re-afferent somatosensory feedback from peripheral hand muscles at intensities exceeding individual resting motor thresholds. This approach therefore offers an initial step in bridging the gap between the behavioural consequences of TMS to the PMd and its physiological reflection, as measured by the BOLD response.

## 7.2 Methods

### 7.2.1 Subjects

9 healthy subjects without any previous neuropsychiatric history (mean age 28 years, range 25-42 years; six females) participated in the study.

### 7.2.2 Experimental protocol

The study comprised three experimental conditions. The order between conditions was randomised. Repetitive TMS was applied at 3 Hz using two different intensities: rTMS at 110% of individual RMT and at 90% of individual AMT. In each session, eight stimulation epochs (9.96 s) alternated with resting periods (23.24 s). Using the same protocol, right index finger dorsiflexion was conducted in a third fMRI session to functionally locate motor regions involved in manual behaviour. Movement periods were indicated by application of rTMS at 15% of stimulator output. Sessions were separated by five minutes to account for carry-over effects of stimulation. Subjects were instructed to keep their eyes closed and to relax their hands. Each subject wore earplugs and headphones to reduce acoustic noise from the discharging TMS coil. The study conformed to presently available safety guidelines for TMS (WASSERMANN, 1998).

### 7.2.3 Magnetic resonance imaging

MRI was performed at 3.0 Tesla (Siemens Trio, Erlangen) using the parameters described in the experimental methods chapter.

### 7.2.4 Transcranial magnetic stimulation

TMS was applied following the details specified in the general methods chapter. Using an posterior-anterior initial current direction, the coil was placed over the presumed location of the dorsal premotor cortex, following previously published procedures (SCHLUTER ET AL., 1998, 1999; JOHANSEN-BERG ET AL., 2002). These studies have revealed a good correspondence of coil position and the probabilistic location of the dorsal premotor cortex when positioning the TMS coil 2 cm anterior and 1 cm medial to the motor hot spot. Prior to scanning, suprathreshold TMS (110% RMT) pulses were applied to the premotor location to ensure the absence of electromyographic activity in the target muscle. In case of electromyographic responses, the TMS coil was shifted anterior for 0.5 cm

### 7.2.5 Electromyographic recordings

Electromyographic recordings were obtained following the details specified in the experimental methods chapter.

### 7.2.6 Interleaved rTMS-fMRI

Functional images were acquired every 166 ms, each image acquisition lasting 91 ms. TMS pulses were applied every 332 ms (3 Hz), starting directly after full acquisition of a single image. As such, waiting periods between TMS pulses and subsequent MR image acquisitions of 75 ms were achieved. In order to avoid mechanical damage to the MR-head coil, direct contact with the TMS coil was always avoided, and the induced magnetic field of the TMS coil was never directed directly onto the MR-head coil frame.

### 7.2.7 Data analysis

Image processing and statistical analysis were carried out using the BrainVoyager 2000 software package (Brain Innovation, Maastricht, The Netherlands). Motion correction, intensity normalisation and linear drift removal was performed prior to statistical analysis. Spatial smoothing was achieved by transformation of functional datasets into 3 mm isotropic resolution. Functional data was co-registered with high-resolution anatomical T1-weighted images. Individual pre-processed volume time courses were analysed using the GLM with stimulation or movement epochs as the effects of interest. Multi-subject analysis was conducted using a fixed effects model to test for significant changes in BOLD MRI signal during each experimental condition at a group level ($P < 0.01$ adjusted for multiple comparisons).

## 7.3 Results

None of the subjects reported any side effects from the experimental procedure. As shown in Figure 7.1 for a representative subject, no evidence for EMG activity was found during suprathreshold rTMS ($P=0.24$) while voluntary finger movement epochs evoked clear electromyographic response

as compared to rest (P<0.01). This indicates that the observed changes in BOLD MRI signal during effective rTMS can not be attributed to a spread of excitation into the adjacent primary motor cortex and a consequent activation of peripheral hand muscles. In the following discussion it will therefore be assumed that the observed activity changes reflect interaction between corticocortical and / or corticosubcortical circuits directly or indirectly targeted by TMS.

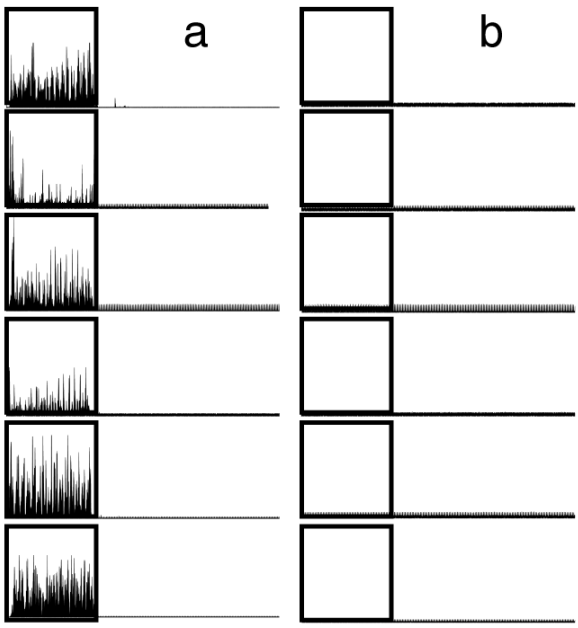


**Figure 7.1.** EMG recordings of finger movement **(a)** and suprathreshold rTMS of the left PMd **(b)** from six representative subjects during fMRI. Stimulation epochs (boxes) were time-locked averaged to the onset of stimulation. Frequency extraction (7-25 Hz) was performed to reduce MRI gradient artefacts. No EMG activity was evidenced in the contralateral FDI muscle during suprathreshold rTMS, indicating that stimulation at 110% resting motor threshold did not spread into the primary motor hand region.

Figure 7.2 reveals that suprathreshold rTMS evoked a localised BOLD response at the site of stimulation in the putative left PMd (mean coordinates of cluster: *x= -40, y= –11, z=54*). Additional activity increases were found in the homologous PMd, the bilateral PMv of the frontal opercular region, the SMA in the medial aspect of the superior frontal gyrus, the CMA, the left posterior middle temporal gyrus, and the entire putative bilateral auditory cortex (AUD), including the superior temporal plane, superior temporal gyrus, and planum temporale (Figure 7.2, Table 7.1). No significant activation was observed in the left M1/S1.

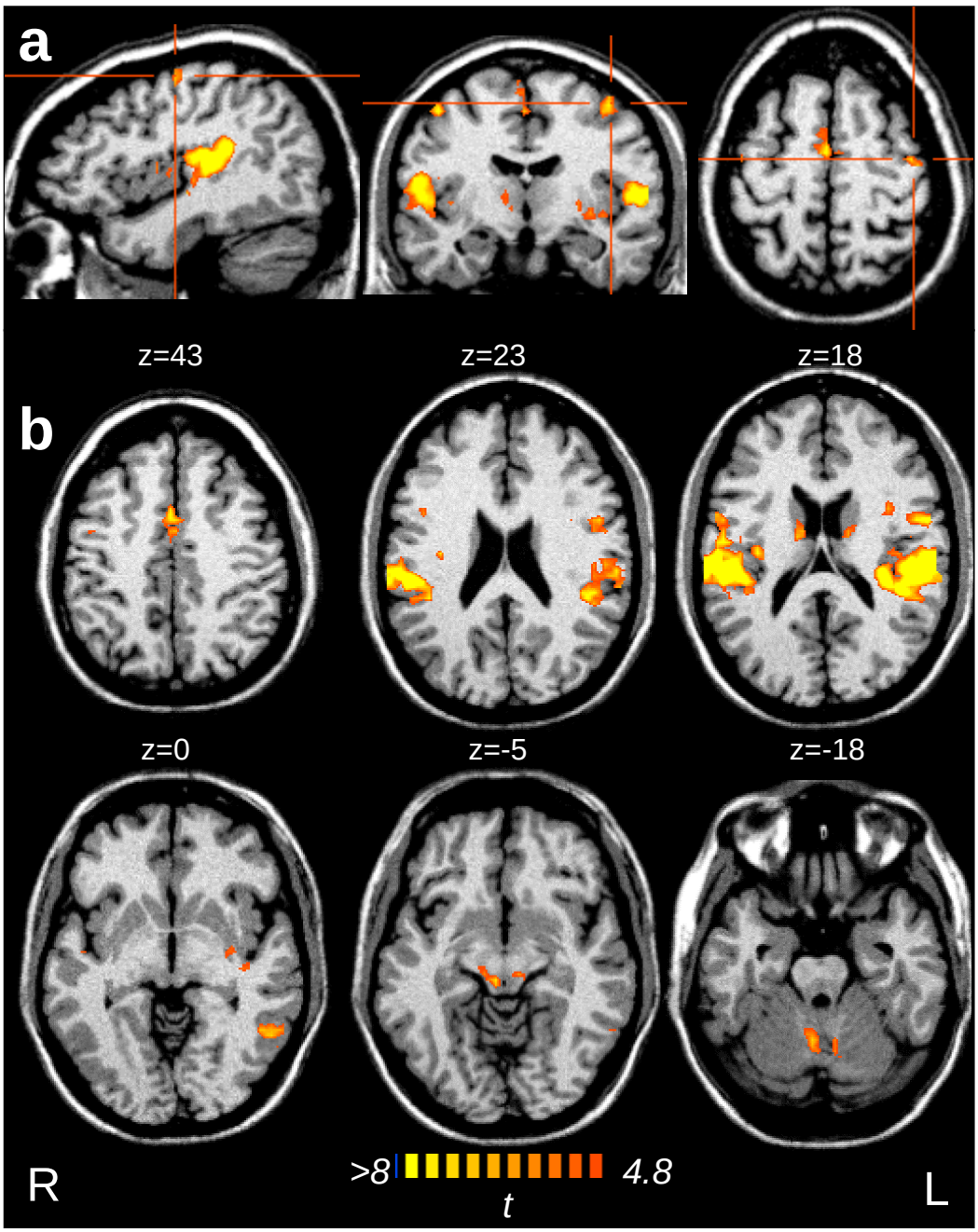


**Figure 7.2.** Brain activations obtained for a group analysis (9 subjects, P < 0.01, corrected) of responses to suprathreshold rTMS of the left PMd. **(a)** Sagittal (*x=-40*), coronal (*y=-11*), and transverse (*z=55*) view of activity in the left PMd. **(b)** Six transverse sections showing activity changes in the CMA, PMv, auditory cortex, caudate nucleus, left posterior temporal lobe, medial geniculate nucleus, and cerebellum. Activation maps are projected on a template brain (Montreal Neurological Institute, MNI).

At the subcortical level, bilateral activity was found in the middle part of the caudate nucleus, as well as the putative motor thalamus of the left hemisphere and the bilateral inferior colliculi. As shown in Figure 7.2, cerebellar activity was localised in the putative hand-arm region (GRODD ET

AL., 2001), with a right-hemispheric preponderance (Table 7.1). Figure 7.3a and Table 7.2 present the good correspondence between brain regions activated during voluntary finger movement and rTMS of the left PMd.

Table 7.1: Activity evoked by suprathreshold rTMS over the left PMd

| | Talairach Coordinates[1] | | | | |
|---|---|---|---|---|---|
| Anatomical/functional location | *x* | *y* | *z* | t-value[2] | Volume[3] |
| L precentral sulcus (PMd) | -40 | -11 | 54 | 8.24 | 438 |
| L inf. precentral gyrus (PMv) | -49 | 1 | 18 | 10.74 | 1544 |
| L auditory cortex[4] | -45 | -27 | 16 | 16.42 | 7854 |
| L posterior temporal lobe | -50 | -52 | 3 | 9.26 | 1317 |
| L thalamus | -11 | -16 | 14 | 6.04 | 118 |
| L caudate | -11 | -4 | 18 | 6.72 | 68 |
| L cerebellar hemisphere | -6 | -59 | -20 | 6.99 | 407 |
| L MGN | -3 | -20 | -2 | 7.00 | 56 |
| BL medial superior frontal gyrus (SMA) | 3 | -6 | 56 | 8.73 | 815 |
| BL cingulate gyrus (CMA) | 3 | 4 | 44 | 9.26 | 1024 |
| R precentral sulcus (PMd) | 43 | -5 | 50 | 9.12 | 410 |
| R precentral sulcus (PMd) | 42 | 7 | 26 | 7.64 | 238 |
| R precentral sulcus (PMv) | 53 | 0 | 13 | 9.14 | 1127 |
| R auditory cortex[4] | 52 | -25 | 18 | 15.72 | 7530 |
| R thalamus | 12 | -11 | 8 | 6.97 | 172 |
| R caudate | 13 | -1 | 15 | 7.42 | 501 |
| R cerebellar hemisphere | 5 | -56 | -15 | 8.38 | 571 |

[1]Coordinates correspond to center of gravity of respective activation clusters. [2]Peak activation within cluster with $P < 0.01$, corrected. [3]Rescaled to voxel size 1 x 1 x 1 mm. [4]Including transverse temporal gyrus, superior temporal gyrus, ventral part of parietal operculum and planum temporale. PMd: dorsal premotor cortex, PMv: ventral premotor cortex, CMA: cingulate motor region, MGN: medial geniculate nucleus, L: left, R: right, BL: bilateral.

The results of subthreshold rTMS are listed in Table 7.3. In principle, activity changes were similar as during suprathreshold rTMS, although much lesser in extent. However, no response at the site of stimulation was found.

A direct comparison of stimulation conditions revealed significantly stronger activity in all implied brain regions during suprathreshold rTMS (Figure 7.4, Table 7.4). As depicted in Figure 7.4, this included activity at the site of stimulation, the mesial motor regions, the dorsal and ventral premotor cortices, and the left posterior temporal cortex. Figure 7.5 further illustrates that suprathreshold, but not subthreshold rTMS evoked a significant BOLD

response at the site of stimulation, whereas both rTMS conditions failed to activate the caudally adjacent M1.

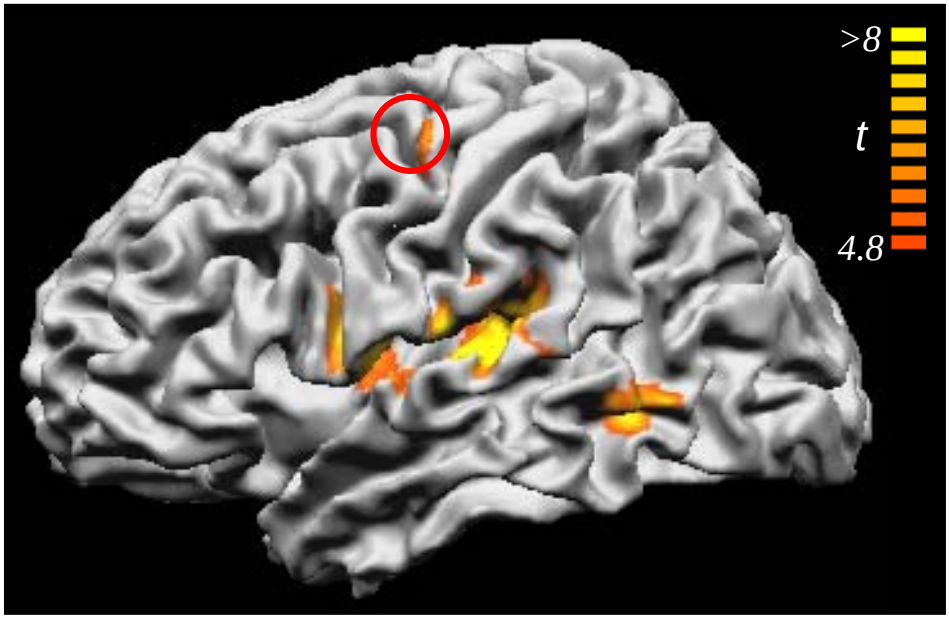


**Figure 7.3.** Brain regions activated by both suprathreshold rTMS of the left PMd and voluntary finger movement projected on a left-hemispheric 3D surface reconstruction (MNI). Importantly, activity increased in the stimulated left PMd (*red circle*). Additional activity in the left hemisphere was evoked in PMv, SMA, CMA, auditory cortices, and left posterior middle temporal gyrus (n=9; P<0.01, corrected). L: left, R: right.

Table 7.2: Conjunction analysis finger tapping – suprathreshold rTMS

| | Talairach Coordinates[1] | | | | |
|---|---|---|---|---|---|
| Anatomical/functional location | *x* | *y* | *z* | t-value[2] | Volume[3] |
| L precentral sulcus (PMd) | -41 | -12 | 55 | 7.54 | 92 |
| L precentral sulcus (PMv) | -50 | 0 | 15 | 9.21 | 1261 |
| L auditory cortex[4] | -46 | -25 | 16 | 13.93 | 6887 |
| L posterior temporal lobe | -50 | -53 | 3 | 9.26 | 1035 |
| L MGN | -5 | -19 | -3 | 6.47 | 119 |
| BL medial superior frontal gyrus (SMA) | 3 | -6 | 55 | 8.72 | 810 |
| BL cingulate gyrus (CMA) | 3 | 4 | 43 | 8.39 | 675 |
| R PMv | 53 | 1 | 14 | 9.14 | 119 |
| R auditory cortex[4] | 53 | -22 | 15 | 14.11 | 5070 |
| R caudate | 13 | -1 | 15 | 6.86 | 195 |
| R cerebellar hemisphere | 5 | -55 | -15 | 8.38 | 588 |

[1]Coordinates correspond to center of gravity of respective activation clusters. [2]Peak activation within cluster with P < 0.01, corrected. [3]Rescaled to voxel size 1 x 1 x 1 mm. [4]Including transverse temporal gyrus, superior temporal gyrus, ventral part of parietal operculum and planum temporale. MGN: medial geniculate nucleus.

Table 7.3: Activity evoked by subthreshold rTMS over the left PMd

| Anatomical/functional location | Talairach Coordinates[1] | | | t-value[2] | Volume[3] |
|---|---|---|---|---|---|
| | *x* | *y* | *z* | | |
| L precentral sulcus (PMd) | -43 | -11 | 53 | 5.10 | 53 |
| L inf. precentral gyrus (PMv) | 53 | -3 | 11 | 7.79 | 1012 |
| L auditory cortex [4] | -45 | -25 | 14 | 12.86 | 7407 |
| L posterior temporal lobe | -49 | -53 | 4 | 7.63 | 702 |
| L thalamus | -7 | -13 | 4 | 6.03 | 130 |
| BL medial superior frontal gyrus (SMA) | 0 | -5 | 52 | 6.02 | 201 |
| BL cingulate gyrus (CMA) | 3 | 6 | 43 | 6.23 | 432 |
| R precentral sulcus (PMv) | 46 | -3 | 46 | 6.04 | 610 |
| R precentral sulcus (PMv) | 53 | -3 | 11 | 7.79 | 1012 |
| R auditory cortex[4] | 49 | -23 | 14 | 12.29 | 6702 |
| R thalamus | 11 | -11 | 9 | 6.63 | 216 |

[1]Coordinates correspond to center of gravity of respective activation clusters. [2]Peak activation within cluster with P < 0.01, corrected. [3]Rescaled to voxel size 1 x 1 x 1 mm. [4]Including transverse temporal gyrus, superior temporal gyrus, ventral part of parietal operculum and planum temporale. For other abbreviations see Table 7.1 and 7.2.

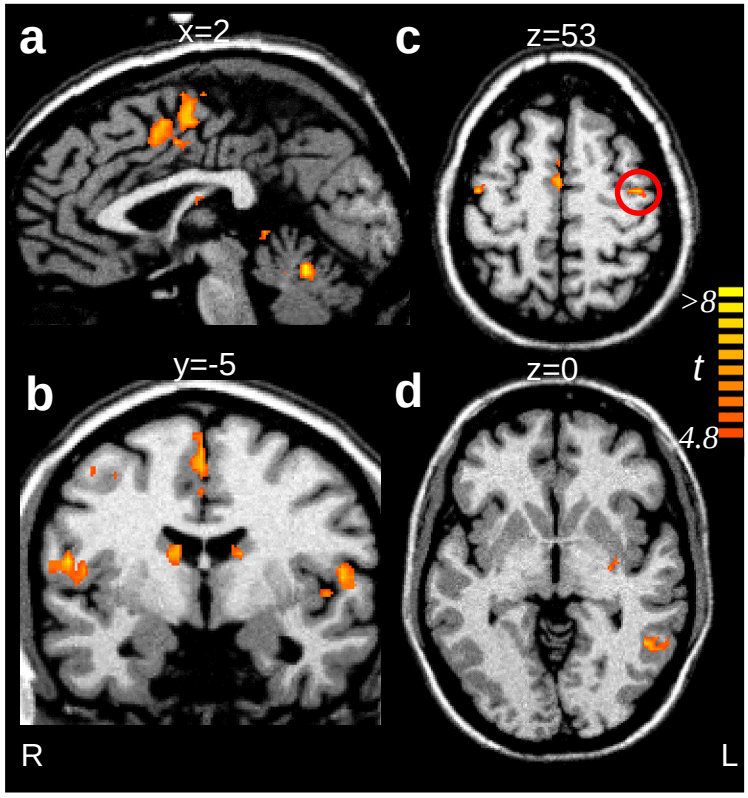


**Figure 7.4.** Comparison of supra- and subthreshold rTMS displayed on a sagittal **(a)**, coronal **(b)**, and two transverse **(c,d)** sections of a reference brain (MNI) with Talairach coordinates indicated. Stimulation at 110% RMT evoked significantly stronger activity changes at the site of stimulation (left PMd, white circle), the right PMd, SMA, CMA, right cerebellum, bilateral superior temporal plane (putative auditory cortices), bilateral caudate nucleus, and left posterior middle temporal gyrus (n=9; P<0.01, corrected). L: left, R: right.

Table 7.4: Activity differences between supra- and subthreshold rTMS

| Anatomical/functional location | Talairach Coordinates[1] x | y | z | t-value[2] | Volume[3] |
|---|---|---|---|---|---|
| L precentral sulcus (PMd) | -37 | -10 | 55 | 8.08 | 157 |
| L precentral sulcus (PMv) | -51 | 1 | 12 | 9.52 | 530 |
| L posterior temporal lobe | -50 | -51 | 3 | 7.96 | 485 |
| L caudate | -10 | -5 | 19 | 7.14 | 55 |
| BL medial superior frontal gyrus (SMA) | 3 | -5 | 55 | 7.53 | 297 |
| BL cingulate gyrus (CMA) | 2 | 5 | 47 | 7.40 | 319 |
| R precentral sulcus (PMd) | 43 | -8 | 52 | 8.79 | 130 |
| Right precentral sulcus (PMv) | 41 | 7 | 26 | 6.80 | 130 |
| R caudate | 13 | 0 | 15 | 7.63 | 418 |
| R cerebellar hemisphere | 5 | -55 | -14 | 8.61 | 336 |

[1]Coordinates correspond to center of gravity of respective activation clusters. [2]Peak activation within cluster with $P < 0.01$, corrected. [3]Rescaled to voxel size 1 x 1 x 1 mm. [4]Including transverse temporal gyrus, superior temporal gyrus, ventral part of parietal operculum and planum temporale. For other abbreviations see Table 7.1 and 7.2.

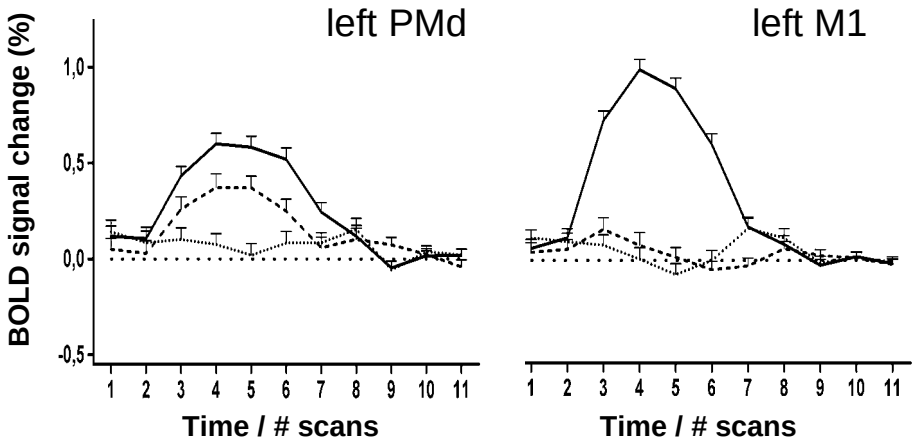


**Figure 7.5.** Mean MRI signal time course averaged across subjects (mean ± s.e.m., n=9) of the left M1 and the stimulated left PMd as determined from an anatomically demarcated Region-of-Interest. Voluntary finger movement (*solid line*) and suprathreshold rTMS (*dashed line*) evoked a response at the site of stimulation, while no significant response was found during subthreshold rTMS (*dotted line*). In the left M1 caudal to the site of stimulation, only finger movement was found to evoke significant activity changes. L: left, R: right.

## 7.4 Discussion

To my best knowledge, the present study is the first demonstration of activity increases at the site of stimulation by means of high resolution fMRI during short trains of rTMS.

The occurrence of a local response modulation by TMS indicates that the effects of TMS in terms of haemodynamic response changes may not be uniform across the brain and across stimulation protocols, as various studies have failed to demonstrate local BOLD changes when accounting for re-afferent feedback (BOHNING ET AL., 1999; BAUDEWIG ET AL., 2001; KEMNA & GEMBRIS, 2003; CHAPTER 4). These studies have either used 1 Hz stimulation (Bohning et al., 1999), short stimulation trains of 1s (BAUDEWIG ET AL., 2001; KEMNA & GEMBRIS, 2003), or low stimulation intensities (CHAPTER 4). One likely explanation for the increased efficacy of suprathreshold rTMS, in contrast to subthreshold stimulation, to evoke local and remote activity changes, is that it activates distant sites by both direct stimulation of subcortical projection fibres as well as activation of corticocortical circuits

Several factors indicate that the PMd was indeed directly targeted rather than the caudally adjoining primary motor cortex, the nearby FEF, or the rostrally located prefrontal cortex. First, the activation center in left caudal PMd during suprathreshold rTMS (*x= -40, y= -11, z=54*) was located 12 mm anterior to the activation center in M1/S1 during finger tapping (*x=33, y=23, z=55*), which is within the range of the probabilistic location of PMd as obtained by previous functional imaging studies (PICARD & STRICK, 2001). In addition, there is a good correspondence between the probabilistic location of the PMd as determined by TMS and the underlying cortical structure (SCHLUTER ET AL., 1998, 1999; JOHANSEN-BERG ET AL., 2002). Second, no activity was evoked in the left M1 during effective rTMS. In particular during suprathreshold rTMS, direct targeting of M1 can be assumed to have resulted in peripheral muscle movements that have been reported to result in eminent activations of M1 (BOHNING ET AL., 1998, 1999; BAUDEWIG ET AL., 2001). Third, stimulation of the FEF has been shown to preferentially target the visual rather than the motor

system (PAUS ET AL., 1997) and would thus make the extensive activity changes within the frontal motor regions difficult to accommodate.

The lack of significant response changes in the left M1/S1 is somewhat surprising when considering recent findings of a significant influence of premotor rTMS on primary motor cortex activity (CIVARDI ET AL., 2001; GERSCHLAGER ET AL., 2001; MUNCHAU ET AL., 2002; SIEBNER ET AL., 2003a) and vice versa (LEE ET AL., 2003; SIEBNER ET AL., 2001a; CHAPTER 4). The present results are, however, in agreement with a previous investigation of 1 Hz rTMS of the left PMd that did not reveal significant blood flow changes in left M1 (CHOUINARD ET AL., 2003). An explanation briefly entertained in this study was that TMS had preferentially activated inter-hemispheric rather than intra-hemispheric connections. Given the intimate coupling between the intra-hemispheric PMd and M1, however, it is difficult to reconcile how TMS would only activate projections to the contralateral hemisphere. The present findings indicate that positive BOLD responses in M1 are not readily evoked by short trains of rTMS to the PMd.

Even single conditioning pulses to the PMd exert an inhibitory influence on M1 (CIVARDI ET AL., 2001). The latency of this effect of 6 ms suggests transsynaptic processes rather than a removal of ongoing tonic activity. Therefore, activation of neurons projecting into M1 might be less susceptible in terms of the resulting haemodynamic impact, and might only be elicited by prolonged stimulation trains (GERSCHLAGER ET AL., 2001; MUNCHAU ET AL., 2002; SIEBNER ET AL., 2003a). The rostral part of M1 receives stronger projections from the PMd and is generally less excitable than the caudal part of M1 (KAAS & STEPNIEWSKA, 2002). This may further indicate that stimulation of the PMd provokes rather subtle changes in M1 that may be readily detected using electrophysiological measures but is less likely to be reflected in significant BOLD MRI signal changes.

The fact that only suprathreshold rTMS elicited significant activity increases at the site of stimulation further supports the notion of a dose-dependent mechanism of action of rTMS. In this regard, the present data reveal that rTMS has differential effects on both local and remote brain circuits

depending on its intensity, and, when compared to the pattern of activity in previous studies, its duration and frequency (e.g. PAUS ET AL., 1998; BAUDEWIG ET AL., 2001; SIEBNER ET AL., 2001a,b; CHOUINARD ET AL., 2003; SPEER ET AL., 2003a, b).

Similarly, the lack of significant activity changes within the intraparietal cortex, which is not only intimately linked to the premotor cortex (WISE ET AL., 1996) but has also found to be activated by rTMS of the PMd (CHOUINARD ET AL., 2003) might be due to insufficient targeting of respective projections. It should be noted that as the location of the PMd was determined by probabilistic rather than functional criterions, slightly different subsets of premotor circuits may have been stimulated more or less efficiently, resulting in variant influence on ipsilateral M1 and parietal cortex activity that precluded reliable activation of these regions across subjects.

While rapid trains of rTMS probe the immediate response of the brain to an external cortical input, prolonged stimulation (CHOUINARD ET AL., 2003; SIEBNER ET AL., 2003a) evokes rather long-term adjustments of the brain. These can not necessarily be assumed to exhibit the same haemodynamic properties as short TMS applications, and previous studies of premotor TMS suggest a considerable degree of non-linearities in the resulting activity changes. For example, whereas stimulation over 30 minutes provokes widespread activity decreases, including M1 (SIEBNER ET AL., 2003a), the suppressive effect of shorter stimulation protocols on electromyographic activity seems to be associated with activity increases (CHOUINARD ET AL., 2003). By contrast, stimulation trains of 1 second (BAUDEWIG ET AL., 2001; KEMNA & GEMBRIS, 2003) have failed to demonstrate significant local activity changes in the vicinity of the PMd. In the present study, local responses in PMd were readily evoked at the site of stimulation at stimulation trains of 10 seconds. These were highly localised to the precentral gyrus rostral to the M1 hand area, clearly indicating that even short stimulation epochs of 10 seconds are capable to increase local activity beyond a threshold for haemodynamic response changes.

With regard to the origin of the activity changes, a recurring question throughout the TMS community is whether the effects of rTMS are evoked by inhibitory or excitatory circuits. It should be noted, however, that TMS elicits its effects on the systems level and thus involves a complex interaction of both inhibitory and excitatory circuits between multifarious brain regions (SIEBNER & ROTHWELL, 2003). TMS-induced BOLD MRI signal changes are the result of the complex interplay both within and between brain regions. Furthermore, while suprathreshold rTMS is likely to have recruited a greater number of intracortical neurons, direct antidromic activation of projections to the site of stimulation and / or increased back-propagation from cortical and subcortical target regions may also contributed to the overall activity increase. This underscores that suprathreshold rTMS, in contrast to subthreshold rTMS activates a complex range of cortical and subcortical elements that make an easy explanation of the mechanism of action difficult. This also implies that the absence of significant local BOLD MRI signal changes during subthreshold rTMS does not foreclose some level of local intracortical activity. It rather indicates that local activity does not always exceed background activity levels.

A remaining question is what mediates remote activity changes? It is tempting to attribute activity increases in the homologous PMd of the right hemisphere during suprathreshold rTMS, for example, to direct targeting of callosal connections between the two hemispheres. This would be congruent with the rich callosal connectivity of the dorsal and ventral premotor cortices (MARCONI ET AL., 2003). However, direct activation of transcallosal fibres may not invariably occur even at suprathreshold intensities as fibres in the premotor cortex have a smaller diameter than fibres in M1 and direct excitation is presumably more difficult. This mechanism would furthermore not account for remote activity changes during subthreshold rTMS. The latter might have modified the efferent function of the area of stimulation by changing the excitability of local neurons. The resulting local redistribution of efferent signals in turn may provoke altered afferent input and local

information processing in remote target regions, resulting in a change of activity as reflected by the BOLD response.

A consistent activity increase was found in the posterior part of the left posterior middle temporal region (putative BA 21/37) in all three experimental conditions. This region has been linked to passive listening of both meaningful and arbitrary sounds, with a left-hemispheric dominance (HUGDAHL ET AL., 2003). Furthermore, the left superior temporal sulcus has been implicated to the processing of auditory phonetic cues irrespective of their intelligibility (SCOTT ET AL., 2000). Assuming that subjects attended to stimulation periods in all conditions, activity in the temporal lobe presumably reflects attentional monitoring of these periods that predominantly affect the left hemisphere (HUGDAHL ET AL., 2003). Although not being verbal stimuli itself, the TMS pulses certainly contained a meaningful signal in that they either indicated movement periods or periods of stimulation during which subjects were instructed to maintain relaxation of the target muscles.

The present findings are important for several reasons. First, it was shown that combined TMS-fMRI over non-primary motor regions allows for the immediate monitoring of brain activity changes. This clearly offers unprecedented opportunities for 'virtual lesion' studies of motor function which generally utilise even shorter stimulation periods (SCHLUTER ET AL., 1998, 1999; RUSHWORTH ET AL., 2003). Here, the effects of stimulation can directly be attributed to a set of brain regions, rather than being restricted to the area of stimulation alone. Second, the results emphasise that remote activity changes may even occur following relatively short stimulation epochs and precursory knowledge regarding such changes may buttress the interpretation of the mechanism of action in TMS studies on motor function. An emerging picture from the available literature on combined TMS and neuroimaging studies clearly shows that not all stimulation protocols exhibit the same haemodynamic properties (PAUS ET AL., 1997, 1998, 2001; BAUDEWIG ET AL., 2001; NAHAS ET AL., 2001; CHOUINARD ET AL., 2003; KEMNA & GEMBRIS, 2003; LEE ET AL., 2003; SIEBNER ET AL., 2001a, 2003a; SPEER ET AL., 2003,a,b). Thus, while causally attributing behavioural changes subsequent to

TMS to the stimulated region alone might be appropriate in some occasions, such a premise may not hold true under all circumstances if remote brain regions also reveal considerable activity changes during rTMS. Clearly, being able to obtain a more capacious view of the mechanism of action of TMS will allow for a better understanding of the causal implication of a brain system during a given task. Third, the sulcal and gyral structure of the brain make a determination of the site of maximal induced current difficult. In that respect, local activity changes may provide an indirect indication of the exact site of effective stimulation. Furthermore, in the absence of behavioural measures such as reaction times, and for brain regions not exhibiting positive phenomena of stimulation such as phosphenes or motor-evoked potentials they provide information whether TMS has effectively interacted with neural function at all. Fourth, the occurrence of a positive BOLD response at the site of stimulation may allow for correlating the given input (i.e. the intensity, duration, and frequency of stimulation) with the direct and local effect of TMS. This has particular importance for connectivity studies that aim to probe cortical reorganisation due to a defined stimulus given to the brain. Notwithstanding the secondary activity changes related to somatosensory and auditory stimulation, TMS applied to the motor system targets distinct cortical and subcortical circuits that highlight the known anatomically relationship between such areas and may serve as a probe to test functional connectivity in an unparalleled fashion for a variety of brain regions.

In summary, rTMS orchestrates activity in a complex network of brain regions. Although this does not imply that the disruptive behavioural effects of rTMS to the PMd are indeed mediated by distant sites or entire brain circuits, careful inspection of activity changes due to TMS are advisable before allocating a brain region to a causal involvement in a certain behaviour. In that respect, combining TMS and fMRI holds the promise of combining the *causal* and the *correlational* for the investigation of human brain function.

# 8 General Discussion

The experiments presented in this thesis have investigated the technical feasibility of interleaved TMS-fMRI as well as the consequences on brain activity patterns following cortical stimulation in humans. The following chapter is intended to summarise and discuss the results presented in Chapters 3-7 with regard to the methodological and functional consequences impinging from these findings. Several main topics will be bound together and discussed in separate sections, with their order not necessarily reflecting their importance.

The technical requirements of combined TMS-fMRI were investigated at field strengths of 2T and 3T in Chapter 3. Extending previous studies, a more detailed description of possible imaging perturbations was conducted. It was concluded that the avoidance of any interference between TMS pulse and MR image acquisition is required for unperturbed fMRI. Unperturbed MR images may be acquired when TMS pulses are temporally separated from MR image acquisition by approximately 60-100 ms. The optimisation of section orientation with respect to the direction of phase- and frequency encoding gradients further minimises static image degradations. Experimental protocols were described for unperturbed interleaved TMS-fMRI and utilised in the subsequent experimental chapters.

In Chapter 4, the use of a high-resolution EPI protocol provided first evidence that short trains of subthreshold rTMS immediately modulate cortical activity in remote brain regions. Activity changes were localised in a confined motor network comprising the PMd and the SMA, as well as the contralateral M1/S1. The absence of detectable BOLD MRI signal changes at the site of stimulation suggested a decoupling of the known electrophysiological effects of rTMS and their reflection in corresponding haemodynamic response changes. Activity changes resulting from suprathreshold rTMS were, at least partially, linked to re-afferent somatosensory feedback evoked by peripheral muscle movements. These signal changes cannot be disentangled from the

haemodynamic component related to the cortical stimulation itself. Chapter 4 also provided the first evidence that TMS may be interleaved with continuous fMRI at frequencies beyond 1 Hz without having to exclude perturbed MR images (as in BAUDEWIG ET AL., 2001) or using stimulation protocols not exceeding 1 s (BAUDEWIG ET AL., 2001; KEMNA & GEMBRIS, 2003).

The context-dependence of TMS-induced haemodynamic changes was demonstrated in Chapter 5 when TMS was applied during or before motor behaviour. Simultaneous rTMS and motor behaviour provided the first demonstration of the modulation of the local BOLD response by TMS. By contrast, when rTMS preceded motor behaviour, attenuated BOLD responses were found in PMd and SMA, but not in the area of stimulation. The effects of TMS therefore depend on the 'state' of the brain. In the primary motor cortex, stimulation during periods of increased cortical excitability seems to be more effective of modulating local activity as compared to stimulation at rest, thus complementing results obtained by previous electrophysiological investigations.

The experiment presented in Chapter 6 extended the knowledge obtained in Chapters 3 and 4 to a higher field MR environment. By profiting from decreased echo-times, faster imaging gradients, and a proposed increase in BOLD sensitivity, activity changes were visualised at high spatial resolution in both cortical and subcortical motor regions, thus overcoming several limitations of Chapter 4. Simultaneous electromyographic recordings from the target muscle confirmed the sub- and suprathreshold nature of the rTMS protocol. Following both sub- and suprathreshold rTMS of the left M1/S1, a motor network comprising SMA, PMd, PMv, left parieto-temporal junction, the left motor thalamic nuclei and dorso-ventral putamen was found to be activated. These activity changes were accompanied by unwanted activity related to auditory and somatosensory (trigeminal) input and illustrate the complex nature of TMS. In addition, this chapter is the first demonstration of the feasibility to interleave TMS-fMRI at 3T.

Finally, TMS-related activity changes were investigated during stimulation of the PMd in Chapter 7. This study provided the first conclusive evidence that

rTMS is capable to elicit local BOLD responses that can not be attributed to re-afferent feedback. Moreover, activity changes were observed in distinct brain regions reflecting the known functional neuroanatomy of the PMd. The results emphasise that rTMS is non-focal *within* a functional system, as it may activate a set of interconnected brain regions. On the other hand, the results show that rTMS is focal *between* functionally segregated systems (e.g. primary motor and dorsal premotor cortex) as it targets distinct regions reflecting the connectivity of a specific region.

## 8.1 The haemodynamic response characteristics of TMS

At first glance, the variety of reported TMS-induced activity patterns nearly match the number of TMS pulses that have been applied in these respective experiments. Even studies using the most commonly applied stimulation frequency of 1 Hz provide little continuity regarding the resulting activity patterns. The variability of TMS pulses, intensity of stimulation, or the targeted brain region complicate a comparison between studies.

**Side note:** Several combined TMS-fMRI and TMS-PET studies have attempted to visualise TMS-evoked brain activity changes in major depression (e.g. SPEER ET AL., 2000; LI ET AL., 2003). In principle, extending the presently available applications of TMS to pathology *before* having fully elucidated its cortical underpinnings in healthy subjects seems an untimely undertaking to approach. Moreover, about 15 years of research have at best provided an indication towards the usefulness of TMS for the treatment of major depression, or even substituting electroconvulsive therapy (for a critical overview see PADBERG & MOLLER, 2002). A thorough discussion of this particular field is thus regarded as beyond the scope of the present work.

### 8.1.1 TMS–fMRI

Table 8.1: Overview of combined TMS-fMRI studies

| Study | Target site | Frequency/ Pulse number/ Train length/ Intensity | Spatial resolution | TMS trains | Local effects | Remote effects |
|---|---|---|---|---|---|---|
| Chouinard et al., 2003 | Left M1<br>Left PMd | 1 Hz/ 900/ 15 min/ 90% RMT | | 1 | M1:yes<br>PMd: no | M1 TMS: R-CMA, L-PUT, rM1, R-VLN, GP, PMd TMS: PMv, R-IPS, BL-CMA, R-PMd, SMA, rPUT |
| Kemna & Gembris, 2003 | Left M1<br>Left PMd<br>Left SPL | 4Hz/ 1 s/ 200/ 10%RMT | 6x6x8mm + 10% gap | 50 | M1: yes | SMA |
| McConnell et al., 2003 | Left M1 | 1 Hz/ 21/ 21 s/ 110% RMT | 5 mm + 1.5 mm gap | 8 | M1: yes | |
| Bohning et al., 2003 | Left M1 | 1 Hz/ 1,2,3,8,16 pulses per epoch/ 120% RMT | 5 mm + 1.5 mm gap | 5 per condition | Yes, increasing with pulse number | BL-AUD, R-M1 |
| Baudewig et al., 2001 | Left M1<br>Left PMd | 10 Hz/ 10/ 1s/ 80, 120% RMT | 2x2x6 mm | 23 | Only in M1 at suprathreshold TMS | BL-AUD, BL-SMA |
| Nahas et al., 2001 | Left DLPFC | 1 HZ/ 21 per train/ 147/ 80, 100, 120% RMT | 5 mm + 1.5 mm gap | 21 per train | Maybe 120 % RMT | BL-AUD, R Middle temporal gyrus, L-insula,<br>at 120% RMT: BL-BA 46, BL-BA 9 |
| Bohning et al., 2000a | Left M1 | Single pulses/ 15 blocks/ 120% RMT | 5 mm + 1.5 mm gap | N/A | yes | BL-AUD, SMA, R-M1 |
| Bohning et al., 2000b | Left M1 | 1 Hz/ 21/ 21s/ 110% RMT | 5 mm + 1.5 mm gap | 8 | yes | R-M1, BL-AUD |
| Bohning et al., 1999 | Left M1 | 1 Hz/ 288/ 18 s/ 110% RMT & 80% RMT | 5 mm + 1.5 mm gap | 6 | Yes, but only at suprathreshold TMS | BL-AUD, BL-M1/S1, R-Cereb, |
| Bohning et al., 1998 | Left M1 | 0.83 Hz/ 20/ 24 s/ 110% RMT | 4.5mm + 1.5 mm gap | 6 | yes | BL-AUD |

AMT: active motor threshold, AUD: auditory cortex, BL: bilateral, BP: binding potential, Cereb: cerebellum, DLPFC: dorsolateral prefrontal cortex, L: left, M1: primary motor cortex, N/A: not applicable, PMd: dorsal premotor cortex, R: right, RMT: resting motor threshold, SMA: supplementary motor area, SPL: superior parietal lobule.

All previous combined TMS-fMRI studies *at rest* failed to demonstrate a significant BOLD response in the vicinity of stimulation when accounting for possible contributions of re-afferent feedback. This may in part be related to technical reasons such as local signal dropouts in the vicinity of the TMS coil. However, peripheral input can drive unit responses in the motor cortex of the anaesthetised monkey (ROSEN & ASANUMA, 1972). Furthermore, movement-related activity, sensitivity to passive joint, or muscle manipulation not only occurs in M1, but is frequently found in the SMA-proper (MATSUZAKA & TANJI, 1996), and re-afferent feedback thus presents a confound to fMRI data.

The occurrence of a positive BOLD response at the site of stimulation has been claimed even at subthreshold intensities (BOHNING ET AL., 1999, NAHAS ET AL., 2001), yet the data presented in these studies lacks evidence for such a conclusion. Studies repeatedly failed to report BOLD MRI signal changes at the site of stimulation even during high-intensity protocols of brain regions other than M1 (BAUDEWIG ET AL., 2001; NAHAS ET AL., 2001; KEMNA & GEMBRIS, 2003). In these studies, significant BOLD MRI signal changes at the site of stimulation were only observed when movements were provoked.

Furthermore, little consensus exists regarding remote activity changes. NAHAS ET AL. (2001) stimulated the dorsolateral prefrontal cortex and reported activity in several brain regions distal and proximal to the TMS coil. At subthreshold and threshold intensities, however, no responses at the site of stimulation were found (their figures 1 and 2) and activation during suprathreshold rTMS seemed to reveal all signs of a spread of activation, or were localised in an interconnected prefrontal brain region rather than at the site of stimulation. Although earlier TMS-fMRI studies were suggestive of remote activity changes even at low intensity TMS, the likely contribution of movement confounds and spreads of activation was recently acknowledged in summary of the work of these authors (BOHNING ET AL., 2003b).

In summary, previous studies have primarily shown that TMS-evoked muscle movements provoke similar haemodynamic responses as voluntary finger movement. Due to the lack of studies extending these approaches, it was recently questioned whether TMS-fMRI offers convincing advantages over TMS-PET studies (PAUS, 2002; SIEBNER ET AL., 2003b). The results of the present thesis may still be subject to limitations, yet they do offer evidence that combined TMS-fMRI provides insight into the mechanisms of action of TMS otherwise not accessible due to its excellent temporal and spatial resolution.

### 8.1.2 TMS–PET

Given the subthreshold nature of cortical stimulation in several TMS-PET studies, remote activity changes can not entirely be attributed to the occurrence of confounding muscle movements or direct excitation of

projecting fibres (see Table 8.1 for an overview of combined TMS-PET studies).

Initial studies lend credence to the idea that the physiological changes induced by TMS of the motor system are echoed in corresponding increases or decreases of rCBF (PAUS ET AL., 1997, 1998). However, rCBF was found to increase after both inhibitory and facilitatory intervals of paired-pulse stimulation (STRAFELLA & PAUS, 2001) and the simple assertion of decreases in rCBF following inhibitory TMS protocols and increases following excitatory TMS protocols is not tenable. Previous studies reported either local activity decreases following low-frequency stimulation (SIEBNER ET AL., 2003a; SPEER ET AL., 2003b), increases (SPEER ET AL., 2003a), rCBF increases paralleling electrophysiological increases in corticospinal excitability (SIEBNER ET AL., 2000, 2001b), or the opposite (PAUS ET AL., 1998). It was argued in the previous chapters that the dose-dependency of rTMS presumably accounts for the variance of results. Compared to previous TMS-PET studies (Table 8.2), the present experiments applied much shorter stimulation trains. It should not be surprising that different stimulation protocols are reflected in different local and remote rCBF or BOLD responses, and, if anything, this bolsters the notion of a dose-dependency for haemodynamic TMS-related changes.

Even subthreshold rTMS at 1Hz over periods of 30 minutes does not lead to reliable activity changes at the site of stimulation (KIMBRELL ET AL., 2002), although activity in secondary cortical and subcortical motor regions is positively correlated with TMS intensity, and local responses may only occur at suprathreshold stimulation (SPEER ET AL., 2003a,b). When comparing stimulation of M1 with prefrontal rTMS, activations evoked by prefrontal TMS seem, at least in part, to be related to discomfort of the subjects, which is concurrent with the observation that this stimulation is generally more uncomfortable (Kai Thilo, *pers. comm.*).

Table 8.2: Overview of combined TMS-PET studies

| Study | Target site | Frequency/ Pulse number/ Train length/ Intensity | PET tracer | TMS trains | Local effects | Remote effects |
|---|---|---|---|---|---|---|
| Chouinard et al., 2003 | Left M1, Left PMd | 1 Hz/ 900/ 15 min/ 90% RMT | $H_2{}^{15}O$ | 1 | M1:yes<br>PMd: no | M1 TMS: R-CMA, L-PUT, rM1, R-VLN, GP, PMd TMS: PMv, R-IPS, BL-CMA, R-PMd, SMA, rPUT |
| Lee et al., 2003 | Left M1 | 1 Hz/ 1800/ 2 x 15 min/ 90% RMT | $H_2{}^{15}O$ | 2 a 15min | Yes | BL-PMd, Cereb, caudal SMA, L-BG, IPL, R-PFC Decrease: R-CMA, L-PMv, STG, R-Cereb, lateral PFC, Reduced effective connectivity with M1: L-PMd, CMA; increased task- related coupling: L-M1, PMd, SMA |
| Siebner et al., 2003 | Left PMd | 1 Hz/ 1800/ 30 min/ 90% RMT | $H_2{}^{15}O$ | 2 a 15min | Yes, decrease | Decrease : SMA, R-PMd, PFC, L-PMd, PMv, L-M1, R-M1, L-PUT, L-temporal lobe, Increase: L-Cereb, R-PUT, R-Insula |
| Speer et al., 2003a | Left M1 | 1 Hz/ 75/ 75 s/ 80, 90, 100, 110, 120% twitch threshold | $H_2{}^{15}O$ | 1 per intensity | After supra-threshold rTMS only | Dose-dependent increase: AUD, L-PMd, Cereb, PUT, Insula<br>Decrease: V1, V5, leg area |
| Speer et al., 2003b | Left PFC | 1 Hz/ 75/ 75 s/ 80, 90,100, 110, 120% twitch threshold | $H_2{}^{15}O$ | 1 per intensity | Dose-dependent decrease after supra.TMS | Ant. Cing, Cereb. Decrease: V1, V5, Med. temp lobe |
| Strafella et al., 2003 | Left M1 | 10 Hz/ 10/ 1s/ 90% RMT | [$^{11}$C] Raclopride | 15 | N/A | Reduced BP in L ventro-lateral PUT, |
| Kimbrell et al., 2002 | Left PFC | 1Hz/ 1800/ 30min/ 80% RMT | $^{18}$FDG | 1 | No | Decrease: R PFC, BL AntCing, BG, Cereb; Increase: BL Temp and Occ |
| Paus et al., 2001 | Left MDLFC | rTMS: 10 Hz/ 10/ 1s; PP 50ms/ 30/ 1 min/ RMT | $H_2{}^{15}O$ | 15/ 4 | Decrease after PP/ Increase following rTMS | PP: CMA/PHG, R-MDLFC, L-IPC |
| Siebner et al., 2001 | Left M1 | 1-5 Hz/ 1min per train/ 90% AMT | $H_2{}^{15}O$ | 9 | Yes, rate dependent CBF increase | L anterior insula, L anterior cingulate |
| Strafella et al., 2001 | MDLFC, OC | 10 Hz/ 10/ 1s/ RMT | [$^{11}$C] Raclopride | 45 over 30min | N/A | Decreased BP in L-Caudate |
| Strafella and Paus, 2001 | Left M1 | PP ITI: 3, 12 ms | $H_2{}^{15}O$ | 20 trials per condition | Yes | MEP suppression correlates with increase in BL-M1, L-PMd. MEP facilitation correlates with increase in L-M1, R-Thal, CMA |
| Siebner et al., 2000 | Left M1 | 5 Hz/ 1800/ 12 min/ ca. 90% RMT | $^{18}$FDG | 36 (50 pulses per train) | Increase | R-M1, caudal SMA |
| Siebner et al., 1998 | Left M1 | 2 Hz/ 120 per train/ 500 ms/ 140% RMT | $^{18}$FDG | 15 a 1 min | Increase | L-M1, SMA |
| Paus et al., 1998 | Left M1 | 10 Hz/ 5, 10, 15, 20, 25, 30 per scan/ 400 ms/ 70% output | $H_2{}^{15}O$ | 1 per condition | Decrease as function of number of pulse | Decrease: SMA, medial parietal region, R-PMd, R-M1 |
| Paus et al., 1997 | Left FEF | 10 Hz/ 5, 10, 15, 20, 25, 30 per scan/ 400 ms/ 70% output | $H_2{}^{15}O$ | 1 per condition | Yes. Covariation with pulse length | Visual, R-SPL, R-SEF |

BG: basal ganglia, CMA: cingulate motor area, FEF: frontal eye-field, GP: globus pallidus, IPC: intra-parietal cortex, MDLFC: mid-dorsolateral prefrontal cortex, OC: occipital cortex, PFC: prefrontal cortex, PHG: parahippocampal gyrus, PMv: ventral premotor cortex, PP: paired pulse, PUT: putamen, SEF: supplementary eye-field, STG: superior temporal gyrus, Thal: thalamus, VLN: ventro-lateral nucleus of the thalamus. Other abbreviations: see Table 8.1.

A detailed investigation of the dose-dependency of rTMS is difficult to conduct. Increased stimulation intensities may induce a spread of excitation into adjacent brain areas or re-afferent feedback when stimulating M1. Comparing different stimulation frequencies does either not match for the number of TMS pulses per experimental condition or the duration of stimulation epochs. This, for example, is illustrated by the lack of local activity changes following 1 Hz rTMS at 90% RMT of M1, whereas local responses were reported following rTMS at 3 Hz and 5 Hz (SIEBNER ET AL., 1999c) and contrasts previous findings reporting local activity changes following 1 Hz rTMS at the same intensity (CHOUINARD ET AL., 2003; LEE ET AL., 2003; SIEBNER ET AL., 2003a).

The absence of remote activity changes following subthreshold rTMS has been attributed to the lack of a spread of activation (SIEBNER ET AL., 2001b). The notion that short subthreshold trains of 1 minute are less prone to induce remote activity changes (irrespective of the frequency) as compared to prolonged stimulation protocols (LEE ET AL., 2003; SIEBNER ET AL., 2000, 2003a) is at odds with the present results which revealed remote activity changes during short epochs of rTMS. Some of these discrepancies are likely to be accounted for by differences in stimulation protocols. From the results of SIEBNER ET AL. (2001b) it does not entirely become clear whether remote rCBF changes were indeed absent at stimulation frequencies also applied in the present experiments. A trend towards significant positive correlations in rCBF in the left anterior insular and left anterior cingulate cortex was indeed reported. As analysis was focused on positive correlations between TMS frequency and rCBF, regions displaying similar degrees of activity to all stimulation protocols (as for example expected for auditory cortices) as well as brain regions being only activated at a specific stimulation frequency would have remained undetected.

### 8.1.3 SPECT and NIRS

At present, only one study has assessed the effects of TMS by using SPECT in healthy subjects (OKABE ET AL., 2003). Importantly, similar to the results obtained in this thesis, rCBF changes were not observed at the site of stimulation. Following 1 Hz rTMS of the left primary motor cortex, decreased responses were found in the contralateral M1, the SMA and PMd, and the parietal cortex. Although the application of monophasic TMS pulses over 60 seconds makes a direct comparison difficult, the important finding of this study are remote activity changes following low intensity rTMS. Congruent with the data presented here, this study provides clear evidence that activity decreases contralateral to the site of stimulation may occur even in the absence of significant local responses. All targeted brain regions corresponded well to those described in this thesis, and were largely confined to motor regions of the frontal lobe and subcortical motor structures.

TMS-NIRS measures local changes in the oxygenation state of tissue haemoglobin and redox state of cytochrome oxidase (cyt aa3), which reflects the overall activity of oxidative metabolism in cells. TMS at 100% of stimulator output was shown to increase metabolic activity and a concomitant increase in rCBF, while TES failed to induce such effects (OLIVIERO ET AL., 1999). At these intensities rTMS is likely to excite subcortical fibres and although TES was not found to change metabolic parameters, significant contributions arising from subcortical or peripheral stimulation may have occurred following TMS. In this regard, NOGUCHI and colleagues (2003) used optical topography and were able to demonstrate local $Hb_{oxy}$ increases following both sub- and suprathreshold single TMS pulses. Although the application of monophasic pulses makes direct comparison difficult, the data is suggestive of local responses even at low stimulation intensities. Increased responses were detected following TMS pulses at 90% RMT but not following stimulation at 70% RMT. While the former did not evoke electromyographic activity, descending volleys may still have occurred (DI LAZZARO ET AL., 1998). Speculating that 70% RMT corresponded to intensities just below active motor thresholds, the lack of a local response at this

intensity would be congruent with the observations presented in this thesis. Either way, the study indicates that NIRS provides a sensitive measure of TMS-induced local metabolic changes.

### 8.1.4 Decreased BOLD responses

Negatively correlated BOLD responses in the contralateral M1/S1 and the occipital cortex were recurrently observed in the present experiments and previous studies (KEMNA & GEMBRIS, 2003). An early explanation offered by Fox and co-workers (FOX ET AL., 1997) stated that TMS induces orthodromic and transsynaptic transmission of neural impulses that lead to a decrease of rCBF in the contralateral M1. Because of the suprathreshold nature of rTMS and the concomitant contribution of re-afferent feedback on neurotransmission levels, however, this explanation can not fully account for negative response changes.

Activity decreases in the homologous motor cortex opposite the stimulated hemisphere following subthreshold stimulation (OKABE ET AL., 2003; SIEBNER ET AL., 2003a) are not likely to result from direct activation of transcallosal projections or re-afferent feedback. Such decreases were more likely mediated by changes in cortical excitability, that in turn influenced motor regions distant from the directly stimulated area. At higher stimulation intensities, several mechanisms such as re-afferent feedback, transcallosal inhibition, and redistribution of ongoing activity will additionally contribute to decreased responses. Decreased responses in the occipital cortex may be explained by cross-modality suppression (PAUS, 2000). Decreased responses in the putative leg area of the mesial motor cortex, however, are subject to speculation that presently can not be resolved. The hand and leg region of the motor cortex are only weakly linked, and a direct interaction seems unlikely as it should have also included other body representations within M1. An alternative, yet speculative explanation holds that these signal decreases reflect interaction with subcortical thalamic or striatal relays.

While decreased BOLD responses could be related to 'vascular steal' from neighbouring regions or reflect an increase in neuronal activity that is for

some reason not accompanied by an increase in blood flow, recent findings suggest that the negative BOLD response is dominated by active neuronal inhibition (SHMUEL ET AL., 2002). In the rat cerebellar cortex, decreased excitatory input (i.e. deactivation) reduces rCBF (GOLD & LAURITZEN, 2002). Generally speaking, the exact physiological origin and pathways mediating negative BOLD responses remain obscure, and it can only be speculated that they indeed reflect active inhibition or deactivation.

Depending on the duration, intensity, and frequency of stimulation, brain activity changes can be presumed to result from different physiological processes, including changes in cortical excitability or long-term potentiation or long-term depression. While the present experiments suggest a dose-dependency for haemodynamic response changes, this is not entirely in synchrony with the known electrophysiological effects of TMS at low intensities. An open issue therefore regards how these effects are translated into haemodynamic changes.

## 8.2 The physiology of TMS-induced haemodynamic response changes

Any discussion regarding the underpinnings of TMS rests upon the foundations set up by the vast amount of electrophysiological TMS studies. However, as TMS interacts with neural tissue in a complex manner whose individual components can not easily be disentangled, previous studies only offer a rapprochement towards a full comprehension of the mechanisms of action of TMS. As recently pointed out by ZIEMANN & ROTHWELL (2000), a good 20 years after the introduction of TMS, and even 50 years after their discovery in the motor cortex by PATTON & AMASSIAN (1954), the exact origin of I waves is still unknown. As most TMS studies of the motor system directly or indirectly measure I-wave interaction, a thorough understanding of the coupling between TMS and cortical haemodynamics can at best be as detailed as our knowledge regarding TMS and neurovascular coupling itself.

There is indeed an incomplete understanding of the linkage between energy usage, neuronal activity, and haemodynamic processes in the brain. Considering the abundant number of fMRI studies, starting back after the original description of deoxyhaemoglobin as endogenous contrast agent (OGAWA ET AL., 1990), the lack of insight into neurovascular coupling has widely been unappreciated for the interpretation of fMRI data. Only recently, a number of studies provided *direct* evidence that the BOLD or CBF response is indeed intimately linked and causally related to neuronal activity (MATHIESEN ET AL., 1998, 2000; LOGOTHETIS ET AL., 2001, 2002; SILVA & KORETSKY, 2002; NIELSEN & LAURITZEN, 2001; LAURITZEN & GOLD, 2003). Although therefore evidently being subject to incompleteness, the following section attempts to provide a preliminary account on the coupling between TMS and neurovascular responses.

At first glance, the lack of activity changes at the site of stimulation may be surprising, however, one may also ask whether local response *should* occur during TMS at all? At very high intensities, a single biphasic TMS pulse that lasts approximately 250 µs generates a series of EPSPs and ISPSs lasting approximately 50-250 ms. Even at high stimulation frequencies, however, the period and number of effectively activated neurons will presumably be small when compared to, for example, activity during voluntary finger movement over the same period of time. Considering that most studies apply stimulation frequencies of 1-10 Hz, the period of cortical 'silence' certainly outlasts the period of TMS-induced activity and this should be reflected in different degrees of haemodynamic response changes. This is indirectly supported by the finding that only high intensity rTMS over the left PMd did evoke local BOLD MRI signal increases.

**What mediates a TMS-evoked BOLD response?** Brain energy usage is determined by ion movements due to postsynaptic currents, action potentials and neurotransmitter re-uptake (ATTWELL & LAUGHLIN, 2001). The majority of energy is required for the reversal of ion movements generating excitatory pre- and postsynaptic currents whereas the reversal of ion flux related to action potentials is considerably smaller (ATTWELL & IADECOLA, 2002). Direct

recordings of multiunit activity in monkey visual cortex during high field fMRI indeed suggest that postsynaptic activity is a major constituent of BOLD MRI signal changes (LOGOTHETIS ET AL., 2001). Further support comes from the observation that glucose consumption and rCBF changes are centred in the principle target area for thalamocortical projections of layer IV (SOKOLOFF, 1999; GERRITS ET AL., 2000; NIELSEN & LAURITZEN, 2001) and can be detected there using high-field fMRI (YANG ET AL., 1996; SILVA & KORETSKY, 2002; LOGOTHETIS ET AL., 2002). In the rat cerebellum and somatosensory cortex activity-dependent increases in rCBF were disproportionate to the spike rate in efferent neurons, and increases in rCBF occurred even though parallel fibre stimulation inhibited or even abolished spiking activity of Purkinje cells (MATHIESEN ET AL., 1998). Therefore, spiking of principle nerve cells does not seem to be a prerequisite for rCBF changes, and on the basis of rCBF increases it is impossible to infer increases or decreases in spiking rate (MATHIESEN ET AL., 1998). In turn, increases in neuronal firing rate may not be the best predictors for increases in either rCBF or BOLD (LAURITZEN, 2001; LAURITZEN & GOLD, 2003; LOGOTHETIS, 2003).

These studies indicate that changes in spiking activity may not generate a haemodynamic response, or that an increase in rCBF may occur following inhibitory synaptic activity without producing any spiking activity (CAESAR ET AL., 2003). Finally, small rCBF changes during activation tasks are unlikely to reveal increased spiking in the population, as simultaneous changes in the contribution from tuning width, response modulation, baseline firing rate and stimulus properties may result in invisible functional changes (SCANNELL & YOUNG, 1999). With respect to the results presented here, one must conclude that the absence of local activity changes during rTMS do not allow for inferring the absence of any changes in neuronal activity. The implication is that brain regions activated during a particular event, under some circumstances, may not reflect the region of task processing but rather the region receiving excitatory input from such an area. This notion nurtures the general criticism of fMRI, in that the observed activation patterns reflect correlational activity, but provide little information regarding causation. This

emphasises the need for additional information regarding connectivity in humans in order to corroborate the linkage of a particular brain activation to a particular event, such as diffusion tensor imaging techniques that allow for a probabilistic assessment of target regions of a specific area (BEHRENS ET AL., 2003), or analysis of functional connectivity (MICHELLI ET AL., 2003).

### 8.2.1 Can a simple model account for TMS-induced BOLD changes?

High intensity TMS depolarises pyramidal neurons at the axon hillock or first or second internode and APs will be generated without preceding synaptic activity. Bearing on the above findings, no local rCBF or BOLD changes then may occur. On the other hand, propagation of these APs would resemble natural synaptic input into a target region and predict an increase in rCBF or BOLD MRI signal in this regions. This simplified view may help to explain the results presented here, in that the artificially induced outgoing signal from the site of stimulation does not elicit a local BOLD response because it is not initially metabolically demanding there.

While this simplified model as preliminary proposed by BAUDEWIG ET AL. (2001) holds some attraction, the complexity of TMS-induced activity in the motor cortex denies such an easy interpretation. TMS of M1 activates a series of cortical interneurons that contribute to the generation of I waves (CHEN, 2004). This local synaptic activity predicts a local BOLD response even during subthreshold TMS. An absence of local BOLD or rCBF changes was recently explained by cancellation of inhibitory and facilitatory activity (CHOUINARD ET AL., 2003). In light of the number of TMS-fMRI and TMS-PET studies failing to detect signal changes in the direct vicinity of stimulation as well as the complexity of intracortical circuitry, such a cancellation seems to be too lucky a case to be considered a satisfying explanation. If at all, it would opt for a local increase in rCBF or BOLD as it predicts both inhibitory and excitatory local synaptic activity. In an elegant study by CAESAR ET AL. (2003), stimulation of both inhibitory and excitatory projections into the rat cerebellar cortex indeed increased rCBF even in the absence of spiking activity from that region.

An alternative explanation would be the absence of *significant levels* of excitatory or inhibitory synaptic intracortical activity. Subthreshold rTMS does not seem to increase local BOLD responses, although known to target the cortex (DI LAZZARO ET AL., 1998; FISHER ET AL., 2002; CHAPTER 4, 6), while suprathreshold rTMS seems to be capable to elevate local synaptic activity significantly (see Chapter 7). This might sufficiently be explained by activation of a greater number of intracortical neurons, but antidromic activation of projections to the site of stimulation or increased back-propagation from target regions may also contribute.

While a threshold for haemodynamic response changes helps to account for the observed results at the site of stimulation, it is more difficult to accommodate response modulations in remote brain regions. The absence of significant local activity changes while observing remote responses has been repeatedly observed (NAHAS ET AL., 2001; KIMBRELL ET AL., 2002; CHOUINARD ET AL., 2003; OKABE ET AL., 2003; SPEER ET AL., 2003a) and increasing evidence supports the idea that local changes of cortical excitability may exert remote effects that are not presumed to result from direct excitation of projecting fibres (GERSCHLAGER ET AL., 2001; MUNCHAU ET AL., 2002; RIZZO ET AL., 2004). As subthreshold rTMS is known to change the functional coupling between motor areas (CHEN ET AL., 2003; LEE ET AL., 2003), a change of cortical excitability may cause redistribution of the efferent function of the area of stimulation.

The occurrence of remote haemodynamic changes during TMS at rest may be explained by the following model. First, short trains of subthreshold rTMS do not elevate local synaptic activity above a threshold that triggers changes in rCBF or BOLD. This does not rule out some level of intracortical activity but proposes that it does not exceed background activity levels. Second, remote activity changes reflect the reaction to an altered efferent function from the site of stimulation. In the case of subthreshold rTMS, the efferent function is presumably influenced by changes in excitability of local neurons rather than altered synaptic neurotransmission. Changes in excitability presumably affect neuronal firing behaviour, either at rest or during motor

activity, and one of the conclusions proposed here is that these are then communicated into a change of activity in respective target regions. It seems feasible to assume that any effect one observes is the sum of direct interactions between local and remote brain regions, influences of thalamic relays projecting back onto remote areas, or even more complex, non-linear interactions.

The latter argument is supported by the notion that the input-output relationship of TMS is indeed non-linear with regard to neuronal interaction (MATTHEWS, 1999; CAPADAY, 1997). Consequently, parametric comparisons of the effects of TMS have to be conducted with caution. It further means that different stimulation intensities will have profoundly different impact on the recruitment of cortical activity and presumably not only concern the quantity of involved elements but also the subtypes of involved pathways, such as inhibitory or excitatory circuits. Again, it seems not too surprising at all that variant stimulation protocols evoke different activity patterns. The present data suggests that TMS-evoked BOLD or rCBF changes are dominated by incoming afferent signals or intracortical processing. There is truly some degree of speculation and uncertainty in this model and rather than offering a full account of TMS-induced changes in cortical haemodynamics it may be seen as a framework for future studies.

In addition, it is worth pointing out that activity changes occur in *some,* but not *all* remote brain regions known to be interconnected. Motor or premotor rTMS, for example, did not unequivocally activate parietal regions despite the strong interconnections of the parietal and frontal cortex. The holds true, for example, for stimulation of the FEF which has been reported to activate superior parietal and medial parieto-occipital regions (PAUS ET AL., 1997). Clearly, these are not the only known targets of the FEF. Similarly, stimulation of the motor cortex does not automatically activate all known frontal motor regions despite their intimate connectivity (Table 8.1, Chapters 6-7). This suggests that the haemodynamic susceptibility to TMS is different in different brain regions. The underlying reasons are currently unknown, but anatomical

features such as the strength of subcortical pathways and the size of neurons in a respective brain region will be the main source of these variations.

As inhibitory or excitatory circuits can not be studied in isolation in humans, the results obtained from invasive animal recordings can not necessarily be transferred humans. Even though we may classify the effects of TMS as inhibitory or excitatory, they reflect fundamentally different processes as those observed in animal studies, where specific subsystems of the brain can be studies in isolation. TMS on the other hand acts on the systems level and its effects will always reflect a complex interaction of local and remote inhibitory and excitatory processes (SIEBNER & ROTHWELL, 2003). While the neurovascular coupling of TMS at the cellular level is certainly far from being understood, combined TMS-fMRI in humans allows to investigate the neurovascular coupling of TMS at a systems level and the entity of the brain. This in itself offers unprecedented opportunities for the elucidation of the mechanism of action of TMS.

### 8.2.2 The context-dependence of TMS

As recently argued, responses in local circuitry depend on the physical configuration of the system. For example, inhibitory stimulation may have a different effect when the level of baseline activity is elevated (TAGAMETS & HORWITZ, 2001). The present experiments emphasise that TMS-mediated BOLD changes are also context dependent and provide a first demonstration of a TMS-modulated BOLD response in the area of stimulation when stimulation was applied *during* motor behaviour. On the other hand, TMS applied *before* contraction periods failed to induce detectable signal changes at the site of stimulation.

At first glance, this is at variance to the conclusions of TAGAMETS & HORWITZ (2001). During task performance little additional variation in activity should occur and therefore TMS should be even less capable for evoking a BOLD response than during motor behaviour. An alternative view proposes that stimulation during pre-innervation reduces the threshold of some intracortical elements, so that neurons are more likely to be targeted by TMS. In such a

case, low intensity stimulation would effectively depolarise more neurons as during rest, consistent with several studies comparing the effects of TMS at rest and during activity (RIDDING ET AL., 1995). This is likely to include local interneurons and may therefore induce sufficient synaptic activity to trigger a local BOLD response. The data shown here reveal that TMS-induced signal changes are context-dependent. The implication is that for any functional application of TMS-fMRI a preceding characterisation of the TMS-evoked BOLD response is mandatory. Even this, however, may not account for non-linear interactions between TMS and task-related activity.

In summary, the present data support the idea that the BOLD MRI signal is dominated by postsynaptic and intracortical activity. The known ability of TMS of modulating activity in remote brain regions is mirrored by the findings that BOLD MRI signal changes were observed in distal and interconnected brain regions. One of the main conclusions that can be derived from the present thesis is the rather nonfocal nature of TMS, and the fact that this can be visualised immediately in combination with fMRI. Moreover, the data is illustrative of previous models predicting a decoupling of low levels of synaptic activity and BOLD (MATHIESEN ET AL., 1998). As shown in Chapter 7, this is unlikely to be an ubiquitous characteristic of the brain, and various stimulation protocols over different brain regions may have different impact on local BOLD changes.

## 8.3 Does TMS-induced activity mirror natural activity patterns?

A germane expression illustrating the reservation whether combined TMS-fMRI visualises cortical networks in a way which allows for inferences about the intact or pathological brain is given in a general criticism of fMRI by Steven Pinker, quoting: "I suspect that when you have people do some artificial task and look at their brains, the strongest activity you'll see is in the parts of the brain that are responsible for doing artificial tasks." With regard to the present thesis this becomes important as the presently available models

of interaction between different inhibitory and excitatory systems in the motor cortex as derived from TMS studies (for recent reviews see ZIEMANN AND ROTHWELL, 2000; CHEN, 2004) do not necessarily reflect activity of these circuits under physiological conditions. Similar to the reservation expressed by PINKER, a common criticism of TMS would state that TMS studies only reveal what occurs under the artificial circumstance of applying an electrical stimulus to the brain.

In this respect, although it seems justified to be cautious in claiming that TMS-fMRI visualises brain activity changes resembling natural activity patterns, several findings suggest that TMS does interact with brain activity in a *meaningful* way. First, TMS-induced rhythmicities of descending volleys occur within physiologically plausible frequencies (AMASSIAN & STEWART, 2003). Second, TMS-evoked changes in cortical activity occur in distinct anatomically linked pathways (Chapters 4-7) and activity changes are confined to 'meaningful' brain regions rather than occurring in all regions known to have anatomical connections to the site of stimulation (STRAFELLA ET AL., 2001, 2003). Third, TMS-induced after effects within the motor system require accurate targeting of specific motor structures and do not unequivocally occur following stimulation of any brain region or any current direction, i.e. TMS is site specific (SIEBNER & ROTHWELL, 2003). Fourth, after effects are not arbitrarily evoked: they can be shaped in a predicted manner by specific frequencies, intensities, and stimulation durations (MODUGNO ET AL., 2001). Finally, cognitive TMS studies have repeatedly induced site-, time-, and task-specific manipulations of behaviour (as reviewed in WALSH & RUSHWORTH, 1999; PASCUAL-LEONE ET AL., 1999, 2000; WALSH & COWEY, 2001). TMS can thus be regarded as an artificial probe of neuronal activity that mimics natural input to some extent, or resembles extremely short and reversible lesions. This is certainly only an approximation with respect to brain function under normal circumstances, and can certainly only approximate the underlying cortical and subcortical circuits involved, yet it offers a hitherto unprecedented opportunity to directly interact non-invasively with brain function at the systems level in healthy humans.

## 8.4 Where should we stimulate?

As stated by the August Krogh principle, for many problems in the biological sciences there is an animal on which it can be most conveniently studied (see KREBS, 1975). In the case of TMS, an analogy may be made by saying that the motor cortex serves as the system in which the effects of TMS can be most conveniently studied because the outcome of stimulation can directly be recorded from peripheral muscles. Furthermore, the motor cortex is easily accessible, and substantial stimulation of facial or neck muscles or trigeminal nerve fibres is less likely. These apparent advantages of M1 stimulation are mirrored by the multitude of TMS studies on the motor system.

As noted in Chapters 4 and 6, however, the contribution of re-afferent feedback does confound the investigation of the direct effects of TMS on brain activity in M1. Moreover, suprathreshold TMS elicits electromyographic responses that reflect a complex interplay of temporal dispersion of descending volleys, combined activity in central and peripheral motor neurons, and contributions from fluctuating levels of excitability of involved synapses (KIERS ET AL., 1993). It would not be surprising had these processes a significant influence on motor cortical activity. By requesting the use of subthreshold stimulation intensities, it limits the applicable range of experimental protocols. As shown in Chapter 7, a solution is the stimulation of non-primary motor regions that allows to circumvent this problem and to visualise the effects of TMS even for intensities which are commonly applied for 'virtual lesion' studies.

On the other hand, one fundamental problem arises when stimulating other brain regions: nothing tells us whether our stimulation has interacted with neural tissue at all. Compared to the granular cortex in area 4, neurons in prefrontal or parietal cortex are much smaller and hence less excitable by TMS. The assumption that suprathreshold TMS over M1 will also be suprathreshold over other brain regions is not necessarily true, especially when using motor thresholds as a surrogate marker for excitability in non-primary motor areas (ROBERTSON ET AL., 2003). This makes it difficult to

conclude that changes in brain activity are indeed a reflection of effective cortical stimulation rather than due to secondary processes related to the unwanted effects of TMS.

This problem may be circumvented by simultaneous behavioural measures. These not only provide a further experimental variable measuring the effectiveness of TMS, but also allow for comparing the quality of behavioural changes with alterations in brain activity. The inherent redundancy of the brain and its capability to compensate for perturbations admittedly may preclude behavioural changes despite effective targeting of cortical neurons. Even stimulation parameters with sufficient physiological impact may not be mirrored by subsequent behavioural changes. The results presented in Chapter 5 underscore this observation: despite BOLD response changes during rTMS in respective motor regions, no behavioural consequences were observed. This finding clearly suggests that the brain is able to perform basic or trivial behaviour despite disruption of one of its subdivisions, and more complex tasks may be needed to reveal behavioural consequences of TMS. Only when TMS elicits behavioural consequences we may conclude that the cortex was effectively targeted.

This issue is particularly important as appropriate control conditions are difficult to conduct in combined TMS-fMRI. For example, stimulation of control sites that are hypothesised to be not causally involved in a specific behaviour of interest is difficult to perform. Such a control would require replacement of the TMS probe which would inevitably result in a position changes of the subject and increase the duration of experiments considerably. As the behavioural consequences of TMS are most consistently observed in the motor system, it does presently represent the most convenient framework on which to study the immediate impact of TMS.

## 8.5 Methodological considerations for combined TMS-fMRI

The experiments presented here have demonstrated the general applicability of TMS-fMRI, and underscored its advantages over alternative neuroimaging methods, such as TMS-PET. Following the initial reports by BOHNING and colleagues (1998, 1999), considerable progress has been made. One achievement of this thesis is the application of rTMS protocols beyond 1 Hz, and the visualisation of the non-focal nature of TMS. Nevertheless, technical challenges and constraints remain, some of which may be solved by technological advance, some of which presumably imposing general constraints to the methodology.

The MR environment is subject to spatial restrictions that seriously limit the brain regions accessible with TMS. At present, stimulation is limited to the dorsolateral and dorsomesial motor regions. Smaller TMS coils may overcome some of these restrictions but have an increased risk of coil overheating and insufficient stimulation power. Preliminary experiments not included in this work show that superior parietal regions can be targeted during fMRI even though it often requires tilting of the head. Occipital regions are theoretically accessible to TMS, yet orienting the TMS-induced magnetic field directly onto the MR head coil increases the risk of mechanical damage to respective copper-shielded coil compartments or electrical circuits. The theoretical considerations presented in Chapter 3 and preliminary experiments furthermore suggest that the torques originating from TMS coil orientations used for occipital stimulation increase and induce additional activity changes related to unwanted effects of the procedure, or even become unpleasant. Round coils only provide a partial solution because of their non-focal stimulation characteristics. TMS over the temporal or frontal cortex provokes facial muscle movements and / or direct stimulation of trigeminal nerve fibres. The resulting head movements and discomfort presumably make stimulation of these regions during fMRI generally impossible.

### 8.5.1 High or low field?

One of the motivations to transfer TMS-fMRI to higher magnetic fields was given by the proposed increase in BOLD sensitivity with increasing $B_0$. The optimal field strength for BOLD-sensitive fMRI has been subject of some debate. In principle, increased $B_0$ should translate into a roughly linear increase in intrinsic SNR. Ideally, such an increase can be translated into an improved temporal and spatial resolution. The SNR in an fMRI experiment is dependent on the fractional change in $T_2^*$ during activation as well as the base image SNR, and is maximal when TE equals $T_2^*$. As briefly summarised before, the BOLD contrast is constituted by four principle components: intravascular $T_2$ changes in capillaries and veins, dephasing between intra- and extravascular compartments, and extravascular static and dynamic averaging effects (NORRIS, 2003). The shortening of venous $T_2$ at higher field strengths is accompanied by an increase in the strength of susceptibility gradients about venous vessels. This increasingly influences the contrast in both $T_2$- and $T_2^*$-weighted images (VAN ZIJL ET AL., 1998). Concurrently, a trend towards improved spatial selectivity resulting from increased contributions of the microvasculature occurs for BOLD-weighted imaging at higher $B_0$. The inhomogeneity in the $B_1$ field, however, makes this gain position dependent as reflected in serious regional SNR variations at higher $B_0$.

Susceptibility artefacts attenuate at shorter TE, which is supported by the observation that static image artefacts were less often encountered at 3T. Here, an echo time of 36 ms with a 128-matrix was found to reveal the best BOLD sensitivity and simultaneous reductions in static imaging artefacts. In addition to these theoretical considerations, TMS-fMRI at 3T was found to profit from decreased RF interference. This renders the use of RF filters obsolete and circumvents TMS pulse attenuation or distortions of the TMS pulse shape.

Mechanical stress exerted onto the TMS coil is increased at 3T which in some subjects, especially with high motor thresholds, may be regarded as unpleasant. While theoretical considerations favour the use of higher field MR

systems in terms of BOLD sensitivity, the increased vibrotactile input at 3T speaks for TMS-fMRI at lower field strength, particularly when oblique TMS coil orientations are desired that increase mechanical stress to the TMS coil due to unbalanced interaction of opposing magnetic fields.

### 8.5.2 Insufficient sensitivity to detect BOLD responses?

In contrast to previous TMS-fMRI studies, the present experiments applied high-resolution fMRI, thus minimising the contribution of partial volume effects. For example, while the spatial resolution in the present thesis was 2 x 2 x 4 $mm^3$ throughout, previous studies used spatial resolutions as low as 4 x 4 x 5 $mm^3$ plus 1.5 mm gap (BOHNING ET AL., 1999; NAHAS ET AL., 2001) or even 6 x 6 x 8 $mm^3$ plus a 10% gap (KEMNA & GEMBRIS, 2003). One might argue that theoretical decreases in SNR at higher spatial resolution prevent detection of subtle signal changes. For the present experiments such a demur can be refuted as subtle BOLD responses were readily detected in several cortical and subcortical brain regions while previous studies failed to detect such signal changes (e.g. KEMNA & GEMBRIS, 2003, BOHNING ET AL., 1999). The spatial resolution applied by KEMNA & GEMBRIS (2003), for example, was 16 times lower than that of the present experiments (288 ml vs. 16 ml) and therefore essentially sacrificed one of the advantages of fMRI. This illustrates an essential observation made in the present experiments: activity changes during subthreshold rTMS are usually small. The use of high resolution MR sequences therefore minimises critical partial volume effects that would otherwise occlude the detection of such signal changes.

As shown in Chapter 3, static image distortions are dependent on the orientation of phase- and frequency-encoding gradients with respect to the TMS probe, rather than the position of the TMS coil itself. The interaction between section orientation, TMS coil orientation, and the direction of phase-encoding gradients is difficult to predict as it will vary between subjects. Consequently, ineffective shimming may occur and prevent sufficient image quality. In fact, approximately one in ten subjects had to be excluded from the experiments due to signal dropouts in one of the regions of interest. This

raises the need for improved functional MR sequences that focus on a reduction of static image artefacts.

Several studies provide evidence that variations and nonlinearities of neurovascular response functions between brain regions or in pathology exist (see, for example, LEE ET AL., 1999 for different BOLD latencies at different brain regions depending on subcomponents of a task; MATHIESEN ET AL., 2000 for CBF data on the rat cerebellar cortex; MORITZ ET AL., 2000 for motor-evoked BOLD responses in different brain regions; MECHELLI ET AL., 2001 for modelling data; BENAR ET AL., 2002 for BOLD responses in interictal epileptic spikes). Recently, AUSTIN ET AL. (2003) reported prolonged BOLD responses to ipsilateral suprathreshold intracortical stimulation of the rat hindlimb region when compared to the responses evoked in the contralateral homotopic area. This further supports the notion that BOLD responses to cortical stimulation may not invariably exhibit the same temporal characteristics in different brain regions. Another study tested for linearities of the TMS-evoked BOLD response and suggested a linear relationship between TMS and BOLD (BOHNING ET AL., 2003b). However, the suprathreshold stimulation intensities in both studies seem only to provide a partial solution to the aforementioned problem.

One of the limitations of this thesis is clearly given by the lack of approaches to detect possible nonlinearities of the haemodynamic response, and future studies may help to clarify the contribution of such non-linearities by application of more sophisticated haemodynamic modelling approaches. As argued in Chapter 6 and 7, however, the fact that activity increases in remote brain regions were well fitted with conventional models of the haemodynamic response strongly suggests that a stimulus-correlated modulation of local activity did occur.

Measures providing a baseline of synaptic activity levels such as PET may be better suited to investigate this issue, as PET allows for the direct comparison of synaptic activity levels between different scanning sessions. It furthermore provides baseline measures of regional synaptic activity over several tens of seconds ($H_2{}^{15}O$-PET) or even minutes ($^{18}$FDG-PET) and the technical

requirements for combined TMS-PET are relatively few (LEE ET AL., 2003). The invasive properties of PET provide one serious constraint with regard to the repeatability of investigations. Technically, the spatial and temporal resolution is relatively poor and high resolution mapping speaks for the use of fMRI. While long stimulation protocols thus favour the use of TMS-PET, the visualisation of the immediate effects on cortical haemodynamics opts for the use of fMRI.

### 8.5.3 Unwanted activity changes

Auditory and vibrotactile inputs are inevitably linked to TMS and provide sources of confounding activity. The high sound-pressure level of TMS pulses does not allow for effective masking, and placebo stimulation does not entirely match for bone conduction to the inner ear (SIEBNER ET AL., 1999a). The data obtained in Chapter 6 furthermore suggests that maximal or near maximal activation may already occur during subthreshold TMS, thus rendering auditory control conditions or parametric variation of stimulation intensities ambiguous. While auditory activation is spatially distinct from motor activity, the vibrotactile or trigeminal input (SIEBNER ET AL., 1999b) provides a more serious confound to motor related activity. Although trigeminal or somatosensory activations may be spatially distinct from motor activations, it is difficult to assess their amount of interaction with motor-related activity. The mere topographical separation of activity does not necessarily indicate functional independence and, again, more elaborate analysis techniques assessing functional connectivity may help to reveal the degree of interaction between the wanted and unwanted activity changes evoked by TMS. It is important to stress that although the auditory and vibrotactile input of TMS during scanning is presumably stronger as compared to outside the MR environment, however, confounding input is also generated in standard TMS settings. The visualisation of brain activity changes related to this input alone is an unprecedented ability of combined TMS-fMRI.

## 8.6 Despite its technical feasibility, what should be done with combined TMS-fMRI

An apparent advantage of TMS-fMRI is the visualisation of the immediate impact of TMS. In light of neurocognitive studies using TMS in a 'virtual lesion' approach, the combination with fMRI promises to assess the immediate consequences of such an interference and correlate these with the behavioural consequences of stimulation. Conversely, the simultaneous assessment of behavioural changes following TMS may help to understand whether TMS-evoked activity increases or decreases in specific brain regions are functionally meaningful. Surely, TMS has introduced a means to manipulate connections over a wide range of brain regions, however, until now, no conceivable way exists to study the dynamics of these networks. The combination of TMS-fMRI may in the future solve this limitation.

In principle, three main applications of combined TMS-fMRI seem to emerge as feasible from the present thesis. First, the method may be used to further characterise the mechanism of action of TMS when applied to the resting brain. This clearly will broaden our understanding of the physiological properties of TMS as for example its coupling with cortical haemodynamics or the occurrence of local and remote activity changes. Second, one can highlight the connectivity between brain regions and how the input given by TMS modulates their interaction. The third application regards the investigation of cortical plasticity or short-term compensation subsequent to a 'virtual lesion', for example during visuomotor behaviour. Compensatory activity in additional brain regions may occur in order to assimilate the disturbances provided by rTMS. These three applications are clearly related to one another: brain regions modulated by TMS during a certain behaviour may be the same as those targeted by TMS at rest, and clearly these regions will determine the localisation and degree of compensatory activity.

The combination of TMS-fMRI with neuro-cognitive studies presupposes a detailed understanding of the physiological properties of TMS itself. As outlined above, neither TMS-PET nor TMS-fMRI studies have fully elucidated

these properties, which might be explained by TMS having differential impact on different regions of the brain. For example, while TMS of the FEF reveals a positive correlation of rCBF in remote brain regions and the number of TMS pulses (PAUS ET AL., 1997), a negative correlation has been reported M1 (PAUS ET AL., 1998). The limited understanding of the mechanism of action of TMS is clearly a motivation for criticism to such ambitious experimental approaches as using combined TMS-fMRI for neurocognitive studies. However, despite its inherent limitations, the method should be seen as an initial opportunity to unravel a more complete picture of brain function. The mere knowledge of both local and remote consequences evoked by TMS and their temporal occurrence alone provides unique information about the mechanisms of action of TMS. Prior knowledge about activity changes in secondary brain regions may help to design appropriate experimental protocols that help to narrow down possible candidates for a specific brain function. Despite the inherent limitations of TMS-fMRI, it is worth recapitulating that both methods on their own also suffer from several (and even more) limitations that did not preclude them from enriching our knowledge about human brain function. Even if TMS-fMRI will remain restricted to regions of the outer convexity of the brain, it opens the unprecedented opportunity to study processes such as visuomotor transformation, action planning, movement selection, or prehensile motor execution in much greater detail as currently possible.

# 9 Conclusion

Combined TMS-fMRI is feasible at high frequencies and for prolonged stimulation epochs. Despite certain technical limitations, it thus allows for the non-invasive visualisation of the mechanisms of action of cortical stimulation in humans.

Within the motor system, a focal disturbance of brain function by means of rTMS may becomes transmitted into interconnected regions. The occurrence of such remote effects seems to be critically dose-dependent. Stimulation does not unequivocally evoke significant activity changes despite the known electrophysiological effects onto the cortex. This indicates a partial decoupling of cortical activity changes as evoked by TMS and its reflection in subsequent haemodynamic response changes.

A further important implication derived from the present studies has to be that the absence of observable behavioural consequences of rTMS does not preclude significant influences of TMS on cortical activity. Combined TMS-fMRI offers to identify structures revealing significant activity changes following stimulation that are not detectable using TMS alone.

Although it remains to be seen whether TMS-fMRI will be successful in demonstrating the causal relationship between brain and behaviour, and at the same time visualise a redistribution (or a lack of it) of brain activity in distinct networks, combined TMS-fMRI promises to link cause and effect. In that, one might reach a further step in knowing the dancer (the brain) from the dance (the behaviour).

# 10 References


Abbruzzese G, Assini A, Buccolieri A, Schieppati M, Trompetto C (1999). Comparison of intracortical inhibition and facilitation in distal and proximal arm muscles in humans. *J. Physiol.* **514:**895-903.

Akgoren N, Dalgaard P, Lauritzen M (1996). Cerebral blood flow increases evoked by electrical stimulation of rat cerebellar cortex: relation to excitatory synaptic activity and nitric oxide synthesis. *Brain Res.* **710:**204-214.

Akgoren N, Mathiesen C, Rubin I, Lauritzen M (1997). Laminar analysis of activity-dependent increases of CBF in rat cerebellar cortex: dependence on synaptic strength. *Am. J. Physiol.* **273:**H1166-1176.

Alexander GE, DeLong MR, Strick PL (1986). Parallel organization of functionally segregated circuits linking basal ganglia and cortex. *Annu. Rev. Neurosci.* **9:**357-381.

Alexander GE, Crutcher MD (1990). Functional architecture of basal ganglia circuits: neural substrates of parallel processing. *Trends Neurosci.***13:**266-271.

Allen GI, Tsukahara N (1974). Cerebrocerebellar communication systems. *Physiol. Rev.* **54:**957-1006.

Allison JD, Meador KJ, Loring DW, Figueroa RE, Wright JC (2000). Functional MRI cerebral activation and deactivation during finger movement. *Neurology* **54:**135-142.

Amassian VE, Weiner H (1966). The effect of (+)-tubocurarine chloride and of acute hypotension on electrocortical activity of the cat. *J. Physiol.* **184:**1-15.

Amassian VE, Stewart M, Quirk GJ, Rosenthal JL (1987). Physiological basis of motor effects of a transient stimulus to cerebral cortex. *Neurosurgery* **20:**74-93.

Amassian VE, Cracco RQ, Maccabee PJ (1989). Focal stimulation of human cerebral cortex with the magnetic coil: a comparison with electrical stimulation. *Electroencephal. Clin. Neurophysiol.* **74:**401-416.

Amassian VE, Cracco RQ, Maccabee PJ, Cracco JB (1992a). Cerebello-frontal cortical projections in humans studied with the magnetic coil. *Electroencephal. Clin. Neurophysiol.* **85:**265-272.

Amassian VE, Eberle L, Maccabee PJ, Cracco RQ (1992b). Modelling magnetic coil excitation of human cerebral cortex with a peripheral nerve immersed in a brain-shaped volume conductor: the significance of fiber bending in excitation. *Electroencephal. Clin. Neurophysiol.* **85:**291-301.

Amasssian VE, Stewart M (2003). Motor cortical and other cortical interneuronal networks that generate very high frequency waves. *Clin. Neurophysiol Suppl.* **56:**119-142.

Andersen P, Hagan PJ, Phillips CG, Powell TP (1975). Mapping by microstimulation of overlapping projections from area 4 to motor units of the baboon's hand. *Proc. R. Soc. Lond. B Biol. Sci.* **188:**31-36.

Arthur DL, Lewis PS, Medvick PA, Flynn ER (1991). A neuromagnetic study of selective auditory attention. *Electroencephal. Clin. Neurophysiol.* **78:**348-360.

Arthurs OJ, Boniface S (2002). How well do we understand the neural origins of the fMRI BOLD signal? *Trends Neurosci.* **25:**27-31.

Asanuma C, Thach WR, Jones EG (1983). Anatomical evidence for segregated focal groupings of efferent cells and their terminal ramifications in the cerebellothalamic pathway of the monkey. *Brain Res.* **286:**267-297.

Ashby P, Reynolds C, Wennberg R, Lozano AM, Rothwell JC (1999). On the focal nature of inhibition and facilitation in the human motor cortex. *Clin. Neurophysiol.* **110:**550-555.

Attwell D, Iadecola C (2002). The neural basis of functional brain imaging signals. *Trends Neurosci.* **25:**621-625.

Attwell D, Laughlin SB (2001). An energy budget for signaling in the grey matter of the brain. *J. Cereb. Blood Flow. Metab*. **21:**1133-1145.

Austin VC, Blamire AM, Grieve SM, O'Neill MJ, Styles P, Matthews PM, Sibson NR (2003). Differences in the BOLD fMRI response to direct and indirect cortical stimulation in the rat. *Magn. Reson. Med.* **49:**838-847.

Bandettini PA, Kwong KK, Davis TL, Tootell RB, Wong EC, Fox PT, Belliveau JW, Weisskoff RM, Rosen BR (1997). Characterization of cerebral blood oxygenation and flow changes during prolonged brain activation. *Hum. Brain Mapp.* **5:**93-109.

Barbas H, Pandya DN (1987). Architecture and frontal cortical connections of the premotor cortex (area 6) in the rhesus monkey. *J. Comp. Neurol.* **256:**211-228.

Barker AT, Jalinous R, Freeston IL (1985). Non-invasive magnetic stimulation of human motor cortex. *Lancet* **1:**1106-1107.

Baudewig J, Paulus W, Frahm J (2000). Artefacts caused by transcranial magnetic stimulation coils and EEG electrodes in T2*-weighted echo-planar imaging. *Magn. Reson. Imaging* **18:**479-484.

Baudewig J, Siebner HR, Bestmann S, Tergau F, Tings T, Paulus W, Frahm J (2001). Functional MRI of cortical activations induced by transcranial magnetic stimulation (TMS). *NeuroReport* **12:**3543-3548.

Baudewig J, Dechent P, Merboldt KD, Frahm (2003). Thresholding in correlation analysis of magnetic resonance functional neuroimaging. *Magn. Reson. Imaging* **21:**1121-1130.

Baumer T, Lange R, Liepert J, Weiller C, Siebner HR, Rothwell JC, Munchau A (2003). Repeated premotor rTMS leads to cumulative plastic changes of motor cortex excitability in humans. *Neuroimage* **20:**550-560.

Behrens TE, Johansen-Berg H, Woolrich MW, Smith SM, Wheeler-Kingshott CA, Boulby PA, Barker GJ, Sillery EL, Sheehan K, Ciccarelli O, Thompson AJ, Brady JM, Matthews PM (2003). Non-invasive mapping of connections between human thalamus and cortex using diffusion imaging. *Nat. Neurosci.* **6:**750-757.

Benar CG, Gross DW, Wang Y, Petre V, Pike B, Dubeau F, Gotman J (2002). The BOLD response to interictal epileptiform discharges. *Neuroimage* **17:**1182-1192.

Ben-Shachar D, Belmaker RH, Grisaru N, Klein E (1997). Transcranial magnetic stimulation induces alterations in brain monoamines. *J. Neural. Transm.* **104:**191-197.

Bestmann S, Thilo KV, Sauner D, Siebner HR, Rothwell JC (2002). Parietal magnetic stimulation delays visuomotor mental rotation at increased processing demands. *Neuroimage* **17:**1512-1520.

Bestmann S, Siebner HR, Modugno N, Amassian VE, Rothwell JC (2004). Inhibitory interactions between pairs of subthreshold conditioning stimuli in the human motor cortex. *Clin. Neurophysiol. (in press)*.

Bilecen D, Seifritz E, Scheffler K, Henning J, Schulte AC (2002). Amplitopicity of the human auditory cortex: an fMRI study. *Neuroimage* **17:**710-718.

Boecker H, Kleinschmidt A, Requardt M, Hanicke W, Merboldt KD, Frahm J (1994). Functional cooperativity of human cortical motor areas during self-paced simple finger movements. A high-resolution MRI study. *Brain* **117:**1231-1239.

Bohning DE, Pecheny AP, Epstein CM, Speer AM, Vincent DJ, Dannels W, George MS (1997). Mapping transcranial magnetic stimulation (TMS) fields in vivo with MRI. *Neuroreport* **8:**2535-2538.

Bohning DE, Shastri A, Nahas Z, Lorberbaum JP, Andersen SW, Dannels WR, Haxthausen EU, Vincent DJ, George MS (1998). Echoplanar BOLD fMRI of brain activation induced by concurrent transcranial magnetic stimulation. *Invest. Radiol.* **33:**336-340.

Bohning DE, Shastri A, McConnell KA, Nahas Z, Lorberbaum JP, Roberts DR, Teneback C, Vincent DJ, George MS (1999). A combined TMS/fMRI study of intensity-dependent TMS over motor cortex. *Biol. Psychiatry* **45:**385-394.

Bohning DE, Shastri A, McGavin L, McConnell KA, Nahas Z, Lorberbaum JP, Roberts DR, George MS (2000a). Motor cortex brain activity induced by 1-Hz transcranial magnetic stimulation is similar in location and level to that for volitional movement. *Invest. Radiol.* **11:**676-683.

Bohning DE, Shastri A, Wassermann EM, Ziemann U, Lorberbaum JP, Nahas Z, Lomarev MP, George MS (2000b). BOLD-fMRI response to single-pulse transcranial magnetic stimulation (TMS). *J. Magn. Reson. Imaging* **11:**569-574.

Bohning DE, Denslow S, Bohning PA, Walker JA, George MS (2003a). A TMS coil positioning/holding device for MR image-guided TMS interleaved with fMRI. *Clin. Neurophysiol.* **114:**1997-2223.

Bohning DE, Denslow S, Bohning PA, Lomarev MP, George MS (2003b). Interleaving fMRI and TMS. *Clin. Neurophysiol. Supp.* **56:**42-54.

Boroojerdi B, Foltys H, Krings T, Spetzger U, Thron A, Topper R (1999). Localization of the motor hand area using transcranial magnetic stimulation and functional magnetic resonance imaging. *Clin. Neurophysiol.* **110:**699-704.

Boxerman JL, Bandettini PA, Kwong KK, Baker JR, Davis TL, Rosen BR, Weisskoff RM (1995). The intravascular contribution to fMRI signal change: Monte Carlo modeling and diffusion-weighted studies in vivo. *Magn. Reson. Med.* **34:**4-10.

Boynton GM, Engel SA, Glover GH, Heeger DJ (1996). Linear systems analysis of functional magnetic resonance imaging in human V1. *J. Neurosci.* **16:**4207-4221.

Brandt SA, Brocke J, Roricht S, Ploner CJ, Villringer A, Meyer BU (2001). In vivo assessment of human visual system connectivity with transcranial electrical stimulation during functional magnetic resonance imaging. *Neuroimage* **14:**366-375.

Brasil-Neto JP, Cohen LG, Panizza M, Nilsson J, Roth BJ, Hallett M (1992). Optimal focal transcranial magnetic activation of the human motor cortex: effects of coil orientation, shape of the induced current pulse, and stimulus intensity. *J. Clin. Neurophysiol.* **9:**132-136.

Brechmann A, Baumgart F, Scheich H (2002). Sound-level-dependent representation of frequency modulations in human auditory cortex: a low-noise fMRI study. *J. Neurophysiol.* **87:**423-433.

Brinkman C (1982). Supplementary motor area (SMA) and premotor area (PMA) of the monkey's brain: distribution of degeneration in the spinal cord after unilateral lesions. *Neurosci. Lett.* **8:**36.

Brown P, Ridding MC, Werhahn KJ, Rothwell JC, Marsden CD (1996). Abnormalities of the balance between inhibition and excitation in the motor cortex of patients with cortical myoclonus. *Brain* **119:**309-317.

Caesar K, Gold L, Lauritzen M (2003). Context sensitivity of activity-dependent increases in cerebral blood flow. *Proc. Natl. Acad. Sci. U. S. A.* **100:**4239-4244.

Campbell AW (1905). Histological studies on the localisation of cerebral function. New York: Cambridge University Press.

Capaday C (1997). Neurophysiological methods for studies of the motor system in freely moving human subjects. *J. Neurosci. Methods* **74:**201-218.

Carpenter M (1978). Neuroanatomy. Williams and Wilkins, London, UK.

Chen R, Classen J, Gerloff C, Celnik P, Wassermann EM, Hallett M, Cohen LG (1997). Depression of motor cortex excitability by low-frequency transcranial magnetic stimulation. *Neurology* **48:**1398-1403.

Chen W, Zhu XH, Kato T, Andersen P, Ugurbil K (1998). Spatial and temporal differentiation of fMRI BOLD response in primary visual cortex of human brain during sustained visual simulation. *Magn. Reson. Med.* **39:**520-527.

Chen WH, Mima T, Siebner HR, Oga T, Hara H, Satow T, Begum T, Nagamine T, Shibasaki H (2003). Low-frequency rTMS over lateral premotor cortex induces lasting changes in regional activation and functional coupling of cortical motor areas. *Clin. Neurophysiol.* **114:**1628-1637.

Chen R (2004). Interactions between inhibitory and excitatory circuits in the human motor cortex. *Exp. Brain Res.* **154:**1-10.

Chouinard PA, Van Der Werf YD, Leonard G, Paus T (2003). Modulating neural networks with transcranial magnetic stimulation applied over the dorsal premotor and primary motor cortices. *J. Neurophysiol.* **90:**1071-1083.

Civardi C, Cantello R, Asselman P, Rothwell JC (2001). Transcranial magnetic stimulation can be used to test connections to primary motor areas from frontal and medial cortex in humans. *Neuroimage* **14:**1444-1453.

Cowey A, Walsh V (2001). Tickling the brain: studying visual sensation, perception and cognition by transcranial magnetic stimulation. *Prog. Brain Res.* **134:**411-425.

Cracco RQ, Amassian VE, Maccabee PJ, Cracco JB (1989). Comparison of human transcallosal responses evoked by magnetic coil and electrical stimulation. *Electroencephal. Clin. Neurophysiol.* **74:**417-424.

Cragg BG (1975). The density of synapses and neurons in normal, mentally defective ageing human brains. *Brain* **98:**81-90.

Cramer SC, Weisskoff RM, Schaechter JD, Nelles G, Foley M, Finklestein SP, Rosen BR (2002). Motor cortex activation is related to force of squeezing. *Hum. Brain Mapp*. **16:**197-205.

Cunningham DJ (1892). Surface anatomy of the cerebral hemispheres. Dublin: Academy House.

Day BL, Dressler D, Maertens de Noordhout A, Marsden CD, Nakashima K, Rothwell JC, Thompson PD (1989). Electric and magnetic stimulation of human motor cortex: surface EMG and single motor unit responses. *J. Physiol.* **412:**449-473.

Dechent P, Frahm J (2003). Functional somatotopy of finger representations in human primary motor cortex. *Hum. Brain. Mapp.* **18:**272-283.

De Graaf RA (1998). In vivo NMR spectroscopy: principles and techniques. Chichester: Wiley.

Deiber MP, Honda M, Ibanez V, Sadato N, Hallett M (1999). Mesial motor areas in self-initiated versus externally triggered movements examined with fMRI: effect of movement type and rate. *J. Neurophysiol.* **81:**3065-3077.

Di Lazzaro V, Restuccia D, Oliviero A, Profice P, Ferrara L, Insola A, Mazzone P, Tonali P, Rothwell JC (1998). Magnetic transcranial stimulation at intensities below active motor threshold activates intracortical inhibitory circuits. *Exp. Brain Res.* **119:**265-268.

Di Lazzaro V, Oliviero A, Profice P, Insola A, Mazzone P, Tonali P, Rothwell JC (1999). Direct recordings of descending volleys after transcranial magnetic and electric motor cortex stimulation in conscious humans. *Electroencephal. Clin. Neurophysiol. Suppl.* **51:**120-126.

Di Lazzaro V, Oliviero A, Meglio M, Cioni B, Tamburrini G, Tonali P, Rothwell JC (2000). Direct demonstration of the effect of lorazepam on the excitability of the human motor cortex. *Clin. Neurophysiol.* **111:**794-799.

Di Lazzaro V, Oliviero A, Pilato F, Saturno E, Insola A, Mazzone P, Tonali PA, Rothwell JC (2002). Descending volleys evoked by transcranial magnetic stimulation of the brain in conscious humans: effects of coil shape. *Clin. Neurophysiol.* **113:**114-119.

Di Lazzaro V, Oliviero A, Pilato F, Mazzone P, Insola A, Ranieri F, Tonali PA (2003). Corticospinal volleys evoked by transcranial stimulation of the brain in conscious humans. *Neurol. Res.* **25:**143-150.

Dum RP, Strick PL (1991). The origin of corticospinal projections from the premotor areas in the frontal lobe. *J. Neurosci.* **11:**667-689.

Dum RP, Strick PL (1996). Spinal cord terminations of the medial wall motor areas in macaque monkeys. *J. Neurosci.* **16:**6513-6125.

Dum RP, Strick PL (2003). An unfolded map of the cerebellar dentate nucleus and its projections to the cerebral cortex. *J. Neurophysiol.* **89:**634-639.

Edgley SA, Eyre JA, Lemon RN, Miller S (1997). Comparison of activation of corticospinal neurons and spinal motor neurons by magnetic and electrical transcranial stimulation in the lumbosacral cord of the anaesthetized monkey. *Brain* **120:**839-853.

Ehrsson HH, Fagergren E, Forssberg H (2001). Differential fronto-parietal activation depending on force used in a precision grip task: an fMRI study. *J. Neurophysiol.* **85:**2613-2623.

Facchini S, Romani M, Tinazzi M, Aglioti SM (2002). Time-related changes of excitability of the human motor system contingent upon immobilisation of the ring and little fingers. *Clin. Neurophysiol.* **113:**367-375.

Fadiga L, Fogassi L, Pavesi G, Rizzolatti G (1995). Motor facilitation during action observation: a magnetic stimulation study. *J. Neurophysiol.* **73:**2608-2611.

Fadiga L, Buccino G, Craighero L, Fogassi L, Gallese V, Pavesi G (1999). Corticospinal excitability is specifically modulated by motor imagery: a magnetic stimulation study. *Neuropsychologia* **37:**147-158.

Ferbert A, Priori A, Rothwell JC, Day BL, Colebatch JG, Marsden CD (1992). Interhemispheric inhibition of the human motor cortex. *J. Physiol.* **453:**525-546.

Fierro B, Piazza A, Brighina F, La Bua V, Buffa D, Oliveri M (2001). Modulation of intracortical inhibition induced by low- and high-frequency repetitive transcranial magnetic stimulation. *Exp. Brain Res.* **138:**452-457.

Fink GR, Frackowiak RS, Pietrzyk U, Passingham RE (1997). Multiple nonprimary motor areas in the human cortex. *J. Neurophysiol.* **77:**2164-2174.

Fisher RJ, Nakamura Y, Bestmann S, Rothwell JC, Bostock H (2002). Two phases of intracortical inhibition revealed by transcranial magnetic threshold tracking. *Exp. Brain Res.* **143:**240-248.

Fitzgerald PB, Brown TL, Daskalakis ZJ, Chen R, Kulkarni J (2002). Intensity-dependent effects of 1 Hz rTMS on human corticospinal excitability. *Clin. Neurophysiol.* **113:**1136-1141.

Foltys H, Meister IG, Weidemann J, Sparing R, Thron A, Willmes K, Topper R, Hallett M, Boroojerdi B (2003). Power grip disinhibits the ipsilateral sensorimotor cortex: a TMS and fMRI study. *Neuroimage* **19:**332-340.

Fox P, Ingham R, George MS, Mayberg H, Ingham J, Roby J, Martin C, Jerabek P (1997). Imaging human intra-cerebral connectivity by PET during TMS. *Neuroreport* **8:**2787-2791.

Frahm J, Merboldt KD, Hanicke W, Kleinschmidt A, Boecker H (1994). Brain or vein–oxygenation or flow? On signal physiology in functional MRI of human brain activation. *N.M.R. Biomed.* **7:**45-53.

Frahm J, Kruger G, Merboldt KD, Kleinschmidt A (1996). Dynamic uncoupling and recoupling of perfusion and oxidative metabolism during focal brain activation in man. *Magn. Reson. Med.* **35:**143-148.

Fransson P, Kruger G, Merboldt KD, Frahm J (1998a). Temporal characteristics of oxygenation-sensitive MRI responses to visual activation in humans. *Magn. Reson. Med.* **39:**912-919.

Fransson P, Kruger G, Merboldt KD, Frahm J (1998b). Physiologic aspects of event related paradigms in magnetic resonance functional neuroimaging. *Neuroreport* **9:**2001-2005.

Fransson P, Kruger G, Merboldt KD, Frahm J (1999a). Temporal and spatial MRI responses to subsecond visual activation. *Magn. Reson. Imaging* **17:**1-7.

Fransson P, Kruger G, Merboldt KD, Frahm J (1999b). MRI of functional deactivation: temporal and spatial characteristics of oxygenation-sensitive responses in human visual cortex. *Neuroimage* **9:**611-618.

Friston KJ, Josephs O, Rees G, Turner R (1998a). Nonlinear event-related responses in fMRI. *Magn. Reson. Med.* **39:**41-52.

Friston KJ, Fletcher P, Josephs O, Holmes A, Rugg MD, Turner R (1998b). Event-related fMRI: characterizing differential responses. *Neuroimage* **7:**30-40.

Gandevia SC, McCloskey DI, Burke D (1992). Kinaesthetic signals and muscle contraction. *Trends Neurosci.* **15:**62-65.

Gangitano M, Mottaghy FM, Pascual-Leone A (2001). Phase-specific modulation of cortical motor output during movement observation. *Neuroreport* **12:**1489-1492.

Ganis G, Keenan JP, Kosslyn SM, Pascual-Leone A (2000). Transcranial magnetic stimulation of primary motor cortex affects mental rotation. *Cereb. Cortex* **10:**175-180.

Gatter KC, Powell TPS (1978). The intrinsic connections of the cortex of area 4 of the monkey. *Brain* **101:**513-541.

Gerardin E, Lehericy S, Pochon JB, Tezenas du Montcel S, Mangin JF, Poupon F, Agid Y, Le Bihan D, Marsault C (2003). Foot, hand, face and eye representation in the human striatum. *Cereb. Cortex* **13:**162-169.

Gerfen CR (1984). The neostriatal mosaic: compartmentalization of corticostriatal input and striatonigral output systems. *Nature* **311:**461-464.

Gerrits RJ, Raczynski C, Greene AS, Stein EA (2000). Regional cerebral blood flow responses to variable frequency whisker stimulation: an autoradiographic analysis. *Brain Res.* **864:**205-212.

Gerschlager W, Siebner HR, Rothwell JC (2001). Decreased corticospinal excitability after subthreshold 1 Hz rTMS over lateral premotor cortex. *Neurology* **57:**449-455.

Geyer S, Ledberg A, Schleicher A, Kinomura S, Schormann T, Burgel U, Klingberg T, Larsson J, Zilles K, Roland PE (1996). Two different areas within the primary motor cortex of man. *Nature* **382:**805-807.

Geyer S, Matelli M, Luppino G, Zilles K (2000). Functional neuroanatomy of the primate isocortical motor system. *Anat. Embryol. (Berl.)* **202:**443-474.

Ghosh S, Brinkman C, Porter R (1987). A quantitative study of the distribution of neurons projecting to the precentral motor cortex in the monkey (M. fascicularis). *J. Comp. Neurol.* **259:**424-444.

Ghosh S, Fyffe RE, Porter R (1988). Morphology of neurons in area 4 gamma of the cat's cortex studied with intracellular injection of HRP. *J. Comp. Neurol.* **277:**290-312.

Gilio F, Rizzo V, Siebner HR, Rothwell JC (2003). Effects on the right motor hand-area excitability produced by low-frequency rTMS over human contralateral homologous cortex. *J. Physiol.* **551:**563-573.

Godschalk M, Lemon RN, Kuypers HG, Ronday HK (1984). Cortical afferents and efferents of monkey postarcuate area: an anatomical and electrophysiological study. *Exp. Brain Res.* **56:**410-424.

Goebel R, Linden DE, Lanfermann H, Zanella FE, Singer W (1998). Functional imaging of mirror and inverse reading reveals separate coactivated networks for oculomotion and spatial transformations. *Neuroreport* **9:**713-719.

Gold L, Lauritzen M (2002). Neuronal deactivation explains decreased cerebellar blood flow in response to focal cerebral ischemia or suppressed neocortical function. *Proc. Natl. Acad. Sci. U. S. A.* **99:**7699-7704.

Graf von Keyserlingk D, Schramm U (1984). Diameter of axons and thickness of myelin sheaths of the pyramidal tract fibres in the adult human medullary pyramid. *Anat. Anz.* **157:**97-111.

Grezes J, Decety J (2001). Functional anatomy of execution, mental simulation, observation, and verb generation of actions: a meta-analysis. *Hum. Brain Mapp.* **12:**1-19.

Grodd W, Hulsmann E, Lotze M, Wildgruber D, Erb M (2001). Sensorimotor mapping of the human cerebellum: fMRI evidence of somatotopic organization. *Hum. Brain Mapp.* **13:**55-73.

Gugino LD, Romero JR, Aglio L, Titone D, Ramirez M, Pascual-Leone A, Grimson E, Weisenfeld N, Kikinis R, Shenton ME (2001). Transcranial magnetic stimulation coregistered with MRI: a comparison of a guided versus blind stimulation technique and its effect on evoked compound muscle action potentials. *Clin. Neurophysiol.* **112:**1781-1792.

Haacke EM, Lai S, Yablonskiy, DA, Lin WL (195). In vivo validation of the BOLD mechanism – a review of signal changes in gardient echo functional MRI in the presence of flow. *Int. J. Imaging Systems Technol.* **6:**153-163.

Hajnal JV, Myers R, Oatridge A, Schwieso JE, Young IR, Bydder GM (1994). Artefacts due to stimulus correlated motion in functional imaging of the brain. *Magn. Reson. Med.* **31:**283-291.

Hamzei F, Dettmers C, Rzanny R, Liepert J, Buchel C, Weiller C (2002). Reduction of excitability ("inhibition") in the ipsilateral primary motor cortex is mirrored by fMRI signal decreases. *Neuroimage* **17:**490-496.

Hanajima R, Furubayashi T, Iwata NK, Shiio Y, Okabe S, Kanazawa I, Ugawa Y (2003). Further evidence to support different mechanisms underlying intracortical inhibition of the motor cortex. *Exp. Brain Res.* **151:**427-434.

Harmer CJ, Thilo KV, Rothwell JC, Goodwin GM (2001). Transcranial magnetic stimulation of medial-frontal cortex impairs the processing of angry facial expressions. *Nat. Neurosci.* **4:**17-18.

Hashimoto R, Rothwell JC (1999). Dynamic changes in corticospinal excitability during motor imagery. *Exp. Brain Res.* **125:**75-81.

He SQ, Dum RP, Strick PL (1993). Topographic organization of corticospinal projections from the frontal lobe: motor areas on the lateral surface of the hemisphere. *J. Neurosci.* **13:**952-980.

He SQ, Dum RP, Strick PL (1995). Topographic organization of corticospinal projections from the frontal lobe: motor areas on the medial surface of the hemisphere. *J. Neurosci.* **15:**3284-3306.

Herwig U, Kolbel K, Wunderlich AP, Thielscher A, von Tiesenhausen C, Spitzer M, Schonfeldt-Lecuona C (2002). Spatial congruence of neuronavigated transcranial magnetic stimulation and functional neuroimaging. *Clin. Neurophysiol.* **113:**462-468.

Hlustik P, Solodkin A, Gullapalli RP, Noll DC, Small SL (2002). Functional lateralization of the human premotor cortex during sequential movements. *Brain Cogn.* **49:**54-62.

Holsapple JW, Preston JB, Strick PL (1991). The origin of thalamic inputs to the "hand" representation in the primary motor cortex. *J. Neurosci.* **11:**2644-2654.

Howseman AM, Porter DA, Hutton C, Josephs O, Turner R (1998). Blood oxygenation level dependent signal time courses during prolonged visual stimulation. *Magn. Reson. Imag.* **16:**1-11.

Howseman AM, Bowtell RW (1999). Functional magnetic resonance imaging: imaging techniques and contrast mechanisms. *Philos. Trans. R. Soc. Lond. B Biol. Sci.* **354:**1179-1194.

Howseman AM, Thomas DL, Pell GS, Williams SR, Ordidge RJ (1999). Rapid T2* mapping using interleaved echo planar imaging. *Magn. Reson. Med.* **41:**368-374.

Hu X, Le TH, Ugurbil K (1997). Evaluation of the early response in fMRI in individual subjects using short stimulus duration. *Magn. Reson. Med.* **37:**877-884.

Hubel DH, Wiesel TN (1962). Receptive fields, binocular interaction and functional architecture in cat's visual cortex. *J. Physiol.* **160:**106-154.

Hugdahl K, Thomsen T, Ersland L, Morten Rimol L, Niemi J (2003). The effects of attention on speech perception: an fMRI study. *Brain Lang.* **85:**37-48.

Humphrey DR, Corrie WS (1978). Properties of pyramidal tract neuron system within a functionally defined subregion of primate motor cortex. *J. Neurophysiol.* **41:**216-243.

Ilinsky IA, Kultas-Ilinsky K (1987). Sagittal cytoarchitectonic maps of the Macaca mulatta thalamus with a revised nomenclature of the motor-related nuclei validated by observations on their connectivity. *J. Comp. Neurol.* **262:**331-364.

Ilmoniemi RJ, Virtanen J, Ruohonen J, Karhu J, Aronen HJ, Naatanen R, Katila T (1997). Neuronal responses to magnetic stimulation reveal cortical reactivity and connectivity. *Neuroreport* **8:**3537-3540.

Jahanshahi M, Ridding MC, Limousin P, Profice P, Fogel W, Dressler D, Fuller R, Brown RG, Brown P, Rothwell JC (1997). Rapid rate transcranial magnetic stimulation–a safety study. *Electroencephal. Clin. Neurophysiol.* **105:**422-429.

Jahanshahi M, Rothwell JC (2000). Transcranial magnetic stimulation studies of cognition: an emerging field. *Exp. Brain Res.* **131:**1-9.

Jalinous R (1991). Technical and practical aspects of magnetic nerve stimulation. *J. Clin. Neurophysiol.* **8:**10-25.

Jancke L, Shah NJ, Posse S, Grosse-Ryuken M, Muller-Gartner HW (1998). Intensity coding of auditory stimuli: an fMRI study. *Neuropsychologia* **36:**875-883.

Jing H, Takigawa M (2000). Observation of EEG coherence after repetitive transcranial magnetic stimulation. *Clin. Neurophysiol.* **111:**1620-1631.

Johansen-Berg H, Rushworth MF, Bogdanovic MD, Kischka U, Wimalaratna S, Matthews PM (2002). The role of ipsilateral premotor cortex in hand movement after stroke. *Proc. Natl. Acad. Sci. U. S. A.* **99:**14518-14523.

Johnson MT, Coltz JD, Hagen MC, Ebner TJ (1999). Visuomotor processing as reflected in the directional discharge of premotor and primary motor cortex neurons. *J. Neurophysiol.* **81:**875-894.

Jones EG, Coulter JD, Burton H, Porter R (1977). Cells of origin and terminal distribution of corticostriatal fibers arising in the sensory-motor cortex of monkeys. *J. Comp. Neurol.* **173:**53-80.

Jones EG, Wise SP, Coulter JD (1979). Differential thalamic relationships of sensory-motor and parietal cortical fields in monkeys. *J. Comp. Neurol.* **183:**833-881.

Jones EG (1983). The nature of the afferent pathways conveying short-latency inputs to primate motor cortex. *Adv. Neurol.* **39:**263-285.

Jones EG (1987). Ascending inputs to, and internal organization of, cortical motor areas. *Ciba Found. Symp.* **132:**21-39.

Kaas JH, Stepniewska I (2002). Motor Cortex. In: Ramachandran VS. Encyclopedia of the Human Brain. Academic Press, San Diego, California.

Keck ME, Sillaber I, Ebner K, Welt T, Toschi N, Kaehler ST, Singewald N, Philippu A, Elbel GK, Wotjak CT, Holsboer F, Landgraf R, Engelmann M (2000). Acute transcranial magnetic stimulation of frontal brain regions selectively modulates the release of vasopressin, biogenic amines and amino acids in the rat brain. *Eur. J. Neurosci.* **12:**3713-3720.

Keller A (1993). Intrinsic synaptic organization of the motor cortex. *Cereb. Cortex* **3:**430-441.

Keller A, Asanuma H (1993). Synaptic relationships involving local axon collaterals of pyramidal neurons in the cat motor cortex. *J. Comp. Neurol.* **336:**229-242.

Kelly RM, Strick PL (2003). Cerebellar loops with motor cortex and prefrontal cortex of a nonhuman primate. *J. Neurosci.* **23:**8432-8444.

Kemna LJ, Gembris D (2003). Repetitive transcranial magnetic stimulation indices different responses in different cortical areas: a functional magnetic resonance study in humans. *Neurosci. Lett.* **336:**85-88.

Kiers L, Cros D, Chiappa KH, Fang J (1993). Variability of motor potentials evoked by transcranial magnetic stimulation. *Electroencephal. Clin. Neurophysiol.* **89:**415-423.

Kim JH, Shin T, Kim JS, Kim HJ, Chung SH (1996). MR imaging of cerebral activation performed with a gradient-echo technique at 1.5 T: sources of activation signals. *A.J.R. Am. J. Roentgenol.***167:**1277-1281.

Kimbrell TA, Dunn RT, George MS, Danielson AL, Willis MW, Repella JD, Benson BE, Herscovitch P, Post RM, Wassermann EM (2002). Left prefrontal-repetitive transcranial magnetic stimulation (rTMS) and regional cerebral glucose metabolism in normal volunteers. *Psychiatry Res.* **115:**101-113.

Kleinschmidt A, Nitschke MF, Frahm J (1997). Somatotopy in the human motor cortex hand area. A high-resolution functional MRI study. *Eur. J. Neurosci.* **9:**2178-2186.

Krebs HA (1975). The August Krogh Principle: "For many problems there is an animal on which it can be most conveniently studied". *J. Exp. Zool.* **194:**221-226.

Kruger G, Kleinschmidt A, Frahm J (1996). Dynamic MRI sensitized to cerebral blood oxygenation and flow during sustained activation of human visual cortex. *Magn. Reson. Med.* **35:**797-800.

Kuhtz-Buschbeck JP, Ehrsson HH, Forssberg H (2001). Human brain activity in the control of fine static precision grip forces: an fMRI study. *Eur. J. Neurosci.* **14:**382-390.

Kujirai T, Caramia MD, Rothwell JC, Day BL, Thompson PD, Ferbert A, Wroe S, Asselman P, Marsden CD (1993). Corticocortical inhibition in human motor cortex. *J. Physiol.* **471:**501-519.

Kuypers HG (1960). Central cortical projections to motor and somato-sensory cell groups. An experimental study in the rhesus monkey. *Brain* **83:**161-184.

Kuypers HG (1987). Some aspects of the organization of the output of the motor cortex. *Ciba Found. Symp.* **132:**63-82.

Landry P, Labelle A, Deschenes M (1980). Intracortical distribution of axonal collaterals of pyramidal tract cells in the cat motor cortex. *Brain Res.* **191:**327-336.

Lasota KJ, Ulmer JL, Firszt JB, Biswal BB, Daniels DL, Prost RW (2003). Intensity-dependent activation of the primary auditory cortex in functional magnetic resonance imaging. *J. Comp. Assist. Tomogr.* **27:**213-218.

Lassek AM (1942). The human pyramidal tract. The effect of pre- and postcentral cortical lesions on the fibre components of the pyramids in monkey. *J. Nerv. Ment. Dis.* **95:**721-729.

Lauritzen M (2001). Relationship of spikes, synaptic activity, and local changes of cerebral blood flow. *J. Cereb. Blood Flow. Metab.* **21:**1367-1383.

Lauritzen M, Gold L (2003). Brain function and neurophysiological correlates of signals used in functional neuroimaging. *J. Neurosci.* **23:**3972-3980.

Lee AT, Glover GH, Meyer CH (1995). Discrimination of large venous vessels in time-course spiral blood-oxygen-level-dependent magnetic-resonance functional neuroimaging. *Magn. Reson. Med.* **33:**745-754.

Lee KM, Chang KH, Roh JK (1999). Subregions within the supplementary motor area activated at different stages of movement preparation and execution. *Neuroimage* **9:**117-123.

Lee L, Siebner HR, Rowe JB, Rizzo V, Rothwell JC, Frackowiak RS, Friston KJ (2003). Acute remapping within the motor system induced by low-frequency repetitive transcranial magnetic stimulation. *J. Neurosci.* **23:**5308-5318.

Lehericy S, van de Moortele PF, Lobel E, Paradis AL, Vidailhet M, Frouin V, Neveu P, Agid Y, Marsault C, Le Bihan D (1998). Somatotopical organization of striatal activation during finger and toe movement: a 3-T functional magnetic resonance imaging study. *Ann. Neurol.* **44:**398-404.

Lemon RN, van der Burg J (1979). Short-latency peripheral inputs to thalamic neurones projecting to the motor cortex in the monkey. *Exp. Brain Res.* **36:**445-462.

Lemon RN, Maier MA, Armand J, Kirkwood PA, Yang HW (2002). Functional differences in corticospinal projections from macaque primary motor cortex and supplementary motor area. *Adv. Exp. Med. Biol.* **508:**425-434.

Leocani L, Cohen LG, Wassermann EM, Ikoma K, Hallett M (2000). Human corticospinal excitability evaluated with transcranial magnetic stimulation during different reaction time paradigms. *Brain* **123:**1161-1173.

Li X, Nahas Z, Lomarev M, Denslow S, Shastri A, Bohning DE, George MS (2003). Prefrontal cortex transcranial magnetic stimulation does not change local diffusion: a magnetic resonance imaging study in patients with depression. *Cogn. Behav. Neurol.* **16:**128-135.

Liebetanz D, Fauser S, Michaelis T, Czeh B, Watanabe T, Paulus W, Frahm J, Fuchs E (2003). Safety aspects of chronic low-frequency transcranial magnetic stimulation based on localised proton magnetic resonance spectroscopy and histology of the rat brain. *J. Psychiatry Res.* **37:**277-286.

Linden DE, Prvulovic D, Formisano E, Vollinger M, Zanella FE, Goebel R, Dierks T (1999). The functional neuroanatomy of target detection: an fMRI study of visual and auditory oddball tasks. *Cereb. Cortex* **9:**815-823.

Lisanby SH, Gutman D, Luber B, Schroeder C, Sackeim HA (2001). Sham TMS: intracerebral measurement of the induced electrical field and the induction of motor-evoked potentials. *Biol. Psychiatry* **49:**460-463.

Liu J, Morel A, Wannier T, Rouiller EM (2002). Origins of callosal projections to the supplementary motor area (SMA): a direct comparison between pre-SMA and SMA-proper in macaque monkeys. *J. Comp. Neurol.* **443:**71-85.

Logothetis NK, Pauls J, Augath M, Trinath T, Oeltermann A (2001). Neurophysiological investigation of the basis of the fMRI signal. *Nature* **412:**150-157.

Logothetis N, Merkle H, Augath M, Trinath T, Ugurbil K (2002). Ultra high-resolution fMRI in monkeys with implanted RF coils. *Neuron* **35:**227-242.

Logothetis NK (2003). The underpinnings of the BOLD functional magnetic resonance imaging signal. *J. Neurosci.* **23:**3963-3971.

Loo CK, Taylor JL, Gandevia SC, McDarmont BN, Mitchell PB, Sachdev PS (2000). Transcranial magnetic stimulation (TMS) in controlled treatment studies: are some "sham" forms active? *Biol. Psychiatry* **47:**325-331.

Lu MT, Preston JB, Strick PL (1994). Interconnections between the prefrontal cortex and the premotor areas in the frontal lobe. *J. Comp. Neurol.* **341:**375-392.

Luppino G, Matelli M, Camarda R, Rizzolatti G (1993). Corticocortical connections of area F3 (SMA-proper) and area F6 (pre-SMA) in the macaque monkey. *J. Comp. Neurol.* **338:**114-140.

Luppino G, Murata A, Govoni P, Matelli M (1999). Largely segregated parietofrontal connections linking rostral intraparietal cortex (areas AIP and VIP) and the ventral premotor cortex (areas F5 and F4). *Exp. Brain Res.* **128:**181-187.

Maccabee PJ, Amassian VE, Eberle LP, Cracco RQ (1993). Magnetic coil stimulation of straight and bent amphibian and mammalian peripheral nerve in vitro: locus of excitation. *J. Physiol.* **460:**201-219.

Maccabee PJ, Nagarajan SS, Amassian VE, Durand DM, Szabo AZ, Ahad AB, Cracco RQ, Lai KS, Eberle LP (1998). Influence of pulse sequence, polarity and amplitude on magnetic stimulation of human and porcine peripheral nerve. *J. Physiol.* **513:**571-585.

Macdonell RA, Jackson GD, Curatolo JM, Abbott DF, Berkovic SF, Carey LM, Syngeniotin A, Fabinyi GC, Scheffer IE (1999). Motor cortex localization using functional MRI and transcranial magnetic stimulation. *Neurology* **53:**1462-1467.

Maeda F, Keenan JP, Tormos JM, Topka H, Pascual-Leone A (2000a). Interindividual variability of the modulatory effects of repetitive transcranial magnetic stimulation on cortical excitability. *Exp. Brain Res.* **133:**425-430.

Maeda F, Keenan JP, Tormos JM, Topka H, Pascual-Leone A (2000b). Modulation of corticospinal excitability by repetitive transcranial magnetic stimulation. *Clin. Neurophysiol.* **111:**800-805.

Magistretti PJ, Pellerin L (1999). Cellular mechanisms of brain energy metabolism and their relevance to functional brain imaging. *Philos. Trans. R. Soc. Lond. B Biol. Sci.* **354:**1155-1163.

Mansfield P (1977). Multi-planar image formation using NMR spin-echos. *J. Phys. C Solid State Phys.* **10:**L55

Marconi B, Genovesio A, Giannetti S, Molinari M, Caminiti R (2003). Callosal connections of dorso-lateral premotor cortex. *Eur. J. Neurosci.* **18:**775-788.

Mathiesen C, Caesar K, Akgoren N, Lauritzen M (1998). Modification of activity-dependent increases of cerebral blood flow by excitatory synaptic activity and spikes in rat cerebellar cortex. *J. Physiol.* **512:**555-566.

Mathiesen C, Caesar K, Lauritzen M (2000). Temporal coupling between neuronal activity and blood flow in rat cerebellar cortex as indicated by field potential analysis. *J. Physiol.* **523:**235-246.

Matsuzaka Y, Tanji J (1996). Changing directions of forthcoming arm movements: neuronal activity in the presupplementary and supplementary motor area of monkey cerebral cortex. *J. Neurophysiol.* **76:**2327-2342.

Matthews PB (1999). The effect of firing on the excitability of a model motoneurone and its implications for cortical stimulation. *J. Physiol.* **518:**867-882.

Mazzocchio R, Rothwell JC, Day BL, Thompson PD (1994). Effect of tonic voluntary activity on the excitability of human motor cortex. *J. Physiol.* **474:**261-267.

McConnell KA, Bohning DE, Nahas Z, Shastri A, Teneback C, Lorberbaum JP, Lomarev MP, Vincent DJ, George MS (2003). BOLD fMRI response to direct stimulation (transcranial magnetic stimulation) of the motor cortex shows no decline with age. *J. Neural Transm.* **110:**495-507.

Mechelli A, Price CJ, Friston KJ (2001). Nonlinear coupling between evoked rCBF and BOLD signals: a simulation study of haemodynamic responses. *Neuroimage* **14:**862-872.

Mechelli A, Price CJ, Noppeney U, Friston KJ (2003). A dynamic causal modeling study on category effects: bottom-up or top-down mediation? *J. Cogn. Neurosci.* **15:**925-934.

Menon RS, Ogawa S, Hu X, Strupp JP, Anderson P, Ugurbil K (1995). BOLD based functional MRI at 4 Tesla includes a capillary bed contribution: echo-planar imaging correlates with previous optical imaging using intrinsic signals. *Magn. Reson. Med.* **33:**453-459.

Meyer G (1987). Forms and spatial arrangement of neurons in the primary motor cortex of man. *J. Comp. Neurol.* **262:**402-428.

Middleton FA, Strick PL (1998). The cerebellum: an overview. *Trends Neurosci.* **21:**367-369.

Modugno N, Nakamura Y, MacKinnon CD, Filipovic SR, Bestmann S, Berardelli A, Rothwell JC (2001). Motor cortex excitability following short trains of repetitive magnetic stimuli. *Exp. Brain Res.* **140:**453-459.

Moritz CH, Meyerand ME, Cordes D, Haughton VM (2000). Functional MR imaging activation after finger tapping has a shorter duration in the basal ganglia than in the sensorimotor cortex. *A.J.N.R. Am. J. Neuroradiol.* **21:**1228-1234.

Mountcastle VB (1957). Modality and topographic properties of single neurons of cat's somatic sensory cortex. *J. Neurophysiol.* **20:**408-434.

Muakkassa KF, Strick PL (1979). Frontal lobe inputs to primate motor cortex: evidence for four somatotopically organized 'premotor' areas. *Brain Res.* **177:**176-182.

Muellbacher W, Ziemann U, Boroojerdi B, Hallett M (2000). Effects of low-frequency transcranial magnetic stimulation on motor excitability and basic motor behavior. *Clin. Neurophysiol.* **111:**1002-1007.

Muir RB, Lemon RN (1983). Corticospinal neurons with a special role in precision grip. *Brain Res.* **261:**312-316.

Muller MB, Toschi N, Kresse AE, Post A, Keck ME (2000). Long-term repetitive transcranial magnetic stimulation increases the expression of brain-derived neurotrophic factor and cholecystokinin mRNA, but not neuropeptide tyrosine mRNA in specific areas of rat brain. *Neuropsychopharmacology* **23:**205-215.

Munchau A, Bloem BR, Irlbacher K, Trimble MR, Rothwell JC (2002). Functional connectivity of human premotor and motor cortex explored with repetitive transcranial magnetic stimulation. *J. Neurosci.* **22:**554-561.

Murray EA, Bussey TJ, Wise SP (2000). Role of prefrontal cortex in a network for arbitrary visuomotor mapping. *Exp. Brain Res.* **133:**114-129.

Nahas Z, Lomarev M, Roberts DR, Shastri A, Lorberbaum JP, Teneback C, McConnell K, Vincent DJ, Li X, George MS, Bohning DE (2001). Unilateral left prefrontal transcranial magnetic stimulation (TMS) produces intensity-dependent bilateral effects as measured by interleaved BOLD fMRI. *Biol. Psychiatry* **50:**712-720.

Nakamura H, Kitagawa H, Kawaguchi Y, Tsuji H (1996). Direct and indirect activation of human corticospinal neurons by transcranial magnetic and electrical stimulation. *Neurosci. Lett.* **210:**45-48.

Nathan PW, Smith MC (1955). Spino-cortical fibres in man. *J. Neurochem.* **18:**181-90.

Nathan PW, Smith MC, Deacon P (1990). The corticospinal tract in man. *Brain* **113:**303-324.

Nielsen A, Lauritzen M (2001). Coupling and uncoupling of activity-dependent increases of neuronal activity and blood flow in rat somatosensory cortex. *J. Physiol.* **533:**773-785.

Nikouline V, Ruohonen J, Ilmoniemi RJ (1999). The role of the coil click in TMS assessed with simultaneous EEG. *Clin. Neurophysiol.* **110:**1325-1328.

Noguchi Y, Watanabe E, Sakai KL (2003). An event-related optical topography study of cortical activation induced by single-pulse transcranial magnetic stimulation. *Neuroimage* **19:**156-162.

Norris DG (2003). High field human imaging. *J. Magn. Reson. Imaging* **18:**519-529.

Ogawa S, Lee TM, Kay AR, Tank DW (1990). Brain magnetic resonance imaging with contrast dependent on blood oxygenation. *Proc. Natl. Acad. Sci. U. S. A.* **87:**9868-9872.

Okabe S, Hanajima R, Ohnishi T, Nishikawa M, Imabayashi E, Takano H, Kawachi T, Matsuda H, Shiio Y, Iwata NK, Furubayashi T, Terao Y, Ugawa Y (2003). Functional connectivity revealed by single-photon emission computed tomography (SPECT) during repetitive transcranial magnetic stimulation (rTMS) of the motor cortex. *Clin. Neurophysiol.* **114:**450-457.

Okamura H, Jing H, Takigawa M (2001). EEG modification induced by repetitive transcranial magnetic stimulation. *J. Clin. Neurophysiol.* **18:**318-325.

Oldfield RC (1971). The assessment and analysis of handedness: the Edinburgh inventory. *Neuropsychologia* **9:**97-113.

Oliviero A, Di Lazzaro V, Piazza O, Profice P, Pennisi MA, Della Corte F, Tonali P (1999). Cerebral blood flow and metabolic changes produced by repetitive magnetic brain stimulation. *J. Neurol.* **246:**1164-1168.

Oliviero A, Strens LH, Di Lazzaro V, Tonali PA, Brown P (2003). Persistent effects of high frequency repetitive TMS on the coupling between motor areas in the human. *Exp. Brain Res.* **149:**107-113.

Padberg F, Moller HJ (2003). Repetitive transcranial magnetic stimulation: does it have potential in the treatment of depression? *CNS Drugs* **17:**383-403.

Parent A (1990). Extrinsic connections of the basal ganglia. *Trends Neurosci.* **13:**254-258.

Parent A, Hazrati LN (1995a). Functional anatomy of the basal ganglia. II. The place of subthalamic nucleus and external pallidum in basal ganglia circuitry. *Brain Res. Brain Res. Rev.* **20:**128-154.

Parent A, Hazrati LN (1995b). Functional anatomy of the basal ganglia. I. The cortico-basal ganglia-thalamo-cortical loop. *Brain Res. Brain Res. Rev.* **20:**91-127.

Pascual-Leone A, Houser CM, Reese K, Shotland LI, Grafman J, Sato S, Valls-Sole J, Brasil-Neto JP, Wassermann EM, Cohen LG, Hallett M (1993). Safety of rapid-rate transcranial magnetic stimulation in normal volunteers. *Electroencephal. Clin. Neurophysiol.* **89:**120-130.

Pascual-Leone A, Valls-Sole J, Wassermann EM, Hallett M (1994). Responses to rapid-rate transcranial magnetic stimulation of the human motor cortex. *Brain* **117:**847-858.

Pascual-Leone A, Bartres-Faz D, Keenan JP (1999). Transcranial magnetic stimulation: studying the brain-behaviour relationship by induction of 'virtual lesions'. *Philos. Trans. R. Soc. Lond. B Biol. Sci.* **354:**1229-1238.

Pascual-Leone A, Walsh V, Rothwell JC (2000). Transcranial magnetic stimulation in cognitive neuroscience - virtual lesion, chronometry, and functional connectivity. *Curr. Opin. Neurobiol.* **10:**232-237

Passingham RE, Myers C, Rawlins N, Lightfoot V, Fearn S (1988). Premotor cortex in the rat. *Behav. Neurosci.* **102:**101-109.

Patton HD, Amassian VE (1954). Single and multiple-unit analysis of cortical stage of pyramidal tract activation. *J. Neurophysiol.* **17:**345-363.

Patton HD, Amassian VE (1960). The pyramidal tract: its excitation and functions. In: The handbook of physiology. Vol. II, Washington, DC: American Physiology Society.

Paus T, Tomaiuolo F, Otaky N, MacDonald D, Petrides M, Atlas J, Morris R, Evans AC (1996). Human cingulate and paracingulate sulci: pattern, variability, asymmetry, and probabilistic map. *Cereb. Cortex* **6:**207-214.

Paus T, Jech R, Thompson CJ, Comeau R, Peters T, Evans AC (1997). Transcranial magnetic stimulation during positron emission tomography: a new method for studying connectivity of the human cerebral cortex. *J. Neurosci.* **17:**3178-3184.

Paus T, Jech R, Thompson CJ, Comeau R, Peters T, Evans AC (1998). Dose-dependent reduction of cerebral blood flow during rapid-rate transcranial magnetic stimulation of the human sensorimotor cortex. *J. Neurophysiol.* **79:**1102-1107.

Paus T (1999). Imaging the brain before, during, and after transcranial magnetic stimulation. *Neuropsychologia* **37**:219-224.

Paus T (2000). Functional anatomy of arousal and attention systems in the human brain. *Prog. Brain Res.* **126:**65-77.

Paus T, Castro-Alamancos MA, Petrides M (2001). Cortico-cortical connectivity of the human mid-dorsolateral frontal cortex and its modulation by repetitive transcranial magnetic stimulation. *Eur. J. Neurosci.* **14:**1405-1411.

Paus T. Combination of transcranial magnetic stimulation and brain mapping. In: Brain mapping: The methods, 2nd edition. Elsevier, 2002.

Peinemann A, Lehner C, Mentschel C, Munchau A, Conrad B, Siebner HR (2000). Subthreshold 5-Hz repetitive transcranial magnetic stimulation of the human primary motor cortex reduces intracortical paired-pulse inhibition. *Neurosci Lett.* **296:**21-24.

Penfield W, Rasmussen T (1950). The cerebral cortex of man. New York: MacMillan.

Picard N, Smith AM (1992). Primary motor cortical responses to perturbations of prehension in the monkey. *J. Neurophysiol.* **68:**1882-1894.

Picard N, Strick PL (1996). Medial wall motor areas: a review of their location and functional activation. *Cereb. Cortex* **6:**342-353.

Picard N, Strick PL (2001). Imaging the premotor areas. *Curr. Opin. Neurobiol.* **11:**663-672.

Porter R, Lemon R (1993). Corticospinal function and voluntary movement. Oxford: Clarendon Press.

Rademacher J, Burgel U, Zilles K (2002). Stereotaxic localization, intersubject variability, and interhemispheric differences of the human auditory thalamocortical system. *Neuroimage* **17:**142-160.

Ragsdale CW Jr, Graybiel AM (1990). A simple ordering of neocortical areas established by the compartmental organization of their striatal projections. *Proc. Natl. Acad. Sci. U. S. A.* **87:**6196-6199.

Reddy H, Lassonde M, Bemasconi N, Bemasconi A, Matthews PM, Andermann F, Amold DL (2000). An fMRI study of the lateralization of motor cortex activation in a callosal patients. *Neuroreport* **11:**2409-2413.

Ridding MC, Taylor JL, Rothwell JC (1995). The effect of voluntary contraction on cortico-cortical inhibition in human motor cortex. *J. Physiol.* **487:**541-548.

Rif J, Hari R, Hamalainen MS, Sams M (1991). Auditory attention affects two different areas in the human supratemporal cortex. *Electroencephal. Clin. Neurophysiol.* **79:**464-472.

Rizzo V, Siebner HR, Modugno N, Pesenti A, Munchau A, Gerschlager W, Webb RM, Rothwell JC (2004). Shaping the excitability of human motor cortex with premotor rTMS. *J. Physiol.* (in press).

Rizzolatti G, Luppino G, Matelli M (1996). The classic supplementary motor area is formed by two independent areas. *Adv. Neurol.* **70:**45-56.

Rizzolatti G, Luppino G, Matelli M (1998). The organization of the cortical motor system: new concepts. *Electroencephal. Clin. Neurophysiol.* **106:**283-296.

Robertson EM, Theoret H, Pascual-Leone A (2003). Studies in cognition: The problems solved and created by transcranial magnetic stimulation. *J. Cogn. Neurosci.* **15:**948-960.

Rockel AJ, Hiorns RW, Powell TP (1980). The basic uniformity in structure of the neocortex. *Brain* **103:**221-244.

Romeo S, Gilio F, Pedace F, Ozkaynak S, Inghilleri M, Manfredi M, Berardelli A (2000). Changes in the cortical silent period after repetitive magnetic stimulation of cortical motor areas. *Exp. Brain Res.* **135:**504-510.

Rosen I, Asanuma H (1972). Peripheral afferent inputs to the forelimb area of the monkey motor cortex: input-output relations. *Exp. Brain Res.* **14:**257-273.

Rossi S, Pasqualetti P, Rossini PM, Feige B, Ulivelli M, Glocker FX, Battistini N, Lucking CH, Kristeva-Feige R (2000). Effects of repetitive transcranial magnetic stimulation on movement-related cortical activity in humans. *Cereb. Cortex* **10:**802-808.

Rossini PM, Rossi S, Pasqualetti P, Tecchio F (1999). Corticospinal excitability modulation to hand muscles during movement imagery. *Cereb. Cortex* **9:**161-167.

Roth BJ, Cohen LG, Hallett M (1991). The electric field induced during magnetic stimulation. *Electroencephal. Clin. Neurophysiol. Suppl.* **43:**268-278.

Rothwell JC (1997). Techniques and mechanisms of action of transcranial stimulation of the human motor cortex. *J. Neurosci. Methods* **74:**113-122.

Rothwell JC (1999). Paired-pulse investigations of short-latency intracortical facilitation using TMS in humans. *Electroencephal. Clin. Neurophysiol. Suppl.* **51:**113-119.

Rothwell JC, Hallett M, Berardelli A, Eisen A, Rossini P, Paulus W (1999). Magnetic stimulation: motor evoked potentials. The International Federation of Clinical Neurophysiology. *Electroencephal. Clin. Neurophysiol. Suppl.* **52:**97-103.

Rouiller EM, Babalian A, Kazennikov O, Moret V, Yu XH, Wiesendanger M (1994). Transcallosal connections of the distal forelimb representations of the primary and supplementary motor cortical areas in macaque monkeys. *Exp. Brain Res.* **102:**227-243.

Rushworth MF, Johansen-Berg H, Gobel SM, Devlin JT (2003). The left parietal and premotor cortices: motor attention and selection. *Neuroimage* **20 S1:**S89-100.

Salimi I, Brochier T, Smith AM (1999). Neuronal activity in somatosensory cortex of monkeys using a precision grip. I. Receptive fields and discharge patterns. *J. Neurophysiol.* **81:**825-834.

Sanes JN, Donoghue JP, Thangaraj V, Edelman RR, Warach S (1995). Shared neural substrates controlling hand movements in human motor cortex. *Science* **268:**1775-1777.

Sanes JN, Schieber MH (2001). Orderly somatotopy in primary motor cortex: does it exist? *Neuroimage* **13:**968-974.

Sanger TD, Garg RR, Chen R (2001). Interactions between two different inhibitory systems in the human motor cortex. *J. Physiol.* **530:**307-317.

Scannell JW, Young MP (1999). Neuronal population activity and functional imaging. *Proc. R. Soc. Lond. B Biol. Sci.* **266:**875-881.

Schambra HM, Sawaki L, Cohen LG (2003). Modulation of excitability of human motor cortex (M1) by 1 Hz transcranial magnetic stimulation of the contralateral M1. *Clin. Neurophysiol.* **114:**130-133

Schieber MH (1999). Voluntary descending control. In: Zigmond, Bloom, Landis, Roberts, Squire (Eds). Fundamental neuroscience. London, UK: Academic Press.

Schlaghecken F, Munchau A, Bloem BR, Rothwell J, Eimer M (2003). Slow frequency repetitive transcranial magnetic stimulation affects reaction times, but not priming effects, in a masked prime task. *Clin. Neurophysiol.* **114:**1272-1277.

Schluter ND, Rushworth MF, Passingham RE, Mills KR (1998). Temporary interference in human lateral premotor cortex suggests dominance for the selection of movements. A study using transcranial magnetic stimulation. *Brain* **121:**785-799.

Schluter ND, Rushworth MF, Mills KR, Passingham RE (1999). Signal-, set-, and movement-related activity in the human premotor cortex. *Neuropsychologia* **37:**233-243.

Schmitt F, Stehling MK, Turner R (1998). Echo-planar imaging: theory, technique and application. Berlin: Springer.

Scholz VH, Flaherty AW, Kraft E, Keltner JR, Kwong KK, Chen YI, Rosen BR, Jenkins BG (2000). Laterality, somatotopy and reproducibility of the basal ganglia and motor cortex during motor tasks. *Brain Res.* **879:**204-215.

Scott SK, Blank CC, Rosen S, Wise RJ (2000). Identification of a pathway for intelligible speech in the left temporal lobe. *Brain* **12:**2400-2406.

Serrien DJ, Strens LH, Oliviero A, Brown P (2002). Repetitive transcranial magnetic stimulation of the supplementary motor area (SMA) degrades bimanual movement control in humans. *Neurosci. Lett.* **328:**89-92.

Shastri A, George MS, Bohning DE (1999). Performance of a system for interleaving transcranial magnetic stimulation with steady-state magnetic resonance imaging. *Electroencephal. Clin. Neurophysiol. Suppl.* **51:**55-64.

Shen L, Alexander GE (1997a). Preferential representation of instructed target location versus limb trajectory in dorsal premotor area. *J. Neurophysiol.* **77:**1195-1212.

Shen L, Alexander GE (1997b). Neural correlates of a spatial sensory-to-motor transformation in primary motor cortex. *J. Neurophysiol.* **77:**1171-1194.

Sherman SM, Guillery RW (2002). The role of the thalamus in the flow of information to the cortex. *Philos. Trans. R. Soc. Lond. B Biol. Sci* **357:**1695-1708.

Shima K, Mushiake H, Saito N, Tanji J (1996). Role for cells in the presupplementary motor area in updating motor plans. *Proc. Natl. Acad. Sci. U. S. A.* **93:**8694-8698.

Shinoda Y, Yokota J, Futami T (1981). Divergent projection of individual corticospinal axons to motoneurons of multiple muscles in the monkey. *Neurosci. Lett.* **23:**7-12.

Shmuel A, Yacoub E, Pfeuffer J, Van de Moortele PF, Adriany G, Hu X, Ugurbil K (2002). Sustained negative BOLD, blood flow and oxygen consumption response and its coupling to the positive response in the human brain. *Neuron* **36:**1195-1210.

Siebner HR, Willoch F, Peller M, Auer C, Boecker H, Conrad B, Bartenstein P (1998). Imaging brain activation induced by long trains of repetitive transcranial magnetic stimulation. *Neuroreport* **9:**943-948.

Siebner HR, Auer C, Roeck R, Conrad B (1999a). Trigeminal sensory input elicited by electric or magnetic stimulation interferes with the central motor drive to the intrinsic hand muscles. *Clin. Neurophysiol.* **110:**1090-1099.

Siebner HR, Peller M, Willoch F, Auer C, Bartenstein P, Drzezga A, Schwaiger M, Conrad B (1999b). Imaging functional activation of the auditory cortex during focal repetitive transcranial magnetic stimulation of the primary motor cortex in normal subjects. *Neurosci. Lett.* **270:**37-40.

Siebner HR, Takano B, Peller M, Bartenstein P, Rossmeier C, Weyh T, Conrad B (1999c). Subthreshold repetitive transcranial magnetic stimulation induced a rate-dependent increase of regional cerebral blood flow in the stimulated primary motor cortex. *Clin. Neurophysiol.* **110(S1):**S81-S82.

Siebner HR, Peller M, Willoch F, Minoshima S, Boecker H, Auer C, Drzezga A, Conrad B, Bartenstein P (2000). Lasting cortical activation after repetitive TMS of the motor cortex: a glucose metabolic study. *Neurology* **54:**956-963.

Siebner H, Peller M, Bartenstein P, Willoch F, Rossmeier C, Schwaiger M, Conrad B (2001a). Activation of frontal premotor areas during suprathreshold transcranial magnetic stimulation of the left primary sensorimotor cortex: a glucose metabolic PET study. *Hum. Brain Mapp.* **12:**157-167.

Siebner HR, Takano B, Peinemann A, Schwaiger M, Conrad B, Drzezga A (2001b). Continuous transcranial magnetic stimulation during positron emission tomography: a suitable tool for imaging regional excitability of the human cortex. *Neuroimage* **14:**883-890.

Siebner HR, Filipovic SR, Rowe JB, Cordivari C, Gerschlager W, Rothwell JC, Frackowiak RS, Bhatia KP (2003a). Patients with focal arm dystonia have increased sensitivity to slow-frequency repetitive TMS of the dorsal premotor cortex. *Brain* **126:**2710-2715.

Siebner HR, Lee L, Bestmann S (2003b). Interleaving TMS with functional MRI: Now that it is technically feasible how should it be used? *Clin. Neurophysiol.* **114:**1997-1999.

Siebner HR, Peller M, Lee L (2003c). Applications of combined TMS-PET studies in clinical and basic research. *Clin. Neurophysiol. Suppl.* **56:**63-72.

Siebner HR, Rothwell JC (2003). Transcranial magnetic stimulation: new insights into representational cortical plasticity. *Exp. Brain Res.* **148:**1-16.

Silva AC, Koretsky AP (2002). Laminar specificity of functional MRI onset times during somatosensory stimulation in rat. *Proc. Natl. Acad. Sci. U. S. A.* **99:**15182-15187.

Sloper JJ, Powell TP (1979). An experimental electron microscopic study of afferent connections to the primate motor and somatic sensory cortices. *Philos. Trans. R. Soc. Lond. B Biol. Sci.* **285:**199-226.

Sokoloff L (1978). Local cerebral energy metabolism: its relationships to local functional activity and blood flow. *Ciba Found. Symp.* **56:**171-197.

Sokoloff L (1999). Energetics of functional activation in neural tissues. *Neurochem. Res.* **24:**321-329.

Sommer M, Lang N, Tergau F, Paulus W (2002). Neuronal tissue polarization induced by repetitive transcranial magnetic stimulation? *Neuroreport* **13:**809-811.

Speer AM, Kimbrell TA, Wassermann EM, D Repella J, Willis MW, Herscovitch P, Post RM (2000). Opposite effects of high and low frequency rTMS on regional brain activity in depressed patients. *Biol. Psychiatry* **48:**1133-1141.

Speer AM, Willis MW, Herscovitch P, Daube-Witherspoon M, Repella Shelton J, Benson BE, Post RM, Wassermann EM (2003a). Intensity-dependent regional cerebral blood flow during 1-Hz repetitive transcranial magnetic stimulation (rTMS) in healthy volunteers studied with $H_2^{15}O$ positron emission tomography: I. effects of primary motor cortex rTMS. *Biol. Psychiatry* **54:**818-825.

Speer AM, Willis MW, Herscovitch P, Daube-Witherspoon M, Repella Shelton J, Benson BE, Post RM, Wassermann EM (2003b). Intensity-dependent regional cerebral blood flow during 1-Hz repetitive transcranial magnetic stimulation (rTMS) in healthy volunteers studied with $H_2^{15}O$ positron emission tomography: II. effects of prefrontal cortex rTMS. *Biol. Psychiatry* **54:**826-832.

Stark DD, Bradley W (1999). Magnetic resonance imaging. St. Louis, MO: Mosby.

Stepniewska I, Preuss TM, Kaas JH (1993). Architectonics, somatotopic organization, and ipsilateral cortical connections of the primary motor area (M1) of owl monkeys. *J. Comp. Neurol.* **330:**238-271.

Strafella AP, Paus T (2001). Cerebral blood-flow changes induced by paired-pulse transcranial magnetic stimulation of the primary motor cortex. *J. Neurophysiol.* **85:**2624-2629.

Strafella AP, Paus T, Barrett J, Dagher A (2001). Repetitive transcranial magnetic stimulation of the human prefrontal cortex induces dopamine release in the caudate nucleus. *J. Neurosci.* **21:**RC157.

Strafella AP, Paus T, Fraraccio M, Dagher A (2003). Striatal dopamine release induced by repetitive transcranial magnetic stimulation of the human motor cortex. *Brain* **126:**2609-2615.

Strens LH, Oliviero A, Bloem BR, Gerschlager W, Rothwell JC, Brown P (2002). The effects of subthreshold 1 Hz repetitive TMS on cortico-cortical and interhemispheric coherence. *Clin. Neurophysiol.* **113:**1279-1285.

Strens LH, Fogelson N, Shanahan P, Rothwell JC, Brown P (2003). The ipsilateral human motor cortex can functionally compensate for acute contralateral motor cortex dysfunction. *Curr. Biol.* **13:**1201-1205.

Symington J, Crymble PT (1913). The central fissure of the cerebrum. *J. Anat. Physiol.* **48:**321-339.

Tagamets MA, Horwitz B (2001). Interpreting PET and fMRI measures of functional neural activity: the effects of synaptic inhibition on cortical activation in human imaging studies. *Brain Res. Bull.* **54:**267-273.

Talairach J, Tournoux P (1988). Co-planar stereotaxic atlas of the human brain. Stuttgart: Thieme.

Tanji J (1985). Comparison of neuronal activities in the monkey supplementary and precentral motor areas. *Behav. Brain Res.* **18:**137-142.

Tanji J (1996). New concepts of the supplementary motor area *Curr. Opin. Neurobiol.* **6:**782-787.

Tanji J, Shima K, Mushiake H (1996). Multiple cortical motor areas and temporal sequencing of movements. *Brain Res. Cogn. Brain Res.* **5:**117-122.

Tanne-Gariepy J, Rouiller EM, Boussaoud D (2002). Parietal inputs to dorsal versus ventral premotor areas in the macaque monkey: evidence for largely segregated visuomotor pathways. *Exp. Brain Res.***145:**91-103.

Taylor JL, Gandevia SC (2001). Transcranial magnetic stimulation and human muscle fatigue. *Muscle Nerve* **24:**18-29.

Thach WT (1999). Fundamentals of motor systems. In: Zigmond, Bloom, Landis, Roberts, Squire (Eds). Fundamental neuroscience. London, UK: Academic Press.

Thielscher A, Kammer T (2002). Linking physics with physiology in TMS: a sphere field model to determine the cortical stimulation site in TMS. *Neuroimage* **17:**1117-1130.

Tiitinen H, Virtanen J, Ilmoniemi RJ, Kamppuri J, Ollikainen M, Ruohonen J, Naatanen R (1999). Separation of contamination caused by coil clicks from responses elicited by transcranial magnetic stimulation. *Clin. Neurophysiol.* **110:**982-985.

Tokuno H, Tanji J (1993). Input organization of distal and proximal forelimb areas in the monkey primary motor cortex: a retrograde double labeling study. *J. Comp. Neurol.* **333:**199-209.

Toma K, Honda M, Hanakawa T, Okada T, Fukuyama H, Ikeda A, Nishizawa S, Konishi J, Shibasaki H (1999). Activities of the primary and supplementary motor areas increase in preparation and execution of voluntary muscle relaxation: an event-related fMRI study. *J. Neurosci.* **19:**3527-3534.

Touge T, Gerschlager W, Brown P, Rothwell JC (2001). Are the after-effects of low-frequency rTMS on motor cortex excitability due to changes in the efficacy of cortical synapses? *Clin. Neurophysiol.* **112:**2138-2145.

Trojano L, Grossi D, Linden DE, Formisano E, Hacker H, Zanella FE, Goebel R, Di Salle F (2000). Matching two imagined clocks: the functional anatomy of spatial analysis in the absence of visual stimulation. *Cereb. Cortex* **10:**473-481.

Trompetto C, Assini A, Buccolieri A, Marchese R, Abbruzzese G (1999). Intracortical inhibition after paired transcranial magnetic stimulation depends on the current flow direction. *Clin. Neurophysiol.* **110:**1106-1110.

Tsuji T, Rothwell JC (2002). Long lasting effects of rTMS and associated peripheral sensory input on MEPs, SEPs and transcortical reflex excitability in humans. *J. Physiol.* **540:**367-376.

Turner R, Le Bihan D, Moonen CT, Despres D, Frank J (1991). Echo-planar time course MRI of cat brain oxygenation changes. *Magn. Reson. Med.* **22:**159-166.

Ugawa Y, Terao Y, Hanajima R, Sakai K, Kanazawa I (1995). Facilitatory effect of tonic voluntary contraction on responses to motor cortex stimulation. *Electroencephal. Clin. Neurophysiol.* **97:**451-454.

Vafaee MS, Marrett S, Meyer E, Evans AC, Gjedde A (1998). Increased oxygen consumption in human visual cortex: response to visual stimulation. *Acta Neurol. Scand.* **98:**85-89.

Vafaee MS, Meyer E, Marrett S, Paus T, Evans AC, Gjedde A (1999). Frequency-dependent changes in cerebral metabolic rate of oxygen during activation of human visual cortex. *J. Cereb. Blood Flow. Metab.* **19:**272-277.

Vafaee MS, Gjedde A (2000). Model of blood-brain transfer of oxygen explains nonlinear flow-metabolism coupling during stimulation of visual cortex. *J. Cereb. Blood Flow. Metab.* **20:**747-754.

van Zijl PC, Eleff SM, Ulatowski JA, Oja JM, Ulug AM, Traystman RJ, Kauppinen RA (1998). Quantitative assessment of blood flow, blood volume and blood oxygenation effects in functional magnetic resonance imaging. *Nat. Med.* **4:**159-167.

Voogd J, Glickstein M (1998). The anatomy of the cerebellum. *Trends Neurosci.* **21:**370-375.

Vogt BA, Vogt O (1919). Allgemeinere Ergebnisse unserer Hirnforschung. *J. Psychol. Neurol. Leipzig* **25:**277-462.

Vorobiev V, Govoni P, Rizzolatti G, Matelli M, Luppino G (1998). Parcellation of human mesial area 6: cytoarchitectonic evidence for three separate areas. *Eur. J. Neurosci.* **10:**2199-2203.

Walsh V, Cowey A (1998). Magnetic stimulation studies of visual cognition, *Trends Cogn. Sci.* **2:**103-110

Walsh V, Rushworth M (1999). A primer of magnetic stimulation as a tool for neuropsychology. *Neuropsychologia* **37:**125-135.

Walsh V, Cowey A (2000). Transcranial magnetic stimulation and cognitive neuroscience. *Nat. Rev. Neurosci.* **1:**73-79.

Ward NS (2003). Reorganisation in the motor system after 1 Hz repetitive transcranial magnetic stimulation to premotor cortex demonstrated with fMRI. *Neuroimage* **19S:**1130.

Ward NS, Frackowiak RS (2003). Age-related changes in the neural correlates of motor performance. *Brain* **126:**873-888.

Wassermann EM, McShane LM, Hallett M, Cohen LG (1992). Noninvasive mapping of muscle representations in human motor cortex. *Electroencephal. Clin. Neurophysiol.* **85:**1-8.

Wassermann EM, Samii A, Mercuri B, Ikoma K, Oddo D, Grill SE, Hallett M (1996). Responses to paired transcranial magnetic stimuli in resting, active, and recently activated muscles. *Exp. Brain Res.* **109:**158-163.

Wassermann EM, Wedegaertner FR, Ziemann U, George MS, Chen R (1998). Crossed reduction of human motor cortex excitability by 1-Hz transcranial magnetic stimulation. *Neurosci. Lett.* **250:**141-144.

Wassermann EM (1998). Risk and safety of repetitive transcranial magnetic stimulation: report and suggested guidelines from the International Workshop on the Safety of Repetitive Transcranial Magnetic Stimulation, June 5-7, 1996. *Electroencephal. Clin. Neurophysiol.* **108:**1-16.

Werhahn KJ, Fong JK, Meyer BU, Priori A, Rothwell JC, Day BL, Thompson PD (1994). The effect of magnetic coil orientation on the latency of surface EMG and single motor unit responses in the first dorsal interosseous muscle. *Electroencephal. Clin. Neurophysiol.* **93:**138-146.

White LE, Andrews TJ, Hulette C, Richards A, Groelle M, Paydarfar J, Purves D (1997). Structure of the human sensorimotor system. I: Morphology and cytoarchitecture of the central sulcus. *Cereb. Cortex* **7:**18-30.

Wiesendanger R, Wiesendanger M (1985). The thalamic connections with medial area 6 (supplementary motor cortex) in the monkey (macaca fascicularis). *Exp. Brain Res.* **59:**91-104.

Wise SP, di Pellegrino G, Boussaoud D (1996). The premotor cortex and nonstandard sensorimotor mapping. *Can. J. Physiol. Pharmacol.* **74:**469-482.

Woolsey CN, Erickson TC, Gilson E (1979). Localization in somatic sensory and motor areas of human cerebral cortex as determined by direct recordings of evoked potentials and electrical stimulation. *J. Neurosurg.* **51:**476-506.

Yang X, Hyder F, Shulman RG (1996). Activation of single whisker barrel in rat brain localized by functional magnetic resonance imaging. *Proc. Natl. Acad. Sci. U. S. A.* **93:**475-478.

Yarowsky PJ, Ingvar DH (1981). Symposium summary. Neuronal activity and energy metabolism. *Fed. Proc.* **40:**2353-2362.

Yousry TA, Schmid UD, Alkadhi H, Schmidt D, Peraud A, Buettner A, Winkler P (1997). Localization of the motor hand area to a knob on the precentral gyrus: a new landmark. *Brain* **120:**141-157.

Ziemann U, Lonnecker S, Paulus W (1995). Inhibition of human motor cortex by ethanol. A transcranial magnetic stimulation study. *Brain* **118:**1437-1446.

Ziemann U, Rothwell JC, Ridding MC (1996a). Interaction between intracortical inhibition and facilitation in human motor cortex. *J. Physiol.* **496:**873-881.

Ziemann U, Lonnecker S, Steinhoff BJ, Paulus W (1996b). Effects of antiepileptic drugs on motor cortex excitability in humans: a transcranial magnetic stimulation study. *Ann. Neurol.* **40:**367-378.

Ziemann U, Bruns D, Paulus W (1996c). Enhancement of human motor cortex inhibition by the dopamine receptor agonist pergolide: evidence from transcranial magnetic stimulation. *Neurosci. Lett.* **208:**187-190.

Ziemann U, Lonnecker S, Steinhoff BJ, Paulus W (1996d). The effect of lorazepam on the motor cortical excitability in man. *Exp. Brain Res.* **109:**127-135.

Ziemann U, Rothwell JC (2000). I-waves in motor cortex. *J. Clin. Neurophysiol.* **17:**397-405.

Zoghi M, Pearce SL, Nordstrom MA (2003). Differential modulation of intracortical inhibition in human motor cortex during selective activation of an intrinsic hand muscle. *J. Physiol.* **550:**933-946.

# 11 Appendix

## 11.1 Publications

The following publication are included in this appendix. The first one represents the work of Chapter 3, the second one is based on upon Chapter 4. The third publication represents Chapter 6, while the last two have been incorporated into Chapter 3 and the general discussion.

Bestmann S, Baudewig J, Frahm J (2003). On the synchronization of transcranial magnetic stimulation and functional magnetic resonance imaging. *J. Magn. Reson. Imaging* **17:**309-316.

Bestmann S, Baudewig J, Siebner HR, Rothwell JC, Frahm J (2003). Subthreshold high-frequency TMS of human primary motor cortex modulates interconnected frontal motor areas as detected by interleaved fMRI-TMS. *Neuroimage* **20:**1685-1696.

Bestmann S, Baudewig J, Siebner HR, Rothwell JC, Frahm J (2004). Functional MRI of the immediate impact of transcranial magnetic stimulation on cortical and subcortical motor circuits. *Eur. J. Neurosci.* **19:**1-13 (in press).

Bestmann S, Baudewig J, Siebner HR, Rothwell JC, Frahm J (2003). Is functional magnetic resonance imaging capable of mapping transcranial magnetic cortex stimulation? *Clin. Neurophysiol. Suppl.* **56:**55-62.*(only uncorrected proof available).*

Siebner HR, Lee L, Bestmann S (2003). Interleaving TMS with functional MRI: now that it is technically feasible how should it be used? *Clin. Neurophysiol.* **114:**1997-1999.